To my family and my students

"Sit down before facts as a little child,
be prepared to give up every preconceived notion,
follow humbly wherever and to whatever abysses nature leads,
or you shall learn nothing"
Thomas Henry Huxley

SUBSTRATE UND LIGANDEN DER PROTEIN-TYROSINE PHOSPHATASE PTPRR IN DER SIGNALTRANSDUKTION NEURONALER ZELLEN

DISSERTATION

zur Erlangung des akademischen Grades
doctor rerum naturalium

vorgelegt dem Rat der Biologisch-Pharmazeutischen Fakultät
der Friedrich Schiller Universität Jena

von Irene Matilde Chesini
aus Verona, Italien

Gutachter:
1.
2.
3.

Tag des Rigorosums:

Tag der öffentlichen Verteidigung:

ZUSAMMENFASSUNG

Zell-Zell-Wechselwirkungen sind von entscheidender Wichtigkeit für eine Vielzahl von Entwicklungs- und Wachstumsprozessen. Die korrekte Verarbeitung von den zwischen Zellen ausgetauschten Signalen wird u.a. durch reversible Tyrosinphosphorylierungen gewährleistet, die auf dem fein abgestimmten Wechselspiel von Rezeptortyrosinkinasen (RTK) und Protein-Tyrosinphosphatasen (PTP) beruhen. Die hier beschriebenen Untersuchungen widmen sich der Identifizierung von Komponenten des PTPRR-Signalweges. Das *Ptprr* Gen der Maus kodiert die vier Protein-Tyrosinphosphatasen PTPBR7, PTP-SL, PTPBSγ-42 und PPBSγ-37. Am Anfang unserer Untersuchungen war schon klar, dass PTPRR Proteine hauptsächlich in neuronalen Zellen exprimiert werden, mit verschiedenen Mitogen-aktivierten Proteinkinasen (MAPK) interagieren, und diese dephosphorylieren, was einen Einfluss auf die Signalaktivität von MAPK nahelegte. *In vivo* Studien in Mäusen mit inaktiviertem Ptprr Gen (knockouts) zeigten, dass die MAPK Phosphorylierung in Hirnzellen dieser Mäuse erhöht war, während die generelle Morphologie des Gehirns unverändert blieb. Interessanterweise zeigten diese Mäuse milde Störungen der Balance und der motorischen Koordination, die wiederum auf eine Dysregulation der MAPK-Signaltransduktion insbesondere in der motorischen Kontollregion des Hirns, dem Cerebellum, hindeuteten. Unpublizierte Daten wiesen auch auf eine Wechselwirkung von PTPRR mit dem neurotrophen Rezeptor TrkA hin. Es wurde gefunden, dass PTPBR7 und PTP-SL TrkA dephosphorylieren können, und die Reifung von TrkA in die voll glykosylierte Form fördern. Dieses interessante Bild der Einbindung von PTPRR in verschiedene Signalwege veranlaßte uns, das Spektrum der Substratanalysen zu erweitern, und auch nach extrazellulären und membranegebundenne potentiellen Ligandenmolekülen für die transmembranale PTPBR7 Isoform zu suchen. Basierend auf einem Screen effizienter Phosphopeptid-Substrate, wurde eine begrenzte Anzahl von Phosphotyrosin-Proteinen (HER4, SHP1, und N-Cadherin) auf ihre mögliche Rolle als PTPRR-Substrate untersucht. Die Validierung dieser Kandidaten-Substrate folgte dabei strikt den etablierten Anforderungen (Tiganis und Bennett 2007), die den Beweis einer direkten Bindung von Substrat und PTP *in vitro* und *in vivo* verlangen, sowie die direkte Beeinflussung der Phosphorylierung der Phosphotyrosin-Spiegel des Substrates bei der Koexpression mit der untersuchten PTP. Diese Kriterien wurden jedoch in unseren experimentellen Ansätzen, welche hauptsächlich auf einer Induktion der Substratphosphorylierung durch Vanadat und der Analyse der PTP-Substrat-Interaktion durch Immunpräzipitation oder „Pulldown"-Ansätzen beruhten, nicht vollständig erfüllt. Es ist möglich, dass diese Untersuchungen durch die, im Gegensatz zu anderen PTP, besonders hohe Empfindlichkeit von PTPRR gegenüber Vanadat-basierten Inhibitoren beeinträchtigt worden sind. Diese ergab sich aus unseren vertiefenden Untersuchungen und könnte sowohl die PTPRR Aktivität, als auch die Kapazität des aktiven Zentrums von PTPRR mit Substraten zu interagieren behindert haben. Die aus dem Phosphopeptid-Screen vorhergesagten Substratinteraktionen könnten entsprechend durch die gewählten experimentellen Bedingungen nicht validierbar gewesen sein. Alternativ, könnte es sich bei diesen Interaktionen um transiente und schwache Wechselwirkungen handeln, die mit den gewählten biochemischen Methoden nicht erfassbar waren.

In einem parallelen Ansatz haben wir die Untersuchung potentieller Liganden von PTPRR im Mäusehirn in Angriff genommen. Unter Verwendung der „Receptor-alkaline Phosphatase (RAP)“ *in situ* Strategie fanden wir, dass die extrazelluläre Domäne der PTPBR7 signifikant in hoch myelinisierten Regionen des Maushirns bindet. Dies erfolgte insbesondere in der weißen Substanz des Cerebellums, was die Auffassung bestärkt, dass PTPRR seinen Einfluss insbesondere in dieser Hirnregion entfaltet. Weitere Experimente schlossen aus, dass es sich bei den vermutlichen PTPRR-Liganden in diesen Hirnarealen um Heparansulfat- oder Chondroitinsulfat-Proteoglykane handelt. Ein affinititäts-gereinigter Pool potentieller Liganden-Kandidaten für PTPBR7 aus dem Maushirn wurde der massenspektrometrischen Identifikation unterzogen. Dabei wurden das Zelladhäsionsprotein Neurotrimin, die heterotrimere G-Protein-Untereinheit Gαo, und die Serin-Threonin-Kinase CaMKII als potentiell interessante Interaktionspartner identifiziert. Gαo und CaMKII sind beide an Calcium-abhängigen Signalprozessen in Neuronen beteiligt. CaMKII wurde durch Massenspektrometrie auch unter potentiellen Substraten von PTPRR gefunden, die mit Hilfe eines GST-pulldown Ansatzes mit der PTPRR Phosphatasedomäne aus Maushirn-Lysaten angereichert worden waren. Störungen der Calcium-Signaltransduktion spielen eine zentrale Rolle für veränderte neuronale Funktionen, wie sie bei verschiedenen neurodegenerativen Prozessen gefunden werden. PTPRR Interaktionen im Gehirn könnten vor allem mit der Regulation von genauen Spiegeln von Calcium-Ionen zusammenhängen, wie sie für eine adäquate neuronale Differenzierung und Funktion erforderlich sind. Neurotrimin ist an der Axon-Faszikulierung und Synaptogenese während der neuronalen Entwicklung beteiligt, insbesondere in granulären und Purkinje-Zellen des Cerebellums. PTPRR könnte zur korrekten neuronalen Reifung und Synaptogenese beitragen, die essentiell für cerebellare Funktionen bei lokomotorischen Prozessen sind.

Zusammengenommen unterstützen diese Befunde das Konzept, dass PTPRR auf der einen Seite Teil von Zell-Zell-Adhäsionskomplexen mit Bedeutung für die Entwicklung des Cerebellums ist und auf der anderen Seite an der Regulation von Calciumionen-abhängigen Prozessen beteiligt ist, die wichtig für die neuronale Entwicklung und Plastizität sind.

SUBSTRATES AND LIGANDS OF THE PROTEIN TYROSINE PHOSPHATASE PTPRR IN NEURONAL CELL SIGNALLING

Thesis

For acquiring the academic degree
Doctor rerum naturalium

Presented to the Faculty of Biology and Pharmacy
Friedrich Schiller University, Jena

By Irene Matilde Chesini,
from Verona, Italy

SUMMARY

Cell-cell communication is a major process that governs a variety of cellular developmental and growth mechanisms. Correct integration of messages to and from the cell is warranted by, among others, reversible tyrosine phosphorylation that results from the fine interplay between Receptor Tyrosine Kinases (RTKs) and Protein Tyrosine Phosphatases (PTPs). The studies here described deal with the identification of components of the PTPRR signalling pathways. The unique *Ptprr* mouse gene encodes for the four protein tyrosine phosphatases PTPBR7, PTP-SL, PTPPBSγ-42 and PTPPBSγ-37. At the start of our studies it was already clear that PTPRR proteins are mainly expressed in neuronal cells and interact with and dephosphorylate several Mitogen-activated Protein Kinases (MAPKs) indicating an alteration of MAPK's regulated signalling. *In vivo* studies on mice knocked-out for *Ptprr* had shown that MAPKs phosphorylation was increased in brain cells of these mice, while the overall morphology of the brain had not changed. Interestingly, these mice displayed, though mildly, balance and motor coordination defects that pointed again at a dysregulation of MAPK signalling, in particular in the motor control centre of the brain, the cerebellum. Unpublished results also pointed at an interaction of PTPRR with the neurotrophic receptor TrkA. So far PTPBR7 and PTP-SL were shown to dephosphorylate and also promote maturation of the fully-glycosylated form of TrkA. This interesting picture of PTPRR intervention in several signalling pathways prompted us to enlarge the spectrum of substrate analysis and venture also the extracellular and membrane-bound pool of potential ligand molecules for the transmembrane PTPBR7 isoform. Based on a screen of efficient phosphopeptide substrates, a small set of phosphotyrosine-containing phosphoproteins (HER4, SHP1 and N-cadherin) were initially tested for being PTPRR substrates. The validation of these candidate phospho-proteins followed the strict requirements indicated by (Tiganis and Bennett 2007) that point at evidencing a direct binding of the phosphatase to its substrates, to be shown both *in vitro* and *in vivo* experimental systems, and a direct modulation of substrate's phosphotyrosine levels upon co-expression with the phosphatase under study. These requirements were not fully met in our experimental set-up, which consisted mainly of vanadate-based induction and maintenance of substrate's phospho-levels, and of immunoprecipitation- or pull down-based detection of stable phosphatase-substrate interactions. These studies may have been compromised by a fact revealed by our in-depth study on the use of vanadate-based inhibitors: PTPRR proteins appear affected more than other protein tyrosine phosphatases by vanadate compounds suggesting that PTPRR activity, and active site-dependent interactions with substrates predicted from the screen may in part not have been detected because of the chosen experimental conditions. Furthermore, the interactions between PTPRR proteins and their substrates may be relatively weak and temporary, and the employed standard biochemical methods may therefore not have been suitable for their validation.

In parallel we approached a study of the potential PTPRR ligands in the mouse brain system. Using the Receptor-alkaline Phosphatase (RAP) *in situ* strategy we found out that PTPBR7 extracellular domain binds significantly to highly myelinated regions of the mouse brain, in particular to the white matter of the cerebellum, strengthening the notion that PTPRR influence is primarily exerted in this part of the brain. Further experiments excluded that heparan-sulphate and chondroitin-sulphate proteoglycans were the putative PTPBR7 ligands

in these brain areas. When we subjected an affinity purified- pool of PTPBR7 potential ligand candidates from the mouse brain to mass-spectrometric identification, the cell adhesion protein neurotrimin, the heterotrimeric G-protein subunit Gαo and the serine/threonine kinase CaMKII were brought to the fore. Gαo and CaMKII participate both to calcium-dependent signalling processes in neurons. CaMKII was found also among potential PTPRR substrates independently obtained by mass-spectrometric identification of GST-pull down-based purifications of PTPRR phosphatase domain from mouse brain lysates. Disturbance of calcium-dependent signalling is at the basis of altered neuronal firing and has been linked to several neurodegenerative processes. PTPRR interactions in the brain may be primarily aimed at maintaining accurate calcium ion levels that are critical for proper neuronal differentiation and functioning. Neurotrimin is involved in axon fasciculation and synaptogenesis during neuronal development, in particular in granular and Purkinje cells of the cerebellum. PTPRR may contribute to proper neuronal maturation and synaptogenesis, which are essential for cerebellar functioning in locomotive processes.

Taken together, these findings support the notion that PTPRR is, on the one hand, part of cell-cell adhesion complexes important for cerebellar development and, on the other hand, involved in calcium ion-regulated events that are instrumental in neuronal development and plasticity.

TABLE OF CONTENTS

1. General introduction…….....6

Purpose and outline of this thesis…….....7

1.1 Cell signalling…….....7

1.1.1 Neuronal networks and signalling…….…….....7

1.1.2 Receptor tyrosine kinase signalling ……..…….....8

1.1.3 The Receptor Tyrosine Kinase family HER/Erb B…….…….....11

1.1.4 cSrc Tyrosine Kinase: activity and regulation.....13

1.1.5 The tyrosine phosphatase SHP1…….....14

1.1.6 The Serine/Threonine calcium/calmodulin-dependent kinase II…….….....14

1.1.7 Cell adhesion molecules of the CNS…….....15

1.1.8 Heterotrimeric G-proteins……..……..…….....18

1.2 Extracellular matrix and proteoglycans in brain development and function.....19

1.3 Protein tyrosine phosphatases…….....21

1.3.1 Regulation of protein tyrosine phosphatases by ligand binding….....21

1.3.2 Protein tyrosine phosphatase substrate-trapping mutants.....24

1.3.3 Approaches to the identification of substrates and ligands for protein tyrosine phosphatases.....24

1.3.4 Orthovanadate and Pervanadate as enhancers of tyrosine phosphorylation.....28

1.3.5 The PTPRR-subfamily of Protein Tyrosine Phosphatases and their biological functions.....29

1.3.6 SCA genes and ataxic phenotypes in humans……...…….....33

1.3.7 Pathways of neuronal degeneration……...…….....….....34

2. Materials and methods…….....36

2.1 Materials…….....….....37

2.1.1. Chemicals.....37

2.1.2. Reagents and Buffers.....38

2.1.3. Antibodies....42
2.1.4. Cell Lines and Media....45
2.1.5. Plasmids and Primers....45
2.2 Methods....46
2.2.1 Cell Culture....46
2.2.2 Cloning....46
2.2.3 Reverse Transcriptase-Polymerase Chain Reaction....47
2.2.4 Transient Transfections....48
2.2.5 Cell lysis, Immunoprecipitation and Blotting....49
2.2.6 Brain tissue sections and lysates....50
2.2.7 GST pull downs....50
2.2.8 Dephosphorylation assays on tyrosine phosphorylated peptides in microplate....51
2.2.9 DiFMUP de-phosphorylation assays....51
2.2.10 Dephosphorylation and co-immunoprecipitation assays *in vitro*....52
2.2.11 Dephosphorylation and co-immunoprecipitation assays in over-expressing cells....52
2.2.12 Alkaline phosphatase assays with conditioned culture media....52
2.2.13 Bradford protein quantification....53
2.2.14 Immunohistochemistry....53
2.2.15 Receptor alkaline phosphate (RAP) *in situ* staining on brain sections....53
2.2.16 GAG ELISA....54
2.2.17 Affinity purification using His-tagged PTPBR7 ectodomain (BR7ecto226-His) in brain lysates....54
2.2.18 Coomassie and silver staining....55
2.2.19 Mass spectrometry analysis of PTPBR7 extracellular domain interacting proteins....55
3. Results....57
3.1 Application of GST fusion proteins in phospho-peptide array screenings and pull-down assays....58

3.1.1 GST fusion protein production and validation…….....58

3.1.2 Phospho-peptide screening…….....59

3.1.3 GST-pull down from brain lysates and mass spectrometry…….....64

3.2 Substrate validation by *in vitro* and *in vivo* approaches…….....70

3.2.1 Dephosphorylation and binding assays *in vitro*…….....70

3.2.1.1 PTPRR does not interact with SHP1 *in vitro*…….....71

3.2.1.2 PTPRR does not interact with HER3 *in vitro*…….....74

3.2.1.3 PTPRR does not interact with HER4 *in vitro*…….....74

3.2.2 Dephosphorylation and binding assays in over-expressing cells.....77

3.2.2.1 PTPPBSγ does not interact with SHP1 when co-expressed in COS-1 cells…...79

3.2.2.2 HER4 remains a candidate substrate of PTPBR7…….....82

3.2.3 PTPBR7 does not interact with N-cadherin…….....85

3.2.4 Validation assays in PC12 cells……..…….....87

3.3 Evaluation of PTPBR7 phosphatase activity in presence of vanadatecompounds..91

3.4 Methods for identifying PTPBR7 extracellular ligands: RAP *in situ* and affinity chromatographic approaches…….....93

3.4.1 PTPBR7 probes for RAP *in situ*…….....94

3.4.2 PTPBR7 extracellular domain binds specifically on myelinated tracts of the mouse cerebrum and cerebellum….....94

3.4.3 PTPBR7 extracellular domain preferentially binds to the white matter in the mouse cerebellum….....97

3.4.4 Assessment of direct binding to heparan- and chondroitin-sulphate GAGs.....100

3.4.5 Candidate protein ligands for the PTPBR7 extracellular domain.....….....100

4. Discussion……..….....104

4.1 Brief summary of obtained results…….....105

4.2 Identification of PTPRR substrates……...….....105

4.3 Is the transmembrane protein PTPBR7 a receptor molecule?.....112

4.4 Implications for the biological role of PTPRR in mouse brain from the identification of putative novel interactions partners……...….....113

5. Conclusion and Outlook……..……...….....120

6. Appendix…….....I

6.1 References…….....….....II

6.2 Abbreviations…….....….....XX

6.3 Plasmid Maps and Vector Constructs…….....….....XXIII

6.4 Supplementary tables……..….....XXVI

6.5 Acknowledgements…….…….....…XXXVII

6.6 Lebenslauf-Curriculum vitae..…….....XL

6.7 Selbstständigkeitserklärung…….....…….....XLI

6.8 Erklärung zur Bewerbung…….....XLII

6.9 List of Posters and Publications……...…….....….....XLIII

Chapter 1

➢ General introduction

"If I saw further than other men,
it was because I stood on the shoulders of giants"
Isaac Newton

Purpose and outline of this thesis

One of the key mechanisms in intracellular signal transduction pathways is the reversible tyrosine phosphorylation of proteins exerted by the essential and reciprocal actions of both protein tyrosine kinases (PTKs) and protein tyrosine phosphatases (PTPs). The mammalian PTP family members have been identified based on sequence homology, but knowledge on their positions within cellular signalling networks is still rudimentary.

In the current study focus has been on the protein isoforms PTPBR7, PTP-SL and PTPPBSγ that are encoded by the mouse gene *Ptprr*. Knock out mice for *Ptprr* display motor coordination defects in multiple locomotion tests and hyperphosphorylation of MAP kinases ERK1/2 in the brain. We have further investigated the modes of action of PTPRR proteins in neuronal cells by searching for physiological substrates and ligands in cell models and in brain tissue sections using biochemical, histochemical and proteomic techniques.

1.1 Cell signalling

Cells in multicellular organisms are continuously exposed to diverse stimuli from the extracellular environment, which comprise endocrine or paracrine factors and signalling molecules on neighbouring cells. It is of great importance that these extracellular signals are correctly interpreted by the cell, in order to achieve an appropriate developmental or proliferative response. Some classes of receptor proteins bind specific ligands and, after conformational modifications such as dimerization and auto- or trans-phosphorylation events on serine, threonine or tyrosine residues, integrate the external stimuli with internal signal transduction pathways that lead to the correct cellular response (Olayioye et al. 2000). In addition to the predominance of protein-protein interactions, in the last years also free or protein-associated sugar moieties have gained more and more recognition in their ability to bind extracellular molecules and induce or contribute to signal transduction mechanisms (Galtrey and Fawcett 2007). Classes of receptors and their signalling mechanisms relevant to our studies are addressed in the following introductive paragraphs.

1.1.1 Neuronal networks and signalling

The nervous system consists of hundreds of billions of neurons interconnected to make up functional neural networks. Neurons innervate and function within a network via specialized cell junctions known as synapses. Synapses are macromolecular structures that regulate intercellular communication in the nervous system, and are the main gatekeepers of information flow within neural networks. The connectivity and functionality of neural networks is determined by where and when synapses form. Synapse formation involves pairing of the pre- and postsynaptic partners at a specific neurospatial coordinate. Multiple developmental events, such as cell fate specification, cell migration, axon guidance, dendritic growth, synaptic target selection and synaptogenesis require precise execution to guarantee the specificity of synapse formation (Juttner and Rathjen 2005; Salie et al. 2005; Waites et al. 2005). During early development of the nervous systems, differentiated neurons migrate to

their proper positions and elongate their axons towards their targets. Growing axons are guided by various attractive or repulsive target-derived cues (Tessier-Lavigne and Goodman 1996). After reaching their target areas, axonal growth cones still need to recognize their appropriate target cells for the formation of synapses. Then, initial contacts are formed between axons and dendrites, and signalling through homophilic and heterophilic receptors induces differentiation of the synaptic specialization (Scheiffele 2003). Most of these interactions and recognitions have been shown to be mediated by cell surface proteins. These molecules interact with each other in between the cells to activate various signalling pathways and bring the apposed cell membranes into contact. Some of these molecules are defined as adhesion molecules and others as signalling molecules. However, as certain adhesion molecules are known to have signalling functions and the signalling molecules often promote cell-cell adhesion, it might not be so easy to distinguish these membrane proteins specifically involved in adhesion or signalling. In addition to neuron-neuron interactions, astrocyte-synapse interactions are also known to play important roles in the formation of neural networks. Astrocyte-synapse communication participates in synapse formation, synaptic transmission and axonal conduction, and may modulate the activity of neuronal networks during development and throughout adult life (Fields and Stevens-Graham 2002). Astrocyte processes ensheath synaptic junctions in the brain, but do not form myelin. Astrocytes are also known to influence synaptic transmission by uptake of neurotransmitters, such as glutamate, ATP and γ-Aminobutyric acid (GABA), from the synaptic cleft through membrane transporters, and release of glutamate upon reversal of the transporter. Other substances (e.g., D-serine, (Wolosker et al. 1999)) released by astrocytes can strengthen synaptic transmission by co-activating N-methyl-D-aspartic acid (NMDA) receptors in the postsynaptic membrane or can reduce it by binding to neurotransmitters (Baranano et al. 2001). During myelination, the process of a myelinating cell wraps around an axon to elaborate a myelin sheath, therefore allowing the establishment of a rapid, saltatory conduction of action potentials along the axon. Myelination is achieved by Schwann cells in the peripheral nervous system, whereas oligodendrocytes are the myelinating cells in the central nervous system (CNS). While a myelinating Schwann cell elaborates a myelin sheath around a single axonal segment, an oligodendrocyte is able, depending on its localization, to myelinate up to 40 axons. This tight interaction implies reciprocal signalling between the oligodendrocytes (or the Schwann cells) and the axons to be myelinated (Coman et al. 2005).

1.1.2 Receptor Tyrosine Kinase signalling

Receptor tyrosine kinases (RTKs) are essential components of signal transduction pathways that play key roles in the majority of cell processes including cell migration, metabolism and survival, as well as cell proliferation and differentiation (Schlessinger 2000). RTKs can be divided in different families depending on the ligands (i.e. growth factors, cytokines) that they bind, on the biological response that they induce or, more rigorously, on their primary structure and homology. All RTKs possess an extracellular ligand binding domain which is usually glycosylated. This is in turn connected to the cytoplasmic region by a single transmembrane helix. The cytoplasmic region contains the protein tyrosine kinase (PTK) domain responsible of the transfer of the γ phosphate of ATP to the tyrosine of target proteins

(Hunter 1998). The PTK domain itself contains also tyrosine sequences that are subject to auto-phosphorylation or to trans-phosphorylation by other tyrosine kinases. RTKs are activated by ligand-induced receptor homo- or heterodimerization that is subsequently stabilized by the action of other receptor regions (Jiang and Hunter 1999). Besides ligand-induced dimerization, it has been shown that active RPTK dimers exist also in the presence of inhibitors or when RPTKs are overexpressed (Schlessinger 2000). Activation leads to auto- or trans-phosphorylation of tyrosine residues in the cytoplasmic region, which in turn serve as recruitment sites for a host of downstream signalling proteins – enzymes and adapter/scaffolding proteins – typically through Src homology-2 (SH2) or phosphotyrosine-binding (PTB) domains in specific sequence contexts (Pawson et al. 2002). The majority of SH2-containing proteins have also enzymatic activity, such as PTK (i.e. Src-family proteins), protein tyrosine phosphatase (PTP) (i.e. SHP1 and SHP2), phospholipase (i.e. PLCγ) or Ras-GTPase activating (i.e. Ras-GAP) activity. Another family of proteins (the so-called adaptor proteins) uses their SH2 and Src homology-3 (SH3) domains to mediate interactions that link proteins involved in signal transduction (Grb2, Nck, Crk, Shc). A simplified view of the structural properties of receptor tyrosine kinases and the protein modules involved in the firsts steps of PTK signal transduction pathways is given in Figure 1.1.

Depending on the type of RTK that is activated, many different signalling pathways can be switched on. A brief overview of the most known pathways will be provided here (see also Figure 1.2), but for an in-depth description we refer to publications that focus on specific pathways.

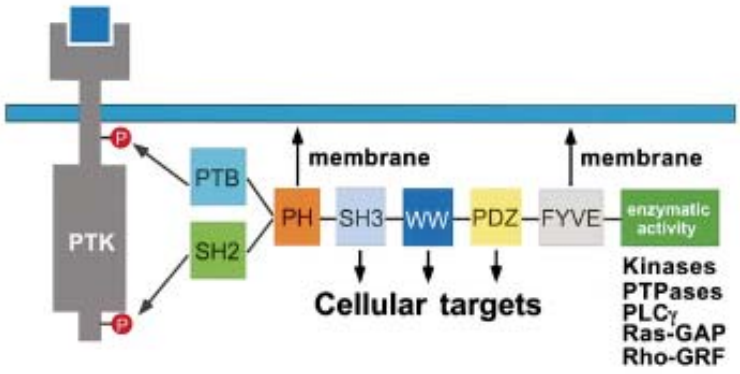

Figure 1.1. Protein modules that participate in signalling via receptor tyrosine kinases. Reprinted with permission from (Schlessinger 2000).

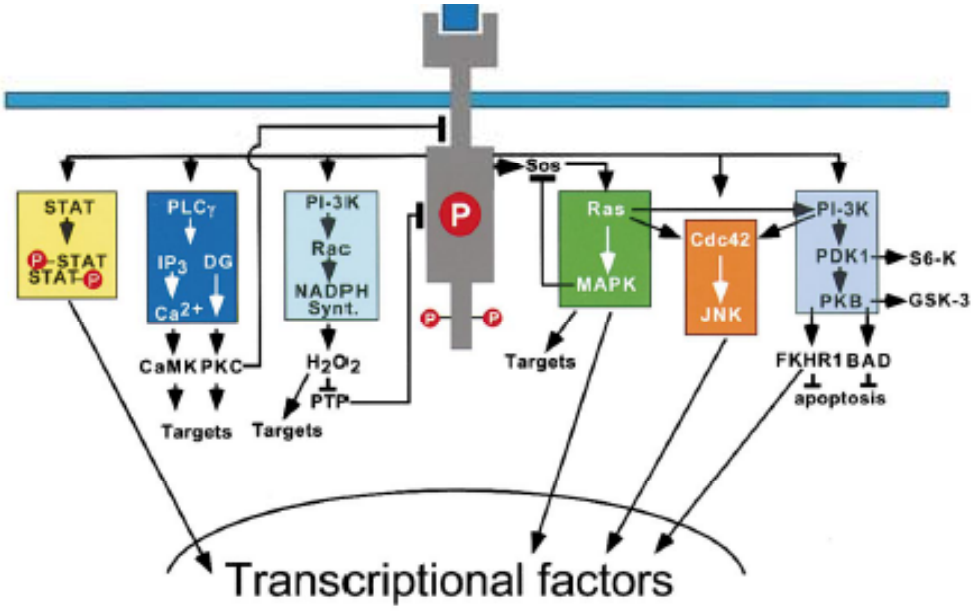

Figure 1.2. Signalling pathways activated by receptor tyrosine kinases. Mechanisms and molecules involved are described in the text. Reprinted with permission from (Schlessinger 2000).

The Ras/MAPK pathway

Many RTKs induce the exchange of GTP for GDP on the small G protein Ras. In this process, after RTK phosphorylation, the adaptor protein Grb2/exhange factor Sos complex is recruited close to the membrane. In this position close to Ras protein, Sos can act and stimulate GTP/GDP exchange (Bar-Sagi and Hall 2000). Other adaptor and docking proteins are known to be involved in specific cases but in any case, once Ras is in the active state, it can interact with many effector proteins such as the Mitogen-activated protein kinase kinase kinase (MAPKKK) Raf or the phosphatidylinositol-3-phosphate kinase (PI3K). The mitogen-activated protein kinase (MAPK) cascade is highly conserved in evolution and several MAPK cascades exists in yeast, invertebrates and vertebrates (Waskiewicz and Cooper 1995; Garrington and Johnson 1999). For example, the MAPKKK Raf activates the MAKK MEK by phosphorylating a key Ser residue in the activation loop and, in turn, MEK phosphorylates the MAPK ERK on Thr and Tyr. Activated MAPK phosphorylates several cytoplasmic and membrane linked substrates and can also translocate to the nucleus where it phosphorylates and activates transcription factors important in key cell processes (Hunter 2000) such as differentiation and proliferation in dividing cells. ERKs are also highly expressed in the adult brain, specifically in mature neurons where ERK is phosphorylated during NMDAR activation in the hippocampal CA1 region during long-term potentiation (LTP) (English and Sweatt 1997) and in cultured embryonic hippocampal neurons [49], demonstrating ERK involvement in synaptic plasticity (Sweatt 2004; Thomas and Huganir 2004).

The PLCγ/CaMK/PKC pathway

Almost all RTKs lead to rapid stimulation of phosphoinositol metabolism and generation of multiple second messengers. Specific phosphotyrosine (pTyr) residues of activated RTKs recruit PLCγ to the membrane where it hydrolizes phosphatidylinositol-(4,5)-diphosphate to

form two second messengers, diacylglycerol (DAG) and inositol-(1,4,5)-triphosphate (IP3). The second binds to specific intracellular receptors and stimulate the release of calcium from intracellular stores. This Ca^{2+} can then be bound by calmodulin which in turn activates $Ca^{2+/}$calmodulin-dependent protein kinases. Both diacylglycerol and Ca^{2+} activate members of the PKC kinase family which phosphorylate several intracellular targets and lead to transcriptional activation (Hunter 2000; Toker and Newton 2000).

The PI3K pathway

The Phosphatidylinositol 3-kinase (PI3K) is activated by almost all RTKs. It contains a regulatory subunit (p85) that allows the binding to pTyr and a catalytic subunit (p110) responsible for the conversion of phosphatidylinositol (4,5) bisphosphate (PIP_2) into phosphatidylinositol-(3,4,5)-triphosphate (PIP_3). PIP_3 mediates the translocation of several signalling proteins to the membrane (i.e. the PTKs Btk and Itk, the docking protein Gab1) where they act on several targets involved in cell survival, apoptosis, sugar metabolism and H_2O_2 generation (Hunter 2000; Toker and Newton 2000). The tumour suppressor phosphatase with tensin homology (PTEN) negatively regulates PI3K signalling by dephosphorylating PIP_3, converting it back to PIP_2 (Cully et al. 2006).

The JAK/STAT pathway

Not only lymphokines but also some growth factors, such as PDGF, EGF and FGF, induce gene transcription by activating the Janus kinase/Signal transducer and activator of transcription (JAK/STAT) signalling pathway (Schlessinger 2000). The binding of these ligands leads to the activation of JAK and subsequent tyrosine phosphorylation of STATs. This is followed by binding of the SH2 domain of STAT to pTyr sites on homotypic or heterotypic STATs enabling the formation of STAT homodimers or heterodimers. The dimeric STATs then migrate to the nucleus to activate transcription on target DNA sequences (Darnell JE. Jr et al. 1994; Ihle JN 1995).

Receptor tyrosine kinases are regulated by several mechanisms that lead to signal attenuation or termination. An important mechanism for signal termination is via receptor endocytosis and degradation (Sorkin and Goh 2008). Also the dephosphorylation by PTPs can inhibit kinase activity or eliminate docking sites, thus terminating signal.
Because our studies pointed to RTKs as being potential candidate ligands or substrates for PTPRR, we will now describe in somewhat more detail the following signalling molecules: the HER/ErbB family, the Src family of PTKs, the PTP protein SHP1, the cell adhesion protein N-cadherin and IgLON protein family, the CaMKII protein complex and the heterotrimeric Go-protein.

1.1.3 The Receptor Tyrosine Kinase family HER/Erb B

ErbB proteins are RTKs expressed in several tissues of epithelial, mesenchymal and neuronal origin. They include the epidermal growth factor receptor EGFR (also known as ErbB1 or HER1), the co-receptor ErbB2 (also called HER2 or Neu), the kinase-impaired receptor ErbB3 (also known as HER3) and the receptor ErbB4 (or HER4). Together with their ligands

they play important roles in proliferation, development and differentiation (Citri and Yarden 2006). Besides this, deregulated expression of ErbB family members has been implicated in the development and malignancy of numerous types of human cancers (Baselga and Swain 2009). Several mechanisms are used to diversify the intracellular signals elicited by receptor activation. First, ErbB members can homo- and heterodimerise as a consequence of ligand binding. Of particular interest, ligands for ErbB2 have thus far not been found but still the receptor can heterodimerise with all other members, hence it is preferentially called a co-receptor. On the contrary, ErbB3 has impaired kinase activity although it does bind ligands, therefore it can only signal upon heterodimerization with enzymatically competent family members. An additional level of ErbB signalling versatility is given by the multiplicity of ligands. For example, neuregulins (NRGs) NRG1 and NRG2 bind to ErbB3 and ErbB4 only. NRG3 and NRG4, however, bind to ErbB4 but not to ErbB3. For a detailed description of ErbB ligand interactions we refer to other publications (Olayioye et al. 2000; Vaskovsky et al. 2000). Likewise, we refer to Sorkin and Goh (2008) for a review on endocytosis and intracellular trafficking of ErbB proteins.

Ligand binding induces receptor dimerization which is followed by activation of the cytoplasmic tyrosine kinase and auto- and trans-phosphorylation of C-terminal tyrosine residues. The phosphorylated tyrosines are bound by adaptor proteins (such as Shc, Crk, Grb2, Grb7 and Gab1), kinases (such as Src, Chk and PI3K via its p85 subunit), tyrosine phosphatases (such as SHP1 and SHP2) and the transcription factor STAT5 (Olayioye et al. 2000; Schulze et al. 2005). A schematic overview of ErbB protein regulation and signal integration is shown in Figure 1.3.

Clear evidence of the importance of ErbB activities in mouse development is given by the lethal or severe phenotypes displayed by null or knock-out mice (Olayioye et al. 2000). Interestingly, ErbB3 deficient mice die at day E13.5 due to heart defects but they show also generalized neural crest defects and absence of Schwann cells precursors (Riethmacher et al. 1997; Erickson et al. 1997). Mice that lack either ErbB2, ErbB3 or NRG1 display impaired neural crest cell migration (Britsch et al. 1998). A similar phenotype is also shown by mice lacking the ErbB4 receptor, together with general defects in axon guidance in the central nervous system (Gassmann et al. 1995; Golding et al. 2000; Tidcombe et al. 2003). The relevance of ErbB proteins in neuronal cell development rendered them interesting for our studies on PTPRR signalling.

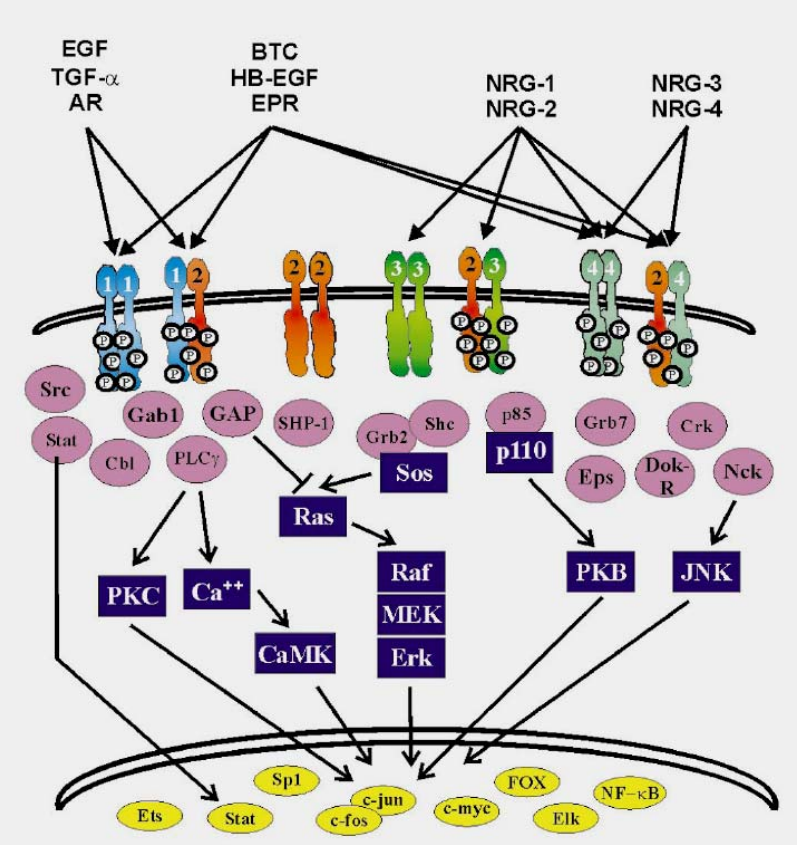

Figure 1.3. ErbB kinase ligand-binding and dimerization profiles and the integration to signalling pathways. Adapted from (Holbro and Hynes 2004).

1.1.4 c-Src Tyrosine Kinase: activity and regulation

Src-family protein tyrosine kinases are proto-oncogenes that have key roles in many cellular processes, such as proliferation, survival, morphology and motility. The founding member of this protein family is called c-Src while v-Src is the oncogenic protein encoded by the avian-cancer-causing Rous sarcoma virus (Martin 2001). The normal Src protein is expressed ubiquitously in vertebrate organisms but brain, osteoclasts and platelets express 5-200 fold higher Src levels than other tissues or cells (Brown and Cooper 1996). Src kinase activity is dormant during most part of the cell cycle, while being activated during G2/M transition. From N- to C-terminus Src contains a 14-carbon myristoyl group, a Src homology-4 (SH4) domain, a unique segment, an SH3 domain, an SH2 domain, an SH2-kinase linker, a tyrosine kinase domain and a C-terminal regulatory tail.

Src tyrosine kinase activity is strictly regulated. Tyr138, Tyr213, Tyr416 and Tyr527 are the tyrosine residues that are involved in Src regulation through reversible phosphorylation. Serine and threonine residues also play important roles but the two most important regulatory sites are Tyr416 and Tyr527. Under physiological conditions 90-95% of Tyr527, located in the C-terminal regulatory tail, is phosphorylated, thereby creating an intramolecular docking site for the Src SH2 domain. In this folded structure the SH2 and SH3 domains are not accessible to engage in interactions with other proteins and the enzyme is inactive because its kinase domain is inaccessible for potential substrate (Yeatman 2004). The protein tyrosine

kinases Chk and Csk are responsible for Tyr527 phosphorylation, ensuring that Src is kept in an inactive state. For Src to become active, the Tyr527 site needs to be dephosphorylated and subsequently Src undergoes an intermolecular autophosphorylation at Tyr416, which is located in the activation loop and promotes Src activity. We refer to Roskosky Jr. R. (2005) for a detailed review on Src regulatory sites. Src in its turn signals to several downstream effectors, among which the regulatory subunit of PI3K p85, Ras-GAP, phosholipase Cγ, various integrin signalling proteins (tensin, vinculin, cortactin, talin and paxillin) and focal adhesion kinase (FAK) (Brown and Cooper 1996).
PTP1B, SHP1, SHP2, CD45, PTPα, PTPε and PTPλ are all protein tyrosine phosphatases able to de-phosphorylate Src on pTyr527, thereby promoting the opening of the folded structure and, thus, Src activation. PTP-Basophil-like (PTP-BL, the mouse homologue of the human PTP-BAS), on the contrary, can dephosphorylate Src on pTyr416 but not on pTyr527, thus leading to Src deactivation. Besides the data *in vitro* and in overexpressing cells, the fact that PTPα, PTPε, PTP-BAS and Src are all well expressed in the brain, provides support for a physiological effect of these phosphatases on Src in this organ (Roskoski Jr. 2005).

1.1.5 The Tyrosine Phosphatase SHP1

SHP1 (also known as PTPN6) is a cytosolic protein tyrosine phosphatase that is expressed primarily in haematopoietic and epithelial cells. It contains two adjacent N-terminal SH2 domains, a tyrosine phosphatase domain and a C-terminal tail (Poole and Jones 2005). In B cells SHP1 substrates include B cell receptor (BCR) Igα-Igβ subunits, CD22, Syk and Src homology 2 domain-containing leukocyte adaptor protein (SLP)-65, suggesting roles for SHP1 in the termination of BCR-proximal tyrosine phosphorylation events and in inhibiting calcium mobilization (Tamir et al. 2000). SHP1 is expressed also in brain. In mouse brain it is expressed in the cortex, cerebellum and cervical spinal cord. Motheaten mice, which have a loss of function mutation in the gene for SHP1, have an allergic asthma phenotype probably due to mast cell dysregulation (Zhang et al. 2010). They also display reduced myelination in the central nervous system, suggesting that SHP1 plays a role in oligodendrocyte differentiation, maturation and survival (Massa et al. 2000). In the same mice, a decreased number of astrocytes and microglia has been observed (Wishcamper et al. 2001). *In vitro* studies in astrocytes showed that SHP1 negatively regulates the cytokine signalling via STAT1, STAT3 and STAT6 and controls the expression of interferon-inducible genes (Massa and Wu 1996; Massa and Wu 1998).

1.1.6 The Serine/Threonine calcium/calmodulin-dependent kinase II

One of the fundamental attributes of the brain is the plasticity of its synapses—namely, a positive or negative change in the efficacy of connections between neurons in response to neuronal activity. This feature is essential for the formation and function of neural circuits, and especially for learning and memory (Kandel 2001). Depending on the specific pattern of stimulation, individual synapses can increase or decrease the strength of their transmission for minutes to months. This long-term potentiation (LTP) or long-term depression (LTD) of

synaptic function has been considered a cellular model for the process of learning. LTP induces the formation of new dendritic spines and increases the volume of existing ones. Conversely, induction of LTD leads to the shrinkage or disappearance of dendritic spines (Okamoto et al. 2007). An increase in intracellular calcium concentration, often acting through the cytosolic Ca^{2+} - binding protein calmodulin (CaM), is a ubiquitous signal that regulates diverse cellular responses. In neurons, most of the diverse actions of Ca^{2+} increases are mediated by protein phosphorylation by three multifunctional $Ca^{2+/}$calmodulin-dependent kinases (CaMKs), CaMKI, CaMKII and CaMKIV (Ishida et al. 2008). These kinases have broad substrate specificities and, through the phosphorylation of various substrate proteins, are involved in a variety of physiological responses, such as neurotransmitter synthesis, neurotransmitter release, LTP and spatial learning (Hudmon and Schulman 2002; Yamauchi 2005). CaMKII is highly abundant in the brain, especially in the postsynaptic density (PSD). In mammals, CaMKII is encoded by a family of four genes, α, β, γ and δ. All these isoforms are found in the brain, but α and β subunits are especially highly expressed. CaMKII is activated following autophosphorylation of Thr286 and phosphorylates a number of proteins included synapsin I, microtubule associated protein 2 (MAP2), tau, myosin light chain, tyrosine hydroxylase and cAMP response-element binding protein (CREB) (Hook and Means 2001). Protein structural studies indicate that CaMKII is an oligomer composed of 10–14 monomers arranged in rotational symmetry (Morris and Torok 2001; Hoelz et al. 2003). CaMKII is crucial for LTP and is also involved in the structural plasticity of spines, and thus plays important roles in the regulation of higher order neuronal functions such as learning and memory. CaMKII is finely regulated by autophosphorylation at an appropriate level and in a timely manner.

Only recently deactivation mechanisms by CaMKII dephosphorylation have been uncovered and they are performed by two classes of Serine/Threonine phosphatases, the PPP and the PPM families. The first includes the phosphatases PP1, PP2A and PP2B and the second PP2C, CaMKP and CaMKP-N (Colbran 2004a). Dephosphorylation of autophosphorylated CaMKII in the post synaptic density (PSD) seems to be mainly catalyzed by PP1 anchored to the PSD through its scaffolding proteins (Strack et al. 1997; Yoshimura et al. 1999). In contrast to PSD-associated CaMKII, cytosolic CaMKII seems to be dephosphorylated *in vivo* mainly by protein phosphatases other than PP1, and PP2A has been proposed (Fukunaga and Miyamoto 2000). PP2B is negatively regulating CaMKII in an indirect way, via dephosphorylation of I-1, which is an inhibitor of PP1 but is inactive if dephosphorylated by PP2B (Ishida et al. 2008). PP2C, belonging to the PPM class of phosphatases, is also a candidate negative regulator of CaMKII. Importantly, mice lacking CaMKIIα expression display impaired spatial learning (Silva et al. 1992) and limbic epilepsy (Butler et al. 1995) and those deficient in the CaMKIV isoform show strong ataxic phenotype consistent with reduced mature Purkinje cell (PC) numbers and altered neurotransmission at excitatory synapses in PCs (Ribar et al. 2000).

1.1.7 Cell adhesion molecules of the CNS

Cell adhesion molecules (CAMs) are involved in many cellular processes during development such as proliferation, differentiation, migration, and morphological changes (Rojas and

Ahmed 1999). Many CAMs belong to one of three structural families: the cadherin (Takeichi et al. 1988), the integrin (Ruoslahti 1988) or the immunoglobulin superfamily (IgSF) (Williams and Barclay 1988). The IgSF proteins, which are defined by the presence of one or more Ig-like domains in their extracellular segments, are particularly abundant in the CNS and have important roles in diverse stages of CNS development (Rougon and Hobert 2003; Sakisaka and Takai 2005) due to their impact on neuronal migration, axon guidance, target recognition, and synapse formation (Williams and Barclay 1988; Salzer and Colman 1989; Schmid and Maness 2008). Until now, the functional importance of IgSF proteins has been investigated mainly in neuronal cells. Several studies now indicate that they play important roles in the proliferation, migration, process guidance, and target recognition of glial cells as well (Fox et al. 2006).

Cadherins

Cadherins are Ca^{2+}-dependent cell-cell adhesion molecules that constitute a superfamily comprised of more than 100 members in vertebrates and can be grouped into two subfamilies designated classic cadherins and protocadherins (Takeichi 2007). Classic cadherins are singlepass transmembrane proteins that have five extracellular cadherin repeat (EC) domains (EC1 to EC5). All classic cadherins are homophilic adhesion molecules that function in conjunction with their cytoplasmic partners, the catenins (Wheelock and Johnson 2003). Catenins are cadherin-binding proteins that connect cadherins to the actin cytoskeleton. These include α-catenin, β-catenin and p120 catenin. Cadherin-catenin complexes are known to regulate actin polymerization, a property important for maintaining cell-cell adhesion. Cadherins and their associated catenins have been observed in many neuronal populations in the CNS. At the ultrastructural level, these proteins were found in synaptic junctions of most regions of the nervous systems, forming a symmetrical adhesion structure in adherens junctions (Uchida et al. 1996). During development, the cadherin-catenin complexes accumulate at early axo-dendritic filopodial contacts, and are retained in many of the mature synapses (Yamagata et al. 1995; Fannon and Colman 1996; Uchida et al. 1996; Benson and Tanaka 1998; Togashi et al. 2002). A remarkable feature of classic cadherins is their binding specificity and region-specific distribution. In the brain, specific subtypes of classic cadherins are expressed by restricted groups of functionally connected regions (Suzuki et al. 1997). Whether cadherin-mediated adhesion contributes to the formation of selective inter-neuronal connections during neural network formation remains unknown.

Protocadherins are a group of transmembrane proteins that belong to the cadherin superfamily and have varying numbers of the EC domains but divergent cytoplasmic domains that do not appear to signal through catenins (Yagi and Takeichi 2000; Hirano et al. 2003). Various protocadherins are expressed in the nervous systems, and some of them are localized at synapses. However, the biological function of most protocadherins is unknown.

Integrins

Integrins are cell surface receptors that mediate interaction between a cell and the extracellular matrix (ECM) and transduce the signal from outside to the cell and viceversa. Integrins consist of two distinct chains, an α- and a β-subunit. Integrins also act at contacts between neurons and astrocytes, where they activate protein kinase C (PKC) signalling and promote synaptogenesis in vitro (Hama et al. 2004). However, the involvement of the

integrins-dependent PKC signalling in synaptogenesis *in vivo* still remains elusive (Togashi et al. 2009).

Ig-CAMs: Nectin, NCAM, L1-CAM and IgLON families

The immunoglobulin superfamily of cell adhesion molecules (Ig-CAMs) comprises at least four types: Nectins, NCAM, L1-CAM and IgLON proteins. Nectins represent a family of Ca^{2+}-independent immunoglobulin (Ig)-like cell-cell adhesion molecules, which consists of four members (Takai and Nakanishi 2003).

Neural cell adhesion molecule (NCAM) is widely expressed in the developing and adult brain and plays crucial roles in migration, axon pathfinding and synaptic plasticity. It is involved in both early synaptogenesis and subsequent synaptic maturation (Polo-Parada et al. 2001; Dityatev et al. 2004). The NCAM extracellular part contains five Ig-like domains and two fibronectin type III repeats, and is engaged in homophilic and heterophilic interactions at synapses with a variety of ligands, such as fibroblast growth factor receptor (FGFR), L1, TAG-1/axonin-1 and heparan-sulphate proteoglycans (Walsh and Doherty 1997; Kiss and Muller 2001). NCAM-deficient mice present poor axonal fasciculation in the hippocampus, which results in impaired synapse formation in the CA3 region (Cremer et al. 1997).

The L1-CAM receptors are a subfamily of the IgG superfamily of transmembrane receptors. In vertebrates, the family consists of a number of different transmembrane receptors, including L1, CHL1 (close homologue of L1), NrCAM (neuron-glia-related CAM) and neurofascin. At the cellular level, the L1-CAM family has been shown to participate in neurite outgrowth, neurite fasciculation and inter-neuronal adhesion (reviewed in (Hortsch 1996; Hortsch 2000)). The discovery that certain neurological disorders in humans are caused by mutations in the gene for neural L1-CAM initially heightened interest in the role of this protein family in the nervous system (De Angelis et al. 2002).

Notable IgSF CAMs are IgSF of the IgLON family. These proteins have three C2-type Ig-like domains, are highly glycosylated and attached to the lipid membrane by a glycosylphosphatidylinositol (GPI)-anchor. The limbic system-associated membrane protein (LSAMP; (Levitt 1984)), opioid-binding cell adhesion molecule (OBCAM, rodent and OPCML, human; (Schofield et al. 1989)), neurotrimin (Ntm; (Struyk et al. 1995)), and neuronal growth factor 1 (NEGR1, human; (Funatsu et al. 1999)) are members of the IgLON family. Most studies of the IgLON proteins involve analyses of CNS expression and function. Several *in vitro* experiments have revealed that LSAMP stimulates the neurite outgrowth of limbic axons (Pimenta et al. 1995), modulates the branching and layer specificity of thalamic axon systems (Zhukareva et al. 1997; Mann et al. 1998), and blocks the neurite outgrowth of dorsal root ganglia neurons. In contrast, Ntm promotes the neurite outgrowth of dorsal root ganglion neurons but inhibits neurite extension of sympathetic neurons (Gil et al. 1998; Gil et al. 2002). An early study showed significant amounts of Ntm mRNA in pontine nuclei, cerebellar GCs and PCs (Struyk et al. 1995).

Ntm expression in rats accompanies the development of projection pathways extending from brainstem nuclei through the cerebellar peduncles into the arbor vitae and disappears with the onset of myelination. These observations suggest that this adhesion molecule plays a role in axonal fasciculation of specific cerebellar systems and in stabilization of selected types of synapses (Chen et al. 2001). OBCAM is a synaptic CAM that controls the number of

dendritic synapses by interacting with other IgLON CAMs (Yamada et al. 2007; Hashimoto et al. 2008; Hashimoto et al. 2009). Two OBCAM isoforms (46 and 51 kDa) were demonstrated to result from different addition of N-linked carbohydrate chains (Hachisuka et al. 1996). OBCAM shows a much more restricted distributional pattern compared with that of LSAMP or Ntm, with the higher expression levels in cerebral cortex and hippocampus (Struyk et al. 1995; Miyata et al. 2003). NEGR1 localizes mainly at axons and presynaptic terminals at early culture stage in hippocampal neurons; however, it is seen at dendritic postsynaptic spine of mature neurons during the later culturing stages. Overexpression of NEGR1 decreases the number of dendritic synapses in young neuronal cultures, whereas the numbers increase again at late culture stages. These results suggest that IgLON CAMs participate in the regulation of synapse formation and neurite outgrowth (Hashimoto et al. 2008; Hashimoto et al. 2009).

1.1.8 Heterotrimeric G-proteins

Guanine nucleotide binding proteins or 'G-proteins' are intracellular molecular switches that alternate between an "on" and "off" state to regulate the duration and intensity of cell signalling. Heterotrimeric G-proteins are partners of seven transmembrane-domain G-protein-coupled receptors (GPCRs). Heterotrimers are composed of three subunits where the GDP-bound Gα subunit binds tightly to the obligate heterodimer Gβγ and the whole molecule associates with the cytosolic part of GPCRs in its "off" state. Upon ligand binding the GPCR acts as a guanine nucleotide exchange factor (GEFs) inducing a conformational change in the Gα subunit that allows it to exchange GDP for GTP. Gβγ dissociates from Gα-GTP and both molecules reach their "on" state and are competent for signalling to their respective effectors. The intrinsic GTPase activity of Gα makes the cycle go back to the basal state corresponding to the Gα-GDP form fastened to the original heterotrimer. The switch to the GDP-bound form is augmented by action of GTPase-accelerating proteins (GAPs) such as the Regulators of G-proteins signaling (RGS) (McCudden et al. 2005). 23 known Gα proteins have been identified in humans and they can be divided into four major classes based on sequence similarities: Gα(s/olf), Gα(i1/i2/i3/o/t-rod/t-cone/gust/z), Gα(q/11/14/16) and Gα(12/13) (Simon et al. 1991). Both palmitoylation and myristoylation are important for Gα membrane localization and interaction with other proteins such as adenylyl cyclase and GPCRs (Myung et al. 1999; Moffett et al. 2000). Palmitoylation results in the stable attachment of Gα to the membrane (Grassie et al. 1994). The Go protein contains a specific Gα subunit and a Gβγ complex that is indistinguishable from that of Gi. In fact, Go was discovered in an attempt to purify Gi from the brain. It makes up to 0.5-1 % of all brain membrane proteins. High densities of Go protein have been observed in the frontal cortex, cerebellum, hypothalamus, hippocampus and substantia nigra (Worley et al. 1986) but also in the peripheral nervous system (Homburger et al. 1987). It is mainly localized at the cytoplasmic face of the plasma membrane especially at cell-to-cell contacts but it was detected also in the cytoplasmic region between the Golgi cisternae and the endoplasmic reticulum (Gabrion et al. 1989). In addition Go has been observed in the heart tissue and in the endocryne system (Homburger et al. 1987). Many GPCRs are coupled to their effectors through Go, including muscarinic cholinergic receptors, GABAb receptors, α_2-adrenergic receptors and somatostatin receptors (Jiang and Bajpayee 2009). Effectors of Go are calcium and sodium channels, rectifying potassium channels,

adenylyl cyclase, diacylglicerol (DAG) kinase and MAP kinases (Jiang and Bajpayee 2009). PC12 cells transfected with Gαo showed activation of Rap1 and mitogen-activated kinase 2 (Ma'ayan et al. 2009). In neuro2A cells it is known that the CBl cannabinoid receptors mediate neurite outgrowth in a pathway that involves Src and STAT3 through Rap1. Overexpression of Gαo results in the activation of Rap1 that eventually promotes neurite outgrowth (He et al. 2005). Go controls also the small GTPase RhoA and phosphatidylinositol 4-kinase (PI4K) and seems involved in actin network reorganization and secretory vesicle movement (Jiang and Bajpayee 2009). Given its high expression in the brain Go is expected to have considerable functional importance. In fact, mice lacking Gαo show neurological deficits that include tremors, seizures and poor motor coordination whereas gross brain morphology is unaltered. Some animals display also a repetitive turning behavior that goes on for hours, abnormal exploration and hyperalgesia when tested on the hot plate. Other Go/i family member knockouts do not show any neurological deficiencies (Jiang and Bajpayee 2009). Interestinlgy GAP-43, a cytosolic protein found at leading edge of growth cones, acts as GEF for Go (Strittmatter et al. 1990) implicating a possible role for Go in neurite extension. When Go1 was overexpressed in NGF-stimulated PC12 cells the number of neurite outgrowths doubled and PKC inhibition along with modulation of Ca^{2+} levels were observed (Strittmatter et al. 1994; Xie et al. 1995). Go protein loss-of function mutants *(goa-1)* of *C. elegans* display misdirected neuronal migration (Kindt et al. 2002). Furthermore, Go-dependent inhibition of neuronal outgrowth by modulation of calcium levels was observed in the moth *Manduca sexta* (Horgan and Copenhaver 1998). All these studies support the notion that Go signalling is involved in neurite outgrowth. Since Ca^{2+} levels are key modulators of axonal extension, cell targeting, cytoskeleton dynamics and synaptic plasticity (Zheng and Poo 2007), it is conceivable that Go acts by translating gradients of extracellular factors into attractant or repellent signals using Ca^{2+} levels as modulators (Jiang and Bajpayee 2009).

1.2 Extracellular matrix and proteoglycans in brain development and function

The ECM contains a plethora of molecules that are secreted and assembled locally. The most abundant components of ECM are: 1) Glycosaminoglycans (GAGs), either in the free form as hyaluronans or in the protein-bound form as proteoglycans; 2) fibrous proteins (e.g. collagen and elastin); 3) adhesive glycoproteins (e.g. fibronectin, laminin, tenascin). Those molecules are arranged in intricate ways and intermingle with a variety of secreted growth factors. Depending on the cells secreting the ECM components, those are organized in different ways and generate diverse forms of ECM (e.g. bone, tendons, cornea) (Alberts B. et al. 2002; Galtrey and Fawcett 2007). GAGs are long, repeating, linear polymers of disaccharides and when attached to a protein core they form proteoglycans. Proteoglycan biosynthesis starts with the addition of xylose to serine residues of the protein scaffold (O-glycosylation), followed by attachment of two galactose and one glucuronic acid residue. Afterwards, alternative addition of N-acetylgalactosamine and glucuronic acid generate chondroitin sulphate (CS) and dermatan sulphate (DS) (if glucuronic acid epimerizes to iduronic acid); otherwise, alternating N-acetylglucosamine and glucuronic acid leads to the formation of heparan sulphate (HS). Keratan sulphate is a polymer of the disaccharide lactosamine, which

is attached to the protein via N- (to asparagine) or O- (to serine) glycosylation of N-acetylglucosamine and galactose dimers. The whole process of GAG synthesis is accompanied by epimerization (the swap in configuration of diasteroisomers) and by sulphation at different residues. Hyaluronan is not attached to any protein and consists of a large polymer of alternating glucuronic acid and N-acetylglucosamine residues (Alberts B. et al. 2002; Zimmermann and Dours-Zimmermann 2008).

The central nervous system has a unique ECM, both in composition and arrangement, because it contains relatively few fibrous proteins and many GAGs (Novak and Kaye 2000). The major GAGs in the CNS are hyaluronan and the lectican family of CSs (aggrecan, versican, neurocan and brevican) (Yamaguchi 2000). Hyaluronan and chondroitin-sulphate are highly present in the perineuronal nets (PNN), agglomerates of extracellular matrix components found around cell bodies and dendrites of certain classes of neurons, whose function is not fully understood yet (Celio et al. 1998). Emerging evidence shows that CS proteoglycans (CS-PGs) are involved in the control of neuronal plasticity, and thus in the refinement of connections during development and in the response to experience, age and injury in the adult CNS (Rhodes and Fawcett 2004; Galtrey and Fawcett 2007). Cortical circuits are sensitive to experience during well-defined intervals of early postnatal development, the so-called critical periods. After the critical period, plasticity is reduced or absent. Several studies have been done in the developing ocular system of higher mammals. CS-PGs appeared instrumental in closing the critical period when the ocular dominance is defined because treatment with the chondroitinase ChABC - that removes CS-GAGs – was found to reopen this critical period (Pizzorusso et al. 2002). CS-PGs also have a role in the plasticity that underlies learning and memory, LTP and LTD. For instance, removal of CS-GAG chains reduced both LTP and LTD in murine hippocampal slice cultures (Bukalo et al. 2001; Saghatelyan et al. 2001) probably due to the release of growth factors (for instance pleiothropin) that bind to the CS-GAG chains of neurocan and phosphacan (Amet et al. 2001). RPTPβ/ζ is a CS-PG protein tyrosine phosphatase receptor that is found in CNS neurons and astrocytes during development and adulthood. Importantly, in RPTPβ/ζ-deficient mice there are no anatomical abnormalities in the brain but still an age-dependent impairment of spatial learning and enhancement of LTP in the hippocampus is evidenced, due to aberrant activation of Rho-associated kinase (Tamura et al. 2006). This may involve the CS chain and pleiothropin/midkine signalling mechanism since RPTPβ/ζ is a receptor for these ligands (Sugahara and Mikami 2007). After traumatic injury of the CNS, CS-PGs have been shown to inhibit axonal regeneration and to restrict plasticity. Treatment of the CNS with the chondroitinase ChABC results in an enhancement of axonal regeneration after nigrostriatal tract lesioning and spinal cord injury (Moon et al. 2001; Bradbury et al. 2002; Yick et al. 2003; Caggiano et al. 2005; Fry et al. 2010) and it induces axonal sprouting of Purkinje cells both in slices cultures (Tanaka et al. 2003) and *in vivo* (Corvetti and Rossi 2005). CS-PGs are thus crucial environmental modulators in the CNS and are expected to interact directly or indirectly with key signaling molecules (e.g. PTKs and PTPs) of the nervous system.

1.3 Protein Tyrosine Phosphatases

Protein tyrosine phosphorylation, as exerted by PTK action, is reversible and thus actively counterbalanced by the effects of protein tyrosine phosphatases (PTPs) (Tonks 2006). The human genome contains 107 PTPs that can be divided into four groups based on their distinct evolutionary origin (Alonso et al. 2004; Andersen et al. 2004). The class I cystein-based PTPs constitute the largest group that can be further subdivided into 61 dual-specificity phosphatases (DUSPs) and 38 tyrosine-specific PTP genes. While the first can dephosphorylate both phospho-tyrosine and phospho-serine/-threonine residues, the second are specific for phospho-tyrosine residues only and constitute the classical PTPs. Classical PTPs (Figure 1.5) are further subdivided into receptor-like (R1-R8) and non-transmembrane (NT1-NT9) subgroups. Non-transmembrane, soluble PTPs all have one PTP domain (Andersen et al. 2001; den Hertog et al. 2008). Twelve receptor-like PTPs (RPTPs) have two catalytic domains in the intracellular region but normally only the one proximal to the transmembrane segment (D1) is active while the distal one (D2) is either inactive or has negligible activity. The functional role of the D2 domain is thought to be related to the regulation of RPTP stability, specificity and dimerization. Furthermore, all RPTPs have an extracellular region that contains diverse domains, some of which are implicated in cell contact and adhesion processes (Aricescu et al. 2007; Coles et al. 2011) as will be discussed further on.

The PTP catalytic domain is around 280 residues long and consists of an α/β structure whose key features include: the CX_5R signature motif with the catalytic site cysteine; the mobile Trp-Pro-Asp (WPD) loop, the catalytically important aspartate residue that is kept in position by the closed WPD loop; and the phospho-tyrosine recognition loop (Barford et al. 1994; Zhang 2002). Despite displaying highly promiscuous activity *in vitro*, PTPs exhibit exceptional substrate specificity *in vivo*. This specificity is generally determined by both structural elements (catalytic domain, post-translational modifications, accessory regulatory domains) and expression patterns (developmental-, tissue-specific expression and subcellular localization) (Tiganis and Bennett 2007; den Hertog et al. 2008; Tabernero et al. 2008). Several mechanisms that regulate PTP activity have been reported, including limited proteolysis, post-translational modifications (i.e. oxidation and phosphorylation), dimerization and ligand binding (Tonks 2006; den Hertog et al. 2008).

1.3.1 Regulation of Protein Tyrosine Phosphatases by ligand binding

In the human genome, 21 of the classical PTPs are called receptor-like PTPs (RPTPs) because of their transmembrane nature and the domain organization of their N-terminal extracellular region that has been proposed to enable the reception of signals outside the cells. Binding of a ligand would trigger conformational changes and/or activation and de-activation of the phosphatase (Hunter 1989). The hypothetical ligand binding region is normally followed by a transmembrane domain and 1 or 2 cytoplasmatic phosphatase domains. This structure reflects the possibility that these proteins may indeed act as transducers of signals from the outside to

the inside of the cell, and perhaps the other way around as well. Despite strong effort only few RPTP ligands have been identified so far and many remain still orphan candidate receptors.
A complicating factor may be the structural variety of extracellular arrangements found in RPTPs: mephrin/A5/RPTPμ (MAM), Ig-like, fibronectin type III- like, carbonic-anhydrase-like and cystein-rich regions, assembled in various order and often subject to alternative splicing and post-translational modifications such as N- or O-linked glycosylation (Tabernero et al. 2008). RPTPδ, an R2A-type RPTP, and RPTPμ, RPTPκ and RPTPλ, all belonging to the R2B type RPTPs, present homophilic interactions that are important in cell adhesion processes (Brady-Kalnay et al. 1993; Sap et al. 1994; Cheng et al. 1997; Gonzalez-Brito and Bixby 2006).
The R2A group displays 3 Ig-like and 8 fibronectin type III-like domains; the R2B group has a MAM domain followed by a single Ig-like domain and only 3 fibronectin type III-like domains. An interesting case is given by RPTPμ, where the trans-dimeric structure has been solved (Aricescu et al. 2007) and appeared to be maintained through interactions between the MAM and Ig domains of one molecule on a cell and the FN1 and FN2 domains of another RPTPμ molecule on the juxtaposed cell. Those features, together with the length of the dimeric structure and the change in intracellular space arising from expression of different RPTPμ mutants, has suggested the involvement of this protein in regulating intercellular spacing in adherens junctions (Aricescu et al. 2007). The R2A members RPTPσ and LAR have both multiple binding partners. RPTPσ binds nucleolin, alpha latroxin, contactin and the heparan-sulphate proteoglycans agrin and collagen XVIII in the nervous system and skeletal muscle (Aricescu et al. 2002; Krasnoperov et al. 2002; Alete et al. 2006; Bouyain and Watkins 2010). Recently, RPTPσ was found to be a receptor for chondroitin-sulphate produced by astroglia and it was suggested to have a role in the inhibition of neuronal regeneration. In fact, RPTPσ disruption was shown to enhance the ability of axons to penetrate regions containing CS-PGs after spinal cord injury (Shen et al. 2009). Furthermore, HS-PGs induce RPTPσ oligomerization on dorsal root ganglia neurons, while CS-PGs are unable to do that and conversely inhibit the HS-PG-mediated effect (Coles et al. 2011). Interactions of R2A type RPTPs have been carefully studied in *Drosophila* where a homologue mediates the development of the neuromuscular junction. Two heparan-sulphate proteoglycans, syndecan and dallylike, bind *Drosophila* LAR at the neuromuscular junction and have respectively a positive and a negative effect on the development of the synapse. In this case a direct effect of the ligand could be demonstrated: dallylike binding to LAR correlates with increased phosphorylation of the LAR substrate Enabled, pointing to dallylike-dependent negative regulation of LAR (Fox and Zinn 2005; Johnson et al. 2006). Additionally, a minor splice form of human LAR binds the laminin-nidogen complex, a major component of the ECM that modulates neurite outgrowth, proliferation and differentiation (O'Grady et al. 1998). DEP-1, an R3-type RPTP was found to be positively regulated by Matrigel^{TM} suggesting the presence of agonist(s) binding to the extracellular domain of this RPTP (Sorby et al. 2001). PTPζ belongs to the R5 group (Figure 1.5) and presents a carbonic anhydrase domain followed by a single fibronectin type III-like domain. It can bind pleiothropin (Pariser et al. 2005b), tenascin (Barnea et al. 1994), contactin (Peles et al. 1995) and TAG-1/axonin (Milev et al. 1996).

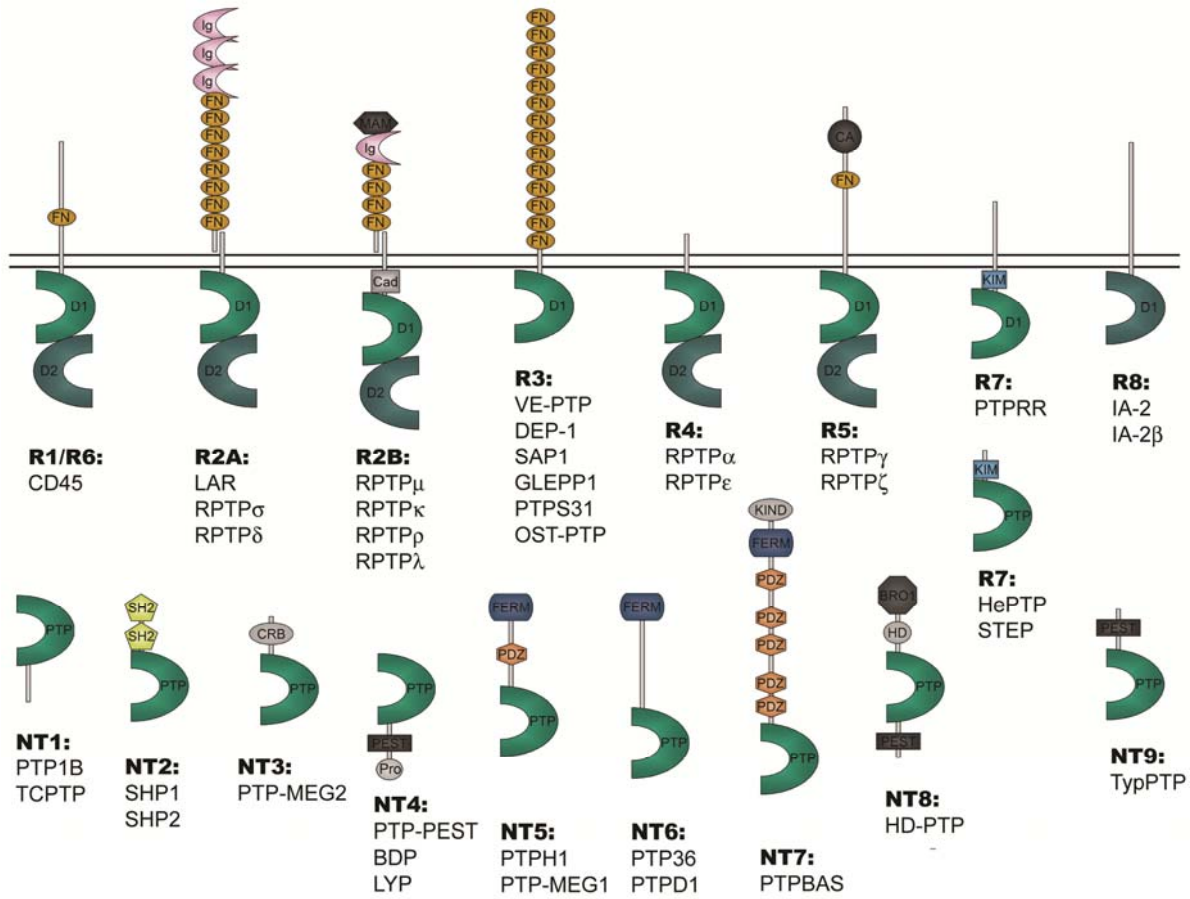

Figure 1.5. Structure of classical PTPs.
Schematic representation of the classical PTP subfamilies grouped as either receptor-like PTPs (R) or non-transmembrane (NT) PTPs. A single protein isoform per subfamily is presented. A single gene may encode other protein isoforms which possess different domain organization due to alternative splicing. Various functional domains are represented: BRO-1, BRO-1 homology; CAH, carbonic anhydrase-like; Cad, cadherin-like juxtamembrane sequence; CRB, cellular retinaldehyde-binding protein-like; FERM, FERM (4.1/ezrin/radixin/moesin) domain; FN, fibronectin type III-like domain; Gly, glycosylated; HD, histidine domain; Ig, immunoglobulin domain; KIM, kinase-interacting motif; KIND, kinase N-lobe-like domain; MAM, mephrin/A5/μ domain; PEST, PEST sequence; Pro, proline-rich; RGDS, RGDS-adhesion recognition motif; SEC14, SEC14/cellular retinaldehyde-binding protein-like; SH2, Src homology 2. Reprinted with permission from (Hendriks et al. 2008).

Among these, only pleiothropin could be demonstrated to have an effect: it inhibits RPTPζ activity, as judged by the increased phosphorylation levels of several RPTPζ substrates, such as β-catenin, β-adducin, p190Rho-GAP and ALK (Meng et al. 2000; Pariser et al. 2005a; Tamura et al. 2006; Perez-Pinera et al. 2007).

Ligand binding itself can thus affect PTP activity and it is tempting to hypothesize that this way of regulation is coupled to RPTP dimerization. Several functional studies have shown that RPTPs are regulated by dimerization (Bilwes et al. 1996; Jiang and Hunter 1999; Nam et al. 2005) and increasing evidences indicate that they can dimerize also in living cells. CD45 (Takeda et al. 1992; Xu and Weiss 2002), RPTPα (Tertoolen et al. 2001; Blanchetot et al. 2002b), SAP-1 (Walchli et al. 2005), RPTPσ (Lee et al. 2007) and RPTPε (Toledano-Katchalski et al. 2003) were encountered as dimers either in chemical cross-linking

experiments or upon co-immunoprecipitation. Dimerization may be driven by the transmembrane domain of RPTPs (Chin et al. 2005) but also the PTP domains are involved (Jiang et al. 2000; Barr et al. 2009). Importantly, for RPTPσ only dimeric ectodomains displayed ligand binding properties, the specificity of which appeared to be regulated by alternative use of extracellular domain components (Lee et al. 2007). Furthermore, post-translational modification, such as H_2O_2 treatment, of the membrane distal PTP domain in RPTPα (RPTPα-D2) generates an inactive dimer (Blanchetot et al. 2002a) and induces a change in rotational coupling in RPTPα that alters the conformation of the extracellular region (van der Wijk et al. 2003). This finding has pushed forward the hypothesis that also intracellular changes in the RPTP drive conformational modifications in the extracellular quaternary structure that in turn alter ligand-binding properties (den Hertog et al. 2008). Therefore, RPTPs could have both outside-in signalling (by ligand-binding influencing catalytic activity intracellularly) and inside-out signalling (by intracellular modifications altering the ligand repertoire).

1.3.2 Protein tyrosine phosphatase substrate-trapping mutants

A typical feature of PTPs is that specific modifications of residues within the catalytic domain confer to the phosphatase an ability to bind and trap its protein substrates (Blanchetot et al. 2005). In the wild type PTP the unprotonated cysteine acts as a nucleophile, by attacking the phosphorous centre of the phosphotyrosine-containing substrate, thereby creating a phosphoryl-cysteine intermediate. Subsequently, the critical aspartate residue of the WPD loop protonates the phenolic oxygen leaving group of the substrate and the final step is the release of the dephosphorylated substrate followed by the release of free phosphate. The replacement of the catalytic site cysteine with serine (a so-called C/S mutant) eliminates the phosphatase activity but still allows the binding of the substrate. This leads to the formation of a stable enzyme-substrate intermediate without release of substrate and free phosphate. Alternatively, mutating the aspartate of the WPD loop into alanine (D/A) has also led to a substrate-trapping mutant but by a different mechanism. In this case, the WPD/A mutant loop still flips over the bound substrate but due to the absence of the protonating activity of the Asp residue it does not allow its release: therefore the D/A mutant is almost catalytically inactive. Some achievements have been obtained also by altering the highly conserved active site Gln (that stabilizes the water molecule together with the WPD Asp) into alanine (Q/A), and by C/D substrate-trapping mutants even though these are still slightly active. In some cases even the combined C/S and D/A mutations have been exploited (Blanchetot et al. 2005).

1.3.3 Approaches to the identification of substrates and ligands for protein tyrosine phosphatases

Protein tyrosine phosphorylation, controlled by the activities of both PTKs and PTPs, plays critical roles in a wide variety of cellular events. However, in contrast to the PTKs, our understanding of the biological functions of PTPs has been limited to date. This is mainly due to difficulties in identifying the substrate and ligand molecules of individual PTPs. The

following will show a brief overview of the various approaches that have been taken thus far and highlight the PTP-specific difficulties that have been encountered.

Substrates. Using a combination of biochemical and genetic approaches quite some functional information has been gathered for specific PTP enzymes. Two reviews (Blanchetot et al. 2005; Tiganis and Bennett 2007) comprehensively describe the techniques used in order to identify candidate PTP substrates and to validate them. All of these techniques rely on the ability of the previously mentioned C/S, D/A, C/S-D/A or D/A-Q/A substrate-trapping PTP mutants to interact stably with their cognate substrate. A good substrate-trapping mutant is expected i) to be inactive or barely active (low K_{cat}); ii) to bind efficiently to its physiological substrate (low K_M); and thus iii) to faithfully mimic the wildtype enzyme's structural integrity. The three main approaches used in the identification of PTP substrates by virtue of such mutants have been: a) the application of D/A substrate-trapping mutants as baits in modified yeast two hybrid screens that have the cDNA library products (the preys) being phosphorylated by constitutively active PTKs (Kawachi et al. 2001; Fukada and Noda 2007); b) the detection of co-immunoprecipitated proteins by western blot after co-expression of the candidate substrate with one of the substrate-trapping mutants for the PTP under study (Xie et al. 2002; Kontaridis et al. 2004); c) the combination of substrate-trapping techniques with mass spectrometry analysis after pull-down or co-immunoprecipitation (Kolli et al. 2004). Recently also the screening of phospho-peptide arrays, exploiting either the dephosphorylation of phospho-peptides by the active enzyme or the phosphopeptide binding to substrate-trapping variants, has been used as an approach to denominate putative PTP substrates (Köhn et al. 2007; Barr et al. 2009; Sacco et al. 2009; Sun et al. 2009). Subsequent validation of the putative substrates is a much more complex effort. Figure 1.6 summarizes the three criteria that need to be fulfilled in order to consider a putative substrate as *bona fide* (Tiganis and Bennett 2007).

The first criterion is a stable interaction of the substrate-trapping mutant with the substrate. This needs to be demonstrated *in vitro* (using the purified substrate-trapping PTP and the tyrosine-phosphorylated substrate) and *in vivo* (after co-expression of the substrate and the PTP trapping mutant in a relevant cell system). To validate that the substrate indeed binds to the catalytic site of the substrate-trapping mutant one may use vanadate as competitor. Vanadate (VO_4^{3-}) is reported to be a competitive inhibitor of PTPs; it binds tightly to the essential cysteine residue in the catalytic pocket of the PTP. Consequently, C/S substrate-trapping mutants are less affected by vanadate than D/A mutants (Blanchetot et al. 2005). For example, 10 mM vanadate was necessary to compete for binding between PTP-PEST-C/S and p130Cas, whereas 1 mM vanadate was already a very good competitor in other cases (Garton et al. 1996).

The second criterion is the demonstration that endogenous tyrosine-phosphorylation levels of the putative substrate are modulated upon alterations in the activity of the PTP under study. This can be achieved by over-expressing the PTP protein in a cell system that also contains the candidate substrate. High levels of the wild type PTP should correlate with low phosphotyrosine levels of the substrate, whereas overexpression of the PTP substrate-trapping mutant should protect the substrate from being dephosphorylated by endogenous PTPs. However, depending upon how the PTP is regulated and on the binding strength of the

substrate-trapping mutant, clear differences in phosphorylation levels might not be easily obtained. In parallel, the type of over-expression approaches discussed here should ideally be complemented by loss-of-function approaches to ensure that any result attained is not an off-target artifact of PTP over-expression.

The third criterion was designed to unequivocally demonstrate that the interaction of enzyme and substrate is direct, and not via other enzymes; *in vitro* dephosphorylation of the substrate by purified wild type PTP should be observed. This is, however, easier said than done. Often only the catalytic phosphatase domain of a specific PTP is used to show dephosphorylation *in vitro* but it is now well established that the additional N- and C-terminal domains are in fact very important in determining the specificity of the PTP under study. This may lead to an overestimation of the number of different substrates that can be dephosphorylated by a given PTP. In addition, a given PTP may well be selective for just one or a few specific phosphotyrosine residues within a multi-phosphorylated substrate protein, which may lead to false-negative results when the total phosphotyrosine content of the substrate is used as read-out (Tiganis and Bennett 2007). Due to the above considerations, in retrospect probably quite a number of established substrates would not satisfy all these criteria. Nevertheless, those three criteria provide highly valuable guidelines when potential PTP substrates have to be put to the test.

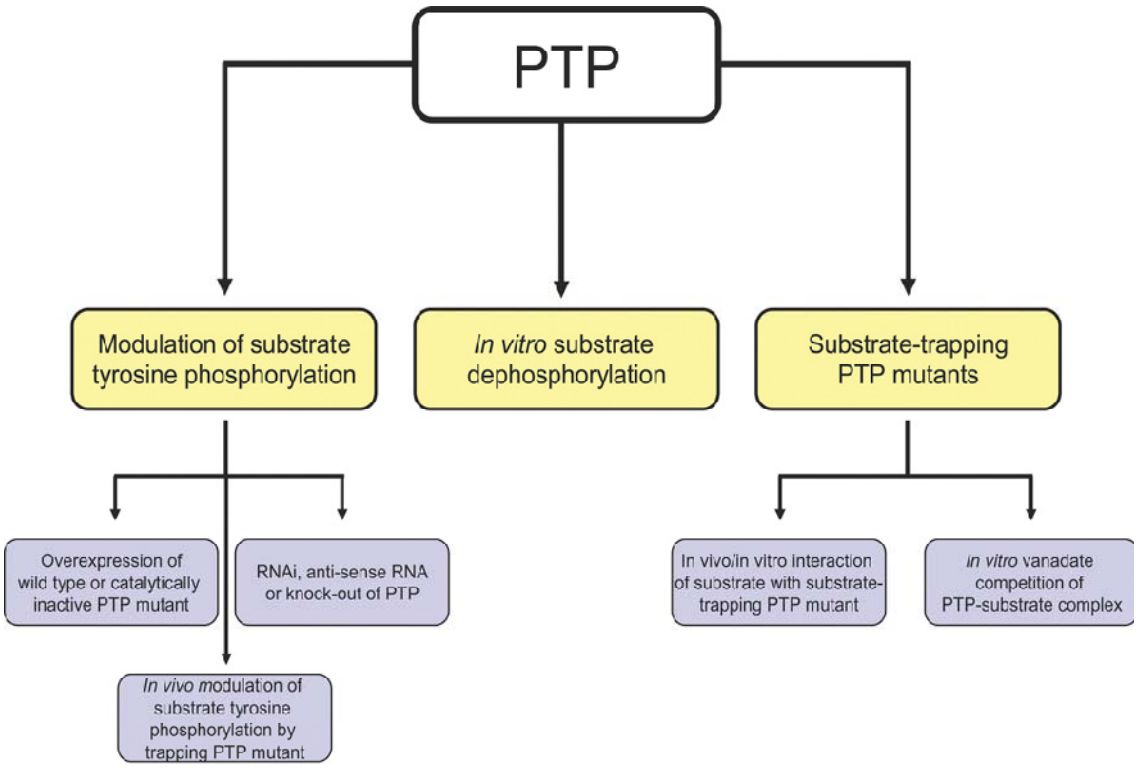

Figure 1.6. Characterization of PTP substrates.

The three proposed criteria for the assignment of a tyrosine-phosphorylated protein as a PTP substrate. To define a tyrosine-phosphorylated protein as a *bona fide* PTP substrate, one should (i) show interaction of the substrate with the PTP substrate-trapping mutant, (ii) observe PTP-dependent modulation of the substrate tyrosine-phosphorylation levels in a cellular context, and (iii) observe dephosphorylation of the substrate *in vitro*. A combination of overexpression of the wild type PTP and substrate-trapping PTP mutant along with underexpression approaches (e.g. RNAi, antisense and knockout cells) can be employed to assess whether a candidate protein is a PTP substrate. Reprinted with permission from (Tiganis and Bennett 2007).

Ligands. As mentioned previously, despite strong efforts over the last 20 years, only few ligands have been identified for RPTPs. Several methods have been set up for this purpose and the most important ones will be briefly discussed here. Flanagan and Leder developed a so-called Receptor Alkaline Phosphatase *in situ* (RAP *in situ* – see Figure 1.7) assay (Flanagan and Leder 1990). This technique depends on the ability of isolated ectodomains from transmembrane proteins to still bind their cognate ligands. To enable detection the ectodomains are fused to a reporter enzyme, in this case placental alkaline phosphatase (PLAP). Binding of such fusion protein probes to either tissue sections or live cultured cells that display the respective ligands can then be monitored by virtue of a standard histochemical procedure. The PLAP is heat stable and therefore its activity can be differentiated from that of endogenous alkaline phosphatases; furthermore the enzymatic reaction is a direct indicator of binding and there is no need of secondary immunodetection. This technique has been successfully applied in the identification of ligands for RPTPσ (Aricescu et al. 2002; Sajnani-Perez et al. 2003; Alete et al. 2006; Shen et al. 2009) and RPTPζ/β (Peles et al. 1995), and for the detection of putative ligands for PTP-NP (Chiang and Flanagan 1996).

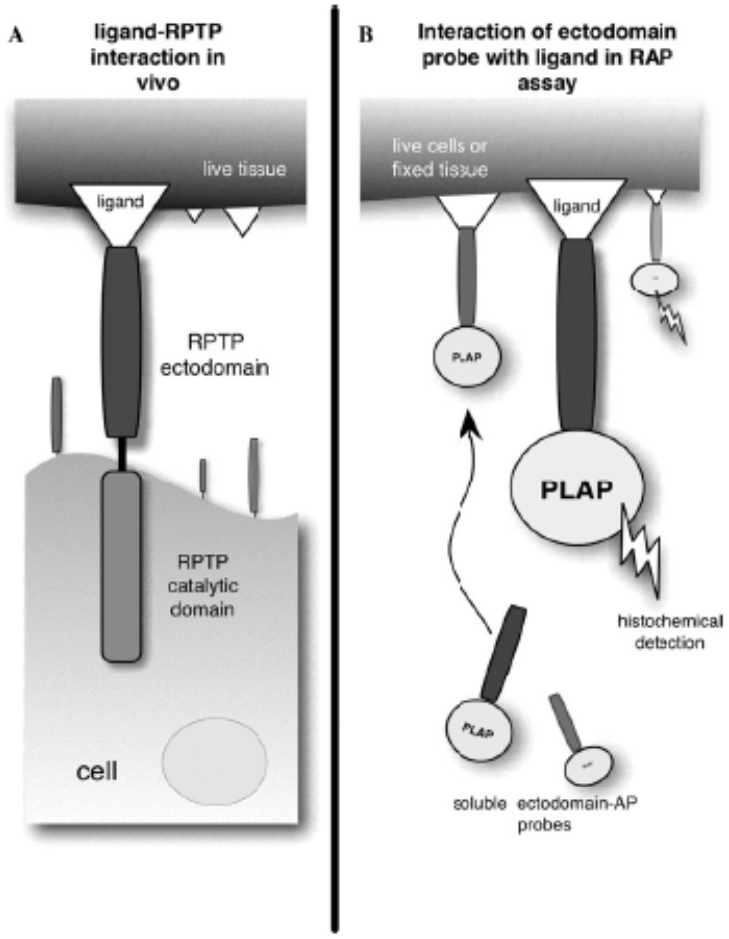

Figure 1.7. Schematic diagram showing the basis for the RAP in situ assay. Panel A shows the native interaction of an RPTP in one cell, with a ligand on another cell or tissue. Panel B shows the ectodomain of the RPTP fused to PLAP as a soluble fusion protein, and this fusion protein binding in vitro to the ligand in live or fixed cells, or the extracellular matrix. Upon addition of the substrate for the PLAP enzyme the location of binding is visualized. Reprinted with permission from (Stoker 2005).

Alternatively, other fusion protein probes can be created by tagging the ectodomain either with Horseradish peroxidase (HRP) domains or Fc immunoglobulin tails. However, these techniques all share the same limitation: they can only indicate the presence or location of

binding sites but do not yield any direct knowledge on the identity of the ligands involved. The main ways leading to the identification of ligands have been the use of affinity purification methods. Affinity chromatography makes use of large amounts of ectodomain protein crosslinked to a column where then tissue or cell lysate can be passed through. The bound ligands are then eluted by standard methods and submitted to, for example, mass spectrometric analysis. In the last years also biosensors have emerged. In this case, the receptor is immobilized on a sensor chip and test solution such as tissue lysates are passed over the chip and Surface Plasmon Resonance is measured to reveal which test solution contained the ligand. In the end, small amounts of ligands are then eluted from the chip and directly subjected to mass spectrometry for further identification (Stoker 2005).

1.3.4 Orthovanadate and Pervanadate as enhancers of tyrosine phosphorylation

As mentioned previously, vanadate is applied as a competitor in the identification of PTP substrates. The methodology for vanadate competition has been described by Blanchetot et al. (2005) and they refer to important pioneering studies by Gregory Huyer and colleagues (Huyer et al. 1997).

Vanadate is a phosphate analog, since it adopts a structure similar to inorganic phosphate (Gresser and Tracey 1990). The X-ray crystal structure of *Yersinia* PTP complexed with vanadate shows that the vanadium molecule occupies the active site within covalent bonding distance of the thiol of the catalytic site cysteine (Denu et al. 1996). Vanadate is chelated by many organic molecules. In particular, addition of EDTA in excess over vanadate reverses immediately and completely the inhibition of PTP1B by the latter in a PTP assay. The fact that EDTA and vanadate are often included together in cell lysis buffers (Huyer et al. 1997) thus implies that depending on the ratio endogenous PTPs may not be completely inhibited. This can have important consequences on the levels of substrate phosphorylation but also suggests a way to circumvent inhibitory effects of vanadate once phosphorylated substrates need to be subjected to PTP activity in *in vitro* assays.

Other studies have focused on another strong inhibitor of PTPs: pervanadate. This term refers to a variety of complexes formed when vanadate is treated with hydrogen peroxide. These complexes appear to be more effective than vanadate in increasing the level of cellular tyrosine phosphorylation. More importantly, pervanadate compounds are irreversible inhibitors of PTPs, and it has been speculated that the mechanism of inhibition may be the oxidation of the catalytic site cysteine (Shaver et al. 1993). Mixing PTP1B with pervanadate completely inactivates the enzyme and generates a cysteine residue with an extra mass that corresponds to the sulfonic acid oxidation state (Huyer et al. 1997). Dithiothreitol (DTT) can reduce pervanadate to vanadate providing a useful way to block any action of excess pervanadate after PTP inhibition has been completed. Consequently, if PTP1B is added to a DTT-containing reaction mix supplemented with either vanadate or pervanadate, its activity can be recovered by the addition of EDTA. When vanadate or pervanadate was added lastly to the reaction mix containing the enzyme, a totally different behavior was observed. Activity can still be completely recovered upon addition of vanadate to the mix, but only a partial recovery is possible in the pervanadate-treated one. This is likely due to the fact that the conversion of pervanadate to vanadate by DTT is not fast enough, allowing for at least some

irreversible inhibition of PTP1B by pervanadate-dependent oxidation (Huyer et al. 1997). Figure 1.8 shows the proposed mechanism of conversion and removal of (per)vanadate compounds (Huyer et al. 1997). Clearly, these properties of (per)vanadate inhibition and conversion must be taken into account when using these compounds to identify and validate putative PTP substrates with the *in vitro* and *in vivo* methods described above.

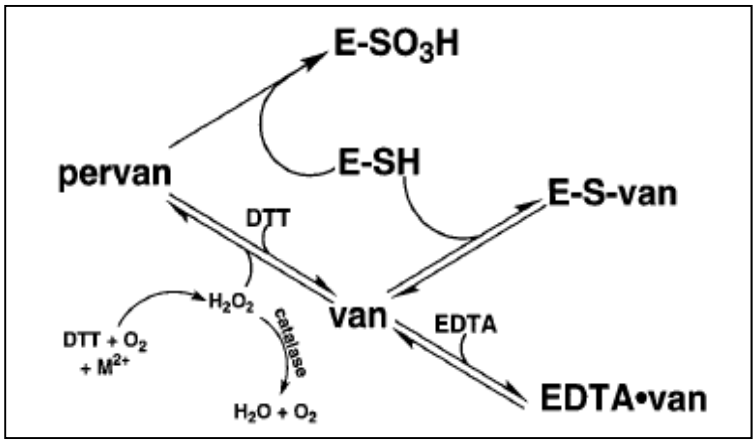

Figure 1.8. **Scheme of (per)vanadate conversion and removal**. Pervanadate (pervan) oxidizes the catalytic cysteine of PTPs (E-SH) to the irreversible sulfonic state (E-SO_3H) but can be reduced to vanadate (van) by excess of DTT. Vanadate occupies the catalytic site of PTPs reversibly (E-S-van) and in presence of EDTA vanadate generates the stable complex EDTA·vanadate. H_2O_2 converts vanadate to pervanadate but can be removed by the enzyme catalase. In addition, DTT can be oxidized in presence of divalent metallic ions generating new H_2O_2. Reprinted with permission from (Huyer et al. 1997).

1.3.5 The PTPRR-subfamily of Protein Tyrosine Phosphatases and their biological functions

The MAPK cascade is a major signalling pathway that is tightly controlled. Some protein tyrosine phosphatases contain a kinase interaction motif (KIM) that mediates selective binding to the MAPK common docking domain (Tanoue and Nishida 2003), ensuring inactivation of the MAPK and - depending on the location of the phosphatase involved - its retention in the cytosol. Three human genes encode KIM containing tyrosine-specific phosphatases and all prove to be MAPK regulators; *PTPN5*, *PTPN7* and *PTPRR*. Gene *PTPRR* orthologues are present in many vertebrates. The mouse gene *Ptprr* encodes four different isoforms (i.e., PTPBR7, PTP-SL, PTPPBSγ-42, and PTPPBSγ-37; (Chirivi et al. 2004)) by the differential use of three distinct transcription start sites (Figure 1.9) (van den Maagdenberg et al. 1999; Chirivi et al. 2004). Alternative inclusion of a 117-nucleotide sequence stretch in the unique 5′ UTR of the shortest mRNA further adds to the complexity (Augustine et al. 2000), but it is the presence of two alternative AUG start codons in these short transcripts that explains why they encode both PTPPBSγ-42 and PTPPBSγ-37. Only the transcripts for the PTPBR7 isoforms are expressed during prenatal development, principally in spinal ganglia and PC precursors (van den Maagdenberg et al. 1999). After birth, in the PCs the PTP-SL mRNAs gradually replace those of PTPTBR7, while the latter remain

expressed throughout all the other brain regions (Augustine et al. 2000). Trace amounts of PTPPBSγ transcripts are present in brain during postnatal development and only these isoforms have also been detected in the gastrointestinal tract and in developing cartilage. PTPBR7 is a type I receptor-like protein located on the membrane of endocytic particles and on the plasmamembrane. PTP-SL is also a transmembrane protein but its location is restricted to endocytic vesicles. It lacks a signal peptide and is therefore classified as a type III transmembrane protein. PTPPBSγ-42 and PTPPBSγ-37 isoforms reside in the cytosol. The four isoforms are identical in the C-terminal part that contains the KIM and the PTP domain. They all have a short half-life, of 3 to 5 hours, and are constitutively phosphorylated, at a Serine residue located in the KIM domain or at a Threonine residue located between the KIM and the PTP domain (Dilaver et al. 2007). The two transmembrane isoforms can homo- and hetero-multimerize thanks to the transmembrane and/or the upstream hydrophobic domain and multimers exhibit decreased phosphatase activity *in vitro* (Noordman et al. 2008). This suggests the possibility that activity of transmembrane PTPRR can be regulated by binding of ligand molecules (Hendriks et al. 2009). The two smallest isoforms, PTPPBSγ-42 and PTPPBSγ-37 do not multimerize (Noordman et al. 2008).

MAPKs are activated by dual phosphorylation on specific Thr and Tyr residues. Inactivation of MAPKs thus can be achieved by phosphatases that are either serine/threonine-specific (PP phosphatases), tyrosine-specific (classical PTPs), or display dual-specificity (DSPs). When PTPRR tyrosine phosphatases bind MAPKs (preferentially ERK1/2/5 and p38) they are first phosphorylated on a threonine residue just between the KIM and the PTP domain by the MAPK. Subsequently they dephosphorylate an essential tyrosine residue of the kinase, thereby inactivating it. Protein kinase A is able to prevent this PTP-MAPK interaction by phosphorylating a serine residue within the KIM domain. By doing so, the MAPK will not be bound and inactivated by the KIM-phosphorylated PTP, can enter the nucleus and phosphorylate its specific substrates (Blanco-Aparicio et al. 1999; Ogata et al. 1999). The above effects were observed in HEK293 and COS-7 cells over-expressing cytosolic PTPRR isoforms. Analysis of PTPRR impact on MAPK phosphorylation and activity in rat PC12 cells, however, revealed that PTPRR isoforms are dispensable for ERK1/2 activity regulation in these cells (Noordman et al. 2006). These observations suggest that cell type-specific factors may modulate PTPRR activity, finally determining their influence on cognate substrates.

It has been proposed that PTPRR proteins serve two possible functions, relating to their MAPK dephosphorylation activity and their transmembrane/vesicle localization pattern, respectively (Hendriks et al. 2009). PTPRR proteins may be implicated in accurate packaging of cargo and vesicle formation, processes that need tight regulation and where tyrosine phosphorylation is one of the mechanisms to do so (Korolchuk and Banting 2003). In fact, in the yeast two-hybrid system it has been observed that PTPRR binds the subunit adaptin β4 of the adaptor complex AP-4 and in neuronal cells PTPRR co-localized with AP-4 at the Golgi apparatus and on endosomes (Dilaver et al. 2003). Adaptor proteins are heterotetrameric complexes involved in the formation of clathrin-coated vesicles in different transport pathways and in the selection of cargo for incorporation into the vesicles. AP-2 mediates rapid endocytosis from the plasma membrane, while AP-1, AP-3, and AP-4 mediate sorting events at the *trans*-Golgi network (TGN) and/or endosomes (Boehm and Bonifacino 2001).

The phosphorylation status of clathrin coat components has been found to influence exocytosis/endocytosis dynamics (Wilde et al. 1999; Lauritsen et al. 2000) suggesting the possibility that also tyrosine phosphorylation would influence vesicle transport (Dilaver et al. 2003).

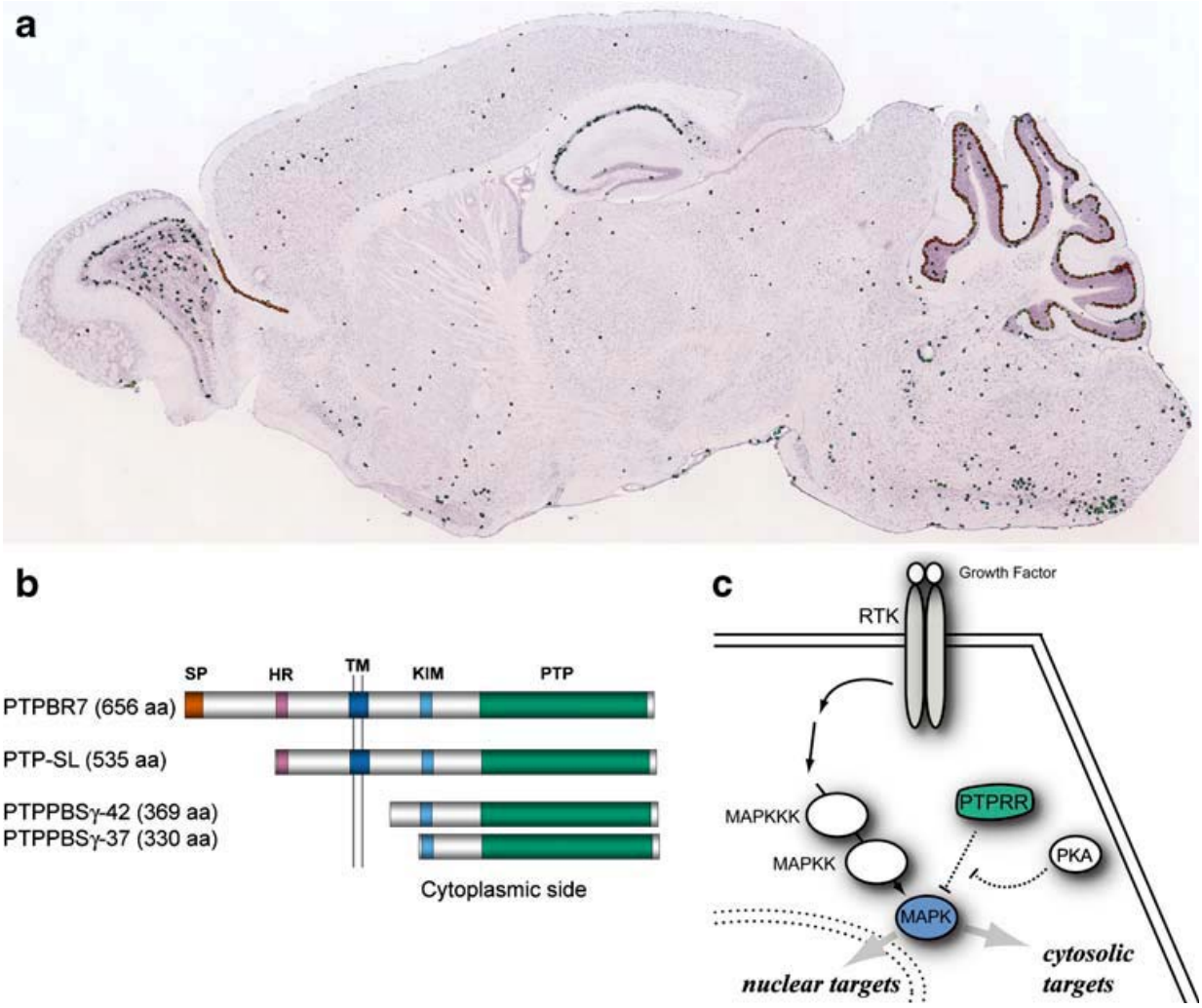

Figure 1.9. *Ptprr* expression patterns in mouse brain, schematic depiction of PTPRR isoforms and their interaction with MAP kinases. (A) PTPRR mRNA expression levels are highest in Purkinje cells of the cerebellum and in specific regions of the hippocampus and the olfactory bulb. (B) The four PTPRR protein isoforms expressed in mouse, with protein names, length and domain indication. SP, signal peptide; HR, hydrophobic region; TM, transmembrane region; KIM, kinase interacting motif; PTP, protein tyrosine phosphatase domain. (C) Example of phosphotyrosine signalling induced by RTK. PTPRR dephosphorylates activated MAPK, an action that can be blocked by PKA. RTK, receptor tyrosine kinase; MAPKKK, MAPKK kinase; MAPKK, MAPK kinase; MAPK, mitogen-activated protein kinase. Reprinted with permission from (Hendriks et al. 2009).

Additionally, a PTPRR control of signalling events via protein scaffolding could be envisaged. For example, the protein Sef is known to anchor activated MEK-ERK complexes in the cytosol, preventing ERK's nuclear activity but not its cytoplasmic effects (Torii et al. 2004). PTPRR may play a similar role by f.i. abrogating vesicle-associated ERK activity.

More conclusive data have come from mice where gene *Ptprr* has been inactivated. Cerebrum and cerebellum tissue lysates displayed a higher level of ERK1/2 phosphorylation when compared to the wild type mice. When brain sections were tested by immunostaining, higher phospho-ERK1/2 levels were observed in the axon hillock of Purkinje cells in the cerebellum of *Ptprr*$^{-/-}$ mice while other brain regions were unchanged. Behavioural and locomotive tests have subsequently shown that nocturnal activity, motor coordination and balance skills are significantly reduced in *Ptprr*$^{-/-}$ mice when compared to wild type animals (Chirivi et al. 2007). This appeared indicative of mild ataxia, but whereas in ataxia patients and mouse models considerable neuronal degeneration is encountered (Pietrobon 2005) the *Ptprr* knock-out animals displayed normal brain morphology (Chirivi et al. 2007).

This combination of locomotive deficiencies without apparent brain morphological abnormalities represents a phenotype that is found in just a few other engineered or spontaneous mutant mice, all having in common that in some way calcium ion homeostasis in the cerebellum is disturbed: junctophilin 3 (Nishi et al. 2002), carbonic anhydrase-related protein VIII (Car8) (Jiao et al. 2005), calbindin (Farre-Castany et al. 2007), and calretinin (Cheron et al. 2004) knockout mice. Junctophilins contribute to the formation of junctional membrane complexes by spanning the endoplasmic/sarcoplasmic reticulum membrane and interacting with the plasma membrane. Car8 is a binding protein for the IP3 receptor expressed in cerebellar Purkinje neurons and it is thought to play a role in fine-tuning of the intracellular calcium level in the dendrites of Purkinje neurons (Turkmen et al. 2009). Calretinin belongs to the large family of EF-hand calcium-binding proteins that apparently confer a general protection against the pathogenic mechanisms of neuron disease. Single or combined inactivation of the genes encoding calretinin and calbindin results in the occurrence of spontaneous 160 Hz local field potential oscillations in the cerebellar cortex of alert mice. Purkinje cells, being the sole output from the cerebellar cortex, occupy an integrative position in the cerebellar network and modifications of Ca^{2+} homeostasis in specific neuron types can alter the dynamics of the global network (Cheron et al. 2004).

As stated previously, mice lacking *Ptprr* show increased ERK1/2 phosphorylation in Purkinje cells (Chirivi et al. 2007). MAPK signalling is a central process in synaptic plasticity (Sweatt 2004; Thomas and Huganir 2004; Marambaud et al. 2009) and chronic activation of ERK has been linked to neurodegeneration (Colucci-D'Amato et al. 2003; Chu et al. 2004). These observations suggest the possibility that altered phosphorylation of ion channels and receptors would hamper their correct functioning, as was proposed for Spinocerebellar ataxia SCA12 (Paulson 2009) and SCA14 (Verbeek et al. 2005; Perlman 2011). In this perspective, the striatal-enriched protein tyrosine phosphatase STEP, a protein homologous to PTPRR, was found to have an important role in neuronal degeneration in Alzheimer's disease (AD) via its substrates ERK1/2, p38 and Fyn (Baum et al. 2010).

It is conceivable that alterations in MAPK activity have an effect on the Ca^{2+} homeostasis in neurons, and notably in PCs this may implicate PTPRR proteins in the fine-tuning of Ca^{2+} levels by either directly or indirectly controlling phosphorylation levels of specific Ca^{2+} signalling-related proteins (Hendriks et al. 2009).

1.3.6 SCA genes and ataxic phenotypes in humans

Interestingly, aberrant Ca^{2+} signalling has been linked to ataxia also in human disorders. Nearly 30 distinct genetic causes of Spinocerebellar ataxia (SCA) are known. They all display cerebellar alterantions and many display disabling noncerebellar features, most commonly brainstem dysfunction. The hallmark symptom in humans is slowly progressive, symmetrical, midline, and appendicular ataxia. Some may also have associated hyperkinetic movements i.e. chorea, dystonia, myoclonus, postural/action tremor, restless legs, rubral tremor and tics (Perlman 2011). Other inherited ataxias are dentatorubropallidoluysian atrophy (DRPLA) and episodic ataxias type 1 and 2 (EA1 and EA2). Most of the human forms of ataxia are caused by DNA repeat expansions occurring inside or outside the protein-coding region of the respective disease genes. Expansion of the coding CAG repeats generate polyglutamine (polyQ) stretches that cause the protein to become toxic for the brain tissue. In the case of expansions in the non-coding region, the toxicity or stress induction is mediated at the RNA level but in both cases the mechanisms involved are not fully understood (Paulson 2009). Although the disease-causing mutations have been identified for a number of these disorders, the normal functions of the proteins involved remain in many cases unknown.
Other alterations in the ataxia disease genes are not due to repeat expansions but instead to conventional mutations in specific genes or genomic segments. In SCA6 a polyQ repeat occurs in the gene *CACNA1* encoding the voltage-dependent calcium channel alpha 1A subunit. Non-repeat mutations in the same gene cause EA2 (Kordasiewicz and Gomez 2007). In several cases mutations that affect calcium and potassium voltage-gated channels (channelopathies) have been found and may be directly linked to alterations in ion homeostasis in cerebellar neurons (Paulson 2009). SCA13, for example, is caused by a mutation in gene *KCNC3* which encodes a voltage-gated potassium channel (Kv3.3). SCA27 is caused by a mutation in the gene encoding the Fibroblas Growth Factor (Fgf) 14 and *Fgf14*$^{-/-}$ mice developed ataxia, had reduced amount of Nav1.6 channels and attenuated Purkinje cells firing (Shakkottai et al. 2009). Mutations in human *SCN8A*, which encodes Nav1.6, are associated with cerebellar atrophy and ataxia (Trudeau et al. 2006). In line with this, mice in which *Scn8a* has been disrupted or that lack Nav1.6 specifically in Purkinje cells display cerebellar ataxia and impaired Purkinje cell firing (Kohrman et al. 1996; Raman et al. 1997; Levin et al. 2006). Some SCA mutations apparently alter the phosphorylation status of neuronal Ca^{2+} channels and receptors and change their membrane localization, activity, and hence functioning in synaptic connectivity and plasticity (Nakanishi 2005). SCA12 and SCA14 are caused by mutations in genes encoding the phosphatase PP2A regulatory subunit PR55/Bb (Holmes et al. 2001) and the kinase PKCγ (Yabe et al. 2003), respectively, and this may well lead to aberrant phosphorylation levels and dysfunctioning of cerebellum calcium channels and receptors. SCA14 mutations results in a PKCγ superkinase that hyper-phosphorylates brain glutamate receptors (Verbeek et al. 2005).The identification of mutations in β-III spectrin in SCA5 patients has lead to another ataxia disease gene, *SPTBN2* (Ikeda et al. 2006). In the brain β-III spectrin binds directly to the excitatory amino acid transporter (EAAT4), the glutamate receptor delta (GluRδ), and various other proteins. Mice lacking intact β-III spectrin develop normally but when they reach six months of age they display a mild nonprogressive ataxia. By one year their cerebellum displays increased dark

Purkinje cells, a thin molecular layer, fewer synapses, a loss of dendritic spines, and a 2-fold expansion of the PC dendrite diameter (Stankewich et al. 2010). Mutations in this cytoskeletal protein have directed attention toward the possible pathogenic role of organelle stability/trafficking and altered membrane protein dynamics in neurons. The fact that partial loss of β-III spectrin causes cerebellar degeneration suggests that mechanical and membrane-dynamical properties of cerebellar neurons may be as important as altered Ca^{2+} homeostasis, transcriptional dysregulation, and impaired protein degradation in causing neurodegeneration (Paulson 2009).

1.3.7 Pathways of neuronal degeneration

Ptprr-deficient mice display mild ataxia in connection with no obvious brain morphological changes, two conditions encountered in junctophilin 3-, Car8-, calbindin- and calretinin-deficient mice that have been linked to ion dyshomeostasis (Cheron et al. 2008; Hendriks et al. 2009), as explained above.

Mechanisms of neuronal degeneration involving altered ion homeostasis have been proposed. Despite the absence of neurodegeneration in *Ptprr*-deficient mice, these mechanisms are particularly interesting when considering the effects of calcium dyshomeostasis on PC firing (Cheron et al. 2008), because they may provide hints to our understanding of PTPRR-related signalling mechanisms.

In the CNS, excessive production of reactive oxygen and nitrogen species (ROS/RNS) has been invoked as a mechanism for neurodegeneration associated with various insults to neurons (Wang et al. 2010). Among all organs in the body, the brain is particularly prone to oxidative stress (OS)-induced damage because of the high oxygen demand, the abundance of redox-active metals (iron and copper), the high level of oxidizable polyunsaturated fatty acids and the fact that neurons are post-mitotic cells with relatively restricted replenishment by progenitor cells during the lifespan of an organism. The involvement of OS in brain aging and neurodegenerative conditions such as ischemia, seizures, calcium dysfunction and glutamate-mediated excitotoxicity have been extensively described (Coyle and Puttfarcken 1993; Sayre et al. 2001; Floyd and Hensley 2002; Valko et al. 2007). Cells have evolved mechanisms to cope with ROS and RNS effects, such as anti-oxidant enzymes (superoxide dismutase, catalase, glutathione peroxidase and thioredoxins) as well as non-protein antioxidants (glutathione, vitamin E, vitamin C, bilirubin and coenzyme Q10).

Vulnerability of neurons to OS varies form one brain region to another. For example, pyramidal neurons of the region CA1 of the hippocampus are extremely sensitive to OS-stress in comparison to CA3 neurons and encounter quickly cell death (Sarnowska 2002; Wang et al. 2005). Outside the hippocampus, OS-inducing agents cause extensive death of neurons in the cerebellar granule cell layer but not in the cerebral cortex. Oxygen tension in the air (around 20%) is sufficient to cause cell death in cerebellar granule neurons under *in vitro* culture conditions (Wang et al. 2009). Selective vulnerability of cerebellar granule neurons to OS might underlie the poor motor coordination and impaired motor learning associated with the ageing process (Wang et al. 2010). But what make these neurons more sensitive than others to OS? It has been proposed that high vulnerability is the result of pre-existing high OS in these neurons (Wang et al. 2010). For example, vulnerable hippocampal CA1 neurons

contain significantly higher levels of superoxide anion than the resistant CA3 neurons (Wang et al. 2005) and CA1 mitochondria release more ROS than those of CA3 neurons (Mattiasson et al. 2003). CA1 neurons express both antioxidant and ROS-producing genes at significantly higher levels than those in CA3 (Wang et al. 2005). Similarly, vulnerable cerebellar granule neurons express higher levels of genes related to OS than the resistant cortical neurons (Wang et al. 2009). The reason for an intrinsic higher OS content seems to lie in the differential requirements of these neurons for ROS and RNS as signalling molecules (Wang and Michaelis 2010).

Some neurons are found to be more responsive to ROS/RNS signaling molecules than others (Wang and Michaelis 2010). Neurons that are vulnerable to OS may have a high demand for ATP to counteract their high intrinsic OS status. These processes include synthesizing anti-oxidant molecules and repairing and degrading oxidized molecules. Limited current data support the negative effects of low ATP levels on vulnerable neurons (Wang et al. 2007; Wang et al. 2009). It is expected that the higher energy demand and low ATP levels in vulnerable neurons can lead to energy crises in case of increased stress, which can seriously affect their ability to mount effective defenses against the stress increase.

There is emerging evidence that suggests neuron-glial crosstalk may play a role as well in the vulnerability of neurons to OS (Park et al. 2001). Astrocytes and microglia contribute to maintenance of CNS homeostasis providing trophic support to neurons, clearing synapses of the released neurotransmitters, re-establishing ionic gradients near the synapse, mediating immune responses in the brain and reducing OS (Dringen et al. 2000). Because properly functioning glia are essential for neuronal health, glial dysfunction can increase the vulnerability of neurons to neurotoxic conditions such as OS.

Finally, increases in intracellular calcium concentration represent a powerful activating stimulus for many signal transduction cascades and abnormal elevations of intracellular calcium may lead to cell dysfunction and ultimately cell death (Wang and Michaelis 2010). It seems then that several mechanisms involving OS are at the basis of the selective vulnerability of certain neurons and the duality of ROS/RNS, being essential signalling molecules as well as dangerous damaging agents, is one of the causes. When this delicate balance is disrupted in vulnerable neurons they appear more prone to synaptic destruction, dendrite and axonal pathology and eventually neuronal death.

In conclusion, the picture emerges that aberrancies in cellular protein phosphorylation signalling due to PTPRR deficiency can deregulate, at the transcriptional and/or the posttranslational level, the calcium-dependent communication circuitry of cerebellar neurons (Hendriks et al. 2009). Calcium dysregulation would lead to deranged ROS/RNS production. Such events involving sensitive cerebellar neurons may cause different levels of damage, ultimately ending in neuron degeneration (Wang and Michaelis 2010). *Ptprr*$^{-/-}$ mice may suffer of mild damages in vulnerable cerebellar neurons, in particular PCs, that have not been inspected yet. Alternatively, balancing mechanisms such as uptake into the ER by the endoplasmic reticulum Ca^{2+} ATPases (SERCAs) and extrusion through the plasma membrane Ca^{2+} ATPases (PMCAs) and the Na^{+}-Ca^{2+} exchanger (NCE) described by (Hartmann and Konnerth 2005), may manage to correct the altered calcium signalling in these neurons, a hypothesis that would explain the mild ataxic behaviour and normal neural morphology of these mice.

Chapter 2

➢ Materials and Methods

"Nature is relentless and unchangeable,
and it is indifferent as to whether its hidden reasons and actions
are understandable to man or not"
Galileo Galilei

2.1. Materials

2.1.1. Chemicals

All general chemicals were purchased either from Merck BV (Darmstadt, Germany), Sigma-Aldrich (St. Louis, MO) or Invitrogen (Carlsbad, CA). Casting and blotting material was from Bio-RAD (Veenendaal, The Netherlands). More specific compounds were purchased from the sources indicated in the following table.

Compound	Company	Cat. No.
Ampicilline	Sigma-Aldrich, St. Louis, MO	A9518-5G
Chondroitinase ABC	Sigma-Aldrich, St. Louis, MO	C2905
Chondroitin Sulphate A	Sigma-Aldrich, St. Louis, MO	C9819
Chondroitin Sulphate C	Sigma-Aldrich, St. Louis, MO	C27043
Chondroitin Sulphate D	Seikagaku, Tokyo, Japan	400676-1A
Chondroitin Sulphate E	Seikagaku, Tokyo, Japan	400678-1A
Coomassie Brilliant Blue G-250	Merck, Darmstadt, Germany	115444
6,8-difluoro-4-methylumbelliferyl phosphate (DiFMUP)	Agilent Technologies, Santa Clara, CA	257001
GSH Sepharose 4B	GE Healthcare Biosciences AB, Uppsala, Sweden	17-0756-01
Hanks' balanced salt solution	Sigma-Aldrich, St. Louis, MO	H6136
Heparan Sulphate sodium salt from bovine kidney	Sigma-Aldrich, St. Louis, MO	H7640
Herculase II Fusion DNA Polymerase	Bio-Connect B.V., Huissen, the Netherlands	600675
His-Select Nickel affinity gel	Sigma-Aldrich, St. Louis, MO	P6611
Influenza hemagglutinin (HA) peptide	Sigma-Aldrich, St. Louis, MO	I2149
p-nitro-phenylphosphate (pNPP)	Eastman Kodak, Rochester, NY	11672
NBT/BCIP	Sigma-Aldrich, St. Louis, MO	72091

NucleoBond XtraMidi	Bioké, Leiden, The Netherlands	740 410.50
Phosphate Sensor	Invitrogen, Carlsbad, CA	PV4406
Protease inhibitor cocktail	Roche Diagnostics GmbH, Mannheim, Germany	11 873 580 001
Protein A Sepharose CL-4B	GE Healthcare Biosciences AB, Uppsala, Sweden	17-0780-01
QIAquick Gel Extraction Kit	QIAGEN, Venlo, The Netherlands	28706
Restriction enzyme buffers and enzymes	Invitrogen, Carlsbad, CA	/
SuperScript first-strand synthesis system	Invitrogen, Carlsbad, CA	11904-018
Tyrosine Phosphatase Substrate Set	JPT Peptide Technologies GmbH, Berlin, Germany	/
VECTOR® M.O.M™ Immunodetection Kit	VECTOR Laboratories, Inc. Burlingame, CA	BMK2202
Vivaspin 15 (5 kDa cut off)	Sartorius Stedim Biotech GmbH, Germany	VS1511

2.1.2. Reagents and Buffers

Cell culture

COS-1 and HEK293T cell medium:
DMEM supplemented with Pyruvate/Glutamine
10% Foetal Calf Serum

PC12 cell medium:
DMEM supplemented with Pyruvate/Glutamine
5% Foetal Calf Serum
5% Horse Serum

Trypsin-EDTA solution:
0.25 % Trypsin
1 mM EDTA

50 mM Pervanadate solution (freshly prepared):
3% H_2O_2 in water
50 mM Sodium orthovanadate
Incubate for 10 minute at RT until solution turns yellow

Bacterial culture

Luria Broth (LB):
10 g Bactotryptone
5 g yeast extract
10 g NaCl
Water up to 1 liter
pH adjusted to 7.0 – 7.4

TSB (for the preparation of competent cells - *E.coli* DH5α):
1 x Luria Broth medium
5 % DMSO
10 mM $MgCl_2$
10 mM $MgSO_4$
10 % PEG 4000

KCM buffer (for transformation):
0.5 M KCl
0.15 M $CaCl_2$
0.25 M $MgCl_2$

Bacterial lysis buffer:
50 mM Tris-HCl, pH 7.5
150 mM NaCl
1 mM PMSF
Complete protease inhibitor cocktail

Cell lysis

COS-1 and HEK293T lysis buffers:
50 mM Tris-HCl, pH 7.5
150 mM NaCl
1% Triton X-100
1mM PMSF
10 mM NaF
Complete protease inhibitor cocktail
Optional: 1 mM Na_3VO_4 (orthovanadate)

Whenever Na_3VO_4 was included this is indicated in the text.
For some experiments 50 mM Hepes pH 7.2 was used as buffering agent instead of Tris-HCl. This will be indicated in the text.

SDS-PAGE and Western BLOT

2 x Sample buffer:
62.5 mM Tris-HCl, pH 6.8
5 % β-Mercaptoethanol or 100 mM Dithiothreitol
10% Glycerol
2% SDS
Bromophenol blue

When necessary, 4 x or 5 x sample buffer was used.

Strip buffer:
62.5 mM Tris-HCl, pH 6.8
100 mM β-Mercaptoethanol
2% SDS

10 x Running buffer:
0.25 M Trizma base
1.92 M Glycine
1% SDS

Transfer Buffer for immunoblot:
39 mM Glycine
48 mM Tris-HCl, pH 9.0
20% Methanol

Blocking buffer:
3% Bovine serum albumin
0.1% Tween 20
in TBS

Coomassie staining solution:
2.5 g/l Coomassie R250
10% Acetic acid
50% Methanol

Destaining solution:
10% Acetic acid
30% Methanol

Silver staining procedure

Silver fixing solution:
50% methanol
12% acetic acid
In milliQ, prepared in sterile glass container

Silver sensitization solution:
0.02% sodium thiosulfate
In milliQ, prepared in sterile glass container

Silver staining solution:
0.04% formalin
0.25% silver nitrate
In milliQ, prepared in sterile glass container

Silver developing solution:
0.04% formalin
6% sodium carbonate

In milliQ, prepared in sterile glass container

Phosphatase activity assays

Two buffers proved to be equally suitable for tyrosine phosphatase assays based on DiFMUP as an artificial substrate. Buffer A was used to test phosphatase activity of GST fusion proteins and buffer B to perform activity tests of immunoprecipitated PTPRR isoforms in the presence of Na_3VO_4 and pervanadate.

DiFMUP buffer A (for phosphatase assay with eluted GST fusion proteins):
50 mM HEPES, pH 7.2
0.1% BSA (Bovine serum albumin)
1 mM DTT (freshly added)

DiFMUP buffer B (for phosphatase assay with immunoprecipitated PTPRR fusion proteins):
50 mM Tris-HCl, pH 7.5
1% Triton X-100
5 mM EDTA
10 mM DTT

2 x SEAP buffer (for alkaline phosphatase assay):
2 M Diethanolamine
1 mM $MgCl_2$

Alkaline phosphate (AP) buffer:
100 mM Tris-HCl, pH 9.5
100 mM NaCl
50 mM $MgCl_2$

NBT-BCIP reaction mix (freshly prepared):
20 µl NBT/BCIP (Sigma Aldrich)
1 ml AP buffer

Phosphate Sensor buffer:
20 mM Tris-HCl, pH 7.5
0.5 mM DTT
0.06% Nonidet P-40
0.25 µM Phosphate Sensor reagent (freshly added)

RAP in situ detection

Hanks' balanced salt solution (HBSS):
20 mM Hepes, pH 7.0
Hanks' balanced salt solution (Sigma)
0.5 mg/ml BSA

RAP in situ washing buffer:
20 mM Hepes, pH 7.0
150 mM NaCl

Chondroitinase ABC buffer :
50 mM Tris-HCl, pH 8.0
60 mM sodium acetate
0.02% BSA

Protein content determination

5 x Bradford reagent (store at 4ºC) :
100 mg Coomassie Brilliant Blue G-250 in 50 ml 95% ethanol
100 ml 85% (w/v) phosphoric acid
50 ml milliQ
Before use, filter through Whatman Filter Paper No. 2

Recombinant protein purification

GSH-beads binding buffer :
Bacterial lysis buffer supplemented with 1% Triton X-100 was used for this purpose

GSH-beads elution buffer :
50 mM Tris-HCl, pH 8.0
10 mM Reduced Glutathione

Nickel-beads washing buffer:
50 mM Tris-HCl, pH 8.0
300 mM NaCl
1 mM PMSF
10 mM Imidazole (freshly added)

Nickel-beads elution buffer:
50 mM Tris-HCl, pH 8.0
300 mM NaCl
1 mM PMSF
1% Triton X-100
250 mM Imidazole (freshly added)

2.1.3. Antibodies

The following tables describe the primary and conjugated antibodies used. Antibody or antiserum name, type, dilution used, and sources (including catalogue number when relevant) are indicated. The various dilutions that were used are dependent on the technique (IB, immunoblotting; IP, immunoprecipitation, GAG-ELISA, glycosaminoglycan-ELISA; IHC, immunohistochemistry) that was applied.

Primary antibodies

Antibody/ antiserum name	Type of antibody	Dilution used	Company/Source	Cat.No.
PY20 (Anti-phospho-tyrosine)	Mouse monoclonal	1:1000 (IB)	Santa Cruz Biotechnologies, Heidelberg, Germany	sc-508
Anti BR7	Rabbit polyclonal	1:3000 (IB)	(Dilaver et al. 2007)	
Anti SL	Rabbit polyclonal	1:3000-1:5000 (IB)	(van den Maagdenberg et al. 1999)	
6A6	Mouse monoclonal	1:1000 (IB); 100 µl per 500 µl lysate (IP)	(Chirivi et al. 2004)	
P5D4 (anti VSV)	Mouse monoclonal	1:10 (in GAG-ELISA)	(Kreis 1986)	
12CA5 (anti HA)	Mouse monoclonal	700 µl per 500 µl lysates (IP)	(Field et al. 1988)	
Y-11 (anti HA)	Rabbit polyclonal	1:1000 (IB)	Santa Cruz Biotechnologies, Heidelberg, Germany	sc-805
B-2 (anti GFP)	Mouse monoclonal	1:1000 (IB)	Santa Cruz Biotechnologies, Heidelberg, Germany	sc-9996
HS4C3 (anti Heparan sulphate)	Single chain variable fragment	1:10 (in GAG-ELISA)	(van Kuppevelt et al. 1998)	
I03H10 (anti Chondroitin Sulphate A/C)	Single chain variable fragment	1:10 (in GAG-ELISA)	(Smetsers et al. 2004)	
GD3G7 (anti Chondroitin Sulphate E)	Single chain variable fragment	1:10 (in GAG-ELISA)	(ten Dam et al. 2007)	
11-5B (anti CNPase)	Monoclonal rabbit	1:100 (IHC)	Millipore, Billerica, MA	MAB326
Anti p44/42	Rabbit	1:1000	Cell Signaling, Bioké, Leiden,	9102

MAP Kinase	polyclonal	(IB)	The Netherlands	
E7 (Anti Tubuline)	Mouse monoclonal	1:2000 (IB)	Hybridoma Bank	/
14C10 (Anti GAPDH)	Rabbit monoclonal	1:1000 (IB)	Cell Signaling, Bioké, Leiden, The Netherlands	2118
52 (anti PTP1C/ SHP1)	Mouse monoclonal	1:1000 (IB)	BD Transduction, Breda , The Netherlands	610125
PY69 (Agarose Anti Phospho-tyrosine)	Mouse monoclonal	25 µl of 50 % slurry per lysates (IP)	BD Transduction, Breda , The Netherlands	610015
1005 (Anti EGFR)	Rabbit polyclonal	1:500 (IB)	Santa Cruz Biotechnologies, Heidelberg, Germany	sc-03
Anti HER3	Rabbit polyclonal	1:1000 (IB)	Provided by Dr. R. Lammers, Tübingen, Germany	
HFR1 (Anti HER4)	Mouse monoclonal	1:300 (IB)	Abcam, Cambridge, UK	ab19391
SRC 2 (anti-c-Src)	Rabbit polyclonal	1:500 (IB)	Santa Cruz Biotechnology, Heidelberg, Germany	sc-18
GC-4 (anti N-cadherin)	Mouse monoclonal	1:1000 (IB)	BD Transduction, Breda , The Netherlands	C3865
EP1829Y (anti CamkIIα)	Rabbit monoclonal	1:500 (IB)	Abcam, Cambridge, UK	ab52476

Conjugated antibodies

Antigen	**Type of antibody**	**Dilution used**	**Company**	**Cat.No.**
Goat anti-mouse Alexa Fluor 488 -labeled	Anti-mouse IgG	1:500 (IHC)	Invitrogen, Carlsbad, CA	A11029
Goat anti-rabbit IRDye680	Anti-rabbit IgG	1:10000 (IB)	LI-COR Biotechnology, Cambridge, UK	926-32220

Rabbit anti-mouse Alkaline-phosphatase-conjugated	Anti-mouse IgG	1:1000 (in GAG-ELISA)	Dakopatts, Glostrup, Denmark	D0486
Goat anti-mouse IRDye800	Anti-mouse IgG	1:10000 (IB)	LI-COR Biotechnology, Cambridge, UK	926-32211

2.1.4. Cell Lines and Media

The HEK293T cell line was kindly provided by Dr. J. Schoeber (Department of Physiology, UMC St. Radboud, Nijmegen). COS-1 (ATCC nr. CRL-1650) and PC12 (ATCC nr.CRL-1721) cell lines were from ATCC (American Type Culture Collection, Manassas, USA). Unless stated otherwise, all cell culture vessels (flasks, dishes and freezing tubes) were purchased from Greiner bio-one (Alphen a/d Rijn, The Netherlands) whereas all cell culture media, i.e. Dulbecco's Modified Eagle Medium (DMEM) and opti-MEM, were purchased from Gibco (Invitrogen, Breda, The Netherlands). Foetal Calf Serum (FCS) was purchased from PAA Laboratories (Pasching, Austria).

2.1.5. Plasmids and Primers

The plasmids pSG8-PTPBR7-HA (wt and C/S mutant), pSG8-PTP-SL-HA (wt and C/S mutant), pSG8-PTPPBSγ (wt and C/S mutant) have been described previously (Noordman et al. 2008). The vector pGEX-SL wt was described in (Hendriks et al. 1995b) and the C/S-D/A mutant in (Noordman et al. 2008). pGEX-BL wt was described in (Hendriks et al. 1995a) and the pGEX-BL C/S mutant and the pGEX-1N-Xho were obtained from Jan Schepens.
The mammalian expression plasmid pBG-flexilinker was generated from pBG (Aricescu et al. 2002) by inserting a linker encoding GGGGSGGGGSP upstream of the PLAP open reading frame (Appendix, Fig. S1). pBG-flexilinker was linearized using HindIII and ClaI in order to introduce an adapter sequence containing EcoRI and KpnI sites (a heteroduplex of oligonucleotides 5'- AGCTGAATTCTTAAGGTACCT-3' and 5'-CGAGGTACCTTAAGAATTC-3'). Both the pHLsec plasmid and pHLsec containing the extracellular domain of RPTPμ (eRPTPμ) were donated by Dr. R. Aricescu (Aricescu et al. 2006; Aricescu et al. 2007).
The mammalian expression plasmids pRK5-EGFR, pRK5-HER2, pRK5-HER3 and pCMV-HER4 were a kind gift of Dr. R. Lammers (Tübingen, Germany). The plasmids pRK5-SHP1, pcDNA3- SHP1 Y538F, pEYFP-C1- SHP1 and pRK5-cSRC were donated by Dr. F.D. Böhmer (Jena, Germany). The pEYFP-N-cadherin expression plasmid was provided by Thomas Brantzos (Oxford, UK).
All primers and oligonucleotides for cloning were purchased from Biolegio BV, Nijmegen, The Netherlands. KpnI and EcoRI sites are indicated in bold and italics, respectively.

Primers used

Primer name	Sequence
BR7ecto forward	5'- TAATACGACTCACTATAGG - 3'
BR7ecto226 reverse	5'- AG**GGTACC**TCCTTCTTTGCTCCAGATC - 3'
BR7ecto225 reverse	5'- AG**GGTACC**TTCTTTGCTCCAGATCTTG - 3'
BR7ecto224 reverse	5'- AG**GGTACC**TTTGCTCCAGATCTTGTC - 3'
BR7ecto223 reverse	5'- AG**GGTACC**GCTCCAGATCTTGTCTGC - 3'
BR7ecto222 reverse	5'- AG**GGTACC**CCAGATCTTGTCTGCTTC - 3'
BR7ecto221 reverse	5'- AG**GGTACC**GATCTTGTCTGCTTCGTG - 3'
BR7ecto220 reverse	5'- TG**GGTACC**CTTGTCTGCTTCGTGCTG - 3'
Oligolinker forward	5'- AGCT*GAATTC*TTAAGGTACCT-3'
Oligolinker reverse	5'- CGA**GGTACC**TTAAGAATTC-3'

2.2 Methods

2.2.1. Cell Culture

COS-1 and HEK293T cells were cultured in Dulbecco's Modified Eagle's Medium (DMEM) reconstituted with Glutamine and Pyruvate, and supplemented with 10% foetal calf serum (FCS). PC12 cells were cultured in DMEM culture medium containing 5% Horse Serum and 5% FCS.
For routine passaging, cells were cultured in 75 cm^2 flasks in an incubator maintained at 37°C, 5% CO_2 and 95% humidity. Cells were allowed to become 60-70% confluent before they were split. For splitting, the medium was removed, the cell layer was washed twice with PBS and cells were detached with a solution of Trypsin-EDTA. Usually, a splitting ratio of 1:6 was used. For freezing purposes, cells were frozen with the usual culture medium containing 10% DMSO (Dimethyl sulfoxide) in a polystyrene container at -80°C overnight, and the next day transferred to and stored in liquid nitrogen. For thawing, cells were removed from the liquid nitrogen, quickly thawed at 37°C and briefly centrifuged to remove DMSO. Cell pellets were then mixed with fresh growth medium and new cultures were initiated.

2.2.2. Cloning

DNA vector extraction from bacterial cells was performed with a NucleoBond XtraMidi Kit according to the producer's indications. To generate the plasmid vector pGEX-PTP-SL-C/S-D/A-ΔKIM, encoding a KIM-deficient substrate-trapping version of PTP-SL phosphatase

domain, the vectors pGEX-SL and pGEX-1N-Xho were digested using XmaI and XhoI restriction enzymes. The XmaI-Xho fragment encoding the region Pro254-Glu535 of PTP-SL (Hendriks et al. 1995b) was subsequently ligated into the linearized pGEX-1N-Xho vector.
An HindIII-ClaI oligolinker containing sites for EcoRI and KpnI was generated by incubating a 1:1 mixture of the forward and reverse oligonucleotide primers for 5 minutes at 70°C and slowly letting the mix cool down at RT. Subsequently, the heteroduplex was stored at -20°C. The mammalian expression plasmid pBG-flexilinker was linearized using HindIII and ClaI and the oligolinker with EcoRI and KpnI sites was introduced to allow subsequent insertion of the seven BR7ecto PCR products.
pHLsec was opened at the restriction sites for EcoRI and KpnI to allow insertion of the BR7ecto226 PCR product in order to generate the pHLsec-BR7ecto226-His plasmid.
All restriction enzyme reactions were performed for 1 hour at 37°C using the indicated restriction enzymes in combination with the appropriate buffer as suggested by the manufacturer. Restriction reaction mixes were prepared as reported:

- Digestion mixes:

15 µl DNA (≈ 1 µg)
4 µl ReACT buffer (10 x stock, typology dependent on the enzyme)
20 µl milliQ water
1 µl restriction enzyme

When possible, two enzymes were used in the same digestion mix. Alternatively, digestion solutions were extracted with Phenol/Chloroform, precipitated and digested with the second enzyme. Otherwise, DNA fragments were size-separated on agarose gels, cut from the gel and purified using the QIAquick Gel Extraction Kit before proceeding with the second digestion.
In all cases, successful digestion was checked by separating the DNA fragments on agarose gel and visualizing them with Ethidium Bromide. DNA fragments were recovered using the QIAquick Gel Extraction Kit and ligations were performed according to the following scheme:

- 10 µl ligation mixes, containing:

x µl vector (10-20 ng)
y µl fragment (3 to 5 x molar excess over vector)
1 µl T4 DNA ligase buffer (10 x stock)
milliQ up to 9 µl
1 µl T4 DNA ligase (1U)

Reactions were performed at RT for 1 hour or overnight at 16°C.

2.2.3 Reverse Transcriptase-Polymerase Chain Reaction (RT-PCR)

C57BL/6 mouse brain RNA preparations (a kind gift of Dr. R. Wansink) were subjected to RT-PCR. Approximately 5 µg of total RNA were used to produce cDNA by random hexamer priming with the SuperScript first-strand synthesis system and the resulting cDNA preparation was subsequently used in a PCR reaction as described below. Stock

concentrations or total amounts are indicated in between brackets. The various steps in the protocol were done as follows:

- Destabilization of RNA secondary structures (mix/sample):

5 µl RNA (5 µg)
1 µl random hexamers (1µg/µl)
Fill with DEPC water up to 12 µl
Mixes were incubated for 5 minutes at 70° C and then quickly chilled on ice

After the RNA secondary structure destabilization, each mix was incubated with components for the reverse transcriptase reaction, as follows.

- Reverse transcriptase reaction (mix/sample):

5 µl SuperScript first strand buffer
1 µl RNAse inhibitor
2 µl dNTPs (10 mM, where each dNTP is 2.5 mM)

The resulting mixtures were incubated for 5 minutes at 25°C and then Reverse Transcriptase (1 µl/sample, 200 U) was added. Mixtures were pre-incubated for 10 minutes at 25°C and then reverse transcription was performed for 60 minutes at 42°C. Reaction was stopped by heating the tubes at 70°C for 10 minutes.

- PCR reaction (mix/sample):

2 µl RT product
10 µl 10x Herculase II buffer
1 µl dNTPs (100 mM, where each dNTP is 25 mM)
1 µl forward primer (100 ng/µl)
1 µl reverse primer (100 ng/µl)
84.5 µl milliQ water
0.5 µl Herculase II

In total, seven samples were prepared, each including the BR7ecto forward primer and one of the BR7ecto reverse primers (see section 2.1.5).
PCR settings implied an initial denaturation at 94°C for 5 minutes, followed by 35 cycles. Each cycle included a denaturation step (1 minute at 94°C), an annealing step (30 seconds at 52°C) and an elongation step (2 minutes at 72°C). At the end of the cycling program a final elongation step at 72°C for 5 minutes was added. Samples were chilled and kept at -20°C until needed.

2.2.4. Transient Transfections

HEK293T or COS-1 cells were transiently transfected using the DEAE-dextran method.
Transfections were performed when cells reached 50% - 60% confluency. Stock concentrations are indicated in brackets.

- For transfection in 6-wells plate (mix/well):

1-2 µl of Chloroquine (100 mM)
50 µl of DEAE-dextran (1 mg/ml)

950 µl OPTIMEM
1 µg of DNA

Cells in the 6-well plate were washed with 1 ml OPTIMEM directly before the DNA-transfection mix was gently added and cells were incubated for 3 hours at 37°C and 7% CO_2. Subsequently, the transfection mix was removed and cells were treated with 10% DMSO in PBS for 2 minutes. The shock medium was carefully removed and fresh medium was added. Transfected cells were then cultured for 24 or 48 hours.

2.2.5. Cell lysis, Immunoprecipitation and Blotting

Cells were usually grown to 70% - 80% confluency either in 6-well plates or in 10 cm dishes. When necessary, serum starvation was performed overnight in serum-free DMEM culture medium and stimulation was usually done with fresh medium containing 10% FCS (unless otherwise specified) for 15 minutes. When appropriate, hyperphosphorylation was induced by treating the cells with 0.1 mM pervanadate for 10 minutes before lysis. For preparing cell extracts, cells were washed with ice cold PBS and lysis was performed using 200 µl buffer per well (in a 6-well plate) or 500 µl per 10 cm dish. Cells were scraped off and incubated for another 40 minutes on ice before being centrifuged at 10,000 rpm at 4°C for 15 minutes. Cell debris were discarded and the cleared lysates were either subjected to immunoprecipitation (IP) or western blotting procedures. In case of IP, lysates were first preincubated with protein A-Sepharose beads for 1 hour at 4°C and, after brief centrifugation, lysates were collected. IP was performed by mixing lysates with the specific antibody coupled to protein A-Sepharose beads and incubating them overnight at 4°C on a rotary wheel. Beads were then washed three times with lysis buffer (with or without Na_3VO_4, as indicated), transferred to a clean tube and washed once more before any subsequent use.
For some applications immunoprecipitated HA-tagged fusion proteins were finally eluted from the bound protein A-Sepharose beads using 200 µl lysis buffer supplemented with 100 µg/ml HA-peptide.
For SDS-PAGE and western blotting of immunoprecipitates, beads were resuspended in 30 µl of 2 x sample buffer, boiled and stored at -20°C. For SDS-PAGE and western blotting of lysates, usually 10% of cell lysates was mixed with 5 x sample buffer, boiled and stored at -20°C before use.
For SDS-PAGE, the acrylamide/bis-acrylamide percentage of the casted gel that was chosen depended on the size of the protein of interest. For quantification of protein expression known amounts of purified BSA protein were also loaded. After size separation, proteins were transferred to PVDF membrane (Millipore, Amsterdam, The Netherlands) by conventional wet electroblotting. Membranes were blocked with blocking buffer, either for one hour at RT or overnight at 4°C. They were then probed with primary antibody diluted in blocking buffer (either for one hour at RT or overnight at 4°C) followed by three washes with TBS including 0.1% Tween20 (TBST). Membranes were then incubated with the appropriate secondary antibody in TBST at RT for another hour. Membranes were finally washed two times with TBST and once with TBS and immunoreactive bands were visualized on an Odyssey infrared imaging system (LI-COR). In cases where the nature of the primary antibodies did not allow

for simultaneous dual-color immuno-detection, membranes were reprobed with another antibody after first being stripped by incubating them with stripping buffer at 50°C for 30 minutes followed by three washes with TBST.
When necessary, quantification of band intensities was performed using the Odyssey infrared imaging system mentioned above. Student's t-test was used for statistical analysis.

2.2.6 Brain tissue sections and lysates

Wild type and *Ptprr* knockout mice of 9 - 12 months of age were anesthetized and perfused with PBS. Whole brains were extracted and snap frozen in liquid nitrogen-cold isopenthane. Brains were then stored at -80°C. Sagittal and coronal cryosections of 10 µm were mounted on glass slides and dried under air flow at RT. Mouse embryonic brain sections were a kind gift of Andrew Stoker. To prepare brain lysates, frozen brains were thawed and homogenized at 4°C in cell lysis buffer. Lysates were centrifuged at 10,000 rpm for 10 minutes at 4°C and cell debris discarded.

2.2.7 GST pull-downs

pGEX-based plasmids harboring cDNA fragments encoding the PTP-SL and PTP-BL phosphatase domain were transformed into the *E.coli* strain BL21 and bacterial cultures were started. In brief, colonies were inoculated into 100 ml Luria Broth containing ampicillin and grown at 37°Cuntil the optical density (OD) at 0.600 nm reached 0.7. Then, protein expression was induced by addition of 0.1 mM IPTG (isopropyl-beta-D-thiogalactopyranoside) and the culture was incubated at 37°C for an additional 5 hours. Bacterial cells were then centrifuged and resuspended in approximately 2.5 ml of bacterial lysis buffer. Bacteria were lysed by two times sonication (LABsonic®P, Sartorius) for 20 seconds. Triton X-100 was then added to a final concentration of 1% and lysates were incubated at 4°C for another 10 min. Subsequently, cell debris was removed by centrifugation at 9,500 rpm at 4°C for 15 minutes in a Sorvall RC-5B (Rotor SM-24). Supernatant was mixed with 160 µl 50% slurry of Glutathione (GSH)-Sepharose beads that had been pre-equilibrated with bacterial lysis buffer. Mixes were incubated on a rotary wheel overnight at 4°C. Beads were briefly centrifuged and washed three times with the bacterial lysis buffer. The GST fusion proteins were finally eluted from the bound GSH beads with 200 µl of GSH beads elution buffer. Aliquots of the eluates were mixed with 5 x sample buffer and separated on SDS-PAGE to monitor recombinant fusion protein production.

For some applications, the GST fusion proteins still bound to the beads were added to cell or brain lysates for dephosphorylation of candidate PTPRR protein substrates or to serve as baits for co-purifying protein complexes.

Alternatively, GST fusion proteins that were eluted from the beads were used for dephosphorylation assays of tyrosine phosphorylated peptides in microplates (see below).

2.2.8 DiFMUP dephosphorylation assays

Phosphatase activity of the GST-PTP-SL and GST-PTP-BL fusion proteins, either bound to GSH-sepharose beads or after elution, was measured according to the instructions in the Signal Scout Phosphatase System. Several dilutions of phosphatase protein (between 1 µg and 20 ng) were mixed with DiFMUP buffer up to a volume of 50 µl which was then added to separate wells of a white fluorescence microplate. Then 50 µl of substrate (a 200 µM DiFMUP solution) were added to each well and fluorescence of the hydrolysed product (DiFMU) immediately measured at 455 nm in a Victor 3 Multilabel Plate reader (Perkin Elmer 1420).
To test for the effect of Na_3VO_4 and Pervanadate on the immunoprecipitates, immune-purified proteins (who had never been treated with phosphatase inhibitors during culture or lysis) were resuspended in DiFMUP buffer B and activity was tested in presence or absence of either 1 mM Na_3VO_4 or 0.1 mM Pervanadate. 50 µl of immune-precipitated protein were added first to each well of a microplate and then 50 µl of DiFMUP buffer B were added. Activity was immediately measured and monitored for 30 minutes. To convert and bind unreacted vanadate compounds, suspensions in each well were treated with 5 mM EDTA and 10 mM DTT (Blanchetot et al. 2005). After 2 hours incubation on ice, again 50 µl of phosphatase protein were added to the wells and activity was measured for another 30 minutes.

2.2.9 Dephosphorylation assays on tyrosine-phosphorylated peptides in microplate

Dephosphorylation assay
To determine candidate protein substrates for the PTPRR PTP domain, dephosphorylation assays on specific phosphotyrosine-containing peptides (JPT Peptide Technologies) were performed in microtiter plates. GST protein alone and the GST-PTP domain fusion of the protein phosphatase PTP-BL were used for comparison. 5 µl preparations containing 25 pmol of each phosphopeptide (1 µM final concentration) were put in separate wells of two 384-well microplates. Subsequently, 2 ng/well and 5 ng/well of eluted GST-PTP-BL or GST-PTP-SL protein, respectively, were added to the Phosphate Sensor reaction mix (Invitrogen) for a total volume of 20 µl/well and the suspension was added to each well in the two microplates separately. Fluorescence was measured at 450 nm after 0, 1.5, 4.0, 6.5 hours and overnight incubation. Wells that lacked the phospho-peptides served as controls. Wells containing increasing concentrations of pure free phosphate were taken along for calibration purposes.

Data processing
Fluorescence intensities appeared unstable up to time point 4 hours. Therefore, the increase in fluorescence intensity between the 6.0 hours and overnight incubation time points were used for calculations and were ranked. Subsequently, due to scattering effects observed in the wells at the borders of the microplate, the corresponding peptides were excluded from the ranking.

2.2.10 Dephosphorylation and co-immunoprecipitation assays *in vitro*

To determine if candidate substrate proteins are directly or indirectly dephosphorylated by PTPRR isoforms, dephosphorylation assays were performed *in vitro*. Tyrosine hyperphosphorylation of proteins was induced by treating cells over-expressing the candidate substrates with pervanadate or by serum induction. Immunoprecipitated PTPRR protein isoforms or pulled-down GST-PTP-SL fusion proteins were resuspended in DiFMUP buffer B. Subsequently, they were incubated with cell lysates containing the over-expressed and phosphorylated candidate substrates (HER3, HER4, SHP1 or N-cadherin). Where indicated, lysates containing the over-expressed substrate candidates were treated with 5 mM EDTA and 10 mM DTT prior to incubation with the phosphatase in order to block remaining PTP inhibitors. Mixtures were incubated at RT for 1 hour or at 4°C overnight on a rotary wheel before aliquots were taken and mixed with 2 x sample buffer to test phosphorylation levels of the candidate substrate by SDS-PAGE and immunoblotting. The remaining mixtures were used to determine co-immunoprecipitation or co-purification of the candidate substrate with PTPRR substrate-trapping mutants. For this purpose, the mixtures were briefly centrifuged at 4°C to collect the GST-fusion protein-containing beads and its associated proteins. Beads were then washed three times in cell lysis buffer containing Na_3VO_4 and then transferred to a clean tube. Following one more wash beads were resuspended in 2 x sample buffer and boiled. Obtained proteins were subjected to SDS-PAGE and immunoblotting.

2.2.11 Dephosphorylation and co-immunoprecipitation assays in over-expressing cells

To determine if candidate substrate proteins are directly or indirectly dephosphorylated by PTPRR isoforms, the candidate substrates and the tagged PTPRR isoforms were co-expressed in COS-1 cells.
Tyrosine hyperphosphorylation of the candidates was induced by treating over-expressing cells with pervanadate or by serum induction as described above. Subsequently cells were lysed and aliquots were mixed with 5 x sample buffer. The remaining lysate was subjected to immunoprecipitiation of either the candidate substrate or the PTPRR isoform. Pre-clearance of lysates for 1 hour at 4°C with protein A - Sepharose beads was followed by overnight incubation at 4°C of supernatants with the specific antibody conjugated to protein A-Sepharose beads . Beads were briefly centrifuged at 4°C and washed three times in cell lysis buffer containing Na_3VO_4. Beads were then transferred to a clean tube and washed again before being resuspended in 2 x sample buffer and boiled. Samples were subjected to SDS-PAGE and immunoblotting as described previously.

2.2.12 Alkaline phosphatase assays on conditioned culture media

Conditioned medium of HEK293T cells that had been transfected with the various PTPBR7 ectodomain-encoding pBG-flexilinker and pHLsec plasmids was collected 48 hours after transfection. Conditioned media were directly sterile-filtered through 20 µm pore size filters and buffered with Hepes 20 mM (pH 7.4) as described (Stoker 2005). The test for alkaline

phosphatase activity in the conditioned medium was performed using pNPP as substrate (Stoker 2005). Briefly, aliquots of conditioned medium were incubated at 65°C for 5 minutes to inhibit all HEK293T endogenous phosphatase activity. Aliquots were then mixed with SEAP buffer up to 1 ml volume and equilibrated at RT for 5 minutes. 20 µl of 200 mM pNPP solution was then added and absorbance at 405 nm was measured every 5 minutes for 15 minutes.

2.2.13 Bradford protein quantification

For the determination of protein concentration, 5 x Bradford reagent was filtered and diluted with milliQ water to obtain 1 ml reagent/sample. The solution was equilibrated for 5 minutes at RT and then added to 1, 5 and 10 µl of either cell or brain lysates. Mixtures were equilibrated for 5 minutes at RT and then absorbance at 595 nm was measured in a WPA Biowave DNA cuvette reader (Isogene LifeScience). Calibration curves were prepared making use of purified BSA (Bradford 1976).

2.2.14 Immunohistochemistry

Cryosections on glass slides were briefly rinsed in TBS at RT and fixed in acetone for 10 minutes at -20°C. After two washes endogenous mouse immunoglobulins were blocked using the VECTOR® M.O.M™ Immunodetection Kit (VECTOR Laboratories, Inc. Burlingame, CA). Subsequently, sections were washed twice in TBS and pre-incubated 10 minutes in primary antibody M.O.M. ™ Diluent in TBS buffer supplemented with 2% Goat Serum. Sections were incubated for 2 hours at RT with anti-CNPase, washed twice in TBS and incubated for 1 hour at RT with goat-anti-mouse-conjugated Alexa Fluor 488. Finally, sections were washed twice in TBS, embedded in Mowiol (Sigma-Aldrich) and analyzed by fluorescence microscopy (Leica DMRA).

2.2.15 Receptor alkaline phosphate (RAP) *in situ* staining on brain sections

Glass slides with tissue cryosections were thawed and left at room temperature for 5 minutes. Subsequently a 3-4 mm thick rectangle was drawn around each section using a wax pen to provide a sort of barrier to prevent solution overflow during subsequent incubation.
Sections were washed in HBSS for 2 minutes and subsequently fixed in methanol at -20 ˚C for 90 seconds. Sections were then again washed twice for 90 seconds in HBSS before being incubated with 200 µl of BR7ecto-containing conditioned medium. Sections were then incubated in a humidified chamber in the dark at RT for 75 minutes.
Sections were washed six times for 60 seconds in cold HBSS and fixed for 2 minutes in 4 % paraformaldehyde. Paraformaldehyde was then removed by washing the sections three times for 90 seconds with HBSS; slides were then placed in a glass Coplin jar containing RAP *in situ* washing buffer at 65 ˚C. Treatment at 65˚C was for 30 minutes, to ensure inactivation of endogenous alkaline phosphatases. Sections were then preincubated in AP buffer for 5 minutes before being incubated with 200 µl of NBT-BCIP reaction mix/section. Slides were incubated in a humidified chamber at RT overnight.

The next day, sections were rinsed in water, embedded in a water/glycerol (9:1 v/v) embedding and examined on Leica DM LB (Leica Microsystem GmbH, Germany) using a Leica HC PL Fluotar objective. In each experiment minimally three sections per condition were analyzed. Three digitized images of cerebellar white matter per section where taken and for each image the mean gray value in three equal areas was determined using ImageJ software (http://rsbweb.nih.gov/ij/). Averaged mean gray values were plotted and analyzed using Student's t-test.
When sections were incubated with RPTPσ ectodomain probes the procedure followed was the same described for BR7ecto probes.
For some applications the conditioned media were first concentrated using Vivaspin 15 membranes with a 5 kDa cut-off (Sartorius Stedim Biotech GmbH, Germany).
For some experiments tissue sections were first subjected to enzymatic digestion of CS by incubation overnight at RT in 1 IU/ml chondroitinase ABC digestion mix (Sigma-Aldrich) or in chondroitinase buffer as a control. Activity of the digesting enzyme under those conditions was confirmed independently using a GAG ELISA (described below).

2.2.16 GAG ELISA

GAG binding to the extracellular domain of PTPBR7 was tested using a modified ELISA set-up (van Kuppevelt et al. 1998). 100 µl per well of HS, CS-A, CS-C, CS-D or CS-E solution (10 µg/ml) were coated in 96-well microplates at RT overnight. To remove excess GAGs wells were washed 6 times in ELISA buffer (0.2 M NaCl in PBST). Wells were blocked by incubation at RT for 1 hour in 3% cold water fish skin gelatin in ELISA buffer. After 6 washes different dilutions of conditioned medium containing PLAP-tagged protein (BR7ecto226) were added to each well. Incubation was for 1.5 hours at RT in the dark. Following another 6 washes, 100 µl of phosphatase reaction mix (1 mg/ml pNPP in SEAP buffer) were added to each well. Absorbance at 405 nm was measured after 2 hours incubation at RT on a Wallac Victor 3 reader (Perkin Elmer).
To monitor the digestion by chondroitinase ABC activity, chondroitin-sulphates CS-A, CS-C or CS-E were coated to a microplate and excess was removed by washing with PBS-0.1%Tween20. Overnight digestion with 1 IU/ml chondroitinase ABC was performed. Next, 100 µl of CS-specific VSV-conjugated single-chain variable fragment antibodies were applied to each well (1:10 dilution) for 1 hour, followed by washing with PBST. Subsequent incubations were done using mouse monoclonal antibody P5D4 to VSV (1:10 dilution) and AP-conjugated rabbit anti-mouse antibody (1:1000). After 6 washes, 100 µl of 1 mg/ml pNPP in SEAP buffer was added per well and absorbance at 405 nm was recorded.

2.2.17 Affinity purification using His-tagged PTPBR7 ectodomain (BR7ecto226-His) as a bait

His-Select Nickel affinity gel (Sigma-Aldrich, St. Louis, MO) was washed in Nickel-beads washing buffer and incubated on an orbital shaker for 2 hours at 4˚C in the presence of conditioned medium from cells that over-expressed BR7ecto226-His, the His-tagged extracellular domain of RPTPµ or with medium from untransfected cells as controls. Beads

were then collected and washed 3 times with washing buffer containing 10 mM Imidazole. Subsequently, beads were incubated with brain lysate overnight at 4°C on an orbital shaker. Beads were then briefly centrifuged and washed in washing buffer with 1% Triton X-100 and 150 mM NaCl. Bound proteins were eluted in Nickel-beads elution buffer containing 250 mM Imidazole. Eluates were mixed with sample buffer and boiled. Samples intended for LC-MS analysis were subjected to SDS-PAGE, stained with Coomassie Brilliant Blue and individual complete lanes were cut out and analyzed as described below.

2.2.18 Coomassie and silver staining

For Coomassie staining, gels were immersed in Coomassie staining solution for 30 minutes at 60°C and destained overnight in destaining solution at RT. If used for mass spectrometric analysis, gels were stored in 1% glacial acetic acid at 4°C.
For silver staining gels were placed in fixing solution immediately following electrophoresis and gently shaken overnight. Gels were washed with 50% methanol for 20 minutes and twice with MilliQ water for 20 minutes. Gels were placed in sensitization solution for 1 minute and washed twice with MilliQ water for 1 minute. Subsequently they were placed in staining solution for 20 minutes and washed twice with MilliQ water for 1 minute. Gels were placed in the developing solution for some minutes until dark bands started to appear (approximately after 2 minutes). Developing solution was discarded and gels were immediately placed in 12% glacial acetic acid to block the reaction. Gels were stored in 1% glacial acetic acid at 4°C.

2.2.19 Mass spectrometry analysis of PTPBR7 extracellular domain interacting proteins

In-Gel digestion
First Coomassie Brilliant Blue-stained gel bands were minced and destained by 3 consecutive washes in 750 µl buffer containing 200 mM ammonium bicarbonate in 50% (v/v) acetonitrile for 30 min at 30°C. After drying the gel pieces in a Speedvac (Thermo Savant, Holbrook, USA), 200 µl trypsin solution (0.002 µg/µl in a 50 mM ammonium bicarbonate buffer solution, pH 8.0) was added and allowed to be absorbed by the gel for 45 min on ice. Gel bands were completely immersed by adding additional 800 µl buffer solution and incubated at 37°C overnight. The supernatant was recovered, and the resulting peptides were extracted twice with 500 µl of 60% (v/v) acetonitrile, 0.1% (v/v) formic acid. The pooled peptide extracts were dried in a SpeedVac and resuspended in 15 µl 2% (v/v) acetonitrile, 0.1% (v/v) formic acid for analysis by liquid chromatography tandem mass spectrometry (LC-MS/MS).

Liquid chromatography coupled to tandem mass spectrometry based on Electrospray Ionization and Fourier Transform (LC-ESI-FT-MS/MS)
A volume of 5 µl of each fraction was analyzed independently using a fully automated LC-MS/MS setup. Peptides were first separated on an Agilent 1200 chromatographic system (Agilent, Santa Clara, CA, USA) and on-line measured on a LTQ-FT Ultra mass spectrometer (Thermo Fisher Scientific, Waltham, MA, USA). The samples were first loaded and desalted

on a (5 mm x 0.3 mm) Zorbax 300SB-C18 trapping column at a 4 µl/min flow rate using a 2% (v/v) acetonitrile, 0.1% formic acid buffer, and then separated on a (150 mm x 75 µm) Zorbax 300SB-C18 analytical column (Agilent) by a 50 min linear gradient ranging from 2% (v/v) to 80% (v/v) acetonitrile, 0.1% formic acid at a 0.3 µl/min flow rate. The LC-effluent was directly coupled to a Triversa NanoMate ESI source (Advion, Ithaca, NY, USA), working in nano-LC mode and equipped with a D-chip whereon a 1.55 kV voltage was supplied. During the LC-separation the FT-ICR mass analyzer acquired MS scans at 100,000 resolution, the 3 most intense precursor peptides for each MS scan were automatically selected and fragmented by the LTQ ion trap mass analyzer.

Mass spectrometry data handling

Raw LC-ESI-FT-MS/MS data were analyzed using Mascot Daemon v2.2.2 (Matrix Science. London, UK). The processed spectra were searched against the SwissProt Mus musculus database (Swiss-Prot release 57.15). Carbamidomethyl (C) and oxidation (HMW) were selected as variable modifications, and two missed cleavages were allowed with trypsin as the cleaving agent. Decoy database searches were done with a tolerance of 10 ppm for the precursor ion and 0.5 Da in the MS/MS mode. Keratins were excluded from the final protein list. Only protein identifications with a calculated protein probability higher than 0.99 and with MS/MS ionscore $\geq$ 30 were retained.

Chapter 3

- Results

"There are two possible outcomes:
if the result confirms the hypothesis, then you've made a measurement.
If the result is contrary to the hypothesis, then you've made a discovery"
Enrico Fermi

3.1 Application of GST fusion proteins in phospho-peptide array screenings and pull-down assays

To understand PTP functioning and regulation it is crucial to gather knowledge on cognate substrates and interacting proteins. Several screening approaches have been used in the last years in order to identify putative substrates for a specific PTP. Such studies have to be followed by validation assays and in some cases this led to the identification of *bona fide* substrates. Aware of the documented promiscuity of PTPs in dephosphorylating phospho-proteins and most of all phospho-peptides *in vitro* (Tiganis and Bennett 2007; Barr et al. 2009), we have performed in parallel a phospho-peptide array dephosphorylation assay for the phosphatase domain of PTPRR and mass spectrometric analysis of proteins obtained by GST-pull down from brain lysates. In the first approach we made use of the wild type phosphatase domain fused to the GST protein. In the second strategy both wild type and C/S-D/A mutant GST-PTP fusion proteins were used in pull down assays. In both approaches the phosphatase domain of PTP-BL, an unrelated protein tyrosine phosphatase belonging to group NT7, was used to monitor specificity of the dephosphorylation and association steps. Production, validation and application of GST fusion proteins are described in the following paragraphs (3.1.1 to 3.1.3).

3.1.1 GST fusion protein production and validation

The plasmids pGEX-SL and pGEX-SL C/S-D/A encoding GST fusions of the wild type PTPRR phosphatase domain and a catalytically inactive C/S-D/A mutant were already available in our group (Hendriks et al. 1995b) . These vectors include sequences that encode the PTPRR Kinase Interacting Motif (KIM), located N-terminally from the phosphatase domain and responsible for interaction with MAPK proteins. In order to favour the selection of PTPRR substrates other than MAPKs, the sequence encoding the KIM domain was deleted yielding plasmids pGEX-PTP-SL and pGEX-PTP-SL C/S-D/A, respectively. The wild type and C/S mutant of the PTP-BL phosphatase domain fused to GST was also produced exploiting previously generated bacterial expression plasmids (Hendriks et al. 1995a). GST fusion proteins were purified with GSH-Sepharose beads. Importantly, all washing steps were performed using Tris-based buffers in order to avoid contamination by phosphate groups derived from common buffers like PBS, which would subsequently interfere with the detection method based on the Phosphate Sensor reagent during the phospho-peptide screening (paragraph 3.1.2). To monitor the yield and purity of fusion protein preparations that were released from the beads, different volumes were compared to standard amounts of pure BSA protein on Coomassie-stained SDS gel (Figure 3.1). The four GST fusion proteins demonstrated expected apparent molecular weights. While GST-PTP-BL variants displayed considerable break-down, GST-PTP-SL samples did not show signs of degradation.

To test whether the wild type fusion proteins adopted a proper, enzymatically active conformation and C/S and C/S-D/A mutants were indeed catalytically dead, phosphatase activity was measured by means of the DiFMUP assay (Figure 3.2). Wild type GST-PTP-SL and GST-PTP-BL proteins both displayed PTP activity, as witnessed by the linear increase in

DiFMU fluorescence. Wild type GST-PTP-BL demonstrated an activity that exceeded at least 10-fold that of the C/S mutant, and this most likely reflects the contribution of the non-degraded full-length component. In comparison, GST-PTP-SL C/S-D/A had about 20,000-fold reduced activity than its wild type counterpart. Based on these findings we chose to make use of the wild type isoforms in a phospho-peptide screening assay (paragraph 3.1.2) and to use GST-PTP-SL C/S-D/A in substrate-trapping assays for the identification of novel PTP-SL substrates.

3.1.2 Phospho-peptide screening

A library of 360 distinct phosphotyrosine peptides from known tyrosine-phosphorylated proteins in a 384-wells microtiter plate format was supplemented with wild type GST-PTP-SL and GST-PTP-BL fusion proteins previously mixed with the Phosphate Sensor reagent. Immediately and at different time points (1.5, 4.0, 6.5 hours and overnight (ON) after addition of the Phosphate Sensor reagent) fluorescence of the released phosphate groups bound to the Phosphate Sensor reagent was registered in an automatic spectrofluorimetric reader. We noticed that many phospho-peptides-containing wells located along the lateral and top border of the microtiter plate returned a fluorescence intensity higher than that of the other wells at all registered time points. This phenomenon may be due to light scattering of plastic borders that eventually sums up generating an artifacted fluorescence measured directly above these peripheral wells by the detector. Despite the reduction of the resulting subset of tested phospho- peptides, we decided then to exclude those wells from our analysis.

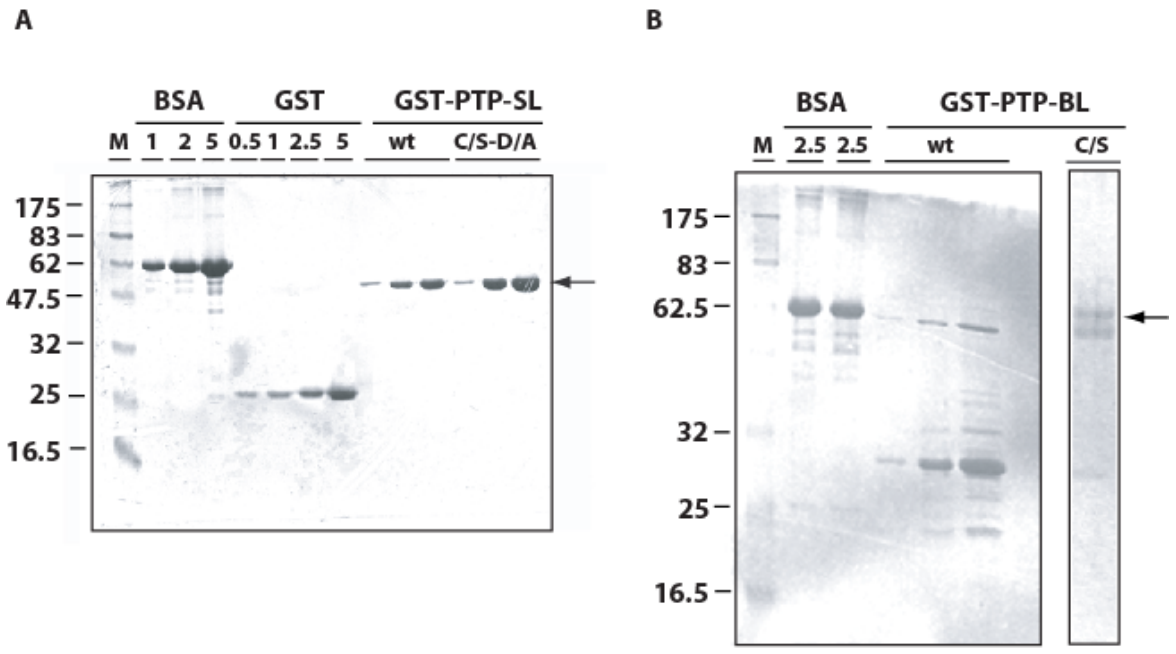

Figure 3.1. GST-PTP-SL and GST-PTP-BL expression and purification. Eluted GST-PTP-SL (A) and GST-PTP BL (B) fusion proteins after purification with GSH-sepharose beads were quantified using known amounts of BSA and GST proteins on Coomassie-stained SDS-gel. Increasing volumes (1.0, 2.0 and 5.0 µl) of fusion protein were loaded together with known amounts of BSA and GST proteins. Arrows indicate full length GST-PTP-SL and GST-PTP-BL, respectively. Molecular weights are given on the left in kDa. Numbers on top of different columns indicate µg of loaded standard protein. M= molecular weight marker lane.

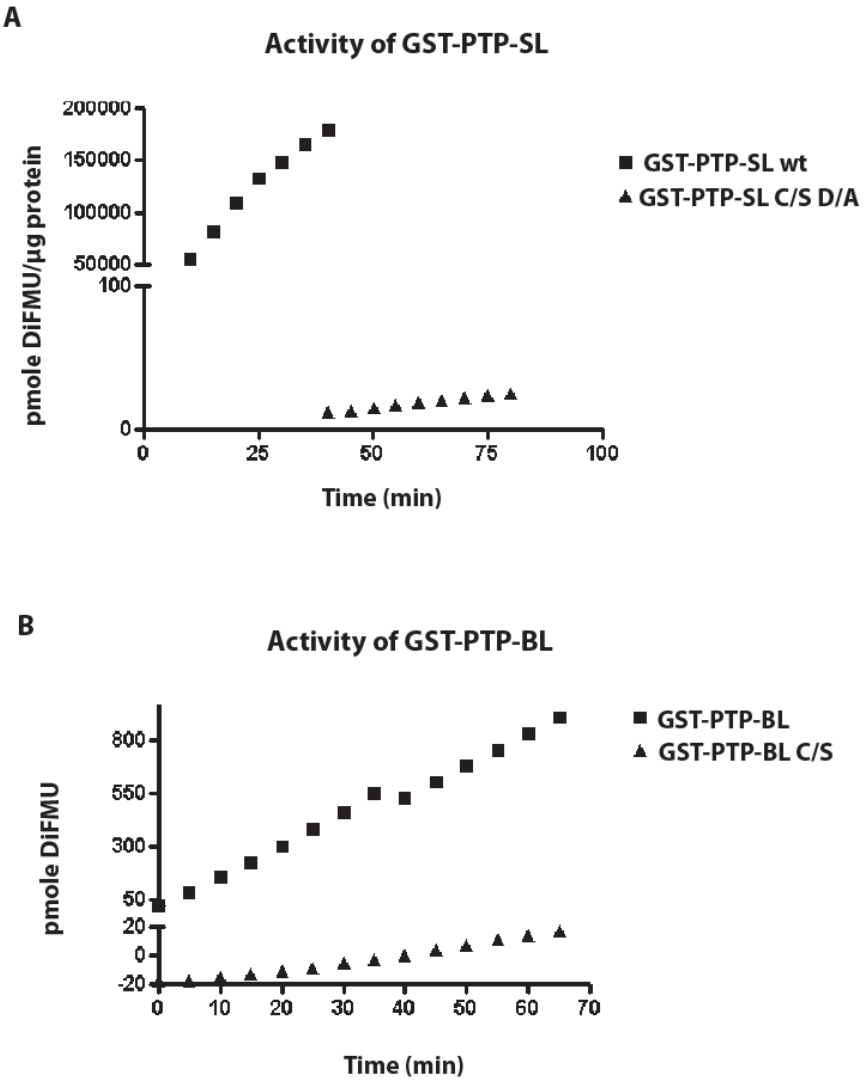

Figure 3.2. GST-PTP-SL (A) and GST-PTP-BL (B) activity. Purified wild type or C/S (-D/A) mutant versions of GST-PTP-SL (A) and GST-PTP-BL (B) were used to measure PTP activity by means of the DiFMUP assay. Activity curves are shown within their range of linear increase. The activity of GST-PTP-SL was normalized to the amount of fusion protein. For GST-PTP-BL this was not possible because of the significant protein degradation (Fig. 3.1).

Subsequently, for each phospho-peptide, the net fluorescence intensity between the time points 6.5 hours and ON was calculated, corrected for the mean fluorescence increase between the same time points of blanco wells (background) that contained no phospho-peptide and ranked. In this way fluorescence intensities correlated to the dephosphorylation efficiency of the specific phospho-peptide. We decided to consider only the phospho-peptides generating the highest fluorescence intensities, hence those around the highest value of the standard curve (whose fluorescence intensity was generated by 160 µM free phosphate). Respectively, Figure 3.3 and Table 3.1 for GST-PTP-SL and Figure 3.4 and Table 3.2 for GST-PTP-BL, report the identity and information about the proteins from which these phospho-peptides were derived.

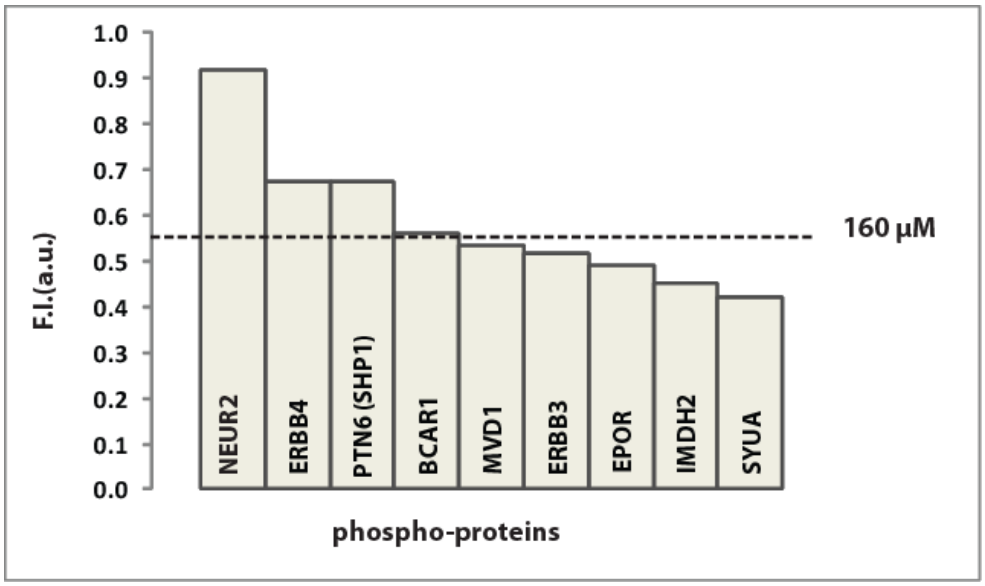

Figure 3.3. Graphical representation of GST-PTP-SL dephosphorylation efficiencies of specific phospho-peptides known proteins. Phospho-proteins, from which the tested phospho-peptides originate, are ranked according to the Fluorescence intensities (F.I.) of the phosphate released by the PTP as measured with the Phosphate Sensor reagent. Standard concentrations of free phosphate in solution served for calibration purposes and the FI that was measured for 160 µM free phosphate is indicated by a dotted line.a.u.: arbitrary units.

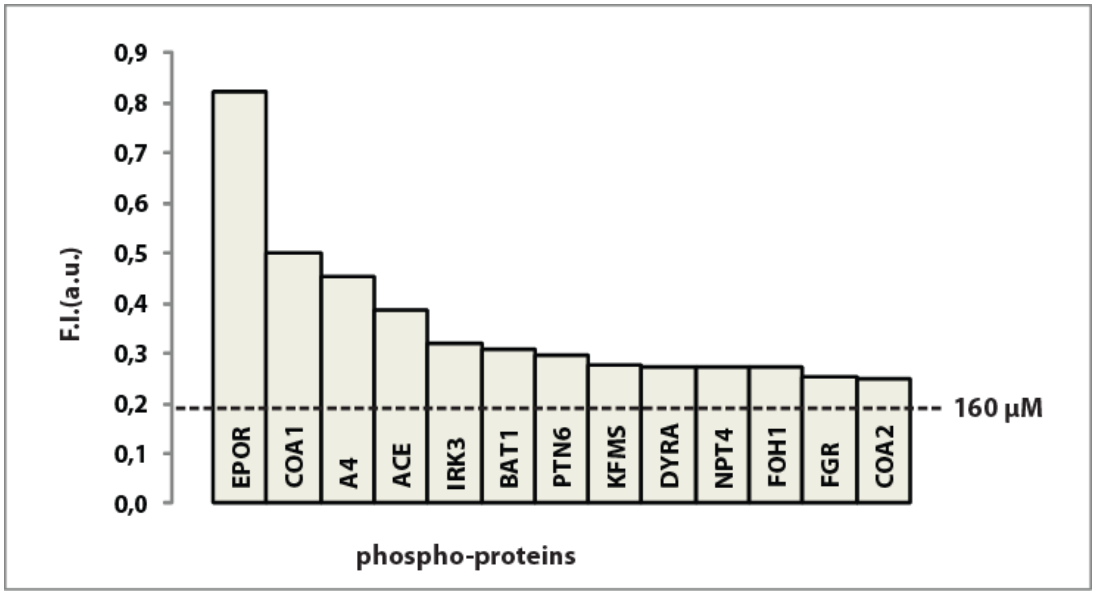

Figure 3.4. Graphical representation of GST-PTP-BL dephosphorylation efficiencies of specific phospho-peptides that correspond to known proteins. Phospho-proteins, from which the tested phospho-peptides originate, are ranked according to the Fluorescence intensities (F.I.) of the phosphate released by the PTP as measured with the Phosphate Sensor reagent. Standard concentrations of free phosphate in solution served for calibration purposes and the FI that was measured for 160 µM free phosphate is indicated by a dotted line. a.u.: arbitrary units.

Table 3.1. Phospho-peptides that were most efficiently dephosphorylated by GST-PTP-SL, listed together with some information on the protein of origin.

Phospho-peptide[a]	Phospho-protein[b]	Description[c]
LYEANDp(Y)EEIVFL	NEUR2 Q9Y3R4	Sialidase 2 binds and hydrolyzes terminal sialic acid residues from various glycoconjugates as well as playing roles in pathogenesis; Tyr360 is not known to be P *in vivo*
YSTKYFp(Y)KQNGRI	ERBB4 Q15303	Protein Tyrosine Kinase ubiquitously expressed in the brain and activated by neuregulins; pTyr1268 is bound by Grb2 and Nck
KGQESEp(Y)GNITYP	PTN6 (SHP1) P29350	Protein tyrosine phosphatase expressed in brain; pTyr536 regulates protein activation
QPEQDEp(Y)DIPRHL	BCAR1 P56945	Breast cancer anti-estrogen resistance protein 1; phosphorylation of Tyr234 directs protein to the membrane
TFPPISp(Y)LNAISW	MVD1 P53602	First enzyme in the biosynthesis of isoprenes. Expressed in heart, skeletal muscle, lung, liver, brain, pancreas, kidney and placenta; Tyr276 is not known to be P *in vivo*.
PASEQGp(Y)EEMRAF	ERBB3 P21860	Protein Tyrosine Kinase expressed in epithelial tissue and brain; pTyr1289 is bound by subunit p85 of PI3K
SAASFEp(Y)TILDPS	EPOR P19235	Erythropoietin receptor; pTyr426 is a known phosphorylated residue that regulates association with other proteins
KYIKDKp(Y)PNLQVI	IMDH2 P12268	Inosine-5'-monophosphate dehydrogenase 2, involved in synthesis of guanine nucleotides; Tyr29 is not known to be phosphorylated *in vivo*
MPSEEGp(Y)QDYEPE	SYUA P37840	Alpha-synuclein is located in neuronal pre-synaptic regions and may be involved in some neuropathologies; Tyr133 is phosphorylated by Syk

a: phospho-peptide with indicated phosphotyrosine.
b: mnemonic identifier and Accession Number of the human isoform of the protein of origin.
c: main features of the protein of origin. In cases where the phosphotyrosine is known to be phosphorylated *in vivo* according to the Phosphosite database (www.phosphosite.org) corresponding relevant information is provided.

Table 3.2. Phospho-peptides that were most efficiently dephosphorylated by GST-PTP-BL, listed together with some information on the protein of origin.

Phospho-peptide[a]	Phospho-protein[b]	Description[c]
SAASFEp(Y)TILDPS	EPOR P19235	Erythropoietin receptor; pTyr426 is a known phosphorylated residue that regulates association with other proteins
MDLLRQp(Y)LRVETQ	ACACA Q13085	Acetyl-CoA carboxylase 1, involved in the biogenesis of fatty-acids. Tyr994 is not known to be phosphorylated *in vivo*
FRHDSGp(Y)EVHHQK	A4 P05067	Amyloid protein A4, important for neurite growth, neuronal adhesion and axonogenesis. Tyr681 is not known to be phosphorylated *in vivo*
RRYGDRp(Y)INLRGP	ACE P12821	Angiotensin-converting enzyme and inhibitor of bradykinin, ubiquitously expressed; Tyr270 is not known to be phosphorylated *in vivo*
RKFGDDp(Y)QVVTTS	IRK3 P48549	Inward rectifier potassium channel controlled by G proteins. Tyrosine phosphorylation of Tyr12 leads to channel deactivation
GIIATIp(Y)IIPGDI	BAT1 P82251	Peptide transporter of the kidney. Tyr365 is not known to be phosphorylated *in vivo*
KGQESEp(Y)GNITYP	PTN6 (SHP1) P29350	Protein tyrosine phosphatase expressed in brain; pTyr536 regulates protein activation
IHLEKKp(Y)VRRDSG	CSF1R P07333	Tyrosine kinase receptor that drives development of monocytes; phosphorylation of Tyr708 regulates molecular association
QLGQRIp(Y)QYIQSR	DYR1A Q13627	Dual specificity kinase highly expressed in brain; pTyr219 is an autophosphrylation site important for activation
LCQSGIp(Y)INVLDI	NPT4 O00476	Sodium/Phosphate cotansporter; Tyr337 is not known to be phosphorylated *in vivo*
EPPPPGp(Y)ENVSDI	FOLH1 Q04609	Glutamate carboxypeptidase that modulates excitatory neurotransmission in the brain; Tyr151 is not known to be phosphorylated *in vivo*
TSAEPQp(Y)QPGDQT	FGR P09769	Tyrosine protein kinase; pTyr523 is a known phosphorylated residue *in vivo*
GPNNNNp(Y)ANVELI	ACACB O00763	Acetyl-CoA carboxylase 2 is involved in fatty acid oxidation; Tyr329 is not known to be P *in vivo*

For footnotes, see Table 3.1.

Importantly, the GST-PTP-SL and GST-PTP-BL fusion proteins clearly show distinct selectivity towards the panel of phospho-peptides analyzed, revealing that at least part of the enzyme's substrate specificity is warranted in the assay. Further studies towards the candidate substrates that result from this phospho-peptide screen using GST-PTP-SL will be described later (paragraph 3.3).

3.1.3 GST-pull down from brain lysates and mass spectrometry

In view of the possible promiscuity of *in vitro* dephosphorylation activity of PTPs towards phosphotyrosine-containing peptides [Blanchetot et al., 2005], we performed additionally GST pull-down experiments on brain lysates and subsequent mass spectrometric analysis to obtain an independent list of candidate interacting proteins. Both wild type and C/S-D/A mutant GST-PTP-SL fusion proteins were used for pull-down assays. The wild type protein is expected to show interactions that are independent from the binding to the active site as it will dephosphorylate and release substrates. In contrast, a substrate trapping mutant should present both these interactions and those due to its trapping abilities towards phosphotyrosine-containing proteins (Blanchetot et al. 2005). As a specificity control we used the GST-PTP-BL fusion protein as well as GST itself. GST (fusion) proteins were incubated with adult mouse brain lysates and, after proper washings, the GST-containing proteins together with their interactors were eluted with GSH elution buffer. Eluates were initially inspected on silver-stained 12% SDS-gels to identify differential bands. Both wild type GST-PTP-SL and the C/S-D/A mutant appear sensitive to degradation under the conditions used here. The degradation products present in the eluates were distinguished on the basis of immunoreactivity, by western blotting using a polyclonal antibody to GST-PTP-SL (Figure 3.5). The polyclonal antibody to GST-PTP-SL did not reveal bands in the range 32-60 kDa of the GST-PTP-SL wild type protein lane indicating the absence of degradation products of this molecular weight while several ones are visible in the GST-PTP-SL C/S-D/A mutant protein lane (Figure 3.5, panel B). The membrane was overexposed to reveal eventual faint bands in the wild type lane. This differential behavior suggests that the silver-stained bands located in the range 32-60 kDa (Figure 3.5, panel A) may be interaction partners of the wild type GST-PTP-SL. Those interaction partners might be overshadowed but yet present in the C/S-D/A lane because of the high amount of degraded products. The GST-PTP-BL lanes display a silver-stained protein pattern in the range 32-60 kDa different from the one of both GST-PTP-SL isoforms, supporting the indication that the just mentioned 32-60 kDa bands in the GST-PTP-SL wild type lane are not sticking aspecifically to the GST-PTP-SL bait. Similar migration patterns were observed in three repeated experiments (not shown).

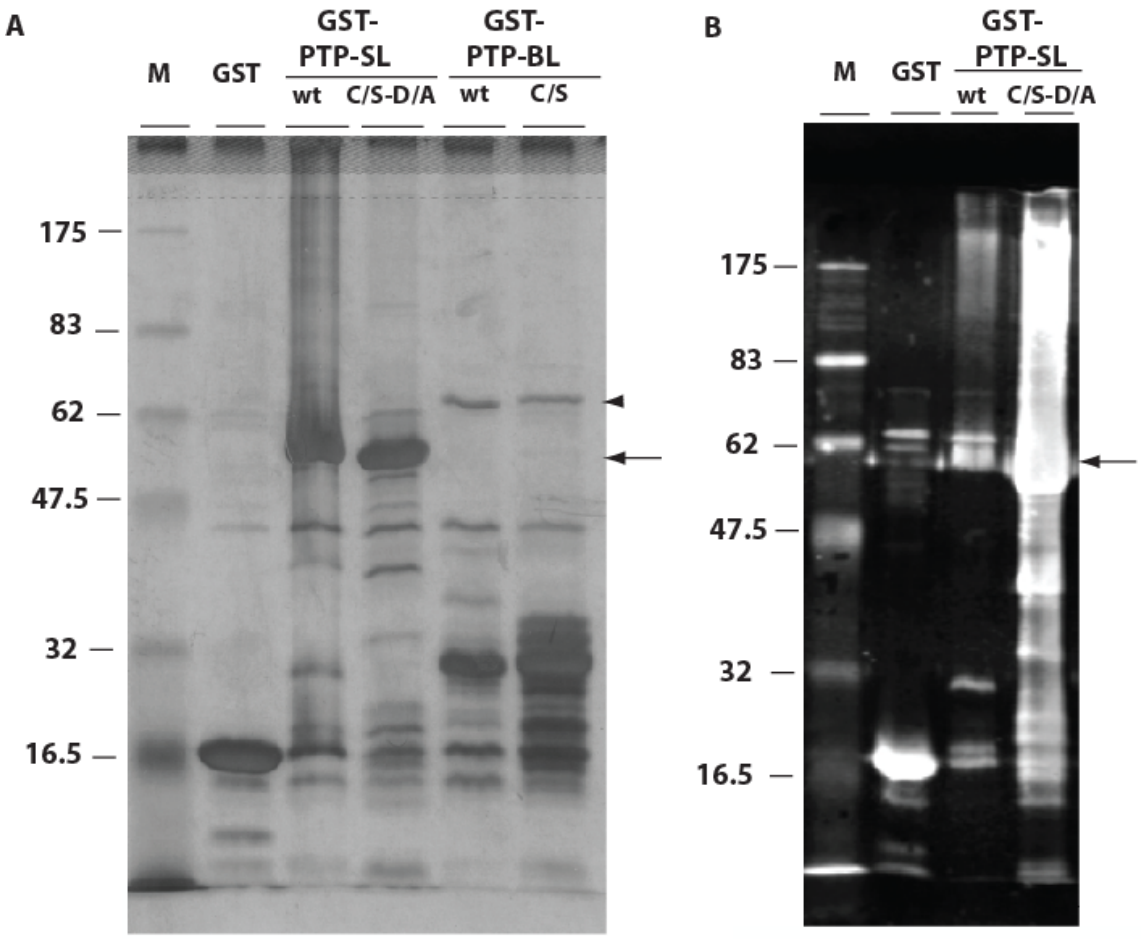

Figure 3.5. Profiling of protein bands after GST-pull down from mouse brain lysates. Aliquots of GST-PTP-SL and GST-PTP-BL eluates (indicated above the lanes, using the name of the applied GST fusion protein bait) were loaded on 12% SDS-gel and (A) stained with silver staining method or (B) blotted on PVDF membrane and incubated with antibody to GST-PTP-SL. As a negative control GST protein (about 26 KDa) was used. Arrows indicate the GST-PTP-SL fusion protein (about 60 KDa) while the arrowhead points to the GST-PTP-BL fusion protein band (about 70 KDa). Molecular weights are given on the left in kDa. M= molecular weight marker lane.

These findings allowed us to attempt an identification of interacting proteins by means of Liquid Chromatography coupled to Mass Spectrometry (LC-MS/MS). To this end, samples were again loaded on gel but now stained with MS-compatible Coomassie Brilliant Blue (CBB) dye. As expected, Coomassie-based staining is less sensitive than silver staining and therefore only few individual bands could be observed by eye (Figure 3.6). Based on the previous findings from silver-stained gels (Figure 3.5), we selected two different regions, one in the 32-45 and one in the 45-55 kDa range, that were cut out for further analysis by MS-based protein identification techniques. We made sure to avoid inclusion of the a-specific band at 45 kDa that is present in all samples, including the GST-purified proteins (Figure 3.6). We reasoned that proteins that may be identified in extracts from the GST control lane segments could then simply be ignored in the results obtained with the lanes of interest that should reveal the GST-PTP-SL and GST-PTP-BL specific interactors.

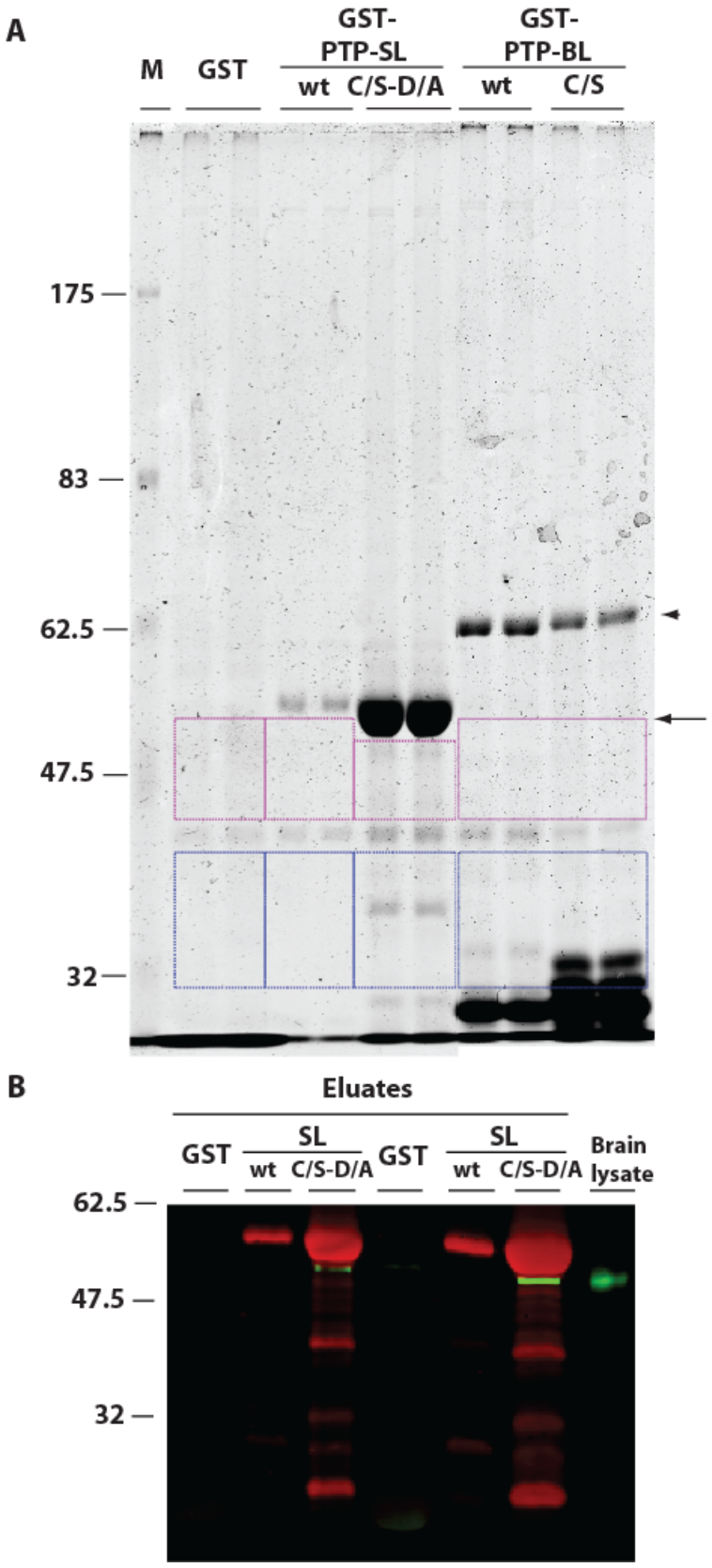

Figure 3.6. Schematic representation of gel region selection for mass spectrometry analysis and detection of CaMKIIα in brain pull downs. (A) Wild type and C/S-D/A GST-PTP-SL fusion proteins were used to affinity-purify associating proteins from mouse brain lysates. Protein complexes were eluated from the glutathione beads, subjected to SDS-PAGE and stained with Coomassie Brilliant Blue dye. For each sample, regions in the range of 45-55 kDa (pink squares) and 32-45 kDa (blue squares) were cut from the gel and collected. As control, the same regions in the GST and in the wild type and C/S GST-PTP-BL lanes were taken along. An a-specific band, around 45 kDa, was not included in the samples. Arrowhead and arrow point to the position of GST-PTP-BL and GST-PTP-SL fusion proteins respectively. Gel pieces were subsequently processed for LC-MS/MS analysis. (B) The presence of CaMKIIα in GST-PTP-SL affinity-purified eluates was confirmed by immunoblot detection on the same eluates using a monoclonal antibody to CaMKIIα (green band). Red bands represent immunostaining to the GST-PTP-SL fusion protein using an anti-GST-GFP antiserum. In the second three lanes twice the amount used in the first three lanes was applied. As a positive control for CaMKIIα immunostaining, total mouse brain lysate was loaded in the seventh lane. Molecular weight markers are indicated in kDa on the left.

The isolated gel pieces were subsequently used for in-gel trypsin digestion and resulting peptides were extracted and analyzed in a tandem liquid chromatography – mass spectrometric set-up. Obtained mass spectra were used to mine mouse protein databases with the Mascot algorithm (reference) and scores above 60 were considered protein candidate interactors for GST-PTP-SL. The full list of proteins identified in the GST-PTP-SL and GST-PTP-BL purified samples are reported in table S1. From these primary data we deduced a shortlist (Table 3.3.) based on the following considerations. Peptides of proteins that were also present in the samples taken from the GST control lanes were considered as GST-associating proteins or as non-specific binders to GSH beads, and therefore excluded. Next the peptides that were enriched in the GST-PTP-SL and GST-PTP-BL pull-down fractions were compared.

Since the GST fusion proteins and their breakdown products are released from the beads together with their interacting proteins when applying GSH-based elution buffers, they serve as internal controls in the mass spectrometry identification. Indeed many peptides that originate from proteins PTPRR and PTPN13 (PTP-BL) were successfully identified in the respective eluates. A PTP-BL-derived peptide was also detected in the samples isolated from the neighbouring GST-PTP-SL C/S-D/A eluate lane (Table S1), pointing to possibly a mild cross-contamination of abundant proteins from the adjacent GST-PTP-BL wt eluate lane (Figure 3.6). With this knowledge we inspected the list of GST-PTP-SL-interaction candidates for proteins that were abundantly represented in the GST-PTP-BL-purified sample. Peptides from interacting proteins are expected to be less abundant than those originating from the bait proteins themselves (GST-PTP-SL and GST-PTP-BL) and any contribution of contaminating peptides from interactors can be estimated based on the proportional occurrence in the respective lanes. After analysis of single cases, these considerations alone did not lead us to exclude any specific protein from the list of potential PTPRR partner proteins. Those excluded were the ones present in the GST lane also when having a Mascot score above 60 (e.g. Breast carcinoma-amplified sequence 1 and FAM164A) or notorious contaminants of affinity purifications (i.e actin, tubulin, Elongation factor 1-alpha).
Likewise, in the GST-PTP-BL eluates peptides were recovered that are obvious cross-contaminants from the GST-PTP-SL C/S-D/A eluates. The amount of GST-PTP-SL derived peptides in the GST-PTP-BL samples is considerable; about one-fifth of the GST-PTP-SL C/S-D/A sample intensities (Table S1). Therefore, we concluded that Calcium/calmodulin-dependent protein kinase II, Homer, Tau and Neuronal growth regulator 1 are to be excluded from the GST-PTP-BL candidate interactors list.

Three major classes of proteins were identified using GST-PTP-SL wt and C/S-D/A mutant proteins as affinity reagents: i) proteins with prominent roles in neuronal functioning (Calcium/calmodulin-dependent protein kinase II, Homer and Sodium/potassium-transporting ATPase); ii) proteins making part of cell-cell adhesion structures (Neuronal growth regulator 1); iii) proteins making part of the cytoskeleton and involved in actin remodeling (Dematin and Tau). The known PTPRR-associating proteins ERK1 and ERK2 (Pulido et al. 1998) were not found among the interactors, reflecting our use of a KIM-deficient PTPRR fusion protein that cannot bind MAPKs.

Interestingly, none of the proposed PTP-BL substrates (IκBα, RIL, Ephrin B, HER2, IRS-1 and STAT4, (Abaan and Toretsky 2008)) was identified in the pull-down experiment using GST-PTP-BL fusions, underscoring the importance of PTP-BL adaptor domains (FERM, KIND and PDZ) in mediating these protein-protein interactions. The proteins that were purified using the PTP-BL phosphatases domain (table S1) are, however, linked to processes in which PTP-BL is suspected to play an important role: cytokinesis, cell-cell adhesion and cytoskeletal organization (Erdmann 2003). Importantly, candidate interacting proteins have been identified that are distinct for the GST-PTP-SL and GST-PTP-BL fusion proteins, indicating that association and elution conditions allowed for PTP-specific binding interactions. Furthermore, it is comforting to note that the proteins that were identified via the Mascot scores of the derived peptides, with the exception of the highly abundant tau protein, are all within the size range expected from the gel pieces used.

When the previous phospho-peptide dephosphorylation approach (Tables 3.1 and 3.2) and the current GST-pull down strategy (Table 3.3) are compared one must conclude that they lead to the candidacy of different proteins. This may reflect the fact that the phospho-peptide array offers a limited and random panel of possible PTP substrates whereas the GST-pull down approach spanned the whole brain proteome as potential interactors. The mass spectrometric analysis identified CaMKII as a candidate substrate of the phosphatase domain of PTPRR proteins (Table 3.3). Much more peptides belonging to CaMKII were retrieved in the eluates obtained from the substrate trapping mutant than from the wild type isoform, indicating that the interaction may be favored by the presence of phosphorylated tyrosine residues. The cytoplasmic protein CaMKIIα contains two known tyrosine phosphorylation sites; at the conserved residues 12 and 230, respectively (Ballif et al. 2008). Presence of CaMKIIα in GST-PTP-SL eluates was subsequently confirmed on western blot (Fig. 3.6).

Table 3.3. Proteins identified by LC/MS-MS and Mascot Search that were affinity-purified from brain lysates using GST-PTP-SL as bait. Proteins are listed that had Mascot scores above 60 and did not purify in isolates using GST as a bait or GST beads alone. Some proteins purified also in isolates using GST-PTP-BL wt and C/S baits and are marked with an #. Data from two independent isolates are shown. A full list of proteins identified in this way is provided as Supplementary Material (Table S1).
Subunits α and β of CaMKII have high sequence identity and the retrieved peptides did not allow to distinguish between the two isoforms.

Protein name Mnemonic identifier Uniprot Accession number	Mass (KDa)	GST-PTP-SL wt		GST- PTP-SL C/S-D/A		Function
		Mascot score	Queries matched	Mascot score	Queries matched	
Calcium/calmodulin-dependent protein kinase II alpha/beta chain KCC2A_MOUSE KCC2B_MOUSE #	54 60	145	3	449	16	Ser/Thr Kinase. Prominent in the central nervous system as it may function in long-term potentiation and neurotransmitter release
Homer protein homolog 1 HOME1_MOUSE #	41	221	5	176	5	Postsynaptic density scaffolding protein that binds and cross-links cytoplasmic regions of several proteins
Dematin DEMA_MOUSE	45	237	7	0	0	Actin-bundling protein
Neuronal growth regulator 1 NEGR1_MOUSE #	38	129	4	94	2	Cell adhesion protein of the IgLON family
Protein FAM98B FA98_MOUSE	45	65	1	120	3	Component of the tRNA-splicing ligase complex
Microtubule-associated protein tau TAU_MOUSE #	76	84	4	32	1	Microtubule-binding protein in neurons
Sodium/potassium-transporting ATPase subunit beta-1 AT1B1_MOUSE	35	78	2	43	1	Regulatory subunit oof the ATPase complex that catalizes the hydrolysis of ATP coupled with the exchange of Na^+ and K^+ ions across the plasma membrane

3.2 Substrate validation by *in vitro* and *in vivo* approaches

To satisfy the requirements for the definition of PTP substrates (Tiganis and Bennett 2007) as discussed in the introductory section, we next performed assays *in vitro* and in over-expressing system. We used either HEK293T or COS-1 cells as mammalian source for the ectopic expression of the candidate substrates in view of the LargeT-mediated episomal replication boost of plasmids that are transfected in and the consequent high expression levels. In all experiments where PTPRR was co-expressed with the candidate substrates we decided to use full-length PTPRR isoforms, most notably PTPBR7, and not the GST fusion proteins applied previously. This to resemble as much as possible the physiological condition at which dephosphorylation and binding of substrates should take place (Tiganis and Bennett 2007). During these studies we noted that PTPRR proteins are only weakly expressed in HEK293T cells (data not shown). On the other hand, COS-1 cells express PTPRR proteins very strongly. We therefore opted for using COS-1 cells in co-expression experiments. This choice, however, sometimes led to an unsuspected effect of PTPRR expression levels on the synthesis of the co-expressed substrate candidates (will be discussed in paragraph 3.2.2). We focused our attention on four putative substrate proteins, three of them – HER4, HER3 and SHP1 – were coined as putative candidates by the phospho-peptide array (Table 3.1) and one – N-cadherin – was proposed as a substrate in a recent study (Barr et al. 2009) based on PTPRR's capability to dephosphorylate a phosphotyrosine-containing peptide originating from N-cadherin. Time constraints kept us from further testing the candidate substrate CaMKIIα that resulted from the MS-based screen (Table 3.3.).

3.2.1 Dephosphorylation and binding assays *in vitro*

Dephosphorylation and binding of cognate substrates by PTPRR were first tested *in vitro* using the purified GST fusion proteins in combination with lysates from cells over-expressing the candidate substrates. For these *in vitro* assays, the COS-1 or HEK293T cells producing the candidate substrate proteins were subjected to appropriate stimuli to induce (hyper-) phosphorylation of the proteins of interest. Furthermore, cells were lysed under conditions that would maximally preserve this phosphorylation status.
Initially, the stimulus for hyper-phosphorylating SHP1 and HER proteins was the treatment with the general PTP inhibitor pervanadate. In some instances SHP1 was co-expressed with cSRC, a well known tyrosine kinase and activator of SHP1 (Frank et al. 2004). During later studies on the HER proteins and on N-cadherin we refrained from the use of the PTP inhibitor since we suspected that any remaining pervanadate might interfere with PTPRR activity during subsequent dephosphorylation assays. Instead, we turned to a more physiological but milder stimulation; serum addition after overnight serum starvation. To preserve the (hyper-)phosphorylation status in protein lysates we included sodium orthovanadate as phosphatase inhibitor in the lysis buffers. The effects of the two types of vanadium compounds on PTPRR activity were studied as well and are described in paragraph 3.3.

3.2.1.1 PTPRR does not interact with SHP1 *in vitro*

Wild type SHP1 and the Y538F mutant form were independently co-expressed with cSRC in HEK293T cells and incubated with either wild type or C/S-D/A mutant GST-PTP-SL that had been produced in bacteria and purified over GSH beads. SHP1 Y538F mutant lacks an important cSRC-dependent phosphorylation site that makes it less active towards cSRC substrates in comparison to wild type SHP1 (Frank et al. 2004). Given the biological importance of this phosphorylation site we investigated whether it is subjected to dephosphorylation by PTPRR and included the Y538F isoform in our experiment. This experimental set-up allowed simultaneously the monitoring of i) dephosphorylation *in vitro* by the wild type phosphatase and ii) binding to the substrate-trapping mutant. SHP1 phospho-levels were unchanged prior and post incubation with GST-PTP-SL fusion proteins, independently on the isoform used (Figure 3.7A). When the mixtures containing cSRC, SHP1 and GST-PTP-SL bound to beads were subjected to pull down SHP1 isoforms could not be retrieved (Figure 3.7B). Test of cSRC expression, equal loading and GST-PTP-SL precipitation by immunodetection confirm the accuracy of the applied procedure. It can therefore be concluded that SHP1 does not bind to the GST-PTP-SL trapping mutant nor that it is dephosphorylated by the wild type GST-PTP-SL.

To test whether perhaps the co-expression of full-length PTPRR proteins in SHP1-expressing cells is required for efficient substrate binding, we repeated the dephosphorylation test using HA-tagged wild type and C/S mutants of the cytoplasmatic PTPRR isoforms (PTPPBSγ-37 and PTPPBSγ-42). YFP-tagged SHP1 was immunoprecipitated from COS-1 cell lysates and incubated with immunoprecipitated HA- tagged PTPPBSγ proteins separately obtained from over-expressing COS-1 cells. The proteins involved were efficiently produced in the transfected cells, and SHP1 phosphorylation levels were clearly detectable. To avoid loss of SHP1 phosphorylation and of HA-tagged protein amounts that would derive from elution, both fusion proteins were tested while still bound to beads. In these conditions we could not observe a significant decrease in YFP-SHP1 phosphorylation levels upon addition of the wild type PTP as compared to its enzymatically dead counterpart (Figure 3.8). Thus, under the conditions used we did not obtain evidence that SHP1 represents a *bona-fide* PTPRR substrate.

Figure 3.7 (next page). SHP1 is not a substrate of GST-PTP-SL *in vitro*. HEK293T cells ectopically co-expressing cSRC and SHP1 wild type (SHP1wt) or SHP1 Y538F mutant (SHP1YF) proteins were lysed in orthovanadate-containing lysis buffer. Lysates were incubated with GSH-beads containing 3 µg of either wild type (wt) or C/S-D/A GST-PTP-SL (mt) protein. (A) SHP1 expression (anti SHP1) and phospho-levels (anti PY20) prior (Lys prior) and post (Lys post) the incubation with GST-PTP-SL were checked by immunoblot analysis. cSRC expression (anti panSrc2) and equal loading (anti GAPDH) were assessed by immunoblot analysis of separate membranes. Immunoreactive bands for cSRC (arrow, cSrc) and SHP1 (arrowhead) are indicated. (B) SHP1 is not bound by GST-PTP-SL. Mixtures containing GST-PTP-SL recombinant protein bound to beads and SHP1-containing lysates were mixed, incubated and centrifuged, and SHP1 pull-down was checked on blot (anti SHP1). Successful pull-down of GST fusion proteins was verified by immunostaining (anti GST-GFP). GST was used as a specificity control. Molecular weights are given in kDa on the left. M= molecular weight marker lane.

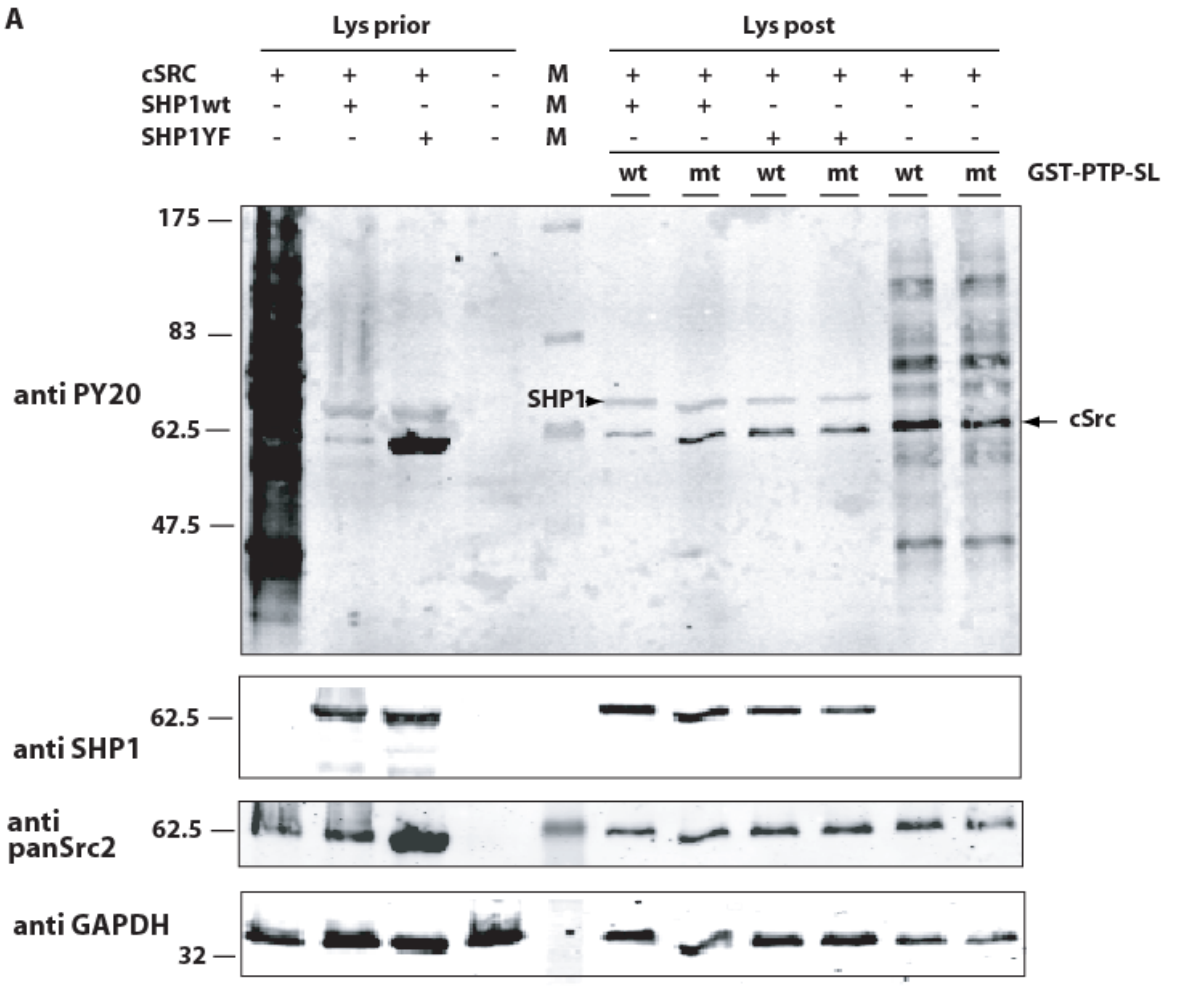
A
Lys prior
Lys post
cSRC + + + - M + + + + + +
SHP1wt - + - - M + + - - - -
SHP1YF - - + - M - - + + - -
wt mt wt mt wt mt GST-PTP-SL
175
83
62.5
47.5
anti PY20
SHP1
cSrc
anti SHP1
62.5
anti panSrc2
62.5
anti GAPDH
32

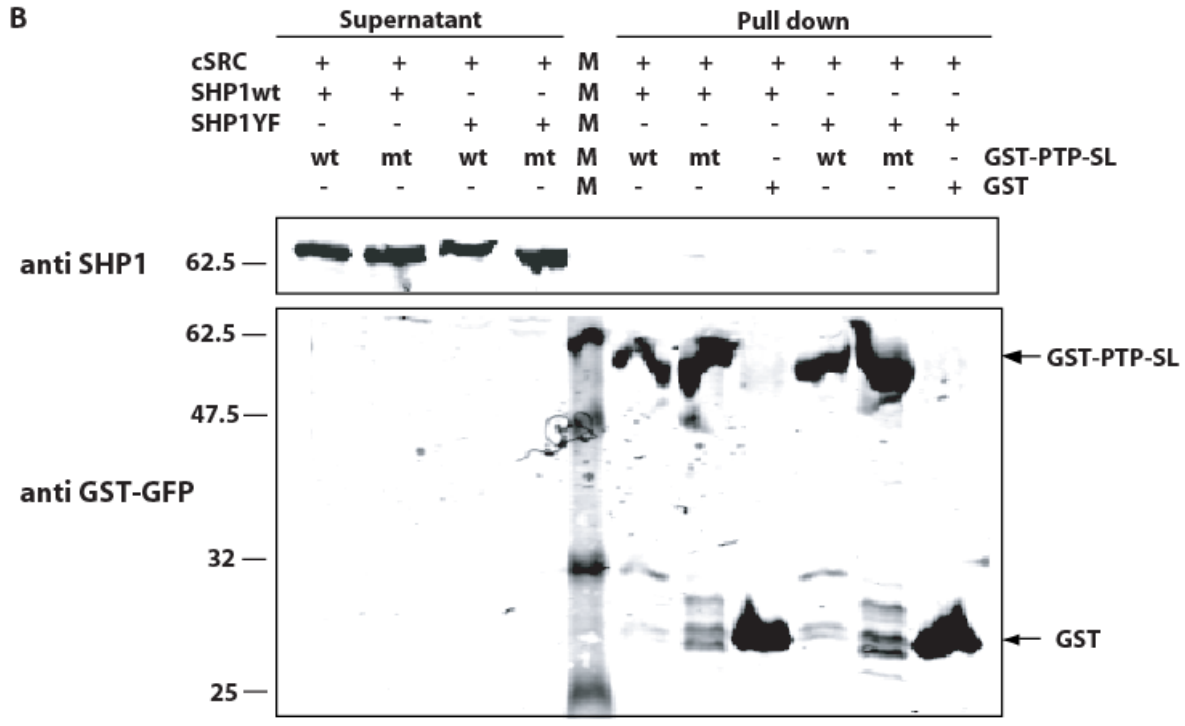
B
Supernatant
Pull down
cSRC + + + + M + + + + + +
SHP1wt + + - - M + + + - - -
SHP1YF - - + + M - - - + + +
wt mt wt mt M wt mt - wt mt - GST-PTP-SL
- - - - M - - + - - + GST
anti SHP1
62.5
62.5
47.5
anti GST-GFP
32
25
GST-PTP-SL
GST

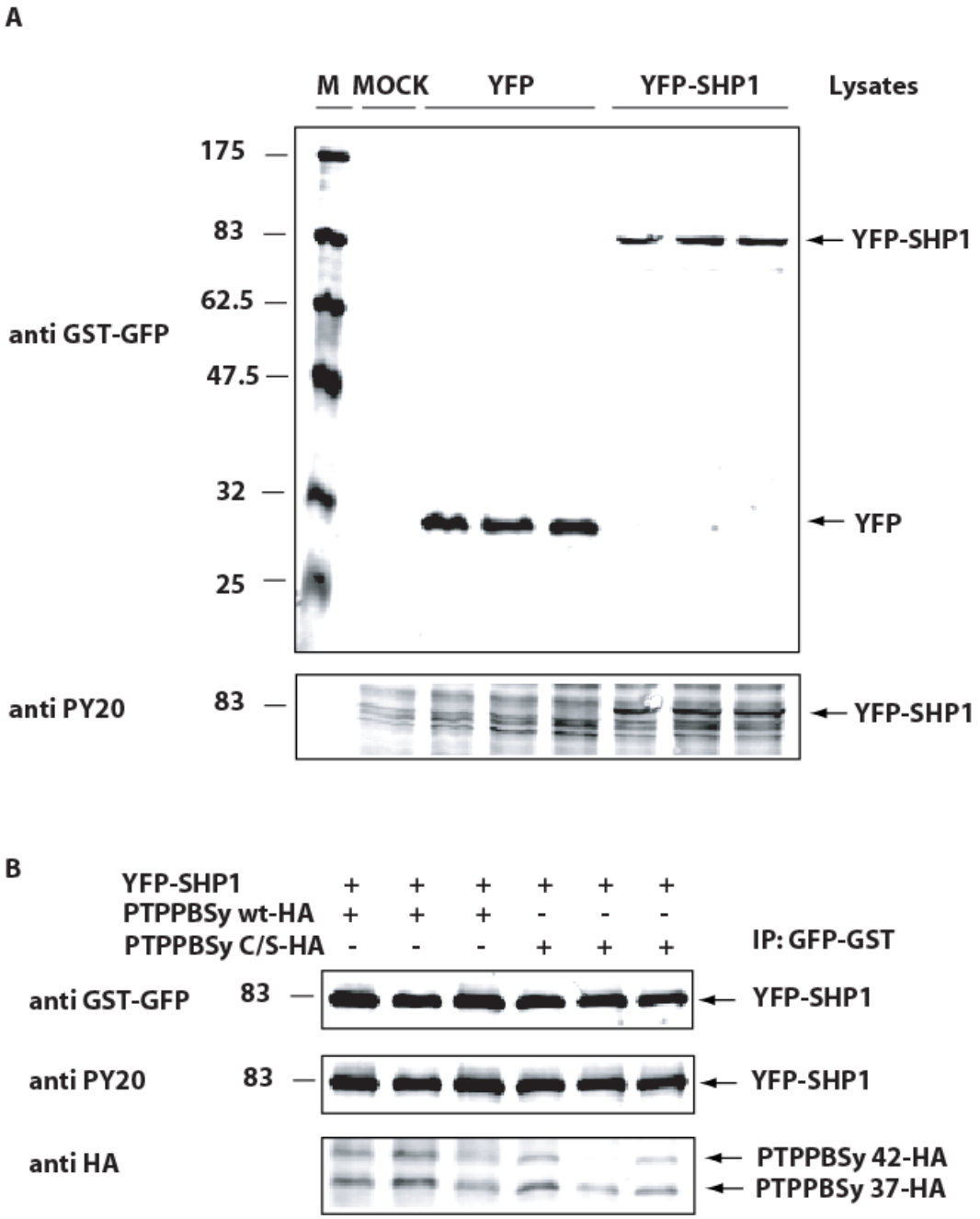

Figure 3.8. YFP-SHP1 is not dephosphorylated by PTPPBSγ *in vitro*. COS-1 cells expressing YFP-tagged SHP1, or YFP as a control, were lysed in orthovanadate-containing lysis buffer after treatment with pervanadate. (A) YFP-SHP1 expression (anti GST-GFP) and phosphorylation (anti PY20) were tested on western blot. Arrows indicate the positions of the corresponding protein bands on the blot. (B) YFP-SHP1 phospho-levels are not changed upon addition of PTPPBSγ**.** Immunoprecipitated YFP-SHP1 (IP: GFP-GST) bound to beads was incubated with either immunoprecipitated PTPPBSγ-HA wild type or C/S mutant bound to beads and YFP-SHP1 dephosphorylation was tested by immunoblotting with anti PY20 antibody. Presence of YFP-SHP1 (anti GST-GFP) and of PTPPBSγ (anti HA) in the mixtures was confirmed. Three replicates per condition are shown. Molecular weights are given in kDa on the left. M= molecular weight marker lane.

3.2.1.2 PTPRR does not interact with HER3 *in vitro*

Phosphorylated HER3 was tested for being pulled-down by GST-PTP-SL C/S-D/A fusion protein. Cells had been incubated with pervanadate to increase tyrosine phosphorylation levels. Resulting lysates were then treated with EDTA and DTT to remove residual, unbound pervanadate. Subsequently, bacterially produced recombinant GST fusion proteins, still bound to GSH-beads, were added. After incubation, the beads were again collected and tested for associating HER3 protein. As shown in Figure 3.9A, no pull-down of HER3 was observed using GST-PTP-SL C/S-D/A fusion protein-coated beads. This may be due to the loss of phosphorylation after EDTA and DTT treatment and overnight incubation. To maintain a high phospho-status of HER3 in the lysates during the incubation we then repeated the experiment without EDTA and DTT treatment. This indeed partially preserved the phosphorylation status in the lysate but no pull-down of phosphorylated HER3 by GST-PTP SL C/S-D/A mutant was observed (Figure 3.9B). Importantly, this experiment clearly indicates that the treatment of pervanadate-subjected lysates with EDTA and DTT does not only neutralize excess PTP inhibitor but also – at least partly - leads to re-activation of endogenous phosphatases in the cell lysate. This coins a difficult experimental paradox; the vanadate compounds are necessary to induce or maintain hyper-phosphorylation of proteins but they need to be inactivated to allow the testing of dephosphorylation performance by the recombinant PTP under study.

3.2.1.3 PTPRR does not bind HER4 *in vitro*

To test HER4's candidacy as a PTPRR substrate, lysates of HER4 overexpressing cells that had been treated with pervanadate were used in a pull–down assay. To this end, GST-PTP-SL C/S-D/A fusion protein-containing beads were added and resulting protein complexes were analysed on immunoblots. Two main bands were recognized by the anti HER4 antibody, the expected band at 180 kDa and the cleaved band around 80 kDa (Sundvall et al. 2008; Muraoka-Cook et al. 2009). Inspection with anti-phosphotyrosine antibodies demonstrates ample phosphorylation on tyrosines in many proteins, including the full-length HER4 protein. Nevertheless, as shown in Figure 3.10A, no pull-down was detectable and the phosphorylated HER4 remained in the supernatant. We did not treat the lysates with EDTA and DTT and therefore excess vanadate compounds may compete for binding to the PTP fusion proteins. We tested also if the interaction is perhaps dependent on the presence of a transmembrane, full-length PTPRR protein. We chose to repeat the assay using the membrane-localized isoform PTPBR7 because hydrophobic domains may be required to allow efficient interaction *in vitro* with the transmembrane HER4 protein. Lysates from cells over-expressing HER4 were incubated with either immunoprecipitated PTPBR7-HA wild type or C/S mutant protein loaded on beads. Subsequently, beads were briefly centrifuged and co-immunoprecipitation of HER4 was tested. We did not observe differential phospho-levels after incubation of HER4 lysates either with the wild type or the C/S mutant of PTPBR7. No co-immunoprecipitation occurred either (Figure 3.10B).

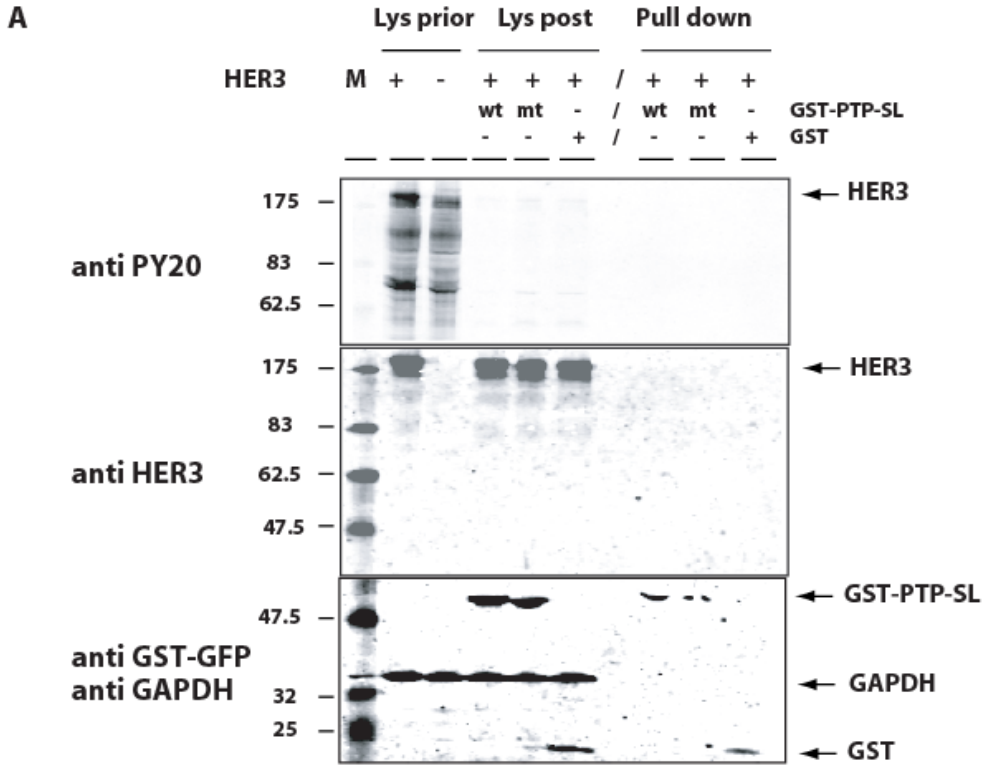
A
Lys prior
Lys post
Pull down
HER3
M
wt
mt
GST-PTP-SL
GST
anti PY20
anti HER3
anti GST-GFP
anti GAPDH
175
83
62.5
47.5
32
25
HER3
GST-PTP-SL
GAPDH
GST

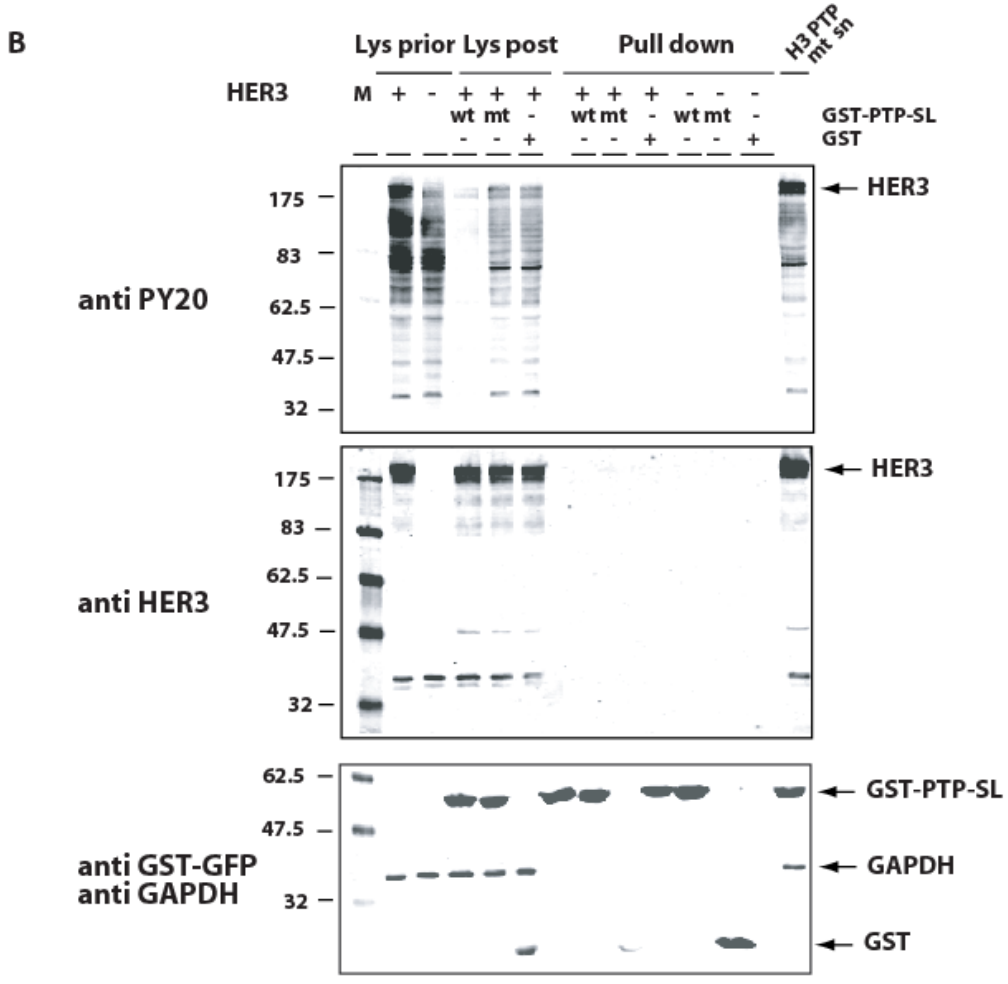
B
Lys prior
Lys post
Pull down
H3 PTP mt sn
HER3
M
wt
mt
GST-PTP-SL
GST
anti PY20
anti HER3
anti GST-GFP
anti GAPDH
175
83
62.5
47.5
32
HER3
GST-PTP-SL
GAPDH
GST

Figure 3.9 (previous page). HER3 is not a substrate of GST-PTP-SL *in vitro*. Pervanadate-treated COS-1 cells ectopically expressing HER3 were lysed in orthovanadate-containing buffer. Lysates were split in two parts and either incubated with 5 mM EDTA and 10 mM DTT (A) or left unaltered (B). Subsequently, samples were incubated with beads containing either 3 µg wild type GST-PTP-SL (wt), C/S-D/A mutant GST-PTP-SL (mt) or GST protein itself. Subsequently, beads were removed again from the lysates and (phospho)proteins remaining in the lysate or associated to the beads were monitored on western blots. HER3 expression (anti HER3) and phosphotyrosine levels (anti PY20) prior (Lys prior) and post (Lys post) the incubation with GST-PTP-SL were immuno-detected. Equal loading was monitored using anti GAPDH. Mixtures containing HER3 and GST-PTP-SL-loaded beads were centrifuged and GST fusion protein (anti GST-GFP) and HER3 (anti HER3) pull-down (pull-down lanes) was checked by immunostaining. An aliquot of the remaining supernatant after the pull-down performed with GST-PTP-SL C/S-D/A (HER3 PTP mt sn) was also tested for the presence of HER3. Molecular weights are given in kDa on the left. M= molecular weight marker lane.

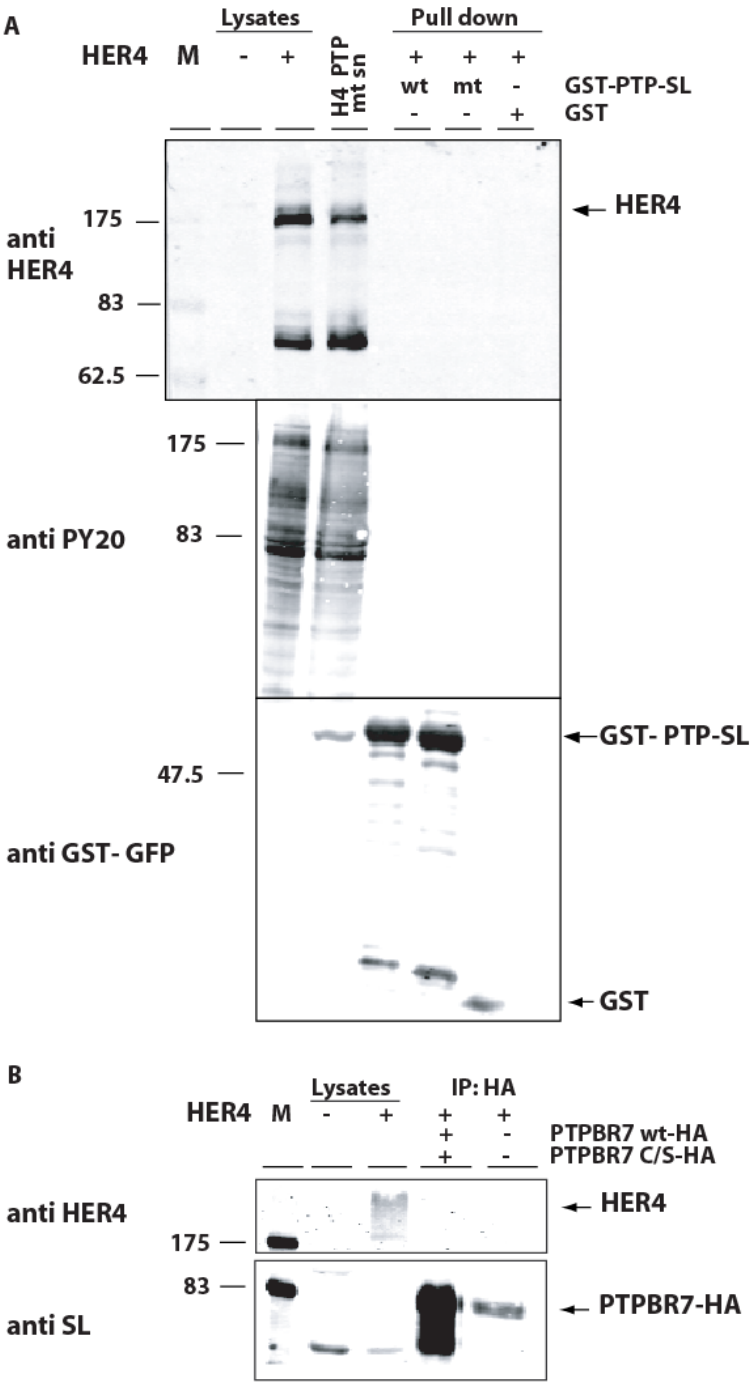

Figure 3.10 (side). HER4 is not bound by the GST-PTP-SL C/S-D/A or PTPBR7 C/S substrate mutants *in vitro*. COS-1 cells ectopically expressing HER4 were lysed in orthovanadate-containing lysis buffer after treatment with pervanadate. Equal volumes of the lysates were incubated with 3 µg of either wild type (wt), C/S-D/A GST-PTP-SL (mt) protein or GST itself coated on GSH-beads. Subsequently, protein complexes associated to the beads were collected and analyzed by western blotting. (A) HER4 expression (anti HER4) and phospho-levels (anti PY20) in lysates (Lysates) and, after incubation, on the GST-PTP-SL or GST-coated beads (Pull down) were checked by immunoblot. Successful pull-down of GST fusion proteins was verified by immunostaining (anti GST-GFP). An aliquot of supernatant from the pull-down performed with GST-PTP-SL C/S-D/A (HER4 PTP mt sn) was included to check for presence of HER4 after the incubation. (B) HER4 lysates were incubated with either immunoprecipitated PTPPBR7-HA wild type or PTPPBR7-HA C/S mutant bound to beads and HER4 co-immunoprecipitation (IP: HA) was tested by immunoblotting with anti HER4 antibody. Presence of PTPBR7 (anti SL) in the mixtures was confirmed. Molecular weights are given in kDa on the left.
M= molecular weight marker lane.

3.2.2 Dephosphorylation and binding assays in over-expressing cells

A second approach to validate the candidacy of SHP1, HER4 and HER3 as PTPRR substrates was to co-express them with either wild type or C/S mutant PTPRR isoforms in COS-1 cells and observe if the subtrate trapping mutant had the ability to bind the substrates and protect them from dephosphorylation relative to the wild type phosphatase. We chose to use COS-1 cells because with several other cell lines (including HEK293T) only very low PTPRR expression levels were obtained. In addition, we observed that PTPRR over-expression considerably hindered the co-expression of HER proteins (Fig 3.11). The effect was most notable for HER3, where increasing plasmid amounts of either transmembrane or cytosolic PTPRR proteins resulted in reduced levels of the HER3 180 kDa protein band. A reduction of the PTPRR plasmid amount used in our transfections was matched by lower cytosolic PTPRR protein levels, while transmembrane PTPRR protein levels were hardly affected by the plasmid amounts. Intriguingly, expression of inactive PTPBR7 protein had no apparent effect on the levels of co-transfected HER3 while an increase in expression of inactive PTPPBSγ did lead to a reduction in HER3 expression levels. Conversely, HER4 levels were affected both by wild type and C/S mutant PTPBR7 levels. In particular, expression of both active and inactive PTPBR7 led to reduced HER4 expression. Since our aim was to obtain detectable levels of both the candidate substrates and their phospho-levels, we decided to reduce the amount of PTPRR plasmid for our co-transfections. Starting from the standard amount of 1 μg/well indicated for DEAE-dextran method we tested lower concentrations of PTPRR encoding plasmid until we reached decent expression levels of HER and SHP1 proteins. Finally, 0.01 μg and 0.1 μg plasmid/well of PTPRR encoding plasmid were used in the case of co-transfection with HER proteins and SHP1, respectively, while plasmid amounts for the candidate substrates were kept constant at 1 μg/well.

Figure 3.11 (next page). HER3 and HER4 expression levels are sensitive to co-expressed PTPRR levels. 1 μg of the CMV-promoter-containing pRK5-HER3 plamid was co-tansfected with (a) 0.5, (b) 0.25 and (c) 0.1 μg of SV40-early-promoter-containing (A) PSG8-PTPBR7-HA, pSG8-PTP-SL-HA or (B) pSG8-PTPPBSγ-HA plasmid in COS-1 cells. Total lysates were collected 24 hours after transfection and HER3 and PTPRR expression levels were analyzed by immunodetection using anti-HER3 and anti 6A6 antibodies, respectively. Equal loading was assessed by immunodetection of tubulin (anti TUB). (C). 1 μg of the CMV-promoter-containing pCMV-HER4 plamid was co-transfected with (a) 0.5, (b) 0.25 and (c) 0.1 μg of SV40-early-promoter-driven PSG8-PTPBR7-HA plasmid in COS-1 cells. Total lysates were collected 24 hours after transfection and HER4 and PTPBR7 expression was analyzed on immunoblots using antibodies specific for HER4 and the cytoplasmatic domain of PTPBR7 (anti SL), respectively. Equal loading was assessed by tubulin immunostaining (anti TUB). Molecular weights are given in kDa on the left. M= molecular weight marker lane.

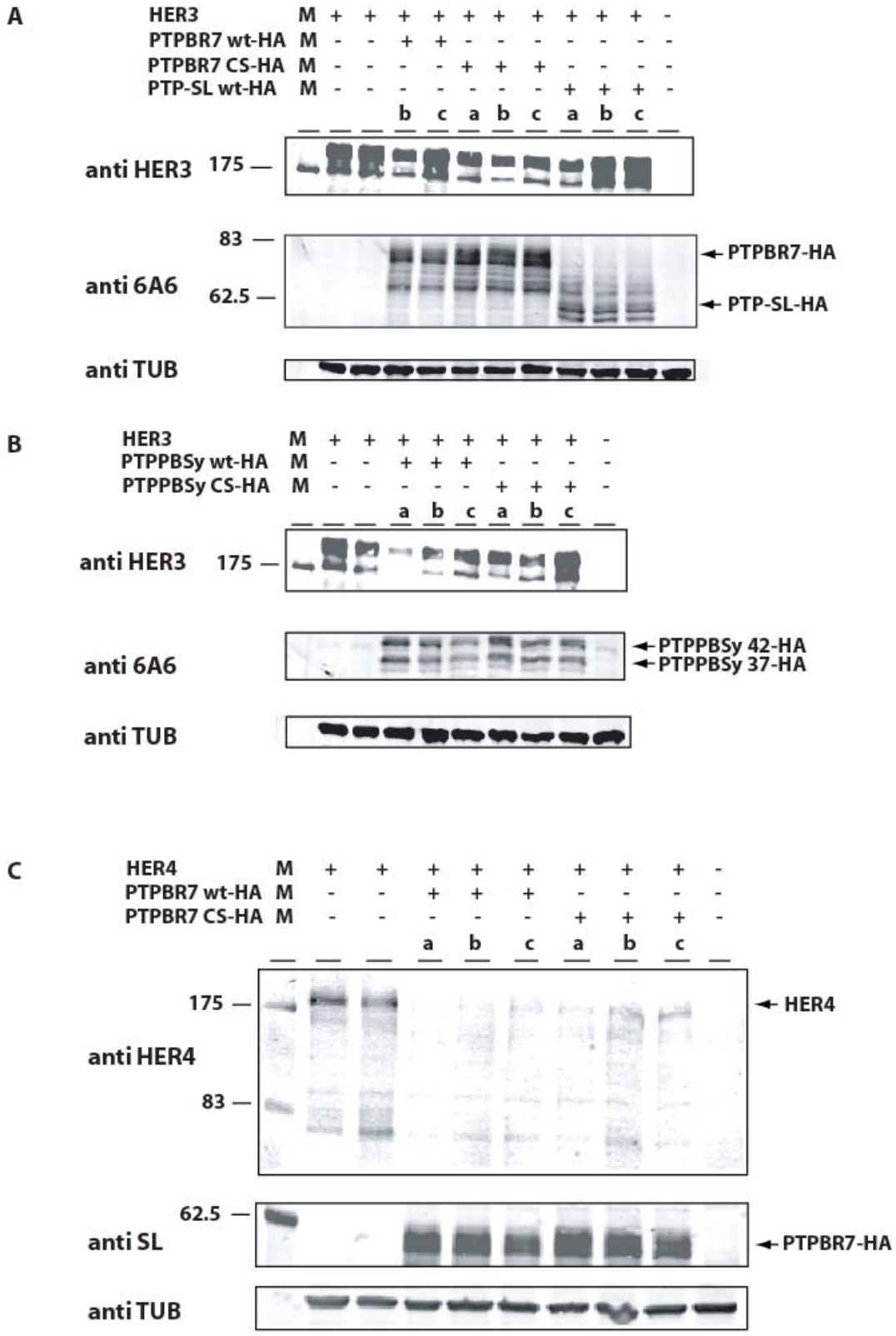
A
HER3 M + + + + + + + + + + -
PTPBR7 wt-HA M - - + + - - - - - - -
PTPBR7 CS-HA M - - - - + + + - - - -
PTP-SL wt-HA M - - - - - - - + + + -
b c a b c a b c
anti HER3
175
83
anti 6A6
62.5
PTPBR7-HA
PTP-SL-HA
anti TUB
B
HER3 M + + + + + + + + -
PTPPBSy wt-HA M - - + + + - - - -
PTPPBSy CS-HA M - - - - - + + + -
a b c a b c
anti HER3
175
anti 6A6
PTPPBSy 42-HA
PTPPBSy 37-HA
anti TUB
C
HER4 M + + + + + + + + -
PTPBR7 wt-HA M - - + + + - - - -
PTPBR7 CS-HA M - - - - - + + + -
a b c a b c
175
anti HER4
83
HER4
62.5
anti SL
PTPBR7-HA
anti TUB

3.2.2.1 PTPPBSγ does not interact with SHP1 when co-expressed in COS-1 cells

Having established the required co-transfection conditions, we set out to investigate the putative interplay between PTPRR and SHP1 proteins. Either SHP1 or YFP-SHP1 was co-transfected with the different PTPPBSγ variants and hyper-phosphorylation of SHP1 variants was induced by cSRC co-transfection or through pervanadate treatment. Following lysis, the PTPRR proteins were immunoprecipitated and obtained complexes were analysed on immunoblots. As shown in Figure 3.12B, we observed co-immunoprecipitation of both wild type and Y538F mutant SHP1 with the PTPPBSγ wt but not with the PTPPBSγ C/S mutant protein. No significant difference in phospho-levels were present, however (data not shown). In contrast, when the YFP-tagged version of SHP1 was assessed, either using pervanadate stimulation or cSRC co-transfection, we could not observe any co-immunoprecipitation with PTPPBSγ isoforms (Figure 3.12D and 3.12F). Furthermore, we did not observe a differential phosphorylation of YFP-SHP1 when co-expressed with PTPPBSγ or PTPBR7 C/S substrate trappers (Figure 3.12C, 3.12E and 3.12G). Perhaps presence of the YFP tag is hampering the interaction with the PTPPBSγ proteins, but then still it remains puzzling why untagged wild type and Y538F mutant SHP1 bound to the PTPPBSγ wild type (and not to the trapping C/S mutant phosphatase). In summary, we did not obtain unequivocal proof that PTPRR and SHP1 signalling pathways are partly intertwined.

Figure 3.12 (next page). SHP1 as candidate substrate of PTPRR in COS-1 over-expression system. (A-B) SHP1 interacts with PTPPBSγ-HA after pre-treatment with pervanadate. COS-1 cells ectopically expressing wild type and Y538F mutant SHP1 and either PTPPBSγ-HA wt or PTPPBSγ-HA C/S mt were pre-treated with pervanadate and lysed in orthovanadate-containing lysis buffer. (A) SHP1 (anti SHP1) and PTPPBSγ-HA (anti SL) expression were confirmed on western blot. (B) Upon immunoprecipitation of PTPPBSγ-HA isoforms (IP: 6A6) from lysates in (A), co-purifying SHP1 was detected on immunoblots using anti-SHP1 antiserum. Presence of PTPPBSγ-HA (anti SL) in the immunoprecipitates was checked by western blotting. (C-D) YFP-SHP1 does not interact with PTPPBSγ-HA after pre-treatment with pervanadate. COS-1 cells ectopically expressing wild type and Y538F mutant YFP-SHP1 together with either PTPPBSγ-HA wt or PTPPBSγ-HA C/S mt were pre-treated with pervanadate and lysed in orthovanadate-containing lysis buffer . (C) YFP-SHP1 expression (anti GST-GFP) and phosphorylation (anti PY20) and PTPPBSγ-HA (anti SL) expression were checked on immunoblots. (D) Upon immunoprecipitation of PTPPBSγ-HA isoforms (IP:HA) from lysates in (C), YFP-SHP1 co-immunoprecipitation and phospho-status were checked with anti GST-GFP and anti PY20 antibodies respectively. Presence of PTPPBSγ-HA (anti HA) in the immunoprecipitates was checked by western blotting. (E-F-G) YFP-SHP1 co-expressed with cSRC does not interact with HA-tagged PTPPBSγ or PTPBR7. COS-1 cells ectopically expressing wild type and Y538F mutant YFP-SHP1 together with cSRC and either PTPPBSγ-HA wt, PTPPBSγ-HA C/S or PTPBR7-HA C/S were lysed in orthovanadate-containing lysis buffer. (E) YFP-SHP1 expression (anti GST-GFP) and phosphorylation (anti PY20), HA-tagged PTPRR variant expression (anti SL) and equal loading (anti GAPDH) were all monitored by western blotting. (F) Upon immunoprecipitation of YFP-SHP1 isoforms (IP:GFP) from lysates in (E), co-immunoprecipitation of HA-tagged PTPRR variants was checked with anti SL antibody. Immunoprecipitation of YFP-SHP1 was verified by immunodetection to GFP (anti GFPmono). Apparent molecular weights are indicated in kDa on the left. M= molecular weight marker lane. (G) Quantitative representation of YFP-SHP1 phospho-levels as observed in (E), expressed as ratios of anti PY20 and anti GFP-GST signals. Values, displayed as arbitrary units (a.u.), represent the mean ± SD.

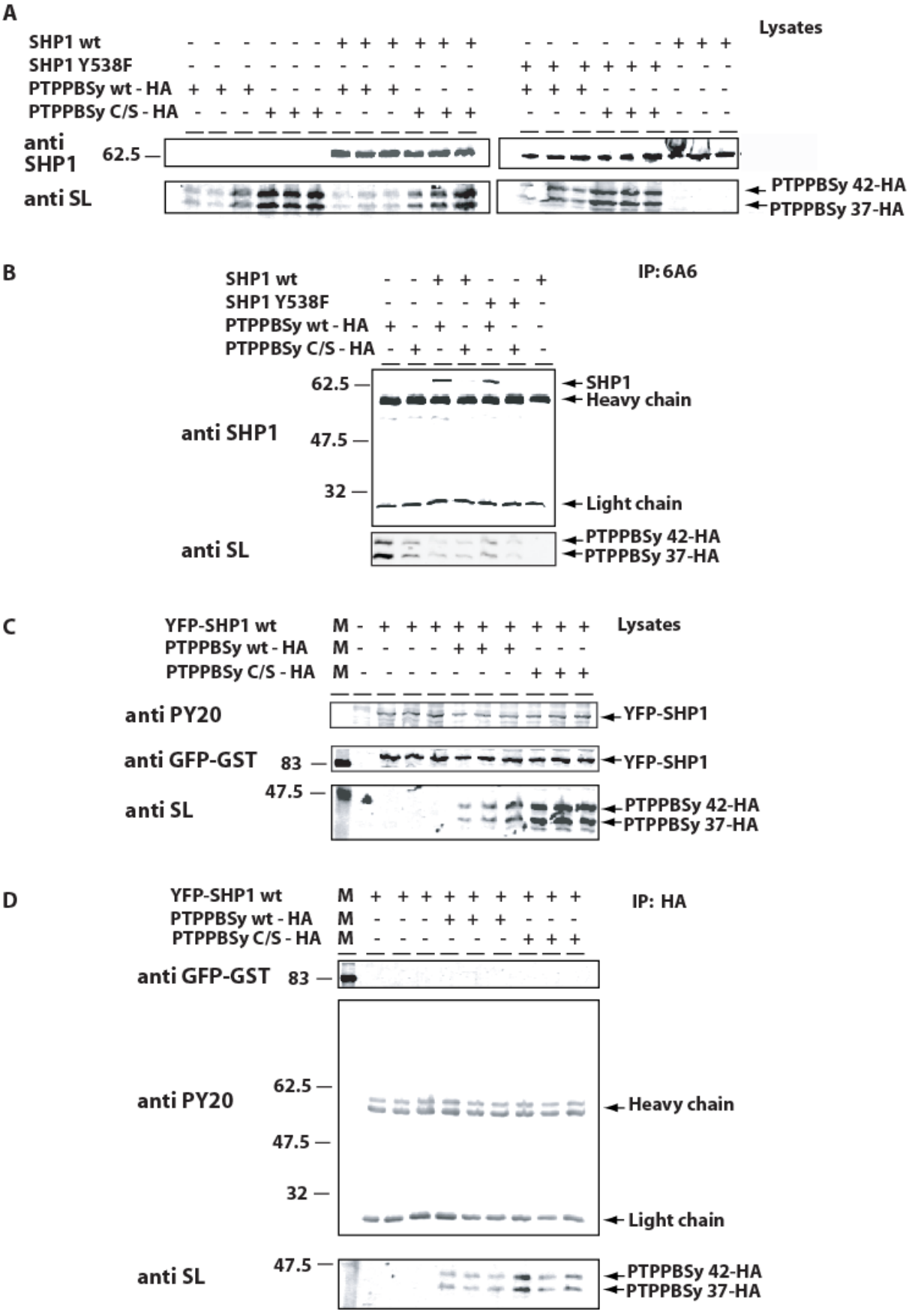
A
Lysates
SHP1 wt
SHP1 Y538F
PTPPBSy wt - HA
PTPPBSy C/S - HA
anti SHP1
62.5
anti SL
PTPPBSy 42-HA
PTPPBSy 37-HA
B
IP: 6A6
SHP1 wt
SHP1 Y538F
PTPPBSy wt - HA
PTPPBSy C/S - HA
62.5
47.5
32
anti SHP1
SHP1
Heavy chain
Light chain
anti SL
PTPPBSy 42-HA
PTPPBSy 37-HA
C
Lysates
YFP-SHP1 wt
PTPPBSy wt - HA
PTPPBSy C/S - HA
M
anti PY20
YFP-SHP1
anti GFP-GST
83
YFP-SHP1
47.5
anti SL
PTPPBSy 42-HA
PTPPBSy 37-HA
D
IP: HA
YFP-SHP1 wt
PTPPBSy wt - HA
PTPPBSy C/S - HA
M
anti GFP-GST
83
anti PY20
62.5
47.5
32
Heavy chain
Light chain
anti SL
47.5
PTPPBSy 42-HA
PTPPBSy 37-HA

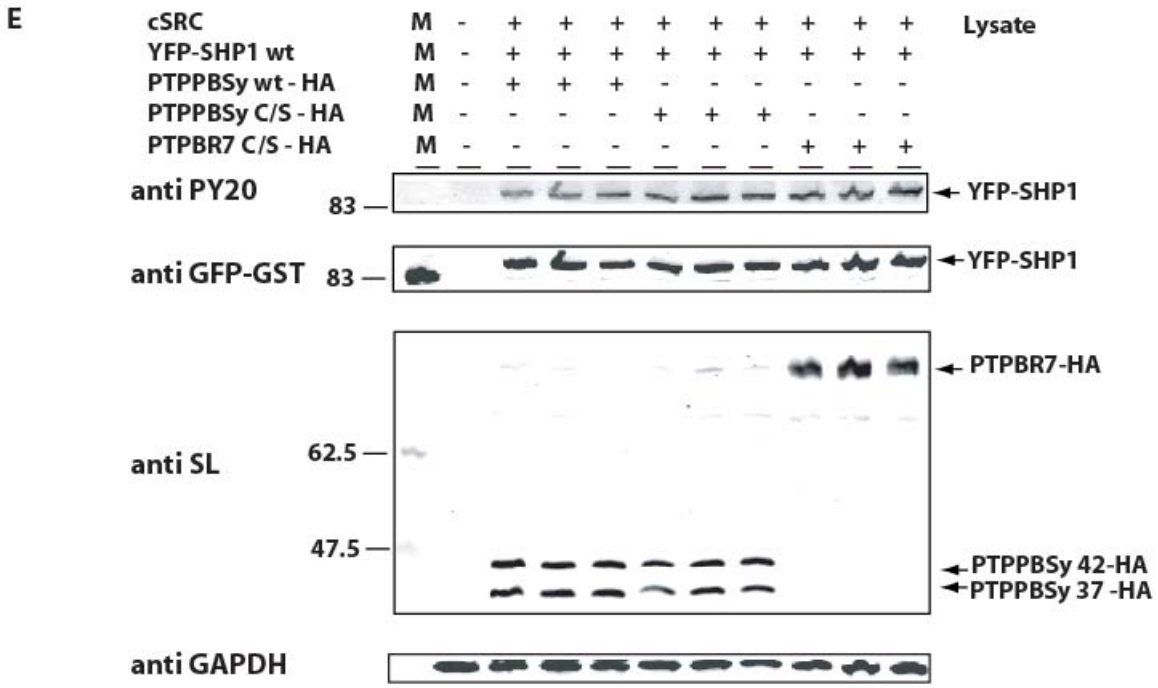
E
cSRC
YFP-SHP1 wt
PTPPBSy wt - HA
PTPPBSy C/S - HA
PTPBR7 C/S - HA
Lysate
anti PY20
83
YFP-SHP1
anti GFP-GST
83
YFP-SHP1
PTPBR7-HA
anti SL
62.5
47.5
PTPPBSy 42-HA
PTPPBSy 37 -HA
anti GAPDH

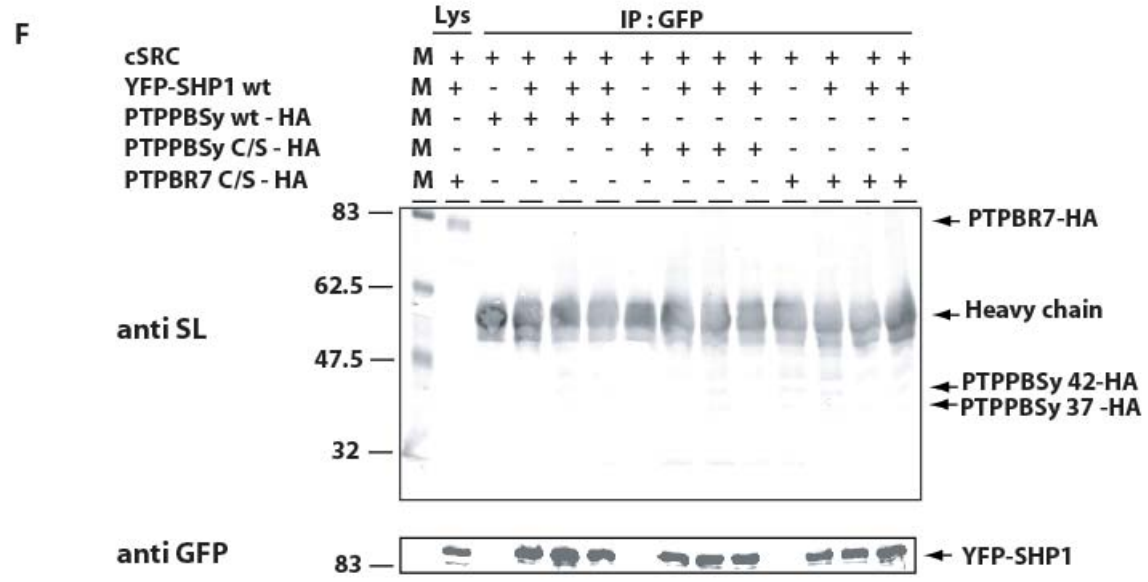
F
Lys
IP : GFP
cSRC
YFP-SHP1 wt
PTPPBSy wt - HA
PTPPBSy C/S - HA
PTPBR7 C/S - HA
83
62.5
47.5
32
PTPBR7-HA
Heavy chain
PTPPBSy 42-HA
PTPPBSy 37 -HA
anti SL
anti GFP
83
YFP-SHP1

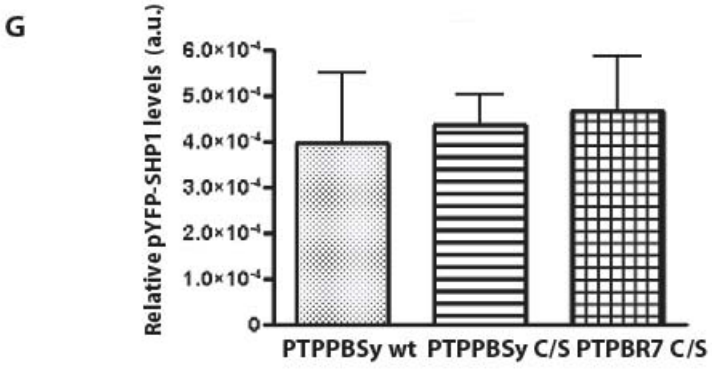
G
Relative pYFP-SHP1 levels (a.u.)
6.0×10⁻⁴
5.0×10⁻⁴
4.0×10⁻⁴
3.0×10⁻⁴
2.0×10⁻⁴
1.0×10⁻⁴
0
PTPPBSy wt
PTPPBSy C/S
PTPBR7 C/S

3.2.2.2 HER4 remains a candidate substrate of PTPBR7

As mentioned previously, achieving proper co-expression of HER4 and PTPRR wild type isoforms turned out complicated and required careful titration of plasmid quantities in the transfection experiments to prevent that high expression of PTPRR isoforms would obstruct expression of HER4 (Figure 3.11). Using relatively low ratios of PTPRR-encoding expression plasmids we eventually managed to obtain detectable steady state levels of expression for both HER4 and PTPRR variants (Fig. 3.13A). HER4 has been reported to display an apparent molecular weight of 180 kDa on SDS-PAGE. Furthermore, due to the many tyrosine phosphorylation sites and proteolytic processing of the receptor tyrosine kinase, many additional protein bands may appear on immunoblots (Kaushansky et al. 2008; Qiu et al. 2008). Under our experimental conditions, when using an anti HER4 antibody, HER4 appeared as a major phosphotyrosine containing species of 180 kDa and in addition also as a cleavage product of about 80 kDa. Several bands appeared inbetween and since we could not find a description in the literature, we initially regarded them as being either yet undescribed HER4-derived proteins or proteins reacting a-specifically with the anti HER4 antibody. Initially cells were stimulated with pervanadate to induce hyper-phosphorylation (Figure 3.13A). We observed co-immunoprecipitation of a 175 kDa phosphorylated band with PTPBR7 C/S mutant and not with PTPPBSγ C/S mutant (Figure 3.13B). Re-analysis with anti the HER4 antibody revealed two bands – one of 175 kDa and one just below – in the sample containing HER4 and PTPBR7 C/S mutant but, as for SHP1 (Fig. 3.12B), the co-immunoprecipitation was not reproducible (Fig 3.13C). In a second moment, we repeated the experiment stimulating cells with serum after overnight serum-starvation. Importantly, no significant dephosphorylation of HER4 was observed when this was co-expressed with wild type PTPBR7 as compared to the substrate trapping C/S version (Figure 3.13D). This may have been hampered by the fact that there are many phosphorylation sites in HER4 and in case PTPRR isoforms display a site-specific PTP activity towards HER4 a resulting partial reduction in phosphotyrosine content may remain unnoticed. Two bands inbetween the 83 and 175 kDa molecular weight markers appeared in lanes over-expressing HER4 but also in the mock lane thus supporting the hypothesis that they represent a-specific reactions of the anti HER4 antibody. In addition, thick bands above 175 kDa were revealed by the anti HER4 antibody (Figure 3.13D). Those ones may well represent phosphorylated isoforms of the 180 kDa-full length HER4 protein thus we proceded with testing whether PTPBR7 isoforms and HER4 establish any stable interaction, as observed in the first case (see Figure 3.13C). Immunoprecipitation of wild type and C/S mutant PTPBR7 revealed the co-precipitation of anti HER4-recognised proteins of molecular weight above 175 kDa. Notably, these bands are above the HER4 band recognized in the lysate (Figure 3.13E) making it difficult to define their identity. Besides this, results were not reproducible thus we can't drive any possible conclusion about an interaction between PTPBR7 and HER4. A clear definition of HER4 status with regard to PTPRR will definitely require the use of site-specific phosphor-antibodies and perhaps several different ways of tagging the proteins involved.

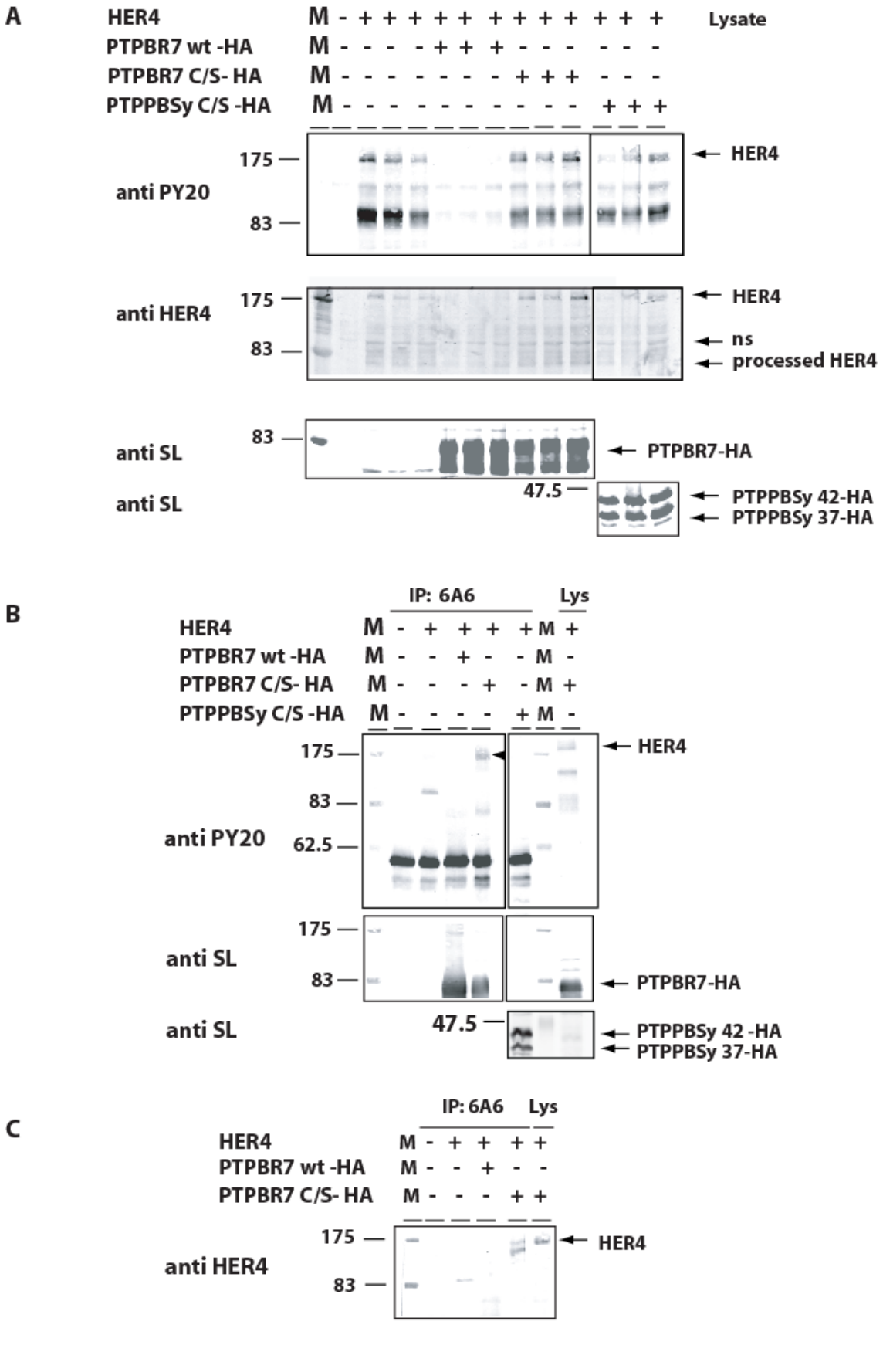

Figure 3.13. Explanation follows.

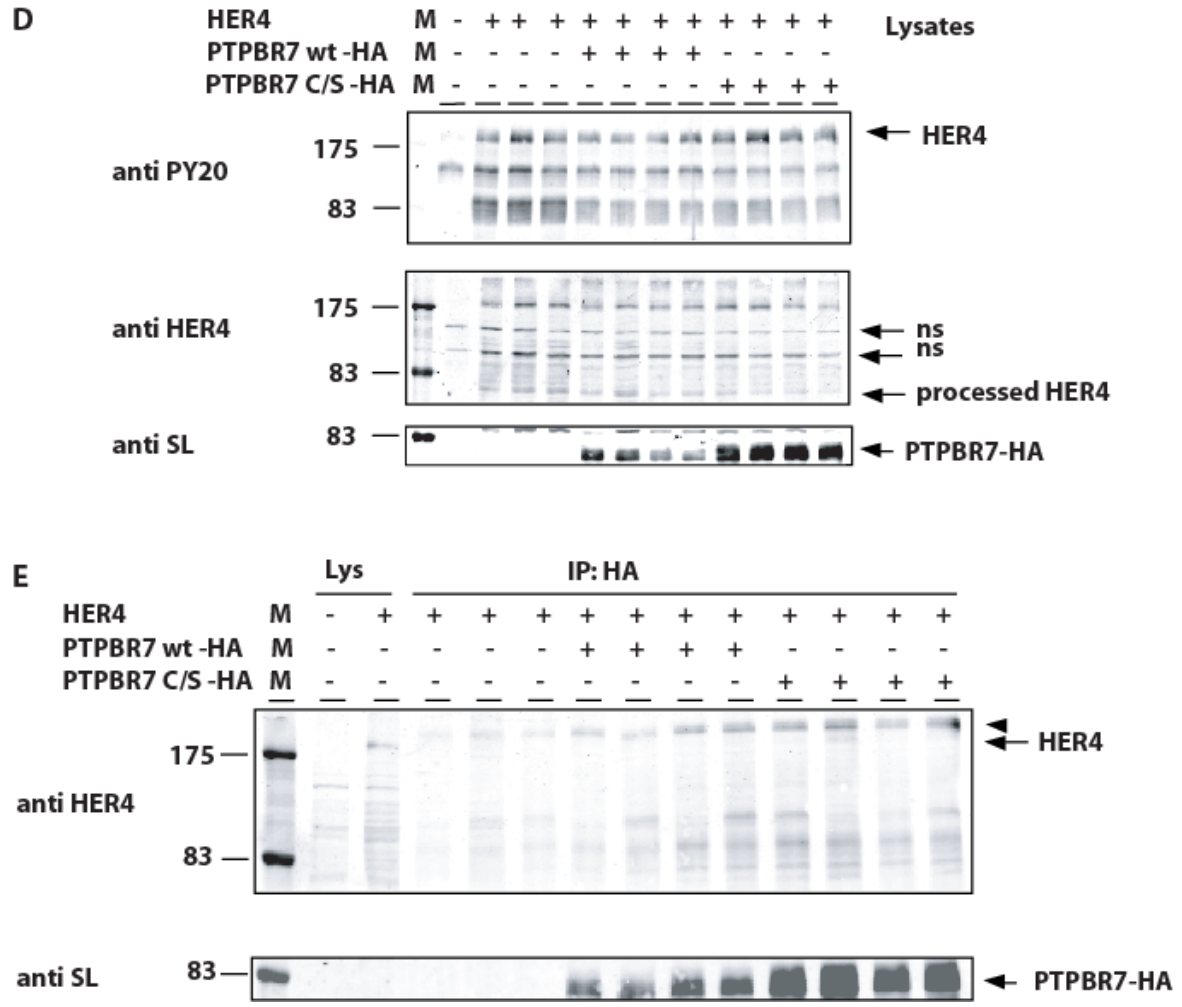

Figure 3.13. HER4 as candidate substrate of PTPRR in COS-1 over-expression system. (A-B-C) HER4 interacts with PTPBR7-HA. COS-1 cells ectopically co-expressing HER4 and either PTPBR7 wt-HA, PTPBR7 C/S-HA or PTPPBSγ C/S-HA were pre-treated with pervanadate before being lysed in orthovanadate-containing lysis buffer. (A) Subsequently, HER4 expression (anti HER4) and phosphorylation (anti PY20) and PTPRR-HA expression (anti SL) were monitored on western blot. ns = nonspecific bands. "processed HER4" indicates the 80 kDa cleavage product (Kaushansky et al. 2008; Qiu et al. 2008). (B) Upon immunoprecipitation of PTPRR isoforms (IP: 6A6) from lysates in (A), a phosphorylated protein species of about 175 kDa (arrowhead), which migrated somewhat faster than the presumed HER4 phosphotyrosine-immunoreactive species in the lysate, co-immunoprecipitated with the PTPBR7 C/S-HA variant. (C) Co-immunoprecipitates as in (B) were again subjected to SDS-PAGE and electroblotted onto membrane. Two bands of approximately 175 kDa were immunodetected by the antibody to HER4 in the immunoprecipitate of PTPBR7 C/S-HA. Comparison was made with the lysate (Lys) expressing HER4 and PTPBR7 C/S-HA. (D-E) Reexamination of HER4 - PTPRR interaction using an alternative experimental set-up. COS-1 cells ectopically co-expressing HER4 and either PTPBR7 wt-HA or PTPBR7 C/S-HA were now serum-stimulated prior to lysis in orthovanadate-containing lysis buffer. (D) HER4 expression (anti HER4) and phosphorylation (anti PY20) and PTPRR-HA expression (anti SL) were checked on blot. ns = nonspecific bands. "processed HER4" indicates the 80 kDa cleavage product (Kaushansky et al. 2008; Qiu et al. 2008). (E) Upon immunoprecipitation of PTPRR-HA isoforms, exploiting an antibody against the HA epitope tag (IP: HA), HER4 co-immunoprecipitation was investigated on immunoblots using anti HER4 antibody. Proper affinity purification of PTPBR7-HA by the immunoprecipitation was confirmed using anti SL. For comparison, MOCK and HER4-expressing lysates were included on the blot. Anti HER4 antibody reveals protein bands (arrowhead) at an apparent molecular weight just above that of the reference protein (arrow) in the lysate. Molecular weights are given in kDa on the left. M = protein size marker.

The candidacy of HER3 as a PTPRR substrate could not be analyzed in co-expression experiments with PTPRR isoforms in COS-1 cells because we never obtained suitable HER3 phosphorylation levels in this set-up (data not shown). In conclusion, both the *in vitro* and the COS-1 cells studies did not contribute additional experimental evidence toward the status of SHP1, HER3 and HER4 as PTPRR substrates. A possible explanation for the difficulties encountered could be that the *in vitro* environment and the cell type used for over-expression are simply not providing the proper conditions for the interaction to occur. We considered performing the tests in rat PC12 cells that endogenously express PTPRR isoforms, and those experiments will be presented in paragraph 3.2.4. Before abandoning the COS-1 over-expression system, however, we will first present our studies towards a putative interaction of PTPBR7 with N-cadherin.

3.2.3 PTPBR7 does not interact with N-cadherin

Barr et al. (Barr et al. 2009) observed that a phospho-peptide derived from N-cadherin could be dephosphorylated by the rat homolog of PTPBR7, PCPTP1. Since N-cadherin-derived phospho-peptides were not present in our peptide array library (see paragraph 3.1.2), we decided to test directly the N-cadherin protein for being a substrate of PTPBR7. COS-1 cells over-expressing YFP-tagged N-cadherin were serum-stimulated and lysed in orthovanadate-containing lysis buffer. YFP-N-cadherin was immuno-purified from cell lysates and subsequently incubated with either PTPBR7 wild type or C/S mutant proteins that had been purified from COS-1 cells in a separate transfection experiment and had been released from beads. The phospho-levels of YFP-N-cadherin were subsequently determined but no indication of relevant phospho-level differences of YFP-N-cadherin due to the PTP were observed (Figure 3.14A-B). Expression of endogenous N-cadherin is shown in Figure 3.14C.
We next turned to a co-expression set-up, anticipating that steady-state differences in N-cadherin phosphotyrosine content would become apparent depending on the use of wild type or C/S mutant PTPs. To this end, YFP-N-cadherin was co-expressed either with PTPBR7 wild type or C/S mutant and serum stimulation of cells was used to boost tyrosine phosphorylation events. Subsequently, cells were lysed and phospho-levels of YFP-N-cadherin were monitored on western blot. YFP-N cadherin phospho-levels were not found to be different under the conditions used, i.e. no effects due to co-transfection of either catalytically active or inactive PTPBR7 were apparent (Figure 3.14D-E-F).

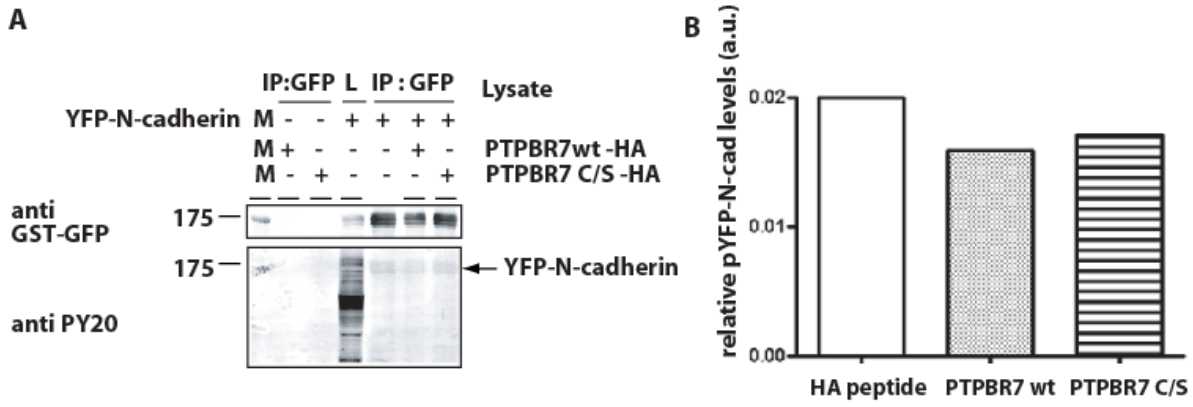

Figure 3.14. Explanation follows.

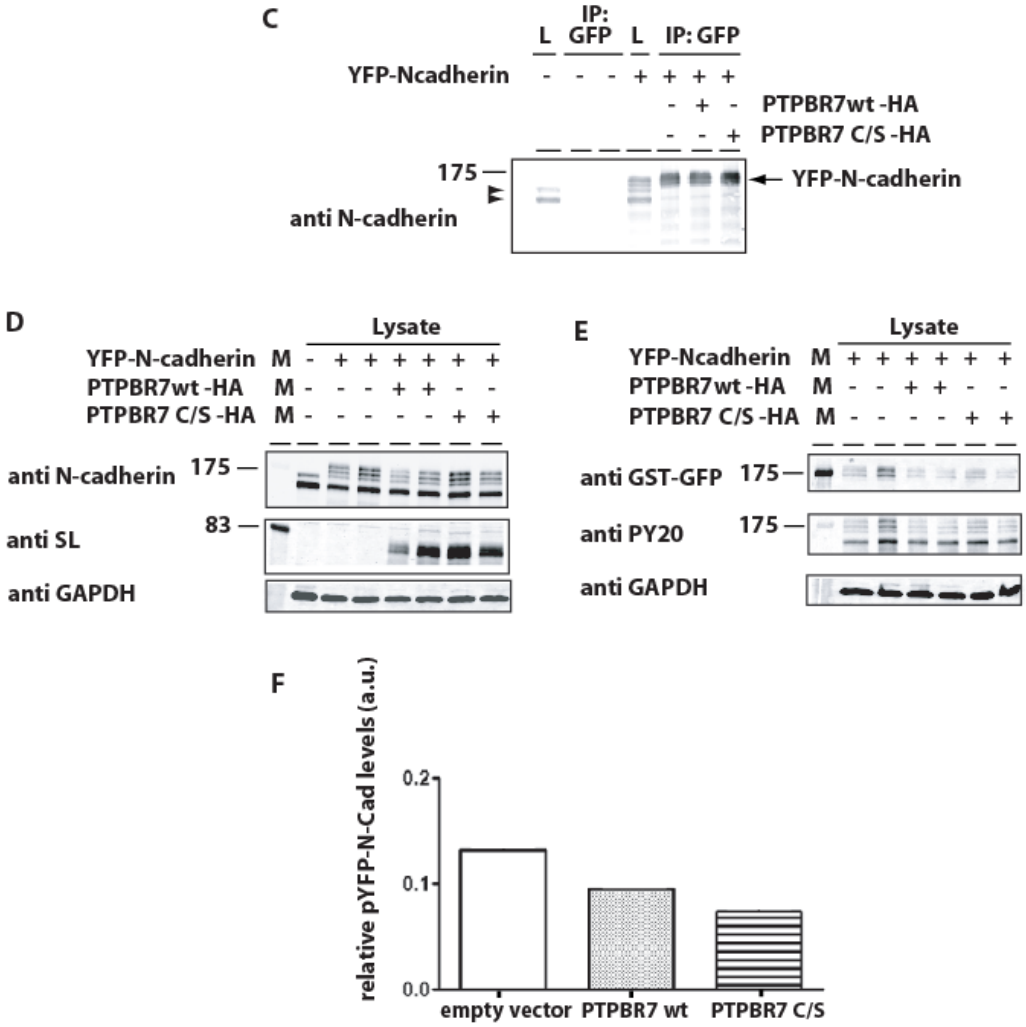

Figure 3.14. YFP-N-cadherin could not be confirmed as a substrate of PTPBR7. (A-B-C) YFP-N-cadherin is not a substrate of PTPPBR7-HA *in vitro*. COS-1 cells ectopically expressing YFP-N-cadherin were serum-stimulated prior to lysis in orthovanadate-containing lysis buffer (L). (A) Immunoprecipitated YFP-N-cadherin (IP:GFP) was incubated with HA peptide or immunoprecipitated PTPBR7 wt-HA or PTPBR7 C/S-HA after release from beads. Efficiency of YFP-N-cadherin immunoprecipitation (anti GST-GFP) and of phosphorylation (anti PY20) was checked on western blot. (B) Quantitative representation of relative phospho-YFP-N-cadherin levels of immunoprecipitated YFP-N-cadherin after incubation with PTPBR7-HA variants or under control conditions. The experiment was performed only once and no relevant difference in YFP-N-cadherin phospho-levels was observed. (C) Anti N-cadherin immunostaining of the YFP-N-cadherin lysates used in (A) on blots revealed in the mock transfected lysates two immune-reactive bands (arrowheads) probably referring to endogenous N-cadherin. Unlike the bands at 175 kDa these were not included in the quantification of YFP-N-cadherin phosphorylation levels in (B). L= lysate. (D-E-F) YFP-N-cadherin is not a substrate of PTPPBR7-HA in COS-1over-expression system. COS-1 cells co-expressing YFP-N-cadherin and either PTPBR7 wt-HA or PTPBR7 C/S-HA were serum-stimulated prior to lysis in orthovanadate-containing lysis buffer. (D) Expression of YFP-N-cadherin (anti N-cadherin and anti GST-GFP) and PTPBR7 isoforms (anti SL) was confirmed on western blots. Two samples per condition were included. (E) Phospho-levels of YFP-N-cadherin (anti PY20) and equal loading (anti GAPDH) were investigated by immunoblotting. (F) Quantitative representation of relative phospho-YFP-N-cadherin levels as determined in (E). As in (C), bands observed also in mock transfected lysates were not included in the quantification of YFP-N-cadherin phosphorylation levels. Empty vector (pSG8 vector without PTPBR7-encoding sequence) refers to lysates where YFP-N-cadherin was over-expressed in absence of any PTPBR7 isoform. Molecular weights are given in kDa on the left. M = protein size marker.

3.2.4 Validation assays in PC12 cells

To test whether the cellular context in which PTPRR proteins and candidate substrates are expressed is important to allow stable interactions we repeated the validation experiments in the rat phaechromocytoma cell line PC12. PC12 cells express endogenously PCPTP1, the rat orthologue of the mouse PTPBR7 transmembrane isoform. We made use of parental PC12 cells and of cell lines derived thereof that were knocked-down for PCPTP1 or stably over-express PTPBR7 (Noordman et al. 2006).

We first tested whether the candidate substrates HER4, HER3, SHP1 and N-cadherin are endogenously expressed in the three PC12 lines mentioned above. The mouse antibody to HER4, HFR1, detected a protein band around 100 kDa that does not correspond to the expected band for HER4. In addition, the rabbit antibody to HER3 did not react with any protein species in PC12 cell lysates (data not shown). We therefore were forced to limit our attention to SHP1 and N-cadherin. Surprisingly, both of these proteins were found up-regulated in the PC12 cells that over-express PTPBR7 (Fig. 3.15). Especially for N-cadherin, that was most strongly up-regulated in PTPBR7 over-expressing PC12 cells, this points to a direct effect of PTPBR7 on N-cadherin expression regulation.

We next tested if PTPBR7 could bind to or regulate phospho-levels of SHP1 and N-cadherin in these cells. Cells were serum-stimulated and lysed in orthovanadate-containing lysis buffer. PTPBR7/PCPTP1 was immunoprecipitated from the three PC12 cell lines but co-immunoprecipitation of either endogenous SHP1 or N-cadherin was not observed. This indicates that at least the wild type PTPBR7 cannot bind stably to these proteins. Furthermore, upon immunoprecipitation of all phosphotyrosine containing proteins in the PC12 cell lines, neither N-cadherin nor SHP1 could be detected (Figure 3.15 C and 3.15D). Intriguingly, we did observe protein bands, at around 130 kDa and 70 kDa, that displayed differential phosphotyrosine levels among the three cell lines (Fig. 3.16A). Upon immunoprecipitation of PTPBR7 from the three cell lines, however, no phosphorylated protein was detectable in the co-immunoprecipitates (Fig. 3.16B) indicating that the catalytically active PTPBR7/PCPTP1 proteins do not support efficient pull-down of phospho-proteins in PC12 cells.

We subsequently tested whether SHP1 and N-cadherin could be co-immunoprecipitated with PTPBR7 C/S mutant protein. The HA-tagged PTPBR7 C/S protein was independently purified from over-expressing COS-1 cells, released from beads and incubated with lysates coming from the three different PC12 cell lines, whose phospho-protein content had been boosted with serum-stimulation. Subsequently, co-immunoprecipitates obtained using the anti HA antibody were checked for SHP1 and N-cadherin co-immunoprecipitation. Neither SHP1 nor N-cadherin co-immunoprecipitated with PTPBR7 C/S mutant, either from cell lysates previously depleted of the endogenous PTPBR7 by immunoprecipitation with antibody 6A6 or from lysates containing both the wild type PTPBR7 and the added C/S substrate trapping isoform (Figure 3.16C). These results make a direct interaction of PTPBR7 with either SHP1 or N-cadherin rather unlikely.

In conclusion, whether using COS-1 or PC12 cells in this set-up, we could not reveal reproducible PTPRR interactions with candidate substrates. This leaves two conclusions: either the phospho-peptide array experiment did not coin names of genuine PTPRR substrates

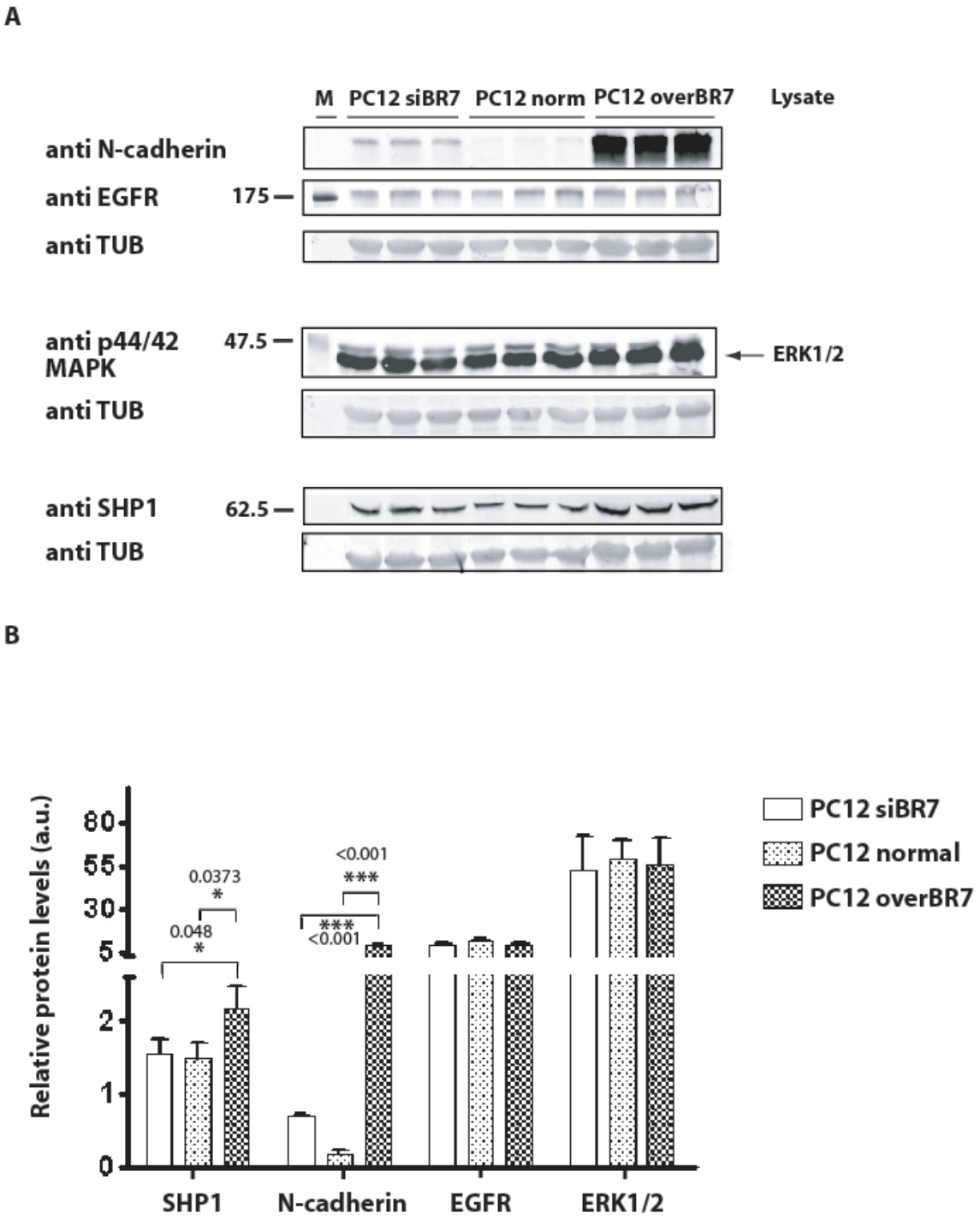

Figure 3.15A-B. SHP1 and N-cadherin are over-expressed in PC12 cell lines over-expressing PTPBR7. PC12 cells knocked-down for PCPTP1 (PC12 siBR7), normal PC12 cells (PC12 norm) and PC12 over-expressing PTPBR7 (PC12 overBR7) were lysed in lysis buffer. (A) Expression levels of SHP1 (anti SHP1) and N-cadherin (anti N-cad) were monitored on western blot. Parallel immunodetection of the unrelated proteins EGFR (anti EGFR), ERK1/2 (anti p44/42 MAP kinase) and tubulin (anti TUB) for loading control was performed. (B) Quantitative representation of protein expression levels as determined in (A). Protein expression levels were corrected for loading differences using the anti TUB signal as control. Student's t-test was performed and statistical significance set at $p<0.05$. Results (n=3) are presented as Mean±SD. p values are indicated on the top of the relevant analysis. Molecular weights are given in kDa on the left. M = protein size marker.

or, alternatively, our experimental verification set-up is somehow preventing efficient interactions. The latter may relate to the cell context or the buffers employed. Paragraph 3.3 focuses on the use of vanadate compounds in PTP research and touches upon such an explanation for our findings in the dephosphorylation and binding assays.

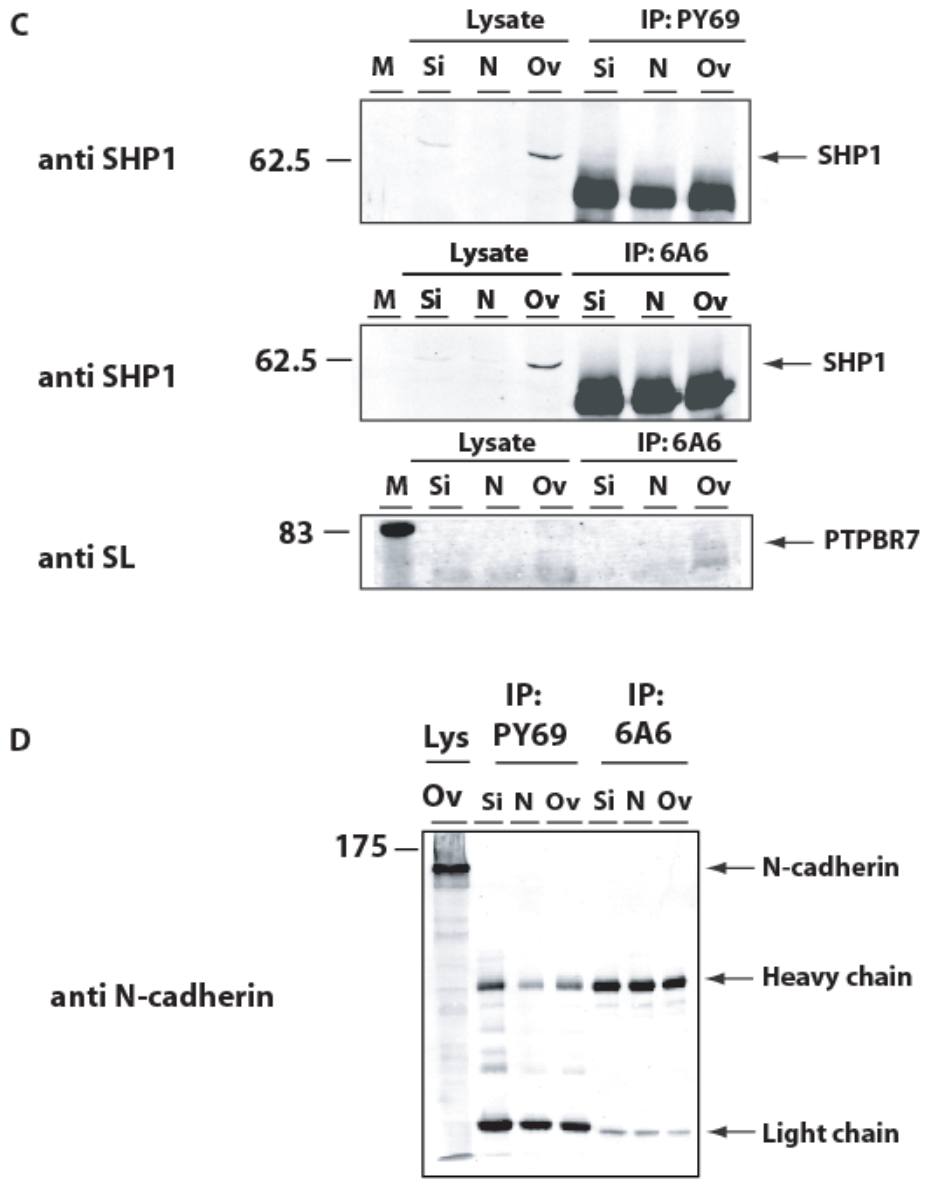

Figure 3.15C-D. SHP1 and N-cadherin do not interact with endogenous PTPRR isoforms in PC12 cells. PC12 cells knocked-down for PCPTP1 (Si), normal PC12 cells (N) and PC12 over-expressing PTPBR7 (Ov) were serum-stimulated prior to lysis in orthovanadate-containing lysis buffer. Subsequently either the total phospho-protein content (IP: PY69) or the PTPRR interactome (IP: 6A6) were immunoprecipitated. (C) SHP1 co-immunoprecipitation (anti SHP1) was investigasted. Efficient PTPBR7 immunoprecipitation (anti SL) was confirmed only for the PTPBR7 over-expressing PC12 cell line. (D) Co-immunoprecipitates as in (C) were again subjected to SDS-PAGE and electroblotted onto membrane. N-cadherin co-immunoprecipitation (anti N-cadherin) was tested and compared with the protein band immunodetected in the PC12 cell line over-expressing PTPBR7 (see figure 3.15A) . Heavy chain, light chain = heavy and light chains of primary antibodies. Molecular weights are given in kDa on the left. M = protein size marker.

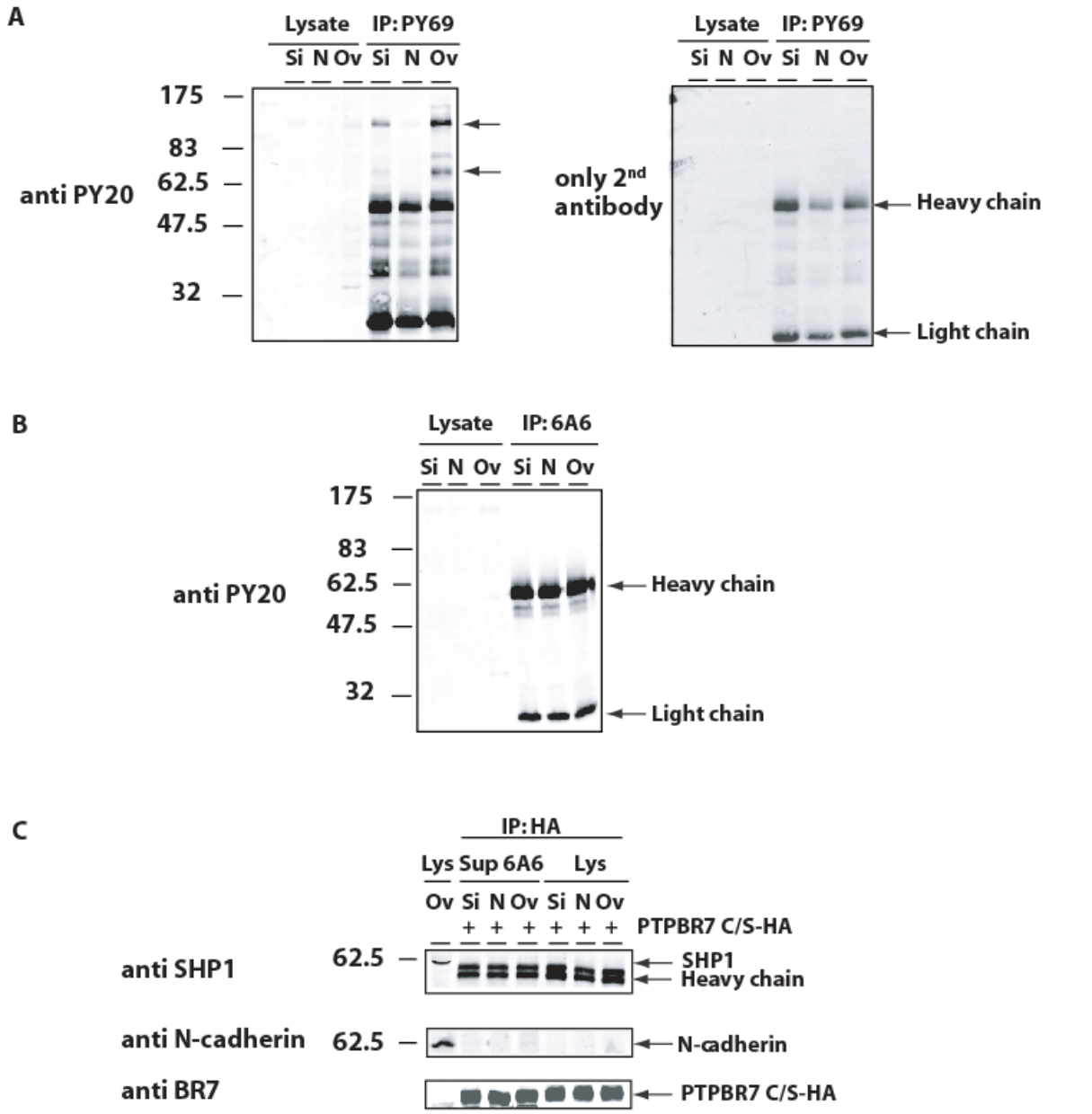

Figure 3.16. Endogenous SHP1 and N-cadherin from PC12 cells do not interact *in vitro* with PTPBR7 C/S isoform in PC12. (A-B) PC12 cells knocked-down for PCPTP1 (Si), normal PC12 cells (N) and PC12 over-expressing PTPBR7 (Ov) were serum-stimulated prior to lysis in orthovanadate-containing lysis buffer. Subsequently, either the total phospho-protein content (IP: PY69) or the PTPRR interactome (IP: 6A6) were immunoprecipitated. (A) Total phospho-proteins were detected using the anti PY20 antibody. Differential bands among the three cell lines were revealed (arrows). Specificity of anti PY20 antibody detection was determined by immunodetection with only the secondary antibody (only 2nd antibody). (B) Immunoprecipitates of the PTPBR7 interactome (IP: 6A6) of lysates as in (A) were tested for presence of phospho-proteins (anti PY20). Heavy chain, light chain = heavy and light chains of primary antibodies. (C) PC12 cell lines knocked-down for PCPTP1 (Si), normal PC12cell lines (N) and PC12 cells over-expressing PTPBR7 (Ov) were serum-stimulated and lysed in orthovanadate-containing lysis buffer. Cell lysates (Sup 6A6) previously deprived of PTPRR isoforms by immunoprecipitation with antibody 6A6 and untreated cell lysates (Lys) were incubated with purified HA-tagged PTPBR7 C/S protein released from beads. Subsequently, PTPBR7 C/S-HA isoforms were immunoprecipitated with antibody to the HA tag (IP: HA). SHP1 (anti SHP1) and N-cadherin (anti N-cadherin) co-immunoprecipitation was investigated by immunodetection. Efficient immunoprecipitation of the exogenous PTPBR7 C/S-HA was confirmed by immunodetection to the N-terminal portion of PTPBR7 (anti BR7). Heavy chain, light chain = heavy and light chains of primary antibodies.

3.3 Evaluation of PTPBR7 phosphatase activity in presence of vanadate compounds

In our *in vitro* and *in vivo* assays used to validate candidate PTPRR substrates we made extensive use of vanadate compounds to induce ample phosphorylation of cellular proteins. As explained in the introductory section of this thesis (paragraph 1.3.4) vanadate compounds are strong phosphatase inhibitors (Swarup et al. 1982). While orthovanadate is a reversible inhibitor and its effect can be abolished by addition of EDTA, pervanadate has irreversible effects on phosphatases. However, before pervanadate reacts with the catalytic site of phosphatases, it can be converted and stably bound by means of DTT and EDTA (Huyer et al. 1997). In our assays we did not observe dephosphorylation of any candidate substrate by PTPRR isoforms, pointing to the possibility that the vanadate compounds strongly inhibit added PTPRR proteins even after DTT and/or EDTA treatment. Furthermore, it has been reported that the catalytic site in enzymatically inactive phosphatase C/S and D/A mutants can still be occuppied by vanadate (Blanchetot et al. 2005), indicating the eventuality that they could compete for binding with candidate substrates. Therefore, we set out to test if the wild type PTPRR fusion proteins would still be enzymatically active when added to vanadate-containing reaction mixtures that had been treated with DTT and EDTA.

First we confirmed that immuno-purified PTPBR7-HA and PTPPBSγ-HA from over-expressing COS-1 cells were active in the buffer used for the *in vitro* dephosphorylation assays (50 mM Tris-HCl pH 7.5; 1% Triton X-100, 5 mM EDTA, 10 mM DTT). The two phosphatases, still bound to the antibody-coated Protein A beads, were indeed catalytically active in this buffer (Figure 3.17). Then we observed that treatment of these phosphatases with either 1 mM orthovanadate or 0.1 mM pervanadate in this same buffer was sufficient to block all phosphatase activity, even though the buffer already contained EDTA and DTT (Figure 3.17). Prior incubation of two hours with EDTA and DTT followed by the addition of fresh PTPRR protein did not allow for PTP activity when samples had been pretreated with orthovanadate. A slow recovery of activity, however, was observed in the case pre-treatment was with pervanadate (Figure 3.18). This was quite unexpected since orthovanadate effects should be reversible whereas pervanadate-mediated PTP inactivation is not (Huyer et al. 1997). The experiment was repeated and again we observed that, in case pervanadate had been applied, activity partially recovered. However, PTP activity decreased again after 20 minutes, suggesting that the phosphatase proteins added were slowly being inactivated over time (Figure 3.19).

These experiments clearly show that PTPRR isoforms are extremely sensitive to oxidation generated by vanadate compounds and inactivation of the phosphatase cannot be blocked or reversed by addition of EDTA and DTT. This indicates that residual amounts of vanadate compounds may have considerably impaired PTPRR activity when tested in de-phosphorylation assays of candidate substrates *in vitro*. Binding to PTPRR C/S mutants, although C/S mutants are known to be less affected than wild type and D/A mutants (Blanchetot et al. 2005), is also conceivable and may hamper binding to cognate substrates. It is tempting to suggest a role of oxidation in regulating PTPRR activity also *in vivo,* as reported for other phosphatases (den Hertog et al. 2008).

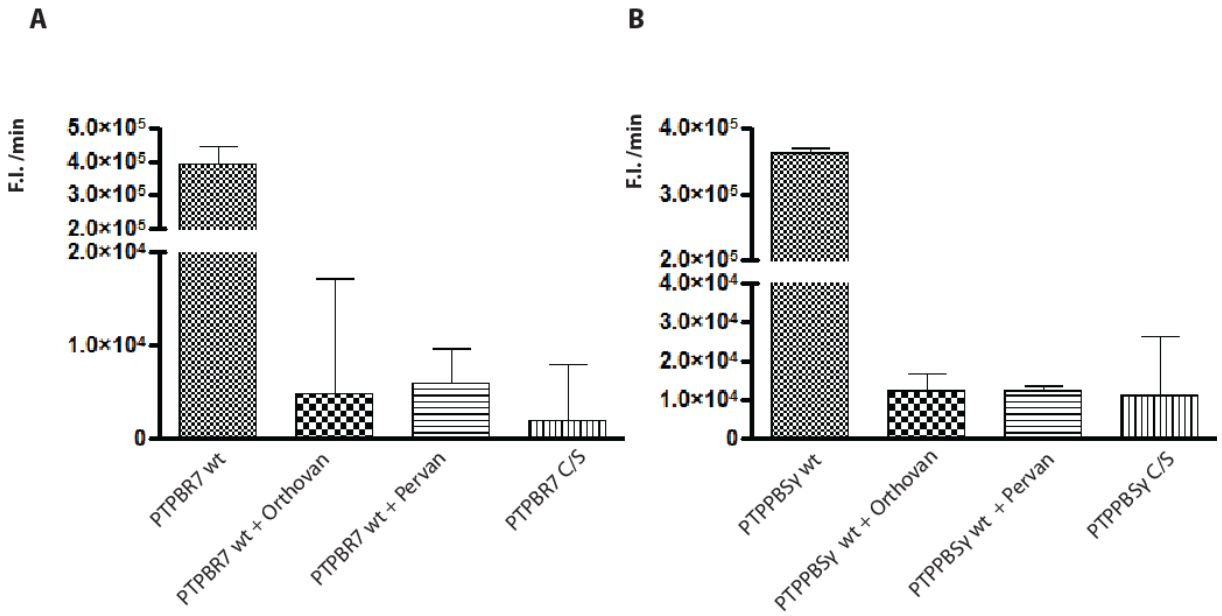

Figure 3.17. PTPBR7 and PTPPBSγ activity is inhibited by vanadate compounds. Respectively 0.24 µg of and 0.16 µg of PTPBR7 wt-HA (A) and PTPPBSγ wt-HA (B) immunoprecipitated from over-expressing cells and bound to beads were tested for phosphatase activity towards DiFMUP in the presence of either 1 mM Orthovanadate (Orthovan) or 0.1 mM Pervanadate (Pervan). Both wild type and C/S mutants were tested. Activities are presented as Fluorescence Intensites per minute (F.I./min) in a linear time range of 25 minutes. Results (n=3) are presented as Mean ± S.D.

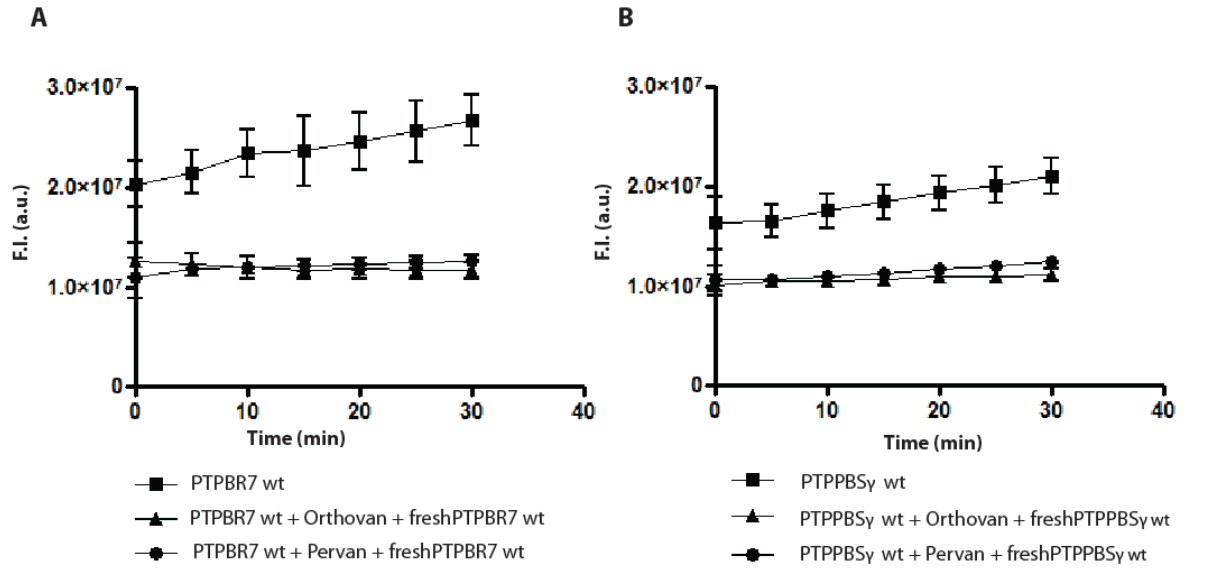

Figure 3.18. Wild type PTPBR7 and PTPPBSγ are sensitive to vanadate inhibitors after treatment with EDTA and DTT. Phosphatase activity of PTPBR7 wt-HA (A)- and PTPPBSγ wt-HA (B)-immunoprecipitates was inhibited by Orthovanadate (Orthovan) or Pervanadate (Pervan) pre-treatment (See Fig. 3.17). Subsequently, immunoprecipitates were treated with 5 mM EDTA and 10 mM DTT before, respectively, 0.24 µg of PTPBR7-HA and 0.16 µg of PTPPBSγ-HA fresh wild type proteins (freshPTPBR7 wt or freshPTPPBSγ wt) loaded on beads was added. Again phosphatase activity towards DiFMUP of the obtained immunoprecipitates was investigated and compared to the one of PTPBR7-HA or PTPPBSγ-HA immunoprecipitates where no vanadate compound had been added. Activities are presented in arbitrary units (a.u.) of Fluorescence Intensity (F.I.). Results (n=3) are presented as Mean ± S.D.

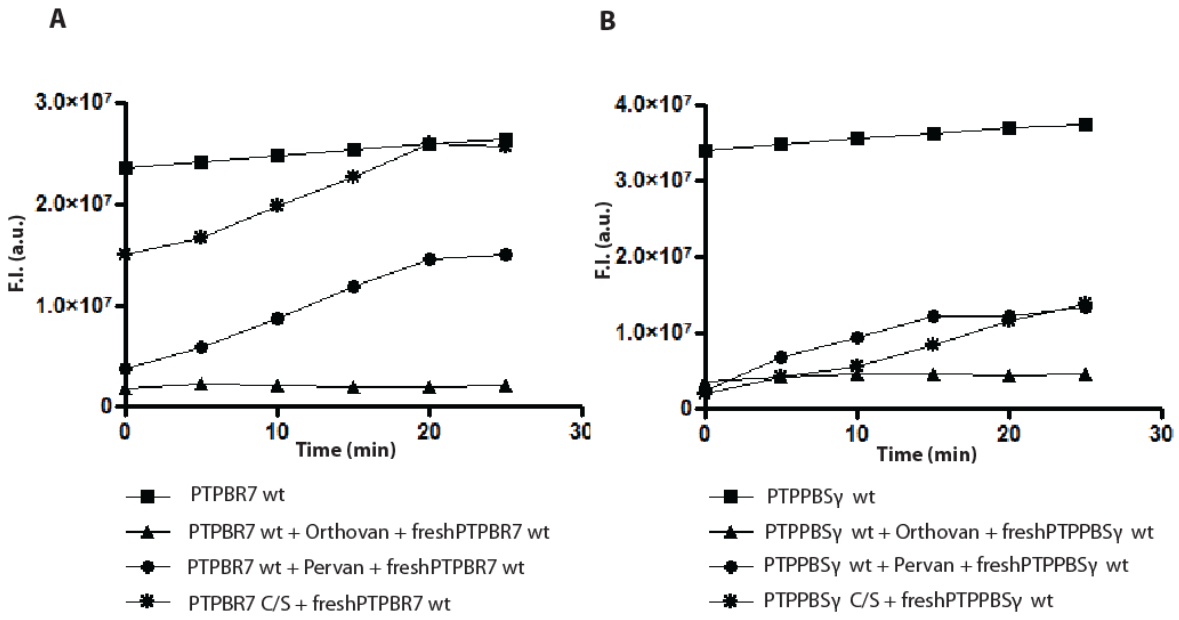

Figure 3.19. Wild type PTPBR7 and PTPPBSγ recover activity after pervanadate inhibition. PTPBR7 wt-HA (A) and PTPPBSγ wt-HA (B) immunoprecipitates where phosphatase activity had been inhibited by Orthovanadate (Orthovan) or Pervanadate (Pervan) were treated with 5 mM EDTA and 10 mM DTT before fresh HA-tagged wild type protein loaded on beads (freshPTPBR7 wt or freshPTPPBSγ wt) was added. Phosphatase activity towards DiFMUP was investigated and compared to the one of PTPBR7 wt-HA or PTPPBSγ-wt-HA immunoprecipitates where no vanadate compound had been added. Activity recovered partially where pervanadate had been applied but tended to decrease after 20 minutes. Activities are presented in arbitrary units (a.u.) of Fluorescence Intensity (F.I.).

3.4 Methods for identifying PTPBR7 extracellular ligands: RAP *in situ* and affinity chromatographic approaches

In his review about methodological approaches to identify ligands of Receptor Tyrosine Phosphatases (Stoker 2005), Stoker suggests the use of the technique Receptor Alkaline Phosphatase (RAP) *in situ* for the identification of cognate ligands for receptor PTPs. The RAP *in situ* technique has been used in our studies to localize candidate ligands of PTPBR7 in the mouse brain. PTPRR transcripts are already detectable in spinal ganglia and parts of the metencephalon of mouse embryos of 14.5 days post conception (van den Maagdenberg et al. 1999). In adult mice PTPRR proteins are expressed in the brain region, mainly in the cerebellum. In brief, our search began from embryos (data not shown) and focused on the adult mouse brain and in particular on the cerebellum (Figs. 3.21 and 3.22). Subsequently, we applied *in situ* and *in vitro* assays to test if the glycosaminoglycans (GAGs) heparan sulphate (HS) and chondroitin sulphate (CS) are candidate ligands. Finally, we turned to affinity chromatography from brain lysates to select proteins interacting with the extracellular domain of PTPBR7. Mass spectrometry analysis of purified proteins led to the identification of candidate ligands that will be tested for interaction with PTPBR7.

3.4.1 PTPBR7 probes for RAP in situ

We first generated a panel of probes to be used in the RAP *in situ* technique (Stoker 2005). Briefly, seven fragments of the extracellular domain of PTPBR7, all starting at amino acid (aa) 1 and ending respectively at amino acid 220, 221, 222, 223, 224, 225 and 226, were fused in frame with the Placental Alkaline Phosphatase (PLAP) enzyme (Figure 3.20A). We chose to create a variety of probes to allow for optimization of fusion protein yield and eventually exploit conformational flexibility in the binding assay. After transfection of HEK293T cells, expression levels and sizes of the ectodomain probes were inspected on western blot using the rabbit polyclonal α-BR7 antiserum (Dilaver et al. 2007). As shown in Figure 3.20B, all probes except BR7ecto225 were expressed in the culture medium and displayed the expected apparent molecular weight (83 kDa). Correct folding of each secreted fusion protein was probed by measuring alkaline phosphatase (AP) activity towards 4-nitrophenyldisodium orthophosphate (pNPP) (Figure 3.20C). All probe-containing conditioned media, except the one for BR7ecto225, displayed phosphatase activities that exceeded the minimal working activity suggested (0.2 ABS/min; (Stoker 2005)). For RAP *in situ* purposes, AP activities were equalized and unfused PLAP-containing conditioned medium was used as negative control.

3.4.2 PTPBR7 extracellular domain binds specifically on myelinated tracts of the mouse cerebrum and cerebellum

Ectodomain probes were used on sagittal sections of adult mouse brain and positive staining was observed in regions ascribed to corpus callosum, alveus, fimbria fornix, anterior commisure of olfactory bulb, hippocampal area in the cerebrum and cerebellar related fiber tracts (Figure 3.21), all regions associated with high myelination (Shiota et al. 1989; Franklin and ffrench-Constant 2008). No qualitative difference was observed in the binding patterns for the different BR7ecto probes indicating comparable binding abilities (data not shown). Those regions of the cerebrum were RAP staining was observed only partially coincide with the pattern of *Ptprr* gene expression observed by RNA *in situ* hybridization (van den Maagdenberg et al. 1999). The patterns are distinct from those obtained using RPTPσ extracellular probes (Aricescu et al. 2002; Sajnani-Perez et al. 2003), underscoring specificity (Fig. 3.25A-B).

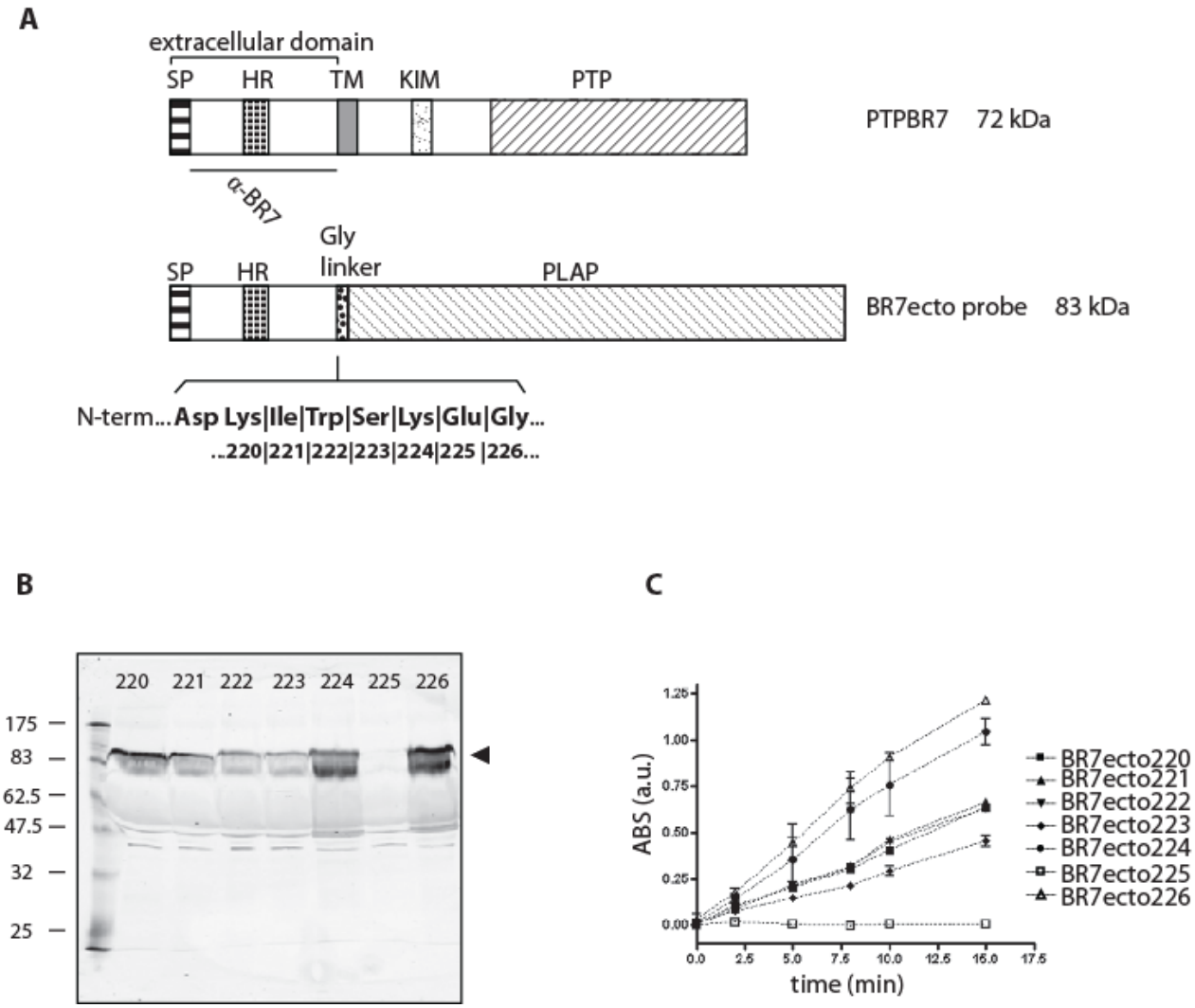

Figure 3.20. Characterization of BR7ecto fusion proteins used for RAP in *situ* assays on mouse brain sections. (A) Schematic representation of the mouse PTPRR protein isoform PTPBR7 (72 KDa) and the BR7ecto probes (83 KDa). Signal peptide (SP), hydrophobic and transmembrane regions (HR, TM), kinase-interacting motif (KIM), catalytic protein tyrosine phosphatase domain (PTP), Glycine linker (Gly linker), Placental alkaline phosphatase (PLAP) enzyme and the segment recognised by the □-BR7 antiserum are indicated. At the junction between the extracellular domain and the Gly linker the seven bridging amino acid (position 220, 221, 222, 223, 224, 225 and 226 from the N-terminus of PTPBR7) corresponding to the seven different probes are highlighted in bold. We indicate each probe with the name BR7ecto followed by the amino acid number. (B) Expression of BR7ecto probes detected by immunoblot. Conditioned culture media of HEK293T cells transiently transfected with expression plasmids pBGflexilinker - BR7ecto220, - BR7ecto221, - BR7ecto222, - BR7ecto223, - BR7ecto224, - BR7ecto225 and - BR7ecto226 were analysed on western blot using the rabbit polyclonal □-BR7 antiserum. Numbers corresponding to the length of each PTPBR7 extracellular segment for each probe are indicated on the top of each lane. Molecular size markers in kDa are indicated on the left in kDa. (B) Graph reporting the alkaline phosphatase activity of each BR7ecto probe containing medium. Activity of each probe containing medium was measured as indicated in Materials and Methods.

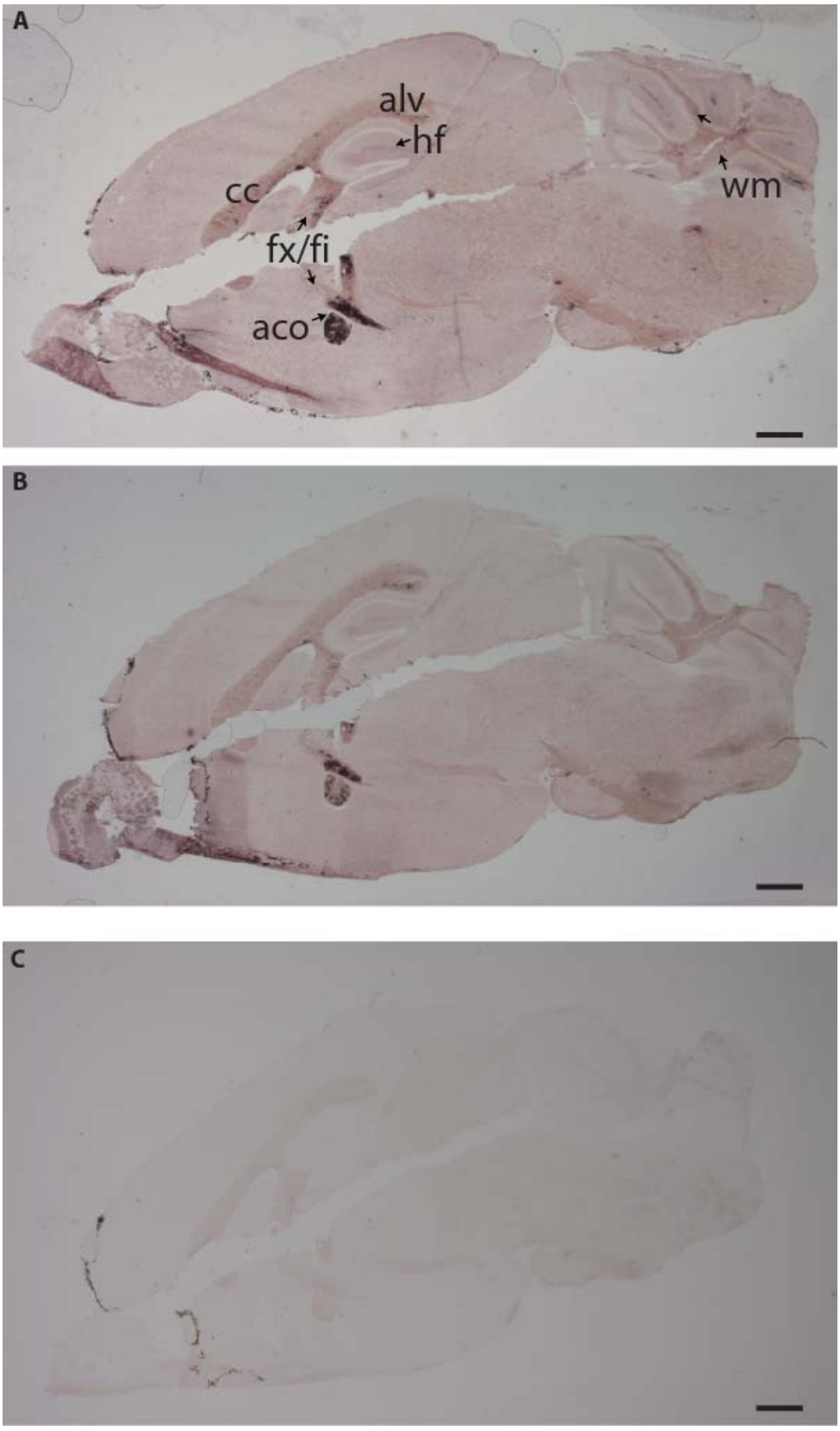

Figure 3.21. BR7ecto probes bind specifically to highly myelinated regions of the mouse brain. RAP *in situ* assays were performed using respectively the BR7ecto226 probe (A), the BR7ecto224 probe (B) and the control PLAP protein (C) on mouse brain sections. Reddish-purple staining was identified in corpus callosum (cc), alveus (alv), fimbria (fi), columns of the fornix (fx), anterior commisure of olfactory bulb (aco), hippocampal fissure (hf) in the cerebrum and cerebellar related fiber tracts (wm). Bar = 1 mm.

3.4.3 PTPBR7 extracellular domain preferentially binds to the white matter in the mouse cerebellum

Past studies showed that PTPRR proteins display highest expression levels in granular layer and Purkinje cells in the adult mouse cerebellum (van den Maagdenberg et al. 1999). In the RAP *in situ* assay the white matter of the cerebellum was positively stained by the BR7ecto probes. Some staining was also present in PCs, single neurons of the granular layer and tracts of the molecular layer (Figure 3.22). The pattern observed in the white matter is reminiscent of myelinating oligodendrocytes and indeed immunostaining for 2'-3'-cyclic-nucleotide 3'-phosphodiesterase (CNPase) revealed a very similar staining pattern (Figure 3.22D).

Next, we tested whether binding of the BR7ecto226 probe could be outcompeted. As competitor we produced a complete PTPBR7 extracellular domain fused to a 6-Histidine tag (BR7ecto226-His), and applied it on brain sections before performing the RAP *in situ*. Unexpectedly, the procedure did not lead to a significant decrease in BR7ecto226 binding to white matter tracts (Figure 3.23).

The BR7ecto226-His molecule behaves very likely as a monomeric protein since it lacks dimerization domains. On the contrary, dimerization of fusion proteins induced by the PLAP tag has been reported (Stoker 2005) and may explain the inability of BR7ecto226-His to outcompete the BR7ecto226 probe. In addition, saturation of ligand binding sites may not be achieved by the BR7ecto226-His protein and allow residual probe binding.

We also examined whether absence of PTPRR proteins may have an influence on the localization and level of expression of putative PTPBR7 ligands. No apparent difference in the BR7ecto226 binding patterns on wild type and *Ptprr* knock out cerebellar sections was observed (Figure 3.24).

Figure 3.22 (next page). Binding patterns of the BR7ecto226 probe in the adult mouse cerebellum. Low (A) and high (B) magnification of the cerebellum show strong staining concentrated in the white matter (wm). Less intense staining is observed in Purkinje cells (pl), in single cells of the granular layer (gl) and in tracts (arrowhead) of the molecular layer (ml). Bar = 1 mm (C) Enlargement of the dashed squared region of figure A showing detailed staining of fiber tracts at the white matter branching. Bar = 0.1 mm. (D) Immunostaining of CNPase by means of the monoclonal antibody 11-5B to CNPase. Positive staining was localised on the white matter (wm) and strongly resembles that observed for BR7ecto226 (see C), with fiber tracts elongating from the white matter into the granular layer (gl). Bar = 0.1 mm.

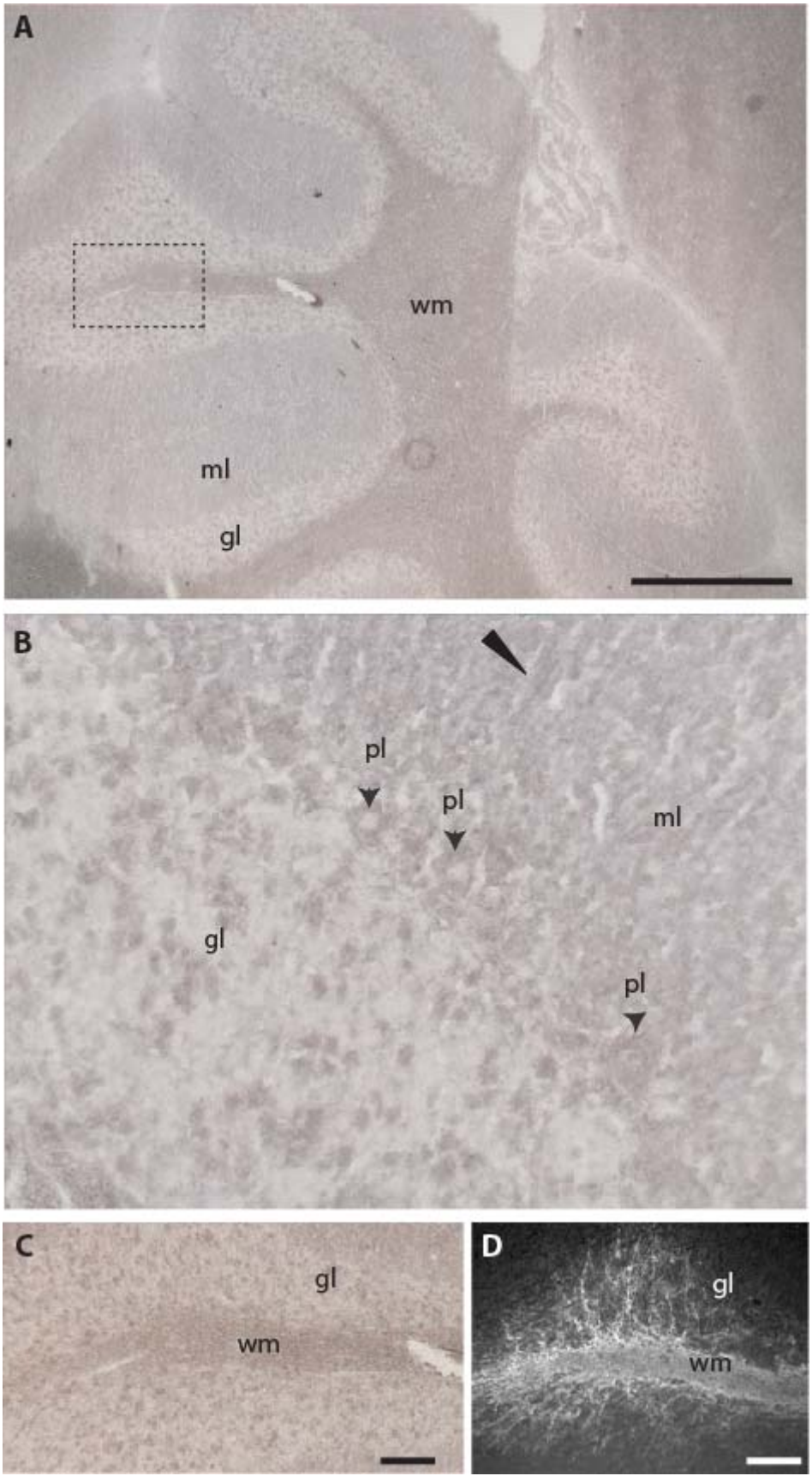
A
wm
ml
gl
B
pl
pl
ml
gl
pl
C
gl
wm
D
gl
wm

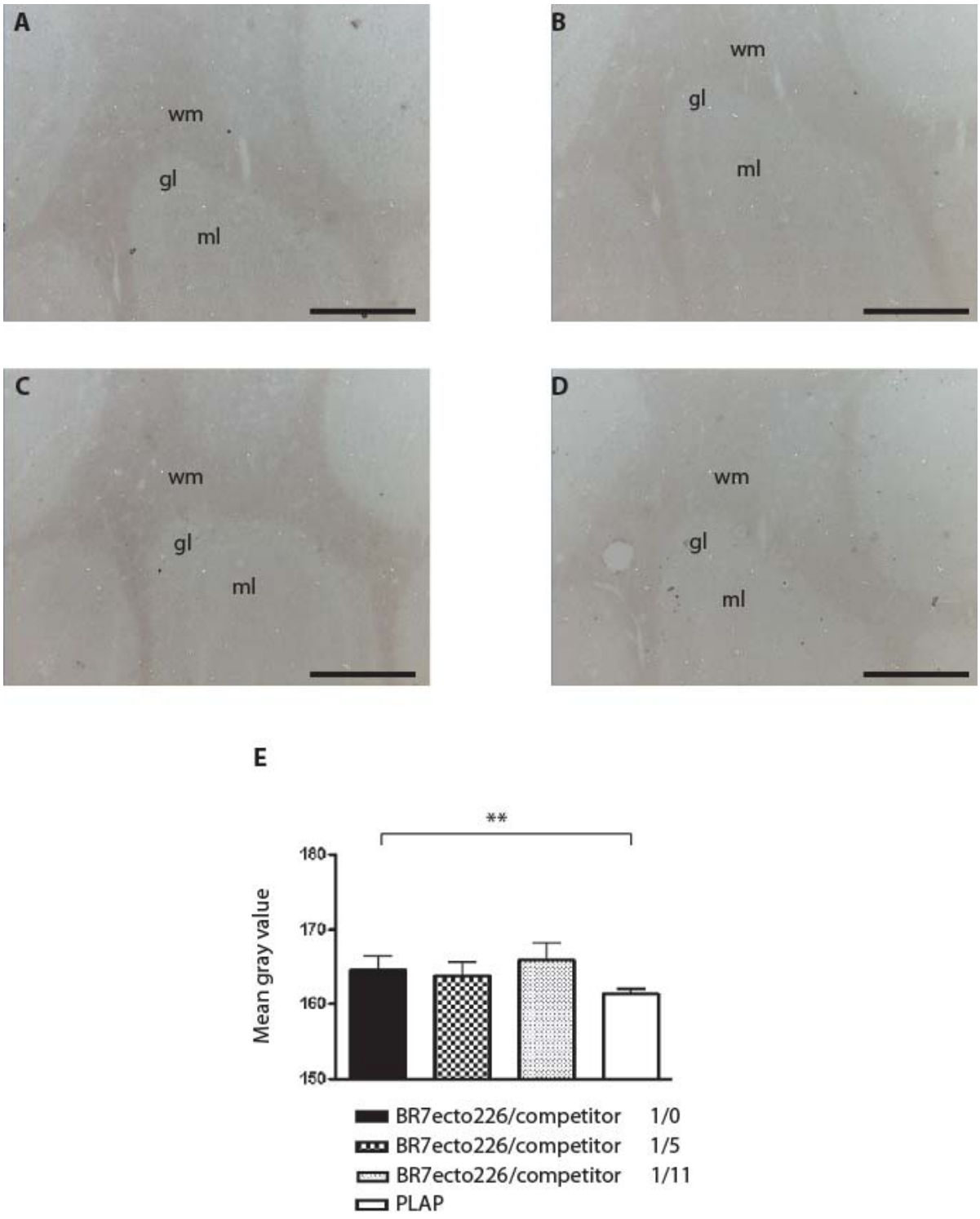

Figure 3.23. The binding of BR7ecto226 probe to the mouse cerebellum is not altered by the PTPBR7 extracellular domain itself. Increasing amounts of BR7ecto226-His protein were mixed with fixed amounts of the BR7ecto226 probe. Molar ratios BR7ecto226/BR7ecto226-His were respectively 1/0 (A), 1/5 (B), 1/11 (C). (D) Comparative staining with the sole PLAP containing conditioned medium after normalization for PLAP activity. Bar = 1 mm. gl = granular layer. ml = molecular layer. (E) Quantification of staining intensity in the white matter (wm) was performed as described in Materials and Methods. Average mean gray values are shown and results (n=6 except for ratio 1/5 where n=5) are presented as Mean ± S.D. No significant decrease in average gray values was observed, except when using the sole PLAP containing medium (p=0.003).

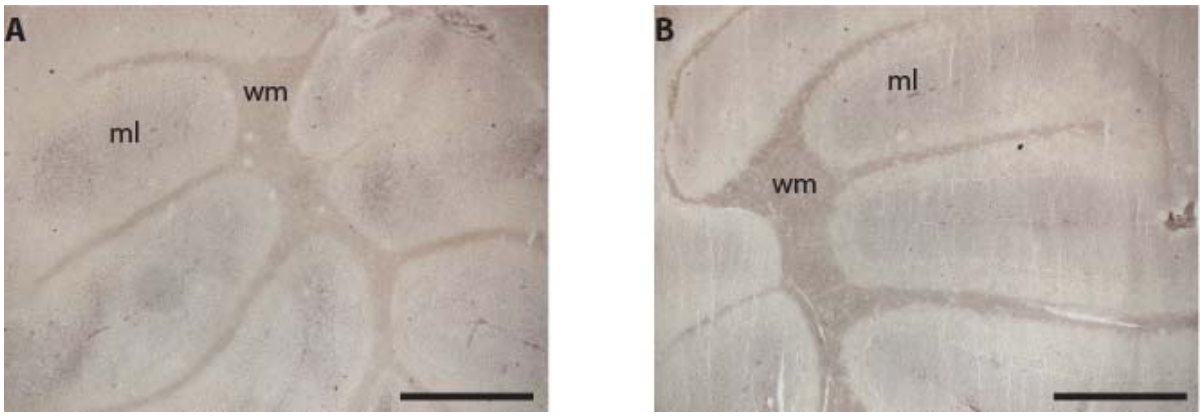

Figure 3.24. Binding patterns of BR7ecto226 probe do not differ in wild-type and *Ptprr* knock out cerebellum. Low magnification of wild-type (A) and *Ptprr* knockout (B) sections of cerebellum do not show any relevant difference in binding patterns. wm = white matter. Bar = 1 mm.

3.4.4 Assessment of direct binding to heparan- and chondroitin-sulphate GAGs

Sulphated GAGs have been found in some instances to be RPTP ligands (den Hertog et al. 2008) and have important roles in development and plasticity in the postnatal brain (Bovolenta and Fernaud-Espinosa 2000; Galtrey and Fawcett 2007). Therefore we investigated if GAGs would be also PTPBR7 ligands. Direct binding of the BR7ecto226 probe to a panel of GAGs was tested using a modified ELISA protocol (van Kuppevelt et al. 1998). Purified HS and CS A, C, D and E chains were coated in wells of a microtiter plate. Application of single chain GAG-specific antibodies in parallel control wells confirmed successful coating (data not shown). Culture medium containing the BR7eco226 protein was incubated in coated wells to allow binding and excess was removed by thorough washing. Binding of the BR7ecto226 probe was determined by detection of AP activity in the wells and results demonstrate that HS and CS do not bind the BR7ecto226 probe in this set-up (Figure 3.25).

As an alternative approach we tested whether chondroitin sulphates, the most abundant GAGs in the CNS, are contributing to BR7ecto226 binding in the RAP in situ assay. Removal of CS by chondroitinase ABC did not alter either the patterns or the staining intensity of BR7ecto226 in the cerebellar white matter (Figure 3.26). Degradation of CS by chondroitinase ABC was confirmed independently by applying the enzyme to wells coated with CS in an ELISA set-up (data not shown). Collectively, these data imply that CS are not the main binding sites for BR7ecto226 in adult mice brain and that HS is not a direct ligand, at least *in vitro*.

3.4.5 Candidate protein ligands for the PTPBR7 extracellular domain

Next we investigated protein molecules as possible candidates exploiting the fusion protein BR7ecto226-His in two independent affinity purification assays from wild-type mouse brain lysates. Proteins binding to the PTPBR7 ectodomain were then separated on SDS-PAGE and visualized with Coomassie staining. Gel lanes were cut and proteins identified by means of

Liquid Chromatography coupled to Mass Spectrometry. A full list of identified proteins is reported in Table S2 (Supplementary Tables, par. 6.4). Three proteins were retrieved reproducibly in both samples analyzed: the guanine nucleotide-binding protein G(o) subunit alpha (Gαo), the putative cell adhesion molecule neurotrimin (Ntm) and the calcium/calmodulin-dependent kinase II alpha/beta (CaMKIIα/β) (Table 3.6).

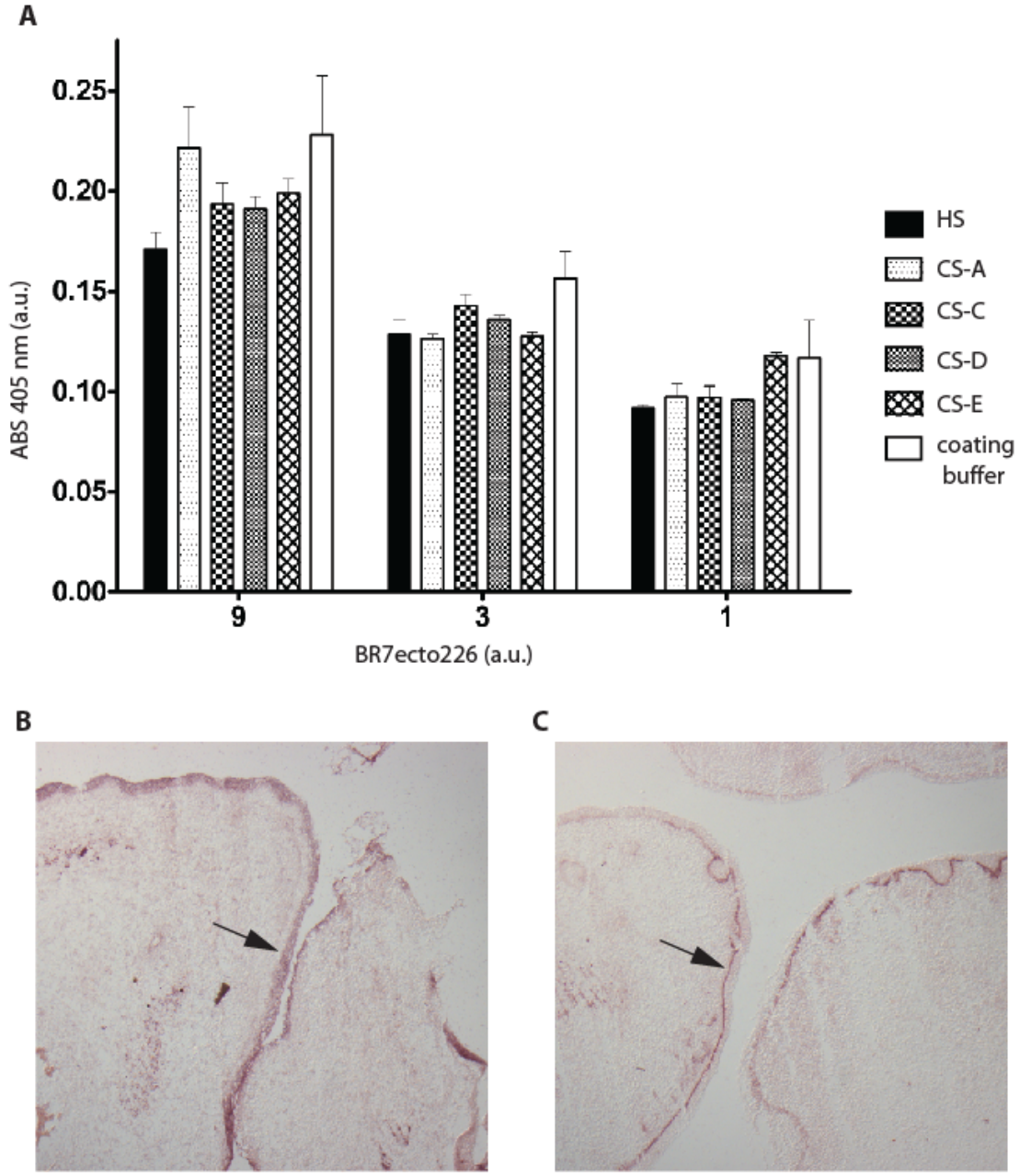

Figure 3.25. The BR7ecto226 probe does not bind to HS and CS *in vitro*. Conditioned medium containing the BR7ecto226 probe was added to the wells of a 96 wells-plate previously coated with one of the indicated GAG chain. The binding was assessed by measuring the ABS at 405 nm. No differential intensity was observed in comparison with the uncoated wells. The successful coating of the GAGs to the wells was separately confirmed by incubation with specific antibodies. Results (n=3) are presented as Mean ± S.D. (B) RAP *in situ* staining of the epidermis (arrow) in mouse embryonic cryosections using BR7ecto226 as a probe. (C) The RPTPσ ectodomain probe displays distinct binding to the basal laminae (arrow), whereas BR7ecto226 does not.

Notably these proteins, with the exception of CaMKIIα/β, were not purified when the Histidine-tagged extracellular domain of an unrelated PTP, RPTPμ, was used as bait. It is of note that CaMKIIα/β subunits were also retrieved in the affinity purification where the GST fusion protein of the phosphatase domain of PTPRR was used (see Table 3.3). Future experiments will be aimed at the validation of the identified candidate binding proteins.

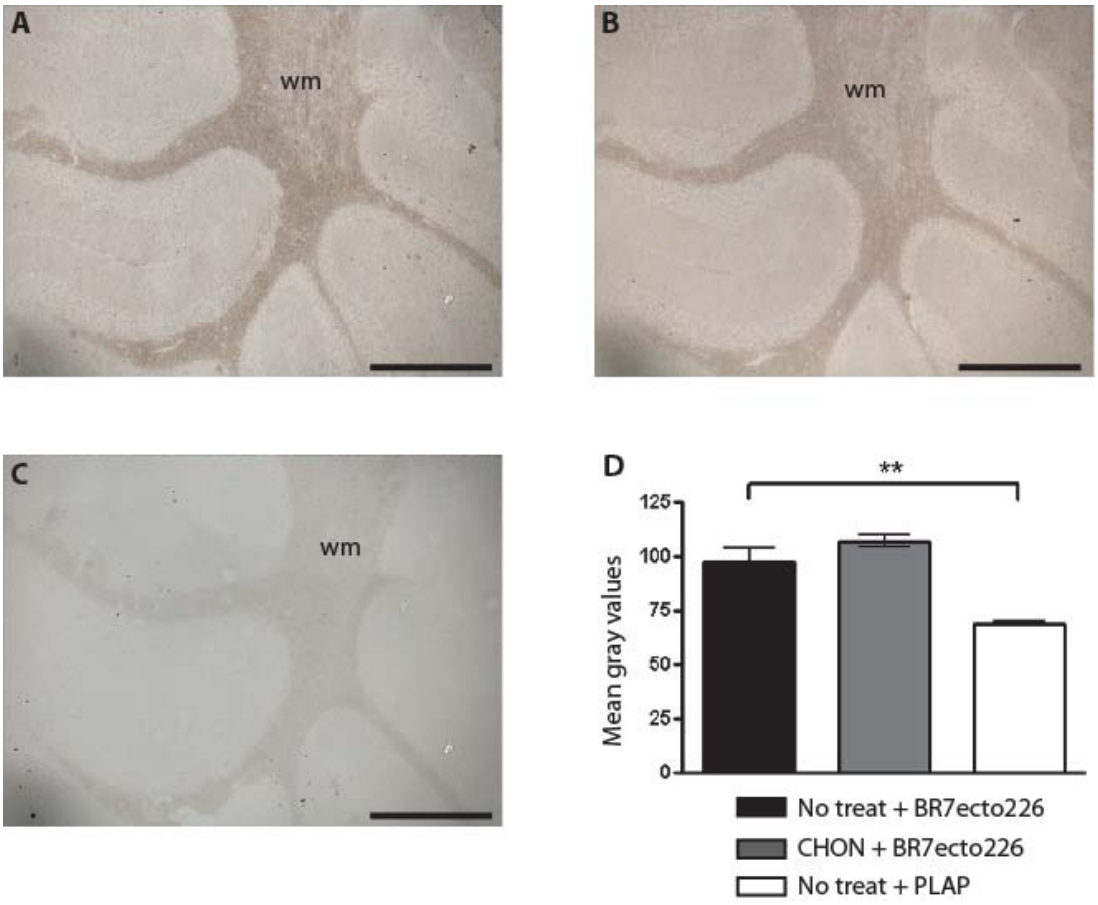

Figure 3.26. Digestion of CS chains does not alter BR7ecto226 staining patterns and intensity in the cerebellar white matter. Conditioned culture medium containing the BR7ecto226 probe was incubated on Chondroitinase ABC - treated and non treated coronal sections of the wild-type cerebellum according to the RAP *in situ* procedure. Low magnification images of non treated (A) and Chondroitinase ABC-treated (B) brain sections do not show any relevant difference in binding patterns. C) Comparative staining with the sole PLAP containing medium after normalization for PLAP activity. Bar = 1 mm. D) Quantification of staining intensity in the white matter. Mean gray values are shown. The experiment was repeated 3 times and only the BR7ecto226 and the PLAP staining intensity were consistently found to be significantly different. Results (n=3) are presented as Mean ± S.D. (p=0.0013). CHON= chondroitinase ABC. No treat = no treatment.

Table 3.6. Proteins identified by LC/MS-MS and Mascot Search that were affinity-purified from brain lysates using BR7ecto226-His as bait. Proteins that had Mascot scores above 60 and did not purify in isolates using an unrelated His-tagged bait or nickel beads alone are listed. Data from two independent isolates are shown. A full list of proteins identified in this way is provided as Supplementary Material (Table S1). *CaMKII protein was detectable in control samples but Mascot scores (38) were below threshold. Subunits α and β of CaMKII have high sequence identity and could not be distinguished in the analysis.

Protein name	**Protein mnemonic identifier**	**Uniprot Accession number**	**Mass** (kDa)	**Mascot scores**	**Queries matched**	**Function**
Guanine nucleotide-binding protein G(o) subunit alpha	Gnao1	GNAO_MOUSE	40	85	2	Modulator / transducer of GPCR signaling. G(o) protein function is not clear. GNAO1 mutation implicated in breast cancer
				139	5	
Neurotrimin	Ntm	NTRI_MOUSE	38	77	5	Neural cell adhesion molecule of the IgLON subfamily of immunoglobulins
				31	1	
Calcium/calmodulin-dependent protein kinase type II	Camk2a Camk2b	KCC2A_MOUSE KCC2B_MOUSE	54 60	153*	4	Prominent kinase in the central nervous system, implicated in long-term potentiation and neurotransmitter release
				200*	5	

Chapter 4

➢ Discussion

"The idea is to try to give all the information
to help others to judge the value of your contribution;
not just the information that leads to judgment
in one particular direction or another"
Richard P. Feynman

"All our knowledge begins with the senses,
proceeds then to the understanding, and ends with reason.
There is nothing higher than reason.
All the interests of my reason, speculative as well as practical,
combine in the three following questions:
What can I know? What ought I to do? What may I hope?"
Immanuel Kant

4.1 Brief summary of obtained results

Protein tyrosine phosphorylation has been recognized as a major signal transduction mechanism in higher eukaryotes. Among the central players in phosphotyrosine-based signalling are protein tyrosine phosphatases (PTPs), which form a functional dyad with the family of protein tyrosine kinases. Aberrant cell signalling may undermine proper functioning of cells and thus contribute to the development of disease states. We have investigated the molecular details of PTPRR–mediated signal transduction in the mouse central nervous system (CNS). Earlier work demonstrated that mice with PTPRR deficiency display reduced motor coordination skills and hyperphosphorylation of the ERK MAP kinases. We have searched for associated intracellular substrates and extracellular ligands of the PTPRR enzymes using a variety of approaches. Screening of short phospho-peptides in an *in vitro* dephosphorylation assay resulted in the candidacy of several proteins (i.e. HER3, HER4 and SHP1) as putative PTPRR substrates. However, phosphorylation levels of full-length candidate substrates were not noticeably reduced by PTPRR activity *in vitro* and in mammalian cells. Similarly, we did not observe altered phospho-levels for N-cadherin, a proposed substrate for rat PTPRR, upon co-expression with PTPRR.
An enzyme-based binding assay was used, on brain sections and *in vitro*, to identify potential ligand molecules that might bind to the PTPRR extracellular portion. Results thus far point to the presence of such ligands in the myelinated fiber tracts and we could exclude the polysaccharides heparan- and chondroitin-sulphate, that serve as ligands for other receptor-type PTPs, as PTPRR-binding molecules. Finally, using PTPRR variants as affinity reagents we purified interacting proteins from mouse brain lysates, and subsequent mass spectrometric analyses indicated the alpha/beta subunits of calcium/calmodulin-dependent kinase II (Camk2a/b), the guanine nucleotide-binding protein G(o) subunit alpha (Gnao1), and the IgLON type cell adhesion molecule neurotrimin (Ntm) as new PTPRR-associating candidates. These preliminary results suggest PTPRR involvement in cell-cell adhesion processes and calcium ion-regulated events that are instrumental in neuronal development and plasticity. Follow-up studies are needed to fully define PTPRR roles in the mouse nervous system.

4.2 Identification of PTPRR substrates

Testing interactions
About twenty years of studies attempting to identify PTPs substrates resulted in three types of biochemical approaches that proved to be successful: a) the combination of a substrate-trapping mutant with modified yeast-two hybrid (Y2H) screens in which cDNA library products are phosphorylated by constitutively active PTKs and D/A substrate-trapping mutants are used as bait (Kawachi et al. 2001; Fukada and Noda 2007); b) the detection of co-immunoprecipitating proteins by western blot following co-expression with one of the substrate-trapping PTP mutants (reviewed in (Blanchetot et al. 2005)); c) the combination of substrate-trapping techniques with mass spectrometric identification of co-purifying proteins (Kolli et al. 2004). The main advantage of the latter method is its versatility; any cell type, tissue or organ can be used. In addition, pervanadate-treatment of cell lysates and tissues can

be applied to boost phosphotyrosine-containing protein content for *in vitro* GST–PTP substrate-trapping mutant pull-down experiments, eliminating the need to know which kinase(s) phosphorylate(s) the substrate (Blanchetot et al. 2005).

Past studies succeeded in identifying the MAP kinases ERK1, ERK2, ERK5 and p38 as PTPRR substrates (Pulido et al. 1998; Ogata et al. 1999; Buschbeck et al. 2002). The techniques used were GST pull-down and co-immunoprecipitation assays, making use of 20-50 mM Hepes or Tris buffers of pH 7.5-8.0 and physiological salt concentrations (150 mM NaCl), with the addition of 0.1-1% non-ionic detergent. In yeast-two-hybrid (Y2H) experiments, that impose karyoplasmic conditions on the associations tested, of the application of PTP-SL cytoplasmic domain (aa142-549) allowed the confirmation of ERK2 and p38 as interacting proteins.

In our attempts to identify additional PTPRR substrates we started off testing the dephosphorylation of phospho-tyrosine (pTyr)-containing peptides by the PTPRR phosphatase domain. The result of this screen was used as a source of putative substrates for further validation by means of *in vitro* binding and dephosphorylation studies and *in vivo* co-expression experiments exploiting PTPRR wild type or substrate-trapping isoform. In particular the proteins HER3, HER4, SHP1 and N-cadherin were included in this assessment. The first three were prominently present in the list of candidate substrates that arose from the peptide-array. N-cadherin was included because PCPTP1, the rat homolog of PTPBR7, demonstrated effective dephosphorylation of an N-cadherin-derived phospho-peptide (Barr et al. 2009). As described in the introductory chapter, HER4, SHP1 and N-cadherin are known to be implicated in brain development or functioning.

Results indicated that, under the conditions that we used, N-cadherin was not bound by the C/S substrate-trapping mutant of PTBR7, neither *in vitro* nor after co-expression in COS-1 cells (Fig. 3.14). Likewise, confirmation of the status of HER4 and SHP1 as PTPRR substrates could not be obtained on the basis of our current data. In particular, SHP1 or HER4 co-immunoprecipitation with PTPRR was observed in some experiments but this could not be reproduced consistently (Fig. 3.12 and 3.13, respectively). In addition, the immunoreactive band that represents HER4 appeared at slightly altered heights on immunoblots (Fig. 3.13), a phenomenon that may mark molecular weight shifts due to differential phosphorylation of the protein. It is of note that thus far nineteen tyrosine phosphorylation sites have been reported for HER4 (Kaushansky et al. 2008). Alternatively, the apparent band shift may be an antibody artifact or it may reflect protein expression and processing imperfections resulting from over-expression. Finally, *in vitro* dephosphorylation assays and assessments of total phosphotyrosine levels of HER4, SHP1 and N-cadherin did not reveal significant differences following incubation or co-expression with wild-type or inactive PTPRR mutants, respectively. For HER3, another candidate substrate derived from the peptide array data, we unfortunately were not in the position to further put it to the test because sufficient phosphorylation levels of the protein could not be obtained, not even when co-expressed with catalytically inactive PTPRR in COS-1 cells.

There remains the possibility that COS-1 cells simply do not provide the optimal environment for neuronal PTPRR interactions. We therefore repeated some of the tests in a much more physiological cell system, namely PC12 rat neuroendocrine cells. PC12 cells are derived from a rat pheochromocytoma tumour and, together with Neuro2A mouse neuroblastoma cells,

provide a model system that is commonly used to study pathways involved in early neuronal differentiation and interactions between cell signalling pathways (Adler et al. 2006; Ma'ayan et al. 2009). PC12 and Neuro2A cells can be driven to differentiate by specific ligands. For example, nerve growth factor (NGF), a neurotrophin and an agonist of the TrkA tyrosine kinase receptor, triggers PC12 cells to differentiate (Lange-Carter and Johnson 1994; York et al. 1998) and HU-210, a cannabinoid receptor agonist, triggers Neuro2A differentiation (He et al. 2005). PTPRR isoforms have been over-expressed in Neuro2A cells and the observed staining patterns (Dilaver et al. 2003) reflect PTPRR protein localisation as observed in both primary neurons and PC12 cells (Hendriks et al. 2009) that display very low endogenous expression levels. Both PTPBR7 and PTP-SL share a common membrane topology (Noordman et al. 2008) and localize at the trans-Golgi network and on endocytic vesicles (van den Maagdenberg et al. 1999; Dilaver et al. 2003). But while PTPBR7 is present also on the plasma membrane, PTP-SL is not.

In view of the above, we turned to PC12 cells and repeated the binding assays for the candidate proteins. Consistent with the knowledge that HER4 is not endogenously expressed in PC12 cells (Vaskovsky et al. 2000), the antibody HFR1 that is directed to HER4 did not identify any band at the HER4 expected molecular weights. Furthermore, although HER3 is expressed in PC12 (Vaskovsky et al. 2000), we did not detect immunoreactivity that could be ascribed to HER3 using the antiserum to HER3 that was kindly provided by dr. R. Lammers (Tübingen). We then focused our attention on endogenous SHP1 and N-cadherin in the parental PC12 cell line and in variants derived thereof in which endogenous PTPRR levels had been knocked-down using stable shRNA expression or in which PTPBR7 was stably over-expressed (Noordman et al. 2006). Upon immunoprecipitation of the total phospho-tyrosine-containing protein content in these cells, different staining patterns were observed for the distinct cell lines (Fig. 3.16A). However, none of these bands corresponded to SHP1 or N-cadherin. Also, SHP1 and N-cadherin could not be co-immunoprecipitated with endogenous PTPBR7 or with added PTPBR7 C/S mutant protein (Fig. 3.16C). Therefore, binding of PTPRR proteins to SHP1 and N-cadherin could not be demonstrated in PC12 cells under the conditions tested. Irrespective, we clearly observed increased expression levels for both SHP1 and N-cadherin in PC12 cell lines that over-express PTPBR7 (Fig. 3.15A-B). We also observed that PTPBR7 over-expressing cells demonstrate increased adherence as compared to the parental PC12 cells and tend to form clumps (JS and YN, personal communication), a phenotype reminiscent of that of cells over-expressing cell adhesion molecules such as N-cadherin (Kim et al. 2011). These observations would suggest the existence of a, perhaps indirect, link between PTPRR and these two candidate substrate proteins that may involve the regulation of protein stability or gene transcription. Clearly, further experiments will be necessary to substantiate these observations and to characterize the relationship between PTPRR and SHP1 or N-cadherin in PC12 cells.

Recent technical advances have made mapping complete and accurate protein interactions a realistic possibility, mostly thanks to yeast-two-hybrid (Y2H) approaches and affinity purifications coupled to mass spectrometric identification (Wright 2009). Both Y2H and affinity purification strategies are, however, regarded as unsuitable for the detection of short-lived interactions between proteins (Wright 2009). Due to the transient nature of the enzyme-

substrate complex, wild-type PTPs are often not suitable to successfully identify substrates and the development of substrate-trapping variants successfully aimed at overcoming this hindrance (Liang et al. 2007). A possible reason why the candidate substrates that we obtained via the phospho-peptide array screen could not be validated in mammalian cell systems may be that we tested the interactions engaged by PTPRR isoforms under too stringent conditions. As mentioned previously, Y2H and biochemical approaches led to the identification of MAPKs as substrates of PTPRR (Pulido et al. 1998; Ogata et al. 1999; Dilaver et al. 2003). Also β4-adaptin resulted from the Y2H screen for PTPRR interacting proteins, and PTPRR transmembrane isoforms co-localized with β4-adaptin in Neuro2A cells (Dilaver et al. 2003). Furthermore, co-expression of PTP-SL and β4-adaptin in Neuro-2A cells led to a redistribution of PTP-SL from a vesicle-associated to a more dispersed, cytoplasmic localisation. However, when direct interaction of these two proteins by GST pull-down and by co-immunoprecipitation from co-expressing COS-1 cells was investigated, no association was observed. ERK2, on the contrary, was readily co-purified with PTP-SL in the same experiment. Several reasons were brought up to explain this phenomenon, including the suggestion that high co-expression of PTPRR and β4-adaptin proteins may create a reciprocal exclusion effect caused by competition for the same subcellular localization, thereby preventing their association. Such a reciprocal exclusion should not be at stake when performing GST pull-down and Y2H assays because the competition effect is absent (Dilaver et al. 2003). Interestingly, the direct interaction of PTP-SL and β4-adaptin was tested making use of buffers similar to those used to reveal MAPK-PTPRR interactions. The PTP-SL construct used as bait for the Y2H, the GST pull-downs and the co-immunoprecipitation assays contained not only the PTP domain but also included the KIM domain that is responsible for the interaction with ERK proteins. Thus, the picture emerges that the presence of the KIM domain is a prerequisite for a sufficiently strong interaction of MAPKs with PTPRR and that the interaction with other proteins, such as β4-adaptin, is of much lower affinity. Normally, buffer types, most notably pH levels and salt and detergent concentrations, are indicated as major determinants for preservation of protein-protein interactions (Brymora et al. 2004; Golemis and Adams 2005). In our assays we made use of low stringency conditions (50 mM Hepes or Tris-HCl pH 7.2-7.5; 150 mM NaCl; 1% Triton X-100) according to peer-reviewed methods for the identification of PTP targets using substrate-trapping techniques (Blanchetot et al. 2005; Tiganis and Bennett 2007). Washes, however, were never less than three and were performed thoroughly, indicating the possibility of a reduction in the amount of bound proteins – perhaps to levels below detection limits. The use of substrate-trapping mutants, either C/S or D/A or a combination of them should increase the stability of the binding of putative substrates, but ironically the status of PTPRR C/S and C/S-D/A mutants as efficient substrate-trappers has not been established yet. After all, in the PTPRR – MAPK association it is the KIM domain that plays the major role. The MAP kinases ERK1 and ERK2 even appear to precipitate less well with the C/S mutant than with wild type PTPRR (Ogata et al., 1999) and ERK5 still associates with PTPRR mutants that completely lack the PTP domain but still contain the KIM segment (Buschbeck et al., 2002). Unpublished work from our lab (Y.N., personal communication) shows that PTPRR can interact with and dephosphorylate the TrkA tyrosine kinase receptor and that the interaction requires the presence of the transmembrane spanning region in both proteins. The picture

therefore emerges that for PTPRR substrate identification one may need much more than just the catalytic PTP domain, be it in wild type or substrate-trapping mode.
Another issue is the specificity of the phospho-peptide dephosphorylation assay. Barr et al. (2009) assessed PTP catalytic activity against a panel of phospho-peptides derived from potential physiological substrates and evidenced that each PTP had a phospho-peptide selectivity profile that correlated with that of the subgroup the PTP belongs to. In this regard, PTPs of the R7 group (PCPTP1, STEP and HEPTP) showed high selectivity in comparison with the R3 group PTPs, which were able to dephosphorylate all presented phospho-peptides. Furthermore, PTP catalytic domains exhibit exceptional substrate specificity *in vivo*, which is conveyed both by the catalytic domain and other regulatory mechanisms including restricted subcellular localization, posttranslational modification events, specific tissue distribution, and accessory or regulatory domains (Tiganis and Bennett 2007). PTP catalytic domains display differences in surface electrostatic potential, a property that is likely to influence substrate recognition, association with regulatory proteins, and regulatory mechanisms such as dimerization (Barr et al. 2009). This implies that – as a mirror image – also the structural surface displayed by the folded PTP substrate is a crucial determinant in the interaction with the enzyme, and this is only partly represented by short phospho-peptide sequences. Therefore, one should use phospho-peptide array screens only as a source of candidate substrates that require further analysis by biochemical approaches that pay tribute to the impact of the full-length substrate structures involved (Tiganis and Bennett 2007). We decided to complement the phospho-peptide array screening strategy with an approach that gives credit to the native structure of the assumed substrates. To this end, we employed the GST-PTP-SL proteins used in the phospho-peptide screen also for affinity purification purposes. GST pull-down of associating proteins from brain lysates was followed by mass spectrometric analysis to identify the purified interactors. The phospho-peptide dephosphorylation approach and the GST-pull down strategy both led to distinct lists of candidate proteins. This is to be expected to some extent since the phospho-peptide array only contained a restricted panel of peptides and thus may lack some physiologically important ones that, in turn, are more likely to be encountered in the pull-down approach. Before describing these results (paragraph 4.4) we will first discuss the methods employed for the dephosphorylation and binding assays.

Performing dephosphorylation assays
We focus here on those conditions employed in our biochemical assays in the light of the inability to show dephosphorylation and binding of the tested candidate substrates by PTPRR. Protein tyrosine phosphatase activity is compatible with commonly used buffer systems that act in the physiological pH range (McCain and Zhang 2002) such as Hepes (20–25mM), acetate (50–100 mM), glycine (100 mM) or Tris (50 mM). Mes, however, being a sulfonic derivative, was shown to be a competitive inhibitor of *Yersinia* Yop51 tyrosine phosphatase with a K_i of 26 mM (Zhang 2002). Depending on the phosphatase, the buffer should be chosen such that its pK_a is close to the optimal pH of the particular phosphatase. For example, Bis–Tris has a p*K*a of 6.5 making it the most suitable buffer salt for PTP1B (Montalibet et al. 2005). Past experiments showed that GST fusions of the PTPRR phosphatase domain are active in Hepes-based buffers of pH 7.2 (Noordman et al. 2008). The physiological ionic

strength of 150 mM is fully compatible with phosphatase assays and can be achieved by adding NaCl to the buffer. Dithiothreitol (DTT) is used to keep reducing conditions, thereby protecting the catalytically essential cysteine from oxidation and thus ensuring phosphatase activity. EDTA is added primarily to chelate iron which can react with thiols, such as DTT, to produce free radicals that will inactivate the enzyme (Montalibet et al. 2005). Again, previous experiments showed that PTPRR is active in buffers containing 1-10 mM DTT and 5 mM EDTA (Noordman Y., unpublished data). Vanadate compounds must be avoided or carefully removed from the reaction environment because they are potent phosphatase inhibitors (Huyer et al. 1997). Vanadate binds to the catalytic pocket even in substrate-trapping mutants, as shown by the application of vanadate competition to validate phosphatase substrates. Importantly, the current data suggest that vanadate compounds have a higher affinity for the enzymatically impaired D/A substrate-trapping mutants than for the catalytically dead C/S variants (Blanchetot et al. 2005). Treatment with EDTA and DTT in lysis buffers (Fig. 1.8) proved successful in chelating unreacted vanadate compounds (Huyer et al. 1997). Finally, detergent concentration must be determined carefully. Triton X-100 is often used to prevent aspecific binding of the phosphatase to itself or to the wells: 0.01% is a sufficient quantity to achieve this effect. Omitting the Triton or using too much (1% and above) results in gradual loss of activity. On the other hand, addition of at least 1% of non-ionic non-denaturing detergent is advised for recovery of transmembrane proteins or, in immunoprecipitation and affinity purification protocols, to prevent sticking of beads to tube walls (Montalibet et al. 2005).

Bearing all the above considerations in mind, we confirmed that the PTPRR isoforms we exploited were indeed active in the buffers used for dephosphorylation assays *in vitro* (Figure 3.17). Nevertheless, phosphorylation levels of all candidate substrates were not altered upon incubation with the wild type PTP as compared to the inactive mutant PTPRR. We also observed that treatment of the phosphatase with 0.1 mM pervanadate or 1 mM orthovanadate was sufficient to completely inhibit its enzymatic activity (Figure 3.17). Use of phosphatase inhibitors is necessary to preserve the phosphorylation status of candidate substrates (Fig. 3.9) and they are therefore included in most cell and tissue lysis buffers (Blanchetot et al. 2005). We asked ourselves whether these very same inhibitors would perhaps interfere with subsequent PTPRR-dependent dephosphorylation reactions. Treatment with EDTA and DTT, to remove remaining unreacted vanadate, turned out not sufficient to allow activity of freshly added phosphatase (Figure 3.18). Pervanadate-treated samples showed partial recovery of phosphatase activity (Fig. 3.18 and 3.19) which may be due to the competing reaction of DTT with pervanadate that would retard the oxidation of the catalytic site cysteine (Huyer et al. 1997). Any remaining vanadate would thus directly inhibit the freshly added phosphatase. Surprisingly, we could not reverse the orthovanadate-induced inactivation of the phosphatase by using EDTA, even though EDTA amounts were at least five times in excess of orthovanadate. This points to a very high sensitivity of PTPRR towards orthovanadate inhibition as compared to PTP1B, for which complete reversibility was observed (Huyer et al. 1997). Past studies showed that 0.5 mM orthovanadate was enough to reduce recombinant PTPRR phosphatase activity to 40% while Ser/Thr phosphatase inhibitors had no influence (Hendriks et al. 1995a). We reasoned that while orthovanadate is being bound by EDTA in the reaction mixture the PTPRR catalytic site is again quickly occupied by residual free

vanadate. This phenomenon would account at least in part for our inability to demonstrate *in vitro* dephosphorylation in all samples in which either pervanadate or orthovanadate was used to either induce or maintain hyper-phosphorylation. The irreversibility of orthovanadate binding to PTPRR may perhaps reflect some unique structural feature of its catalytic pocket. It is known that, upon substrate recognition, the WPD loop is reoriented to optimize salt-bridge interactions with the substrate phosphate so that the catalytic site cysteine can commence a nucleophilic attack on the phospho-tyrosine phosphorus atom (Eswaran et al. 2006). The flexibility of the WPD loop affects the size and shape of ligands that bind to the active site and therefore has major implications on any drug-design strategy. Interestingly, in crystallization experiments the PTPRR PTP domain adopted an open WPD loop conformation, while in PTP1B crystals the WPD loop is closed (Eswaran et al. 2006). The Tyr-Lys-Thr recognition loop in all KIM-containing PTPs contrasts with the Tyr-Arg-Asp loop found in PTP1B and has been suggested to reduce substrate affinity and limit catalytic activity of these PTPs (Eswaran et al. 2006; Barr et al. 2009). On the other hand, the catalytic efficiency (*k*cat/*K*m) was not significantly different for PTP1B and all R7-group PTPs when measured using DiFMUP as a substrate (Eswaran et al. 2006). It has been reported that incidentally DTT can combine with O_2 and generate hydrogen peroxide that subsequently could convert vanadate into pervanadate (Fig. 1.8) and thus trigger permanent inhibition of PTPs by oxidation (Huyer et al. 1997). We cannot exclude this possible *in situ* generation of pervanadate in our experiments and perhaps this forms the explanation for the permanent inhibition we observed upon orthovanadate addition. In fact we observed permanent inhibition when orthovanadate was present in the buffer before the PTP was added and also when it was supplemented later on. These considerations indicate that other strategies for induction and preservation of phosphorylation levels may be required when studying PTPRR substrates.

Similar to what we observed for the *in vitro* phosphatase assays, assessment of phospho-levels of candidate substrates following co-expression with PTPRR isoforms did not reveal significant changes. These results underscore the importance of the correct reaction environment but in addition point at another possible culprit. Phospho-peptide dephosphorylation by the PTPRR phosphatase domain can be scored on the basis of release of inorganic phosphate. Detection of changes in phosphotyrosine content of target proteins, both in *in vitro* and in-cells studies, may require availability of antibodies that are directed against individual, phosphorylation-sensitive epitopes in these proteins. Many proteins can be phosphorylated at multiple sites and PTPRR enzyme activity will likely address only a restricted subset of pTyr sites, making it quite hard to detect overall changes in phosphotyrosine levels using general anti-pTyr antibodies. In absence of suitable antibodies, (semi-)quantitative MS-based identification of phospho-peptides in the target proteins under study may represent an appealing alternative.

In conclusion, thus far most studies dealt with stable PTP-substrate complexes that have been identified via trial and error and based on intuition and clues about the signalling pathways involved (Tiganis and Bennett 2007). Identification heavily relied on the existence of available antibodies revealing the trapped substrate protein at an expected molecular weight. It appears that only a combination of approaches, high-throughput and high-affinity biochemical methods, ultimately may lead to the identification of PTPRR substrates.

4.3 Is the transmembrane protein PTPBR7 a receptor molecule?

Vertebrate RPTPs show strong developmental expression in the central (CNS) and peripheral nervous system, coinciding with significant events such as axogenesis, target contact, synaptogenesis and plasticity (Stoker and Dutta 1998; Van Vactor 1998; Paul and Lombroso 2003; Stepanek et al. 2005). Immunoglobulin-like domains and Fibronectin type III domains, typically found in neural CAMs, are present in many RPTPs suggesting they could be receptors for contact-mediated cues encountered by growth cones. Indeed, for some CAM-like RPTPs a number of ligands have been discovered over the past years (den Hertog et al. 2008). For example, the R2A family members RPTPσ and PTP-LAR have both multiple binding partners. RPTPσ binds nucleolin, alpha latroxin and the heparan-sulphate (HS) proteoglycans agrin and collagen XVIII in the nervous system and skeletal muscle and chondroitin-sulphate (CS) produced by astroglia (den Hertog et al. 2008; Fry et al. 2010). The R2B family members RPTPμ, RPTPκ and RPTPλ, and the R2A member RPTPδ all display homophilic interactions that are important in cell adhesion processes (den Hertog et al. 2008).
Given that PTPBR7 is a member of the transmembrane receptor-like PTP subfamily, we set out to determine the ligand binding potential of the extracellular segment of PTPBR7 in the adult mouse brain. The biophysical properties of extracellular protein-protein interactions range from very high-affinity interactions (K_D in the nM to pM range, in the case of soluble ligands) to extremely low-affinity interactions (K_D in the μM to mM range, typical for membrane-bound protein partners) (van der Merwe and Barclay 1996). Biochemical affinity purifications are generally regarded as being less suitable to detect extracellular protein-protein interactions. An important reason for this is that extracellular regions of proteins often contain structurally important posttranslational modifications, for example large hydrophilic sugar chains. The necessity of such modifications eliminates convenient and scalable expression methods, such as prokaryotic or cell-free systems, as a means to produce the extracellular proteins in an active conformation. Additionally, the amphipathic nature of transmembrane proteins may require the use of strong ionic detergents for solubilization, which then may turn incompatible with maintenance of the protein's native conformation. In addition, long and stringent washing steps are likely to undermine low-affinity and transient interactions (Wright 2009).
The expression pattern of the PTPRR gene suggests that potential extracellular ligands for the PTPBR7 isoform have to be located in mouse CNS. Given that the extracellular segment of PTPBR7 lacks any similarity to known protein-protein interaction motifs, we decided to adopt a technique that combines the reproduction of the *in vivo* conditions with the direct detection of binding sites, the RAP *in situ* method (Flanagan and Leder 1990; Flanagan et al. 2000). In this strategy, the alkaline phosphatase moiety that is fused to the PTPBR7 ectodomain can serve both as a detection means and as a dimerization tag, which may increase ectodomain avidity (Wright 2009). Forced ectodomain dimerisation may, on the other hand, also hamper protein interactions if the protein under study normally operates as a monomer *in vivo* (Stoker 2005). It is therefore of note that PTP-SL and PTPBR7 can homo- and hetero-multimerize (Noordman et al. 2008), thus indicating that dimerization induced by the alkaline phosphatase tag in this case can be viewed as an advantage. We successfully produced different variants of the soluble PTPBR7 ectodomain (called "BR7ecto" followed by the number of amino acids

included in the probe) that consistently displayed binding to highly myelinated areas in the brain, such as the white matter of the mouse cerebellum (Figs. 3.21 and 3.22).
The RAP *in situ* technique itself does not lead to the identity of any ligand molecule that may be detected. Bearing in mind that highly sulphated GAGs proved to be ligands of RPTPσ and PTP-LAR (Fox and Zinn 2005; Johnson et al. 2006; Shen et al. 2009), we tested whether GAGs are among the PTPBR7 ligands. We did not find evidence, however, for interactions of the PTPBR7 extracellular domain with HS and CS *in vitro* or *in situ* (Fig 3.25 and 3.26). As a means to confirm specificity, we attempted to compete for AP-tagged BR7ecto226 binding to the brain tissue by adding increasing amounts of a His-tagged PTPBR7 ectodomain probe, but this was unsuccessful (Fig. 3.23). This could be explained by assuming that only the dimeric form of the receptor, mimicked by the AP-tagged extracellular probe (Stoker 2005), and not the monomeric His-tagged variant is able to bind the potential ligand(s). This type of behavior has been observed for RPTPσ binding to heterophilic ligands (Lee et al. 2007). Alternatively, it may be that up to eleven-fold excess of competitor over AP-tagged fusion protein, as used in our assay, was simply not sufficient to saturate the PTPBR7 extracellular domain binding sites present in adult brain material. It is worth mentioning that the PTPBR7 ectodomain binding pattern was not altered in PTPBR7-deficient mice (Fig. 3.24) that display impaired motor coordination (Chirivi et al. 2007). This observation suggests that PTPBR7 – ligand interactions *in vivo* are not required to ensure ligand protein stability or routing.
In conclusion, the specificity of BR7ecto226 binding to mouse brain sections remains an issue but direct involvement of sugar moieties seems unlikely. We therefore turned to the search for protein ligands and, as was done for substrates, applied affinity purification from brain lysates in combination with mass spectrometric analysis to detect candidate protein ligands. A discussion of these results and the biological meaning of resulting candidate interactors is presented in paragraph 4.4.

4.4 Implications for the biological role of PTPRR in mouse brain from the identification of putative novel interactions partners

Many human inherited neurodegenerative disorders affect the cerebellum and result in motor coordination and balancing problems. Recent studies have suggested that altered Ca^{2+} homeostasis (exitotoxicity), transcriptional dysregulation, and impaired protein degradation are all possible causative mechanisms of neuronal degeneration at the basis of ataxic disorders (Paulson 2009). More general causes of neuronal death are reactive oxygen and nitrogen species (ROS and RNS) that both can act as signalling molecules and oxidizing agents. When the levels of these molecules are increased, vulnerable neurons will become prone to synaptic destruction, dendrite and axonal pathology and eventually neuronal death (Wang and Michaelis 2010).
In view of the locomotive deficits observed in PTPRR deficient mice (Chirivi et al. 2007), the identification of candidate PTPBR7 interacting proteins from brain lysates may help understand the mechanism(s) underlying ataxic disorders. The proteins that were co-purified (Tables 3.3 and 3.6) can be grouped in three major functional classes, namely proteins involved in neuronal functioning and morphology, cell-adhesion and cytoskeletal proteins. In

our affinity purifications we did not retrieve PSD-95, the most abundant membrane-associated protein of the postsynaptic density (PSD) fraction (Cho et al. 1992; Kistner et al. 1993), supporting the specificity of the procedures applied. Interestingly, CaMKII subunits were co-purified using either the PTPBR7 extracellular segment or the intracellular catalytic domain. Furthermore, CaMKII subunits were identified reproducibly by mass spectrometry in two independent co-purifications using the PTPBR7 extracellular domain as an affinity reagent on mouse brain lysates. CaMKII is a serine/threonine kinase that is highly expressed in brain and that phosphorylates several substrates upon activation by increased calcium ion levels (Colbran 2004b; Colbran and Brown 2004). A link between PTPRR functioning and Ca^{2+} regulation has been suggested before (Hendriks et al. 2009) and the present findings, once confirmed, shed light on a possible mechanism. Many studies have shown that CaMKII is concentrated in the PSD fraction (Gleason et al. 2003; Petersen et al. 2003) and that it is critically involved in the synaptic plasticity that underlies processes of learning and memory (Lee et al. 2009). In hippocampal CA1 pyramidal cells CaMKII enhances AMPA receptor-mediated synaptic transmission (Derkach et al. 1999) and contributes to the maintenance of dendritic spine structure via bundling of F-actin (Okamoto et al. 2007). Furthermore, mice lacking CaMKIIα expression display impaired spatial learning (Silva et al. 1992) and limbic epilepsy (Butler et al. 1995), and those deficient in the CaMKIV isoform show strong ataxic phenotype consistent with reduced amount of mature PC number and altered neurotransmission at excitatory synapses in PCs (Ribar et al. 2000).

Why are calcium and its regulation so important for the neuronal environment? Most Purkinje cells express the fast and slow calcium buffering proteins calbindin-D28k and parvalbumin, whereas basket, stellate and Golgi cells express only the slow buffer protein parvalbumin. These proteins regulate and are regulated by intracellular calcium level. They are, directly or indirectly, influencing the sensitivity of calcium channels, and may block further calcium entry into the cells (Schwaller et al. 2002). The absence of calcium buffering proteins results in marked abnormalities in cell firing, with alterations in simple and complex spikes or transformation of depressing synapses into facilitating synapses (Bastianelli 2003; Hartmann and Konnerth 2005). Abnormal calcium increases may result from diminished transport of cytosolic calcium to the extracellular environment, decreased sequestration into mitochondria and binding to intracellular Ca^{2+}-binding proteins or enhanced influx through voltage-gated calcium channels. The elevation in calcium concentration can lead to further release of calcium from the endoplasmic reticulum and also inhibit mitochondrial complex I thereby causing the formation of reactive oxygen species (ROS) (Starkov et al. 2004). During oxidative stress, ROS/RNS usually activate Ca^{2+} channels and repress Ca^{2+} pumps (Ermak and Davies 2002), resulting in elevation of calcium concentration. Ca^{2+} dysregulation has been regarded as an important contributor to the aging process (Foster 2007; Toescu and Vreugdenhil 2009). Ca^{2+}-buffering proteins such as calbindin D-28K and parvalbumin provide a direct link between calcium dysregulation and selective neuronal vulnerability in their specific distribution among different classes of neurons (Wang and Michaelis 2010).

Another protein that has been linked to calcium-dependent signalling is Gαo (Strittmatter et al. 1994; Xie et al. 1995; Horgan and Copenhaver 1998). The study of ionic currents in mouse hippocampal CA3 neurons revealed that modulation of Ca^{2+} currents by G protein-coupled receptors is changed and much slower recovery kinetics are displayed when Gαo isoforms are

lacking (Greif et al. 2000). Gαo deficient animals have normal brain morphology but suffer from tremors and occasional seizures, display severe motor control impairment and have a reduced life span of only two months (Valenzuela et al. 1997; Jiang et al. 1998). This finding is intriguing since locomotive impairment combined with normal brain morphology was also observed in *Ptprr*$^{-/-}$ mice (Chirivi et al. 2007) and in several mouse models that lack cerebellar calcium binding proteins (Hendriks et al. 2009). These findings suggest that slight modifications in calcium levels of specific neuronal cells have important consequences and strong alterations of calcium concentrations may even lead to neurodegeneration (Wang and Michaelis 2010). Also a calcium-dependent Homer1 protein has been identified as PTPRR candidate interactor in our co-purifications (Table 3.3). Homer1 proteins function as molecular bridges that link metabotropic glutamate receptors mGluR1 and mGluR5 to the inositol 1,4,5-trisphosphate receptors (IP_3Rs) on the endoplasmic reticulum and to additional synaptic ion channels such as calcium channels. Homer1 proteins, by virtue of their ability to form multimers, connect mGluR1 and mGluR5 also to components of the NMDA receptor signalling complex (Tappe and Kuner 2006). Together with proteins that bind calcium directly, Homer proteins are also regarded as calcium buffering proteins that ensure a high spatial and temporal fidelity of the Ca^{2+} signalling (Worley et al. 2007). These findings suggest that PTPBR7 could participate to calcium regulation via interaction with the above mentioned proteins. The regulatory subunit of the ion pump Na^+/K^+ ATPase, another candidate interactor of the PTPRR phosphatase domain (Table 3.3), targets the α subunit of the pump to the plasma membrane and functions as an intercellular adhesion protein (Geering 2008). The primary stimulus for the Na^+, K^+-ATPase is an increase in intracellular concentration of Na^+, and to a lesser extent increase in extracellular K^+. Intracellular Ca^{2+} inhibits enzyme activity by competing with Mg^{2+}, which is critical for ATP hydrolysis. Most ATP consumption in the nervous system is to supply energy for Na^+, K^+-ATPase, which maintains the electrochemical gradients that are continuously affected by neuronal activity and synaptic transmission. Impaired activity of the Na^+, K^+-ATPase is a primary mechanism of acute injury of neurons and glial cells in the setting of hypoxia, ischemia, hypoglycemia, and other conditions associated with failure of oxidative mitochondrial metabolism and ATP production. These processes lead to injury of the gray and white matter (Benarroch 2011).

Neurotrimin is a member of the IgLON family of neural cell-cell adhesion molecules that further comprises LSAMP, Neuronal growth regulator 1 and OBCAM. *In vitro* studies indicate a bifunctional activity of IgLON members in either enhancing or inhibiting neurite outgrowth depending on the subpopulations of cells in which they act (Gil et al. 2002; Reed et al. 2004; Schäfer et al. 2005). Interestingly, several IgLON family members were identified in co-purifications with PTPBR7 domains suggesting an involvement of PTPBR7 in cell-adhesion processes. Incidentally, we observed that PC12 cells over-expressing PTPBR7 adhere to each other and form clumps (see paragraph 4.2), a phenotype that is absent in the parental cell line. This implies that the increased adhesive properties in these cells are brought about by PTPBR7 expression and function. Notably, the PTPBR7 over-expressing cells had markedly higher levels of N-cadherin, which may in part contribute to the adhesion phenotype.

In addition, also tau and dematin were encountered as intracellular candidate PTPBR7 interactors (Table 3.3). Tau is predominantly expressed in neurons where its main function

concerns the stabilization of microtubules through binding via its microtubule-binding domain, particularly in axons. In this way tau regulates morphology of neurons and influences transport of molecules and organelles along microtubule filaments (Roy et al. 2005). Tau interacts also with actin (Gallo 2007), with the plasma membrane and with several proteins involved in signal transduction (De Vos et al. 2011). Tau phosphorylation, by specific kinases such as CaMKII, and dephosphorylation, together with proteolytic processing affects intensively its association with microtubules and signalling effectors (Thies and Mandelkow 2007). Ultimately, aberrant tau phosphorylation can lead to cellular aggregation of tau filaments and altered microtubule and actin organization, which leads to cytotoxic events (Stamer et al. 2002) and neurodegeneration as observed in Alzheimer Disease (De Vos et al. 2011). Dematin, an actin binding and bundling phospho-protein has recently been implicated in regulating cell motility, adhesion and morphology by suppressing RhoA activation in mouse embryonic fibroblasts (Mohseni and Chishti 2009).

Looking at the RAP *in situ* binding patterns, we found that highly myelinated tracts are sites of ligand localization (Fig. 3.21 and 3.22), also in PTPBR7 deficient mice (Fig. 3.24). The strong concordance of ligand(s) localization with myelinating oligodendrocytes in the white matter of the cerebellum (Fig. 3.22) opens interesting questions on the position of PTPBR7 in the process of myelination. Other RPTPs, such as RPTPζ/β, have an important role in the process of remyelination. Its expression is induced in multiple sclerosis lesions and specifically in remyelinating oligodendrocytes in these lesions (Harroch et al. 2002). Additionally, oligodendrocytes and astrocytes also synthesize several of the proteins that make up gap junctions (GJs), namely connexins (Cx). Among the different connexin types, Cx43 is very interesting in this context. Specific Cx43 knock-out in astrocytes (Theis et al., 2003) resulted in enhanced stroke volume after middle cerebral artery occlusion (Nakase et al., 2004), accelerated spreading depression, and motor impairments (Theis et al., 2003; Frisch et al., 2003). Furthermore, mice double-knockout for Cx43 and Cx30 show a dysmyelinating phenotype and hippocampal CA1 vacuolation together with impairment in sensorimotor and spatial memory tasks, supporting the hypothesis that oligodendrocyte structural and functional integrity is influenced by astrocyte GJs communication (Lutz et al. 2009). Interestingly, another key protein in the process of myelination is the cell-adhesion protein contactin-1, a protein whose activity stabilizes sodium channel clusters at the nodes of Ranvier (Shah et al. 2004). At these structures the myelin sheath is shortly interrupted to allow concentration of the saltatory conduction generated by the Na^+/K^+ voltage-gated channels. Although neurodegeneration in *Ptprr*$^{-/-}$ mice has not been observed, deregulation of ion levels is a mechanism at the basis of neurodegenerative diseases (Wang and Michaelis 2010), and PTPRR may have a fine-regulatory role that would account for the mild-ataxic behavior of these mice.

The protein candidates identified in our affinity purifications suggest that PTPBR7 may be involved in at least two major processes. On the one hand as part of cell-cell adhesion and cytoskeletal complexes during cerebellar development; on the other hand in calcium ion-regulated events that are instrumental in neuronal development and plasticity (Malenka and Bear 2004). These two mechanisms may be nicely integrated in the general view that PTPRR participates in ion level regulation in neurons, most notably in the cerebellum. Two of the three proteins that were purified using the PTPBR7 extracellular domain as bait are

intracellular proteins, at first a surprising finding. However, since PTPBR7 is able to form homo-multimers (Noordman et al. 2008) it is conceivable that the PTPBR7 ectodomain stably associates with endogenous, full-length PTPBR7 and all its associating proteins in mouse brain lysates. Alternatively, other Gαo- or CaMKII-associated transmembrane proteins may mediate such an indirect interaction with the PTPBR7 ectodomain probe.

The effect of PTPRR over-expression on co-expressed proteins offers another interesting aspect. We observed that the addition of PTPRR expression plasmids was paralleled by a concomitant reduction of HER3 or HER4 expression (Fig 3.11). Since the plasmids used harbor distinct promoters (CMV promoter versus SV40 early promoter) to drive expression, squelching of jointly needed but limiting transcription factors in the transfected cells seems an unlikely cause. Regulation of co-expressed protein levels by transmembrane PTPRR isoforms is not unprecedented. The catalytically active, transmembrane PTPRR isoforms PTPBR7 and PTP-SL, and not the cytosolic PTPPBSγ isoforms, promote maturation and cell surface expression of TrkA (YN, personal communication). PTP-enhanced maturation of RTKs has been observed also for FLT-3 (Schmidt-Arras et al. 2005) and expression of a particularly effective substrate-trapping PTP1B mutant effectively interfered with insulin receptor cell surface expression (Boubekeur et al. 2011). Our data are too fragmentary to extract a role of PTPRR in regulating maturation of transmembrane proteins but it certainly would be interesting to further investigate a putative role in the transport of proteins to the plasma membrane. Recently it has been reported that Trk neurotrophin receptors cause accumulation of auto-activated receptors in the ER–Golgi intermediate compartment (Schecterson et al. 2010). Auto-activated Trk receptors not only inhibit their own Golgi-mediated processing but also that of other co-expressed transmembrane proteins, apparently by inducing fragmentation of the Golgi apparatus. In addition, it has been shown that auto-activating mutations of FGFR2 are implicated in intracellular retention and degradation of this N-glycosilated receptor (Hatch et al. 2006). It would be interesting to see whether PTPRR isoforms – most notably PTP-SL – can protect the Golgi apparatus from being fragmented due to (over)expression of prematurely activated RTKs, especially since Golgi fragmentation has been noted as an early event in the neuronal pathology associated with neurodegenerative diseases (Gonatas et al. 2006; Fan et al. 2008; Wang and Michaelis 2010). Figure 4.1 focuses on calcium signalling in neuronal cells and depicts a summarized view of the PTPRR interactions described in this chapter together with relevant players in ataxic disorders.

In conclusion, further experiments that focus on the identified candidate ligands and substrates are strongly required in order to clarify the role of PTPRR and its interaction partners in health and disease.

Figure 4.1 (next page). Calcium signalling and putative PTPRR interactions in a neuronal environment. A neuron, such as a Purkinje cell where PTPRR is expressed, is exemplified. The cell body (A) and a synaptic junction at dendrites (B) are enlarged in the respective panels. Molecules co-purified with PTPRR in affinity purifications are highlighted in bold and italics.
(A) PTPRR signalling at the cell body. PTPRR and receptor tyrosine kinases RTKs exert counteracting action on extracellularly-regulated kinase (ERK) proteins. Protein Kinase A (PKA) phosphorylates PTPRR thereby inactivating it and allowing phosphorylated ERKs to enter the nucleus and initiate gene expression. RTK membrane expression is modulated by their integration in the trans-Golgi network and PTPRR may influence RTK trafficking leading to differential maturation and expression of RTKs.
(B) Growth factor- and Ca^{2+}- induced signalling at the postsynaptic terminal. Glutamate binding to AMPA receptors (AMPAR) in Purkinje neuron spines is followed by negligible Ca^{2+} influx through the receptor channel (dashed arrow). The Na^{+} influx, in contrast, is sufficient to depolarize the postsynaptic membrane and activate voltage-gated sodium (NaV) and calcium channels (VGCCs), mostly of the P/Q-type with the subunit Cav2.1. Ca^{2+} accumulates in the cell and is bound by the mobile Ca^{2+}-binding proteins (CaBP). In the dendritic shaft, Ca^{2+} entry through VGCCs activates Ca^{2+}-induced Ca^{2+} release (CICR) through ryanodine receptors RyRs (not shown). Ca^{2+} returns to resting levels through uptake into the ER by the endoplasmic reticulum Ca^{2+} ATPases (SERCAs) and by extrusion through the plasma membrane Ca^{2+} ATPases (PMCAs) and the Na^{+} - Ca^{2+}-exchanger (NCE). A direct interaction between the glutamate transporter mGluR1 and Cav2.1 modulates the depolarization-induced Ca^{2+} influx through VGCCs. Go proteins are coupled to heptameric G-protein-coupled receptors (GPCRs) and inhibit VGCCs. IP3 receptors (IP3Rs) on the ER interact with mGluR1 via the Homer protein and binding of IP3 to IP3R induces Ca^{2+} release from the ER. CamKII interacts with mGluR1 and Calmodulin (CaM). CaM binds Ca^{2+} and activates CamkII which in turn phosphorylates AMPAR and enhances its activity. In Purkinje cells glutamate is removed from the intracellular environment by the high-affinity excitatory aminoacid tranporter EAAT4. EAAT4 membrane localization is stabilized by the cytoskeletal protein spectrin β3 (Spnβ3) which interacts with actin. The Na^{+}/K^{+} ATPases help in re-polarizing the postsynaptic terminal by pumping out Na^{+} ions. IGLON proteins are exposed on the plasmamembrane. RTKs activate the signalling cascades that converge on ERK phosphorylation. PTPRR dephosphorylates ERKs counteracting RTK signalling. RTKs can be translocated to the cell body by retrograde transport. PSD-95 ensures structural stabilization of the postsynaptic density. Purkinje cells do not express NMDA receptors.

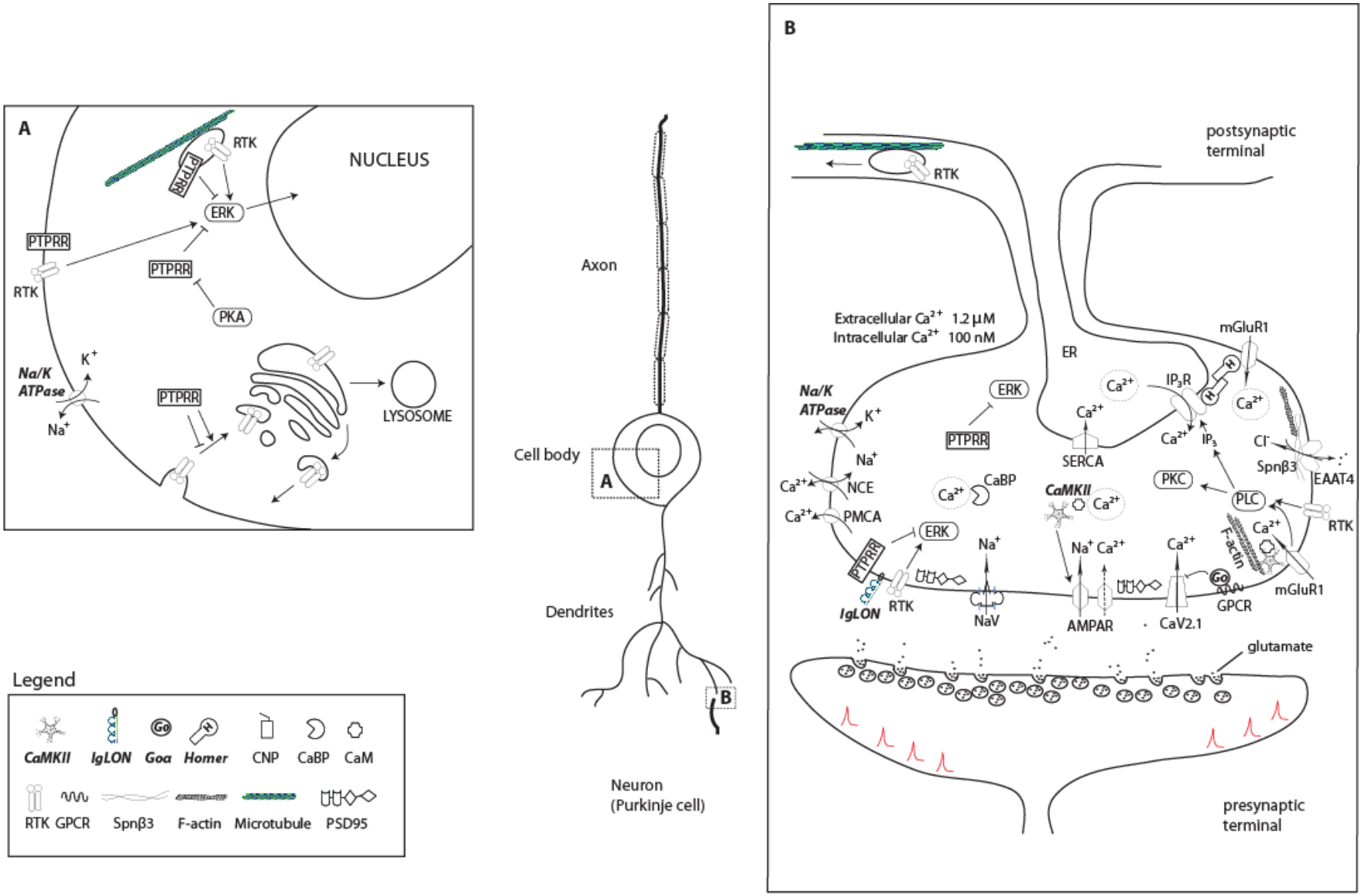
A
NUCLEUS
RTK
PTPRR
ERK
PTPRR
PTPRR
RTK
PKA
Na/K ATPase
K+
Na+
PTPRR
LYSOSOME
Axon
Cell body
A
Dendrites
B
Neuron (Purkinje cell)
B
postsynaptic terminal
RTK
Extracellular Ca2+ 1.2 µM
Intracellular Ca2+ 100 nM
ER
mGluR1
Na/K ATPase
K+
Na+
ERK
PTPRR
Ca2+
IP3R
Ca2+
Ca2+
IP3
Cl-
Spnβ3
EAAT4
SERCA
Ca2+
NCE
Ca2+
CaBP
Ca2+
CaMKII
Ca2+
PKC
PLC
Ca2+
PMCA
Ca2+
ERK
Na+
Na+ Ca2+
Ca2+
F-actin
RTK
PTPRR
Go
mGluR1
IgLON
RTK
NaV
AMPAR
CaV2.1
GPCR
glutamate
presynaptic terminal
Legend
CaMKII
IgLON
Goα
Homer
CNP
CaBP
CaM
RTK
GPCR
Spnβ3
F-actin
Microtubule
PSD95

Chapter 5

➢ Conclusion and Outlook

"There is the greatest practical benefit in making a few failures early in life"
Thomas Henry Huxley

Our studies focused on the identification of PTPRR intracellular substrates and extracellular ligands by means of a combination of biochemical techniques and mass spectrometry-based identification. These studies led to test some candidate substrates (HER4, SHP1, N-cadherin) according to procedures indicated by (Tiganis and Bennett 2007). In the applied conditions these substrates could not be validated according to the accepted criteria for the definition of *bona fide* PTP substrates (Tiganis and Bennett 2007). This may reflect that PTPRR proteins are generally engaged in very weak interactions that would not be revealed by these standard biochemical methods involving stringent test conditions. Additionally, we provided evidence that remaining traces of vanadate compounds may have severely hindered the structural and/or enzymatic interaction of PTPRR enzyme and candidate substrate. Since vanadate compounds are commonly used in candidate-validation assays (Blanchetot et al. 2005), our observations would suggest that PTPRR is more sensitive to vanadate than other PTPs. Thus, in future other methods – that allow the avoidance of vanadate inhibitors – should be applied when testing PTPRR interactions. We successfully used the RAP *in situ* technique to localize putative PTPBR7 ligands in highly myelinated regions of the mouse cerebellum. PTPBR7 ectodomain staining overlapped with oligodendrocyte localization patterns but the specificity of PTPBR7 binding to these brain regions could not be established by our current set-up. This may indicate that PTPBR7-ligand(s) interactions rely on multimeric forms of the receptor. Finally, co-purification studies followed by mass spectrometry indicated candidate substrates and ligand molecules for PTPRR that, once validated, will help in understanding the biological role of PTPRR in the mouse brain. In particular, confirming the interaction of PTPRR with calcium-regulated proteins would be of particular interest in view of the current hypothesis of a role for PTPRR in the regulation of calcium levels (Hendriks et al. 2009). PTPRR interaction with proteins involved in cell adhesion should also be addressed because it may indicate new unknown functions of PTPRR isoforms. Interestingly, PTPRR influences the expression of other transmembrane proteins, most notably RTKs, suggesting a PTPRR role in the delivery of proteins to the plasma membrane along the trans-Golgi network. Approaches suitable for weak and transient interactions, e.g.. phosphoproteomics (Dengjel et al. 2007) and ELISA-style assays such as AVEXIS and MYTH (Sanderson 2008; Petschnigg et al. 2011), will be applied to study PTPRR interacting partners and overcome constraints given by standard biochemical methods. Also, exploitation of *Ptprr*-deficient neurons, e.g. for the detection of any altered Ca^{2+}-dependent processes and phosphorylation-dependent de-regulation of ion channel functioning or trafficking, may prove useful to add information on PTPRR signalling pathways and characterize the spatio-temporal regulation of PTPRR substrate phospho-levels.

Chapter 6

- Appendix

6.1 References

Abaan OD, Toretsky JA (2008) PTPL1: a large phosphatase with a split personality. Cancer Metastasis Rev 27: 205-214

Adler EM, Gough NR, Blundon JA (2006) Differentiation of PC12 cells. Sci STKE 2006: tr9

Alberts B. , Johnson Alexander , Lewis Julian , Raff Martin, Roberts Keith, Peter W (2002) Molecular Biology of the Cell. Garland Science, New York

Alete DE, Weeks ME, Hovanession AG, Hawadle M, Stoker AW (2006) Cell surface nucleolin on developing muscle is a potential ligand for the axonal receptor protein tyrosine phosphatase-sigma. Febs J 273: 4668-4681

Alonso A, Sasin J, Bottini N, Friedberg I, Friedberg I, Osterman A, Godzik A, Hunter T, Dixon J, Mustelin T (2004) Protein Tyrosine Phosphatases in the Human Genome. Cell 117: 699-711

Amet LE, Lauri SE, Hienola A, Croll SD, Lu Y, Levorse JM, Prabhakaran B, Taira T, Rauvala H, Vogt TF (2001) Enhanced hippocampal long-term potentiation in mice lacking heparin-binding growth-associated molecule. Mol Cell Neurosci 17: 1014-1024

Andersen JN, Jansen PG, Echwald SM, Mortensen OH, Fukada T, Del Vecchio R, Tonks NK, Moller NP (2004) A genomic perspective on protein tyrosine phosphatases: gene structure, pseudogenes, and genetic disease linkage. Faseb J 18: 8-30

Andersen JN, Mortensen OH, Peters GH, Drake PG, Iversen LF, Olsen OH, Jansen PG, Andersen HS, Tonks NK, Moller NP (2001) Structural and evolutionary relationships among protein tyrosine phosphatase domains. Mol Cell Biol 21: 7117-7136

Aricescu AR, Hon W-C, Siebold C, Lu W, van der Merwe PA, Jones EY (2006) Molecular analysis of receptor protein tyrosine phosphatase [mu]-mediated cell adhesion. 25: 701-712

Aricescu AR, McKinnell IW, Halfter W, Stoker AW (2002) Heparan Sulfate Proteoglycans Are Ligands for Receptor Protein Tyrosine Phosphatase {sigma}. Mol. Cell. Biol. 22: 1881-1892

Aricescu AR, Siebold C, Choudhuri K, Chang VT, Lu W, Davis SJ, van der Merwe PA, Jones EY (2007) Structure of a Tyrosine Phosphatase Adhesive Interaction Reveals a Spacer-Clamp Mechanism. Science 317: 1217-1220

Augustine KA, Silbiger SM, Bucay N, Ulias L, Boynton A, Trebasky LD, Medlock ES (2000) Protein tyrosine phosphatase (PC12, Br7,S1) family: expression characterization in the adult human and mouse. Anat Rec 258: 221-234

Ballif BA, Carey GR, Sunyaev SR, Gygi SP (2008) Large-scale identification and evolution indexing of tyrosine phosphorylation sites from murine brain. J Proteome Res 7: 311-318

Bar-Sagi D, Hall A (2000) Ras and Rho GTPases: a family reunion. Cell 103: 227-238

Baranano DE, Ferris CD, Snyder SH (2001) Atypical neural messengers. Trends Neurosci 24: 99-106

Barford D, Keller JC, Flint AJ, Tonks NK (1994) Purification and crystallization of the catalytic domain of human protein tyrosine phosphatase 1B expressed in Escherichia coli. J Mol Biol 239: 726-730

Barnea G, Grumet M, Milev P, Silvennoinen O, Levy JB, Sap J, Schlessinger J (1994) Receptor tyrosine phosphatase beta is expressed in the form of proteoglycan and binds to the extracellular matrix protein tenascin. J Biol Chem 269: 14349-14352

Barr AJ, Ugochukwu E, Lee WH, King ON, Filippakopoulos P, Alfano I, Savitsky P, Burgess-Brown NA, Muller S, Knapp S (2009) Large-scale structural analysis of the classical human protein tyrosine phosphatome. Cell 136: 352-363

Baselga J, Swain SM (2009) Novel anticancer targets: revisiting ERBB2 and discovering ERBB3. Nat Rev Cancer 9: 463-475

Bastianelli E (2003) Distribution of calcium-binding proteins in the cerebellum. Cerebellum 2: 242-262
Baum ML, Kurup P, Xu J, Lombroso PJ (2010) A STEP forward in neural function and degeneration. Commun Integr Biol 3: 419-422
Benarroch EE (2011) Na+, K+-ATPase: functions in the nervous system and involvement in neurologic disease. Neurology 76: 287-293
Benson DL, Tanaka H (1998) N-cadherin redistribution during synaptogenesis in hippocampal neurons. J Neurosci 18: 6892-6904
Bilwes AM, den Hertog J, Hunter T, Noel JP (1996) Structural basis for inhibition of receptor protein-tyrosine phosphatase-alpha by dimerization. Nature 382: 555-559
Blanchetot C, Chagnon M, Dube N, Halle M, Tremblay ML (2005) Substrate-trapping techniques in the identification of cellular PTP targets. Methods 35: 44-53
Blanchetot C, G.J.Tertoolen L, den Hertog J (2002a) Regulation of receptor protein-tyrosine phosphatase [alpha] by oxidative stress. EMBO J 21: 493-503
Blanchetot C, Tertoolen LG, Overvoorde J, den Hertog J (2002b) Intra- and intermolecular interactions between intracellular domains of receptor protein-tyrosine phosphatases. J Biol Chem 277: 47263-47269
Blanco-Aparicio C, Torres J, Pulido R (1999) A novel regulatory mechanism of MAP kinases activation and nuclear translocation mediated by PKA and the PTP-SL tyrosine phosphatase. J Cell Biol 147: 1129-1136
Boehm M, Bonifacino JS (2001) Adaptins. The Final Recount. In, vol 12, pp 2907-2920
Boubekeur S, Boute N, Pagesy P, Zilberfarb V, Christeff Nvn, Issad T (2011) A New Highly Efficient Substrate-trapping Mutant of Protein Tyrosine Phosphatase 1B (PTP1B) Reveals Full Autoactivation of the Insulin Receptor Precursor. J Biol Chem 286: 19373-19380
Bouyain S, Watkins DJ (2010) The protein tyrosine phosphatases PTPRZ and PTPRG bind to distinct members of the contactin family of neural recognition molecules. Proc Natl Acad Sci U S A 107: 2443-2448
Bovolenta P, Fernaud-Espinosa I (2000) Nervous system proteoglycans as modulators of neurite outgrowth. Progress in Neurobiology 61: 113-132
Bradbury EJ, Moon LD, Popat RJ, King VR, Bennett GS, Patel PN, Fawcett JW, McMahon SB (2002) Chondroitinase ABC promotes functional recovery after spinal cord injury. Nature 416: 636-640
Bradford MM (1976) A rapid and sensitive method for the quantitation of microgram quantities of protein utilizing the principle of protein-dye binding. Anal Biochem 72: 248-254
Brady-Kalnay SM, Flint AJ, Tonks NK (1993) Homophilic binding of PTP mu, a receptor-type protein tyrosine phosphatase, can mediate cell-cell aggregation. J Cell Biol 122: 961-972
Britsch S, Li L, Kirchhoff S, Theuring F, Brinkmann V, Birchmeier C, Riethmacher D (1998) The ErbB2 and ErbB3 receptors and their ligand, neuregulin-1, are essential for development of the sympathetic nervous system. Genes Dev 12: 1825-1836
Brown MT, Cooper JA (1996) Regulation, substrates and functions of src. Biochim Biophys Acta 1287: 121-149
Brymora A, Valova VA, Robinson PJ (2004) Protein-protein interactions identified by pull-down experiments and mass spectrometry. Curr Protoc Cell Biol Chapter 17: Unit 17 15
Bukalo O, Schachner M, Dityatev A (2001) Modification of extracellular matrix by enzymatic removal of chondroitin sulfate and by lack of tenascin-R differentially affects several forms of synaptic plasticity in the hippocampus. Neuroscience 104: 359-369

Buschbeck M, Eickhoff J, Sommer MN, Ullrich A (2002) Phosphotyrosine-specific phosphatase PTP-SL regulates the ERK5 signaling pathway. J Biol Chem 277: 29503-29509
Butler LS, Silva AJ, Abeliovich A, Watanabe Y, Tonegawa S, McNamara JO (1995) Limbic epilepsy in transgenic mice carrying a Ca2+/calmodulin-dependent kinase II alpha-subunit mutation. Proc Natl Acad Sci U S A 92: 6852-6855
Caggiano AO, Zimber MP, Ganguly A, Blight AR, Gruskin EA (2005) Chondroitinase ABCI improves locomotion and bladder function following contusion injury of the rat spinal cord. J Neurotrauma 22: 226-239
Celio MR, Spreafico R, De Biasi S, Vitellaro-Zuccarello L (1998) Perineuronal nets: past and present. Trends Neurosci 21: 510-515
Chen S, Gil O, Ren Y, Zanazzi G, Salzer J, Hillman D (2001) Neurotrimin expression during cerebellar development suggests roles in axon fasciculation and synaptogenesis. Journal of Neurocytology 30: 927-937
Cheng J, Wu K, Armanini M, O'Rourke N, Dowbenko D, Lasky LA (1997) A novel protein-tyrosine phosphatase related to the homotypically adhering kappa and mu receptors. J Biol Chem 272: 7264-7277
Cheron G, Gall D, Servais L, Dan B, Maex R, Schiffmann SN (2004) Inactivation of calcium-binding protein genes induces 160 Hz oscillations in the cerebellar cortex of alert mice. J Neurosci 24: 434-441
Cheron G, Servais L, Dan B (2008) Cerebellar network plasticity: From genes to fast oscillation. Neuroscience 153: 1-19
Chiang MK, Flanagan JG (1996) PTP-NP, a new member of the receptor protein tyrosine phosphatase family, implicated in development of nervous system and pancreatic endocrine cells. Development 122: 2239-2250
Chin CN, Sachs JN, Engelman DM (2005) Transmembrane homodimerization of receptor-like protein tyrosine phosphatases. FEBS Lett 579: 3855-3858
Chirivi RG, Dilaver G, van de Vorstenbosch R, Wanschers B, Schepens J, Croes H, Fransen J, Hendriks W (2004) Characterization of multiple transcripts and isoforms derived from the mouse protein tyrosine phosphatase gene Ptprr. Genes Cells 9: 919-933
Chirivi RG, Noordman YE, Van der Zee CE, Hendriks WJ (2007) Altered MAP kinase phosphorylation and impaired motor coordination in PTPRR deficient mice. J Neurochem 101: 829-840
Cho KO, Hunt CA, Kennedy MB (1992) The rat brain postsynaptic density fraction contains a homolog of the Drosophila discs-large tumor suppressor protein. Neuron 9: 929-942
Chu CT, Levinthal DJ, Kulich SM, Chalovich EM, DeFranco DB (2004) Oxidative neuronal injury. European Journal of Biochemistry 271: 2060-2066
Citri A, Yarden Y (2006) EGF-ERBB signalling: towards the systems level. Nat Rev Mol Cell Biol 7: 505-516
Colbran RJ (2004a) Protein phosphatases and calcium/calmodulin-dependent protein kinase II-dependent synaptic plasticity. J Neurosci 24: 8404-8409
Colbran RJ (2004b) Targeting of calcium/calmodulin-dependent protein kinase II. Biochem J 378: 1-16
Colbran RJ, Brown AM (2004) Calcium/calmodulin-dependent protein kinase II and synaptic plasticity. Curr Opin Neurobiol 14: 318-327
Coles CH, Shen Y, Tenney AP, Siebold C, Sutton GC, Lu W, Gallagher JT, Jones EY, Flanagan JG, Aricescu AR (2011) Proteoglycan-Specific Molecular Switch for RPTPσ Clustering and Neuronal Extension. In, vol 332, pp 484-488
Colucci-D'Amato L, Perrone-Capano C, di Porzio U (2003) Chronic activation of ERK and neurodegenerative diseases. Bioessays 25: 1085-1095

Coman I, Barbin G, Charles P, Zalc B, Lubetzki C (2005) Axonal signals in central nervous system myelination, demyelination and remyelination. J Neurol Sci 233: 67-71
Corvetti L, Rossi F (2005) Degradation of chondroitin sulfate proteoglycans induces sprouting of intact purkinje axons in the cerebellum of the adult rat. J Neurosci 25: 7150-7158
Coyle JT, Puttfarcken P (1993) Oxidative stress, glutamate, and neurodegenerative disorders. Science 262: 689-695
Cremer H, Chazal G, Goridis C, Represa A (1997) NCAM is essential for axonal growth and fasciculation in the hippocampus. Mol Cell Neurosci 8: 323-335
Cully M, You H, Levine AJ, Mak TW (2006) Beyond PTEN mutations: the PI3K pathway as an integrator of multiple inputs during tumorigenesis. 6: 184-192
Darnell JE. Jr, Kerr IM, GR S (1994) Jak-STAT pathways and transcriptional activation in response to IFNs and other extracellular signaling proteins. Science 264: 1415-1421
De Angelis E, Watkins A, Schafer M, Brummendorf T, Kenwrick S (2002) Disease-associated mutations in L1 CAM interfere with ligand interactions and cell-surface expression. Hum. Mol. Genet. 11: 1-12
De Vos A, Anandhakumar J, Van den Brande J, Verduyckt M, Franssens V, Winderickx J, Swinnen E (2011) Yeast as a model system to study tau biology. Int J Alzheimers Dis 2011: 428970
den Hertog J, Ostman A, Bohmer FD (2008) Protein tyrosine phosphatases: regulatory mechanisms. Febs J 275: 831-847
Dengjel J, Akimov V, Olsen JV, Bunkenborg J, Mann M, Blagoev B, Andersen JS (2007) Quantitative proteomic assessment of very early cellular signaling events. Nat Biotechnol 25: 566-568
Denu JM, Lohse DL, Vijayalakshmi J, Saper MA, Dixon JE (1996) Visualization of intermediate and transition-state structures in protein-tyrosine phosphatase catalysis. Proc Natl Acad Sci U S A 93: 2493-2498
Derkach V, Barria A, Soderling TR (1999) Ca2+/calmodulin-kinase II enhances channel conductance of alpha-amino-3-hydroxy-5-methyl-4-isoxazolepropionate type glutamate receptors. Proc Natl Acad Sci U S A 96: 3269-3274
Dilaver G, Schepens J, van den Maagdenberg A, Wijers M, Pepers B, Fransen J, Hendriks W (2003) Colocalisation of the protein tyrosine phosphatases PTP-SL and PTPBR7 with beta4-adaptin in neuronal cells. Histochem Cell Biol 119: 1-13
Dilaver G, van de Vorstenbosch R, Tarrega C, Rios P, Pulido R, van Aerde K, Fransen J, Hendriks W (2007) Proteolytic processing of the receptor-type protein tyrosine phosphatase PTPBR7. Febs J 274: 96-108
Dityatev A, Dityateva G, Sytnyk V, Delling M, Toni N, Nikonenko I, Muller D, Schachner M (2004) Polysialylated neural cell adhesion molecule promotes remodeling and formation of hippocampal synapses. J Neurosci 24: 9372-9382
Dringen R, Gutterer JM, Hirrlinger J (2000) Glutathione metabolism in brain metabolic interaction between astrocytes and neurons in the defense against reactive oxygen species. Eur J Biochem 267: 4912-4916
English JD, Sweatt JD (1997) A requirement for the mitogen-activated protein kinase cascade in hippocampal long term potentiation. J Biol Chem 272: 19103-19106
Erdmann KS (2003) The protein tyrosine phosphatase PTP-Basophil/Basophil-like. Interacting proteins and molecular functions. Eur J Biochem 270: 4789-4798
Erickson SL, O'Shea KS, Ghaboosi N, Loverro L, Frantz G, Bauer M, Lu LH, Moore MW (1997) ErbB3 is required for normal cerebellar and cardiac development: a comparison with ErbB2-and heregulin-deficient mice Development 124 4999-5011

Ermak G, Davies KJ (2002) Calcium and oxidative stress: from cell signaling to cell death. Mol Immunol 38: 713-721
Eswaran J, von Kries JP, Marsden B, Longman E, Debreczeni JE, Ugochukwu E, Turnbull A, Lee WH, Knapp S, Barr AJ (2006) Crystal structures and inhibitor identification for PTPN5, PTPRR and PTPN7: a family of human MAPK-specific protein tyrosine phosphatases. Biochem J 395: 483-491
Fannon AM, Colman DR (1996) A model for central synaptic junctional complex formation based on the differential adhesive specificities of the cadherins. Neuron 17: 423-434
Farre-Castany MA, Schwaller B, Gregory P, Barski J, Mariethoz C, Eriksson JL, Tetko IV, Wolfer D, Celio MR, Schmutz I, Albrecht U, Villa AE (2007) Differences in locomotor behavior revealed in mice deficient for the calcium-binding proteins parvalbumin, calbindin D-28k or both. Behav Brain Res 178: 250-261
Field J, Nikawa J, Broek D, MacDonald B, Rodgers L, Wilson IA, Lerner RA, Wigler M (1988) Purification of a RAS-responsive adenylyl cyclase complex from Saccharomyces cerevisiae by use of an epitope addition method. Mol Cell Biol 8: 2159-2165
Fields RD, Stevens-Graham B (2002) New insights into neuron-glia communication. Science 298: 556-562
Flanagan JG, Cheng H-J, Feldheim DA, Hattori M, Lu Q, Vanderhaeghen P (2000) Alkaline phosphatase fusions of ligands or receptors as in situ probes for staining of cells, tissues, and embryos. Methods in Enzymology. In: Jeremy Thorner SDEaJNA (ed) Applications of Chimeric Genes and Hybrid Proteins - Part B: Cell Biology and Physiology. Academic Press, pp 19-35
Flanagan JG, Leder P (1990) The kit ligand: a cell surface molecule altered in steel mutant fibroblasts. Cell 63: 185-194
Floyd RA, Hensley K (2002) Oxidative stress in brain aging. Implications for therapeutics of neurodegenerative diseases. Neurobiol Aging 23: 795-807
Foster TC (2007) Calcium homeostasis and modulation of synaptic plasticity in the aged brain. Aging Cell 6: 319-325
Fox AN, Zinn K (2005) The heparan sulfate proteoglycan syndecan is an in vivo ligand for the Drosophila LAR receptor tyrosine phosphatase. Curr Biol 15: 1701-1711
Fox MA, Afshari FS, Alexander JK, Colello RJ, Fuss B (2006) Growth conelike sensorimotor structures are characteristic features of postmigratory, premyelinating oligodendrocytes. Glia 53: 563-566
Frank C, Burkhardt C, Imhof D, Ringel J, Zschornig O, Wieligmann K, Zacharias M, Bohmer FD (2004) Effective dephosphorylation of Src substrates by SHP-1. J Biol Chem 279: 11375-11383
Franklin RJM, ffrench-Constant C (2008) Remyelination in the CNS: from biology to therapy. 9: 839-855
Fry EJ, Chagnon MJ, Lopez-Vales R, Tremblay ML, David S (2010) Corticospinal tract regeneration after spinal cord injury in receptor protein tyrosine phosphatase sigma deficient mice. Glia 58: 423-433
Fukada M, Noda M (2007) Yeast substrate-trapping system for isolating substrates of protein tyrosine phosphatases. Methods Mol Biol 365: 371-382
Fukunaga K, Miyamoto E (2000) A working model of CaM kinase II activity in hippocampal long-term potentiation and memory. Neurosci Res 38: 3-17
Funatsu N, Miyata S, Kumanogoh H, Shigeta M, Hamada K, Endo Y, Sokawa Y, Maekawa S (1999) Characterization of a novel rat brain glycosylphosphatidylinositol-anchored protein (Kilon), a member of the IgLON cell adhesion molecule family. J Biol Chem 274: 8224-8230

Gabrion J, Brabet P, Nguyen Than Dao B, Homburger V, Dumuis A, Sebben M, Rouot B, Bockaert J (1989) Ultrastructural localization of the GTP-binding protein Go in neurons. Cell Signal 1: 107-123
Gallo G (2007) Tau is actin up in Alzheimer's disease. Nat Cell Biol 9: 133-134
Galtrey CM, Fawcett JW (2007) The role of chondroitin sulfate proteoglycans in regeneration and plasticity in the central nervous system. Brain Res Rev 54: 1-18
Garrington TP, Johnson GL (1999) Organization and regulation of mitogen-activated protein kinase signaling pathways. Current Opinion in Cell Biology 11: 211-218
Garton AJ, Flint AJ, Tonks NK (1996) Identification of p130(cas) as a substrate for the cytosolic protein tyrosine phosphatase PTP-PEST. Mol Cell Biol 16: 6408-6418
Gassmann M, Casagranda F, Orioli D, Simon H, Lai C, Klein R, Lemke G (1995) Aberrant neural and cardiac development in mice lacking the ErbB4 neuregulin receptor. Nature 378: 390-394
Geering K (2008) Functional roles of Na,K-ATPase subunits. Curr Opin Nephrol Hypertens 17: 526-532
Gil OD, Zanazzi G, Struyk AF, Salzer JL (1998) Neurotrimin mediates bifunctional effects on neurite outgrowth via homophilic and heterophilic interactions. J Neurosci 18: 9312-9325
Gil OD, Zhang L, Chen S, Ren YQ, Pimenta A, Zanazzi G, Hillman D, Levitt P, Salzer JL (2002) Complementary expression and heterophilic interactions between IgLON family members neurotrimin and LAMP. J Neurobiol 51: 190-204
Gleason MR, Higashijima S, Dallman J, Liu K, Mandel G, Fetcho JR (2003) Translocation of CaM kinase II to synaptic sites in vivo. Nat Neurosci 6: 217-218
Golding JP, Trainor P, Krumlauf R, Gassmann M (2000) Defects in pathfinding by cranial neural crest cells in mice lacking the neuregulin receptor ErbB4. Nat Cell Biol 2: 103-109
Golemis EA, Adams PD (2005) Protein-protein interactions. CSHLP, New York
Gonatas NK, Stieber A, Gonatas JO (2006) Fragmentation of the Golgi apparatus in neurodegenerative diseases and cell death. Journal of the Neurological Sciences 246: 21-30
Gonzalez-Brito MR, Bixby JL (2006) Differential activities in adhesion and neurite growth of fibronectin type III repeats in the PTP-delta extracellular domain. Int J Dev Neurosci 24: 425-429
Grassie MA, McCallum JF, Guzzi F, Magee AI, Milligan G, Parenti M (1994) The palmitoylation status of the G-protein G(o)1 alpha regulates its activity of interaction with the plasma membrane. Biochem J 302 (Pt 3): 913-920
Greif GJ, Sodickson DL, Bean BP, Neer EJ, Mende U (2000) Altered Regulation of Potassium and Calcium Channels by GABAB and Adenosine Receptors in Hippocampal Neurons From Mice Lacking GÎ±o. In, vol 83, pp 1010-1018
Gresser MJ, Tracey AS (1990) Vanadium in Biological Systems. In: Chasteen ND, ed (ed). Kluwer Academic Publishers, The Netherlands, pp 63-79
Hachisuka A, Yamazaki T, Sawada J, Terao T (1996) Characterization and tissue distribution of opioid-binding cell adhesion molecule (OBCAM) using monoclonal antibodies. Neurochem Int 28: 373-379
Hama H, Hara C, Yamaguchi K, Miyawaki A (2004) PKC signaling mediates global enhancement of excitatory synaptogenesis in neurons triggered by local contact with astrocytes. Neuron 41: 405-415
Harroch S, Furtado GC, Brueck W, Rosenbluth J, Lafaille J, Chao M, Buxbaum JD, Schlessinger J (2002) A critical role for the protein tyrosine phosphatase receptor type Z in functional recovery from demyelinating lesions. Nat Genet 32: 411-414
Hartmann J, Konnerth A (2005) Determinants of postsynaptic Ca2+ signaling in Purkinje neurons. Cell Calcium 37: 459-466

Hashimoto T, Maekawa S, Miyata S (2009) IgLON cell adhesion molecules regulate synaptogenesis in hippocampal neurons. Cell Biochem Funct 27: 496-498
Hashimoto T, Yamada M, Maekawa S, Nakashima T, Miyata S (2008) IgLON cell adhesion molecule Kilon is a crucial modulator for synapse number in hippocampal neurons. Brain Res 1224: 1-11
Hatch NE, Hudson M, Seto ML, Cunningham ML, Bothwell M (2006) Intracellular Retention, Degradation, and Signaling of Glycosylation-deficient FGFR2 and Craniosynostosis Syndrome-associated FGFR2C278F. In, vol 281, pp 27292-27305
He JC, Gomes I, Nguyen T, Jayaram G, Ram PT, Devi LA, Iyengar R (2005) The G alpha(o/i)-coupled cannabinoid receptor-mediated neurite outgrowth involves Rap regulation of Src and Stat3. J Biol Chem 280: 33426-33434
Hendriks W, Dilaver G, Noordman Y, Kremer B, Fransen J (2009) PTPRR Protein Tyrosine Phosphatase Isoforms and Locomotion of Vesicles and Mice. The Cerebellum 8: 80-88
Hendriks W, Schepens J, Bachner D, Rijss J, Zeeuwen P, Zechner U, Hameister H, Wieringa B (1995a) Molecular cloning of a mouse epithelial protein-tyrosine phosphatase with similarities to submembranous proteins. J Cell Biochem 59: 418-430
Hendriks W, Schepens J, Brugman C, Zeeuwen P, Wieringa B (1995b) A novel receptor-type protein tyrosine phosphatase with a single catalytic domain is specifically expressed in mouse brain. Biochem J 305 (Pt 2): 499-504
Hendriks WJAJ, Elson A, Harroch S, Stoker AW (2008) Protein tyrosine phosphatases: functional inferences from mouse models and human diseases. FEBS Journal 275: 816-830
Hirano S, Suzuki ST, Redies C (2003) The cadherin superfamily in neural development: diversity, function and interaction with other molecules. Front Biosci 8: d306-355
Hoelz A, Nairn AC, Kuriyan J (2003) Crystal structure of a tetradecameric assembly of the association domain of Ca2+/calmodulin-dependent kinase II. Mol Cell 11: 1241-1251
Holbro T, Hynes NE (2004) ErbB receptors: directing key signaling networks throughout life. Annu Rev Pharmacol Toxicol 44: 195-217
Holmes SE, Hearn EO, Ross CA, Margolis RL (2001) SCA12: an unusual mutation leads to an unusual spinocerebellar ataxia. Brain Res Bull 56: 397-403
Homburger V, Brabet P, Audigier Y, Pantaloni C, Bockaert J, Rouot B (1987) Immunological localization of the GTP-binding protein Go in different tissues of vertebrates and invertebrates. In, vol 31, pp 313-319
Hook SS, Means AR (2001) Ca(2+)/CaM-dependent kinases: from activation to function. Annu Rev Pharmacol Toxicol 41: 471-505
Horgan AM, Copenhaver PF (1998) G protein-mediated inhibition of neuronal migration requires calcium influx. J Neurosci 18: 4189-4200
Hortsch M (1996) The L1 family of neural cell adhesion molecules: old proteins performing new tricks. Neuron 17: 587-593
Hortsch M (2000) Structural and functional evolution of the L1 family: are four adhesion molecules better than one? Mol Cell Neurosci 15: 1-10
Hudmon A, Schulman H (2002) Neuronal CA2+/calmodulin-dependent protein kinase II: the role of structure and autoregulation in cellular function. Annu Rev Biochem 71: 473-510
Hunter T (1989) Protein modification: phosphorylation on tyrosine residues. Curr Opin Cell Biol 1: 1168-1181
Hunter T (1998) The Croonian Lecture 1997. The phosphorylation of proteins on tyrosine: its role in cell growth and disease. Philos Trans R Soc Lond B Biol Sci 353: 583-605
Hunter T (2000) Signaling--2000 and Beyond. Cell 100: 113-127
Huyer G, Liu S, Kelly J, Moffat J, Payette P, Kennedy B, Tsaprailis G, Gresser MJ, Ramachandran C (1997) Mechanism of inhibition of protein-tyrosine phosphatases by vanadate and pervanadate. J Biol Chem 272: 843-851

Ihle JN (1995) Cytokine receptor signalling. Nature 377: 591-594
Ikeda Y, Dick KA, Weatherspoon MR, Gincel D, Armbrust KR, Dalton JC, Stevanin G, Durr A, Zuhlke C, Burk K, Clark HB, Brice A, Rothstein JD, Schut LJ, Day JW, Ranum LP (2006) Spectrin mutations cause spinocerebellar ataxia type 5. Nat Genet 38: 184-190
Ishida A, Sueyoshi N, Shigeri Y, Kameshita I (2008) Negative regulation of multifunctional Ca2+/calmodulin-dependent protein kinases: physiological and pharmacological significance of protein phosphatases. Br J Pharmacol 154: 729-740
Jiang G, den Hertog J, Hunter T (2000) Receptor-like protein tyrosine phosphatase alpha homodimerizes on the cell surface. Mol Cell Biol 20: 5917-5929
Jiang G, Hunter T (1999) Receptor signaling: When dimerization is not enough. Current Biology 9: R568-R571
Jiang M, Bajpayee NS (2009) Molecular Mechanisms of Go Signaling. Neurosignals 17: 23-41
Jiang M, Gold MS, Boulay G, Spicher K, Peyton M, Brabet P, Srinivasan Y, Rudolph U, Ellison G, Birnbaumer L (1998) Multiple neurological abnormalities in mice deficient in the G protein Go. In, vol 95, pp 3269-3274
Jiao Y, Yan J, Zhao Y, Donahue LR, Beamer WG, Li X, Roe BA, Ledoux MS, Gu W (2005) Carbonic anhydrase-related protein VIII deficiency is associated with a distinctive lifelong gait disorder in waddles mice. Genetics 171: 1239-1246
Johnson KG, Tenney AP, Ghose A, Duckworth AM, Higashi ME, Parfitt K, Marcu O, Heslip TR, Marsh JL, Schwarz TL, Flanagan JG, Van Vactor D (2006) The HSPGs Syndecan and Dallylike bind the receptor phosphatase LAR and exert distinct effects on synaptic development. Neuron 49: 517-531
Juttner R, Rathjen FG (2005) Molecular analysis of axonal target specificity and synapse formation. Cell Mol Life Sci 62: 2811-2827
Kandel ER (2001) The Molecular Biology of Memory Storage: A Dialogue Between Genes and Synapses. In, vol 294, pp 1030-1038
Kaushansky A, Gordus A, Budnik BA, Lane WS, Rush J, MacBeath G (2008) System-wide investigation of ErbB4 reveals 19 sites of Tyr phosphorylation that are unusually selective in their recruitment properties. Chem Biol 15: 808-817
Kawachi H, Fujikawa A, Maeda N, Noda M (2001) Identification of GIT1/Cat-1 as a substrate molecule of protein tyrosine phosphatase zeta /beta by the yeast substrate-trapping system. Proc Natl Acad Sci U S A 98: 6593-6598
Kim SA, Tai C-Y, Mok L-P, Mosser EA, Schuman EM (2011) Calcium-dependent dynamics of cadherin interactions at cell-cell junctions. In, vol 108, pp 9857-9862
Kindt KS, Tam T, Whiteman S, Schafer WR (2002) Serotonin promotes G(o)-dependent neuronal migration in Caenorhabditis elegans. Curr Biol 12: 1738-1747
Kiss JZ, Muller D (2001) Contribution of the neural cell adhesion molecule to neuronal and synaptic plasticity. Rev Neurosci 12: 297-310
Kistner U, Wenzel BM, Veh RW, Cases-Langhoff C, Garner AM, Appeltauer U, Voss B, Gundelfinger ED, Garner CC (1993) SAP90, a rat presynaptic protein related to the product of the Drosophila tumor suppressor gene dlg-A. J Biol Chem 268: 4580-4583
Köhn M, Gutierrez-Rodriguez M, Jonkheijm P, Wetzel S, Wacker R, Schroeder H, Prinz H, Niemeyer C, Breinbauer R, Szedlacsek S, Waldmann H (2007) A Microarray Strategy for Mapping the Substrate Specificity of Protein Tyrosine Phosphatase. Angewandte Chemie International Edition 46: 7700-7703
Kohrman DC, Smith MR, Goldin AL, Harris J, Meisler MH (1996) A missense mutation in the sodium channel Scn8a is responsible for cerebellar ataxia in the mouse mutant jolting. J Neurosci 16: 5993-5999

Kolli S, Zito CI, Mossink MH, Wiemer EAC, Bennett AM (2004) The Major Vault Protein Is a Novel Substrate for the Tyrosine Phosphatase SHP-2 and Scaffold Protein in Epidermal Growth Factor Signaling. Journal of Biological Chemistry 279: 29374-29385
Kontaridis MI, Eminaga S, Fornaro M, Zito CI, Sordella R, Settleman J, Bennett AM (2004) SHP-2 Positively Regulates Myogenesis by Coupling to the Rho GTPase Signaling Pathway. In, vol 24, pp 5340-5352
Kordasiewicz HB, Gomez CM (2007) Molecular pathogenesis of spinocerebellar ataxia type 6. Neurotherapeutics 4: 285-294
Korolchuk V, Banting G (2003) Kinases in clathrin-mediated endocytosis. Biochem Soc Trans 31: 857-860
Krasnoperov V, Bittner MA, Mo W, Buryanovsky L, Neubert TA, Holz RW, Ichtchenko K, Petrenko AG (2002) Protein-tyrosine phosphatase-sigma is a novel member of the functional family of alpha-latrotoxin receptors. J Biol Chem 277: 35887-35895
Kreis TE (1986) Microinjected antibodies against the cytoplasmic domain of vesicular stomatitis virus glycoprotein block its transport to the cell surface. Embo J 5: 931-941
Lange-Carter CA, Johnson GL (1994) Ras-dependent growth factor regulation of MEK kinase in PC12 cells. Science 265: 1458-1461
Lauritsen JPH, Menné C, Kastrup J, Dietrich J, Ødum N, Geisler C (2000) [beta]2-Adaptin is constitutively de-phosphorylated by serine/threonine protein phosphatase PP2A and phosphorylated by a staurosporine-sensitive kinase. Biochimica et Biophysica Acta (BBA) - Molecular Cell Research 1497: 297-307
Lee S-JR, Escobedo-Lozoya Y, Szatmari EM, Yasuda R (2009) Activation of CaMKII in single dendritic spines during long-term potentiation. 458: 299-304
Lee S, Faux C, Nixon J, Alete D, Chilton J, Hawadle M, Stoker AW (2007) Dimerization of Protein Tyrosine Phosphatase {sigma} Governs both Ligand Binding and Isoform Specificity. Mol. Cell. Biol. 27: 1795-1808
Levin SI, Khaliq ZM, Aman TK, Grieco TM, Kearney JA, Raman IM, Meisler MH (2006) Impaired motor function in mice with cell-specific knockout of sodium channel Scn8a (NaV1.6) in cerebellar purkinje neurons and granule cells. J Neurophysiol 96: 785-793
Levitt P (1984) A monoclonal antibody to limbic system neurons. Science 223: 299-301
Liang F, Kumar S, Zhang Z-Y (2007) Proteomic approaches to studying protein tyrosine phosphatases. Molecular BioSystems 3: 308-316
Lutz SE, Zhao Y, Gulinello M, Lee SC, Raine CS, Brosnan CF (2009) Deletion of astrocyte connexins 43 and 30 leads to a dysmyelinating phenotype and hippocampal CA1 vacuolation. J Neurosci 29: 7743-7752
Ma'ayan A, Jenkins SL, Barash A, Iyengar R (2009) Neuro2A differentiation by Galphai/o pathway. Sci Signal 2: cm1
Malenka RC, Bear MF (2004) LTP and LTD: an embarrassment of riches. Neuron 44: 5-21
Mann F, Zhukareva V, Pimenta A, Levitt P, Bolz J (1998) Membrane-associated molecules guide limbic and nonlimbic thalamocortical projections. J Neurosci 18: 9409-9419
Marambaud P, Dreses-Werringloer U, Vingtdeux V (2009) Calcium signaling in neurodegeneration. Mol Neurodegener 4: 20
Martin GS (2001) The hunting of the Src. 2: 467-475
Massa PT, Saha S, Wu C, Jarosinski KW (2000) Expression and function of the protein tyrosine phosphatase SHP-1 in oligodendrocytes. Glia 29: 376-385
Massa PT, Wu C (1996) The role of protein tyrosine phosphatase SHP-1 in the regulation of IFN-gamma signaling in neural cells. J Immunol 157: 5139-5144
Massa PT, Wu C (1998) Increased inducible activation of NF-kappaB and responsive genes in astrocytes deficient in the protein tyrosine phosphatase SHP-1. J Interferon Cytokine Res 18: 499-507

Mattiasson G, Friberg H, Hansson M, Elmer E, Wieloch T (2003) Flow cytometric analysis of mitochondria from CA1 and CA3 regions of rat hippocampus reveals differences in permeability transition pore activation. J Neurochem 87: 532 - 544
McCain DF, Zhang ZY (2002) Assays for protein-tyrosine phosphatases. Methods Enzymol 345: 507-518
McCudden C, Hains M, Kimple R, Siderovski D, Willard F (2005) G-protein signaling: back to the future. Cellular and Molecular Life Sciences 62: 551-577
Meng K, Rodriguez-Pena A, Dimitrov T, Chen W, Yamin M, Noda M, Deuel TF (2000) Pleiotrophin signals increased tyrosine phosphorylation of beta beta-catenin through inactivation of the intrinsic catalytic activity of the receptor-type protein tyrosine phosphatase beta/zeta. Proc Natl Acad Sci U S A 97: 2603-2608
Milev P, Maurel P, Haring M, Margolis RK, Margolis RU (1996) TAG-1/axonin-1 is a high-affinity ligand of neurocan, phosphacan/protein-tyrosine phosphatase-zeta/beta, and N-CAM. J Biol Chem 271: 15716-15723
Miyata S, Matsumoto N, Taguchi K, Akagi A, Iino T, Funatsu N, Maekawa S (2003) Biochemical and ultrastructural analyses of iglon cell adhesion molecules, kilon and obcam in the rat brain. Neuroscience 117: 645-658
Moffett S, Brown DA, Linder ME (2000) Lipid-dependent Targeting of G Proteins into Rafts. In, vol 275, pp 2191-2198
Mohseni M, Chishti AH (2009) Regulatory models of RhoA suppression by dematin, a cytoskeletal adaptor protein. Cell Adh Migr 3: 191-194
Montalibet J, Skorey KI, Kennedy BP (2005) Protein tyrosine phosphatase: enzymatic assays. Methods 35: 2-8
Moon LD, Asher RA, Rhodes KE, Fawcett JW (2001) Regeneration of CNS axons back to their target following treatment of adult rat brain with chondroitinase ABC. Nat Neurosci 4: 465-466
Morris EP, Torok K (2001) Oligomeric structure of alpha-calmodulin-dependent protein kinase II. J Mol Biol 308: 1-8
Muraoka-Cook RS, Sandahl MA, Strunk KE, Miraglia LC, Husted C, Hunter DM, Elenius K, Chodosh LA, Earp HS, 3rd (2009) ErbB4 splice variants Cyt1 and Cyt2 differ by 16 amino acids and exert opposing effects on the mammary epithelium in vivo. Mol Cell Biol 29: 4935-4948
Myung C-S, Yasuda H, Liu WW, Harden TK, Garrison JC (1999) Role of Isoprenoid Lipids on the Heterotrimeric G Protein gamma Subunit in Determining Effector Activation. In, vol 274, pp 16595-16603
Nakanishi S (2005) Synaptic mechanisms of the cerebellar cortical network. Trends Neurosci 28: 93-100
Nam HJ, Poy F, Saito H, Frederick CA (2005) Structural basis for the function and regulation of the receptor protein tyrosine phosphatase CD45. J Exp Med 201: 441-452
Nishi M, Hashimoto K, Kuriyama K, Komazaki S, Kano M, Shibata S, Takeshima H (2002) Motor discoordination in mutant mice lacking junctophilin type 3. Biochem Biophys Res Commun 292: 318-324
Noordman YE, Augustus ED, Schepens JTG, Chirivi RGS, Ríos P, Pulido R, Hendriks WJAJ (2008) Multimerisation of receptor-type protein tyrosine phosphatases PTPBR7 and PTP-SL attenuates enzymatic activity. Biochimica et Biophysica Acta (BBA) - Molecular Cell Research 1783: 275-286
Noordman YE, Jansen PA, Hendriks WJ (2006) Tyrosine-specific MAPK phosphatases and the control of ERK signaling in PC12 cells. J Mol Signal 1: 4
Novak U, Kaye AH (2000) Extracellular matrix and the brain: components and function. J Clin Neurosci 7: 280-290

O'Grady P, Thai TC, Saito H (1998) The laminin-nidogen complex is a ligand for a specific splice isoform of the transmembrane protein tyrosine phosphatase LAR. J Cell Biol 141: 1675-1684
Ogata M, Oh-hora M, Kosugi A, Hamaoka T (1999) Inactivation of mitogen-activated protein kinases by a mammalian tyrosine-specific phosphatase, PTPBR7. Biochem Biophys Res Commun 256: 52-56
Okamoto K, Narayanan R, Lee SH, Murata K, Hayashi Y (2007) The role of CaMKII as an F-actin-bundling protein crucial for maintenance of dendritic spine structure. Proc Natl Acad Sci U S A 104: 6418-6423
Olayioye MA, Neve RM, Lane HA, Hynes NE (2000) The ErbB signaling network: receptor heterodimerization in development and cancer. Embo J 19: 3159-3167
Pariser H, Herradon G, Ezquerra L, Perez-Pinera P, Deuel TF (2005a) Pleiotrophin regulates serine phosphorylation and the cellular distribution of beta-adducin through activation of protein kinase C. Proc Natl Acad Sci U S A 102: 12407-12412
Pariser H, Perez-Pinera P, Ezquerra L, Herradon G, Deuel TF (2005b) Pleiotrophin stimulates tyrosine phosphorylation of beta-adducin through inactivation of the transmembrane receptor protein tyrosine phosphatase beta/zeta. Biochem Biophys Res Commun 335: 232-239
Park LC, Zhang H, Gibson GE (2001) Co-culture with astrocytes or microglia protects metabolically impaired neurons. Mech Ageing Dev 123: 21-27
Paul S, Lombroso PJ (2003) Receptor and nonreceptor protein tyrosine phosphatases in the nervous system. Cell Mol Life Sci 60: 2465-2482
Paulson HL (2009) The spinocerebellar ataxias. J Neuroophthalmol 29: 227-237
Pawson T, Raina M, Nash P (2002) Interaction domains: from simple binding events to complex cellular behavior. FEBS Letters Protein Domains 513: 2-10
Peles E, Nativ M, Campbell PL, Sakurai T, Martinez R, Lev S, Clary DO, Schilling J, Barnea G, Plowman GD, Grumet M, Schlessinger J (1995) The carbonic anhydrase domain of receptor tyrosine phosphatase beta is a functional ligand for the axonal cell recognition molecule contactin. Cell 82: 251-260
Perez-Pinera P, Zhang W, Chang Y, Vega JA, Deuel TF (2007) Anaplastic lymphoma kinase is activated through the pleiotrophin/receptor protein-tyrosine phosphatase beta/zeta signaling pathway: an alternative mechanism of receptor tyrosine kinase activation. J Biol Chem 282: 28683-28690
Perlman SL (2011) Spinocerebellar degenerations. Handb Clin Neurol 100: 113-140
Petersen JD, Chen X, Vinade L, Dosemeci A, Lisman JE, Reese TS (2003) Distribution of postsynaptic density (PSD)-95 and Ca2+/calmodulin-dependent protein kinase II at the PSD. J Neurosci 23: 11270-11278
Petschnigg J, Snider J, Stagljar I (2011) Interactive proteomics research technologies: recent applications and advances. Current Opinion in Biotechnology 22: 50-58
Pietrobon D (2005) Function and dysfunction of synaptic calcium channels: insights from mouse models. Curr Opin Neurobiol 15: 257-265
Pimenta AF, Zhukareva V, Barbe MF, Reinoso BS, Grimley C, Henzel W, Fischer I, Levitt P (1995) The limbic system-associated membrane protein is an Ig superfamily member that mediates selective neuronal growth and axon targeting. Neuron 15: 287-297
Pizzorusso T, Medini P, Berardi N, Chierzi S, Fawcett JW, Maffei L (2002) Reactivation of ocular dominance plasticity in the adult visual cortex. Science 298: 1248-1251
Polo-Parada L, Bose CM, Landmesser LT (2001) Alterations in transmission, vesicle dynamics, and transmitter release machinery at NCAM-deficient neuromuscular junctions. Neuron 32: 815-828

Poole AW, Jones ML (2005) A SHPing tale: perspectives on the regulation of SHP-1 and SHP-2 tyrosine phosphatases by the C-terminal tail. Cell Signal 17: 1323-1332
Pulido R, Zuniga A, Ullrich A (1998) PTP-SL and STEP protein tyrosine phosphatases regulate the activation of the extracellular signal-regulated kinases ERK1 and ERK2 by association through a kinase interaction motif. Embo J 17: 7337-7350
Qiu C, Tarrant MK, Choi SH, Sathyamurthy A, Bose R, Banjade S, Pal A, Bornmann WG, Lemmon MA, Cole PA, Leahy DJ (2008) Mechanism of Activation and Inhibition of the HER4/ErbB4 Kinase. Structure (London, England : 1993) 16: 460-467
Raman IM, Sprunger LK, Meisler MH, Bean BP (1997) Altered subthreshold sodium currents and disrupted firing patterns in Purkinje neurons of Scn8a mutant mice. Neuron 19: 881-891
Reed J, McNamee C, Rackstraw S, Jenkins J, Moss D (2004) Diglons are heterodimeric proteins composed of IgLON subunits, and Diglon-CO inhibits neurite outgrowth from cerebellar granule cells. J Cell Sci 117: 3961-3973
Rhodes KE, Fawcett JW (2004) Chondroitin sulphate proteoglycans: preventing plasticity or protecting the CNS? J Anat 204: 33-48
Ribar TJ, Rodriguiz RM, Khiroug L, Wetsel WC, Augustine GJ, Means AR (2000) Cerebellar defects in Ca2+/calmodulin kinase IV-deficient mice. J Neurosci 20: RC107
Riethmacher D, Sonnenberg-Riethmacher E, Brinkmann V, Yamaai T, Lewin GR, Birchmeier C (1997) Severe neuropathies in mice with targeted mutations in the ErbB3 receptor. Nature 389: 725-730
Rojas AI, Ahmed AR (1999) Adhesion receptors in health and disease. Crit Rev Oral Biol Med 10: 337-358
Roskoski Jr. R (2005) Src kinase regulation by phosphorylation and dephosphorylation. Biochemical and Biophysical Research Communications 331: 1-14
Rougon G, Hobert O (2003) New insights into the diversity and function of neuronal immunoglobulin superfamily molecules. Annu Rev Neurosci 26: 207-238
Roy S, Zhang B, Lee VM, Trojanowski JQ (2005) Axonal transport defects: a common theme in neurodegenerative diseases. Acta Neuropathol 109: 5-13
Ruoslahti E (1988) Versatile mechanisms of cell adhesion. Harvey Lect 84: 1-17
Sacco F, Tinti M, Palma A, Ferrari E, Nardozza AP, Hooft van Huijsduijnen R, Takahashi T, Castagnoli L, Cesareni G (2009) Tumor suppressor density-enhanced phosphatase-1 (DEP-1) inhibits the RAS pathway by direct dephosphorylation of ERK1/2 kinases. J. Biol. Chem.: M109.002758
Saghatelyan AK, Dityatev A, Schmidt S, Schuster T, Bartsch U, Schachner M (2001) Reduced perisomatic inhibition, increased excitatory transmission, and impaired long-term potentiation in mice deficient for the extracellular matrix glycoprotein tenascin-R. Mol Cell Neurosci 17: 226-240
Sajnani-Perez G, Chilton JK, Aricescu AR, Haj F, Stoker AW (2003) Isoform-specific binding of the tyrosine phosphatase PTPsigma to a ligand in developing muscle. Mol Cell Neurosci 22: 37-48
Sakisaka T, Takai Y (2005) Cell adhesion molecules in the CNS. J Cell Sci 118: 5407-5410
Salie R, Niederkofler V, Arber S (2005) Patterning molecules; multitasking in the nervous system. Neuron 45: 189-192
Salzer JL, Colman DR (1989) Mechanisms of cell adhesion in the nervous system: role of the immunoglobulin gene superfamily. Dev Neurosci 11: 377-390
Sanderson CM (2008) A new way to explore the world of extracellular protein interactions. Genome Res 18: 517-520
Sap J, Jiang YP, Friedlander D, Grumet M, Schlessinger J (1994) Receptor tyrosine phosphatase R-PTP-kappa mediates homophilic binding. Mol Cell Biol 14: 1-9

Sarnowska A (2002) Application of organotypic hippocampal culture for study of selective neuronal death. Folia Neuropathol 40: 101-106
Sayre LM, Smith MA, Perry G (2001) Chemistry and biochemistry of oxidative stress in neurodegenerative disease. Curr Med Chem 8: 721-738
Schäfer M, Bräuer AU, Savaskan NE, Rathjen FG, Brümmendorf T (2005) Neurotractin/kilon promotes neurite outgrowth and is expressed on reactive astrocytes after entorhinal cortex lesion. Molecular and Cellular Neuroscience 29: 580-590
Schecterson LC, Hudson MP, Ko M, Philippidou P, Akmentin W, Wiley J, Rosenblum E, Chao MV, Halegoua S, Bothwell M (2010) Trk activation in the secretory pathway promotes Golgi fragmentation. Molecular and Cellular Neuroscience 43: 403-413
Scheiffele P (2003) Cell-cell signaling during synapse formation in the CNS. Annu Rev Neurosci 26: 485-508
Schlessinger J (2000) Cell signaling by receptor tyrosine kinases. Cell 103: 211-225
Schmid RS, Maness PF (2008) L1 and NCAM adhesion molecules as signaling coreceptors in neuronal migration and process outgrowth. Curr Opin Neurobiol 18: 245-250
Schmidt-Arras DE, Bohmer A, Markova B, Choudhary C, Serve H, Bohmer FD (2005) Tyrosine phosphorylation regulates maturation of receptor tyrosine kinases. Mol Cell Biol 25: 3690-3703
Schofield PR, McFarland KC, Hayflick JS, Wilcox JN, Cho TM, Roy S, Lee NM, Loh HH, Seeburg PH (1989) Molecular characterization of a new immunoglobulin superfamily protein with potential roles in opioid binding and cell contact. Embo J 8: 489-495
Schulze WX, Deng L, Mann M (2005) Phosphotyrosine interactome of the ErbB-receptor kinase family. Mol Syst Biol 1: 2005 0008
Schwaller B, Meyer M, Schiffmann S (2002) 'New' functions for 'old' proteins: the role of the calcium-binding proteins calbindin D-28k, calretinin and parvalbumin, in cerebellar physiology. Studies with knockout mice. Cerebellum 1: 241-258
Shah BS, Rush AM, Liu S, Tyrrell L, Black JA, Dib-Hajj SD, Waxman SG (2004) Contactin associates with sodium channel Nav1.3 in native tissues and increases channel density at the cell surface. J Neurosci 24: 7387-7399
Shakkottai VG, Xiao M, Xu L, Wong M, Nerbonne JM, Ornitz DM, Yamada KA (2009) FGF14 regulates the intrinsic excitability of cerebellar Purkinje neurons. Neurobiol Dis 33: 81-88
Shaver A, Ng JB, Hall DA, Lum BS, Posner BI (1993) Insulin mimetic peroxovanadium complexes: preparation and structure of potassium oxodiperoxo(pyridine-2-carboxylato)vanadate(V), K2[VO(O2)2(C5H4NCOO)].2H2O, and potassium oxodiperoxo(3-hydroxypyridine-2-carboxylato)vanadate(V), K2[VO(O2)2(OHC5H3NCOO)].3H2O, and their reactions with cysteine. Inorganic Chemistry 32: 3109-3113
Shen Y, Tenney AP, Busch SA, Horn KP, Cuascut FX, Liu K, He Z, Silver J, Flanagan JG (2009) PTPsigma is a receptor for chondroitin sulfate proteoglycan, an inhibitor of neural regeneration. Science 326: 592-596
Shiota C, Miura M, Mikoshiba K (1989) Developmental profile and differential localization of mRNAs of myelin proteins (MBP and PLP) in oligodendrocytes in the brain and in culture. Brain Res Dev Brain Res 45: 83-94
Silva AJ, Paylor R, Wehner JM, Tonegawa S (1992) Impaired spatial learning in alpha-calcium-calmodulin kinase II mutant mice. Science 257: 206-211
Simon MI, Strathmann MP, Gautam N (1991) Diversity of G proteins in signal transduction. In, vol 252, pp 802-808
Smetsers TFCM, van de Westerlo EMA, ten Dam GB, Overes IM, Schalkwijk J, van Muijen GNP, van Kuppevelt TH (2004) Human Single-Chain Antibodies Reactive with Native

Chondroitin Sulfate Detect Chondroitin Sulfate Alterations in Melanoma and Psoriasis. 122: 707-716
Sorby M, Sandstrom J, Ostman A (2001) An extracellular ligand increases the specific activity of the receptor-like protein tyrosine phosphatase DEP-1. Oncogene 20: 5219-5224
Sorkin A, Goh LK (2008) Endocytosis and intracellular trafficking of ErbBs. Exp Cell Res 314: 3093-3106
Stamer K, Vogel R, Thies E, Mandelkow E, Mandelkow EM (2002) Tau blocks traffic of organelles, neurofilaments, and APP vesicles in neurons and enhances oxidative stress. J Cell Biol 156: 1051-1063
Stankewich MC, Gwynn B, Ardito T, Ji L, Kim J, Robledo RF, Lux SE, Peters LL, Morrow JS (2010) Targeted deletion of betaIII spectrin impairs synaptogenesis and generates ataxic and seizure phenotypes. Proc Natl Acad Sci U S A 107: 6022-6027
Starkov AA, Fiskum G, Chinopoulos C, Lorenzo BJ, Browne SE, Patel MS, Beal MF (2004) Mitochondrial alpha-ketoglutarate dehydrogenase complex generates reactive oxygen species. J Neurosci 24: 7779-7788
Stepanek L, Stoker AW, Stoeckli E, Bixby JL (2005) Receptor tyrosine phosphatases guide vertebrate motor axons during development. J Neurosci 25: 3813-3823
Stoker A (2005) Methods for identifying extracellular ligands of RPTPs. Methods 35: 80-89
Stoker A, Dutta R (1998) Protein tyrosine phosphatases and neural development. Bioessays 20: 463-472
Strack S, Barban MA, Wadzinski BE, Colbran RJ (1997) Differential inactivation of postsynaptic density-associated and soluble Ca2+/calmodulin-dependent protein kinase II by protein phosphatases 1 and 2A. J Neurochem 68: 2119-2128
Strittmatter SM, Fishman MC, Zhu XP (1994) Activated mutants of the alpha subunit of G(o) promote an increased number of neurites per cell. J Neurosci 14: 2327-2338
Strittmatter SM, Valenzuela D, Kennedy TE, Neer EJ, Fishman MC (1990) G0 is a major growth cone protein subject to regulation by GAP-43. Nature 344: 836-841
Struyk AF, Canoll PD, Wolfgang MJ, Rosen CL, D'Eustachio P, Salzer JL (1995) Cloning of neurotrimin defines a new subfamily of differentially expressed neural cell adhesion molecules. J Neurosci 15: 2141-2156
Sugahara K, Mikami T (2007) Chondroitin/dermatan sulfate in the central nervous system. Curr Opin Struct Biol 17: 536-545
Sun H, Tan LP, Gao L, Yao SQ (2009) High-throughput screening of catalytically inactive mutants of protein tyrosine phosphatases (PTPs) in a phosphopeptide microarray. Chem Commun (Camb): 677-679
Sundvall M, Korhonen A, Paatero I, Gaudio E, Melino G, Croce CM, Aqeilan RI, Elenius K (2008) Isoform-specific monoubiquitination, endocytosis, and degradation of alternatively spliced ErbB4 isoforms. Proc Natl Acad Sci U S A 105: 4162-4167
Suzuki SC, Inoue T, Kimura Y, Tanaka T, Takeichi M (1997) Neuronal circuits are subdivided by differential expression of type-II classic cadherins in postnatal mouse brains. Mol Cell Neurosci 9: 433-447
Swarup G, Cohen S, Garbers DL (1982) Inhibition of membrane phosphotyrosyl-protein phosphatase activity by vanadate. Biochem Biophys Res Commun 107: 1104-1109
Sweatt JD (2004) Mitogen-activated protein kinases in synaptic plasticity and memory. Curr Opin Neurobiol 14: 311-317
Tabernero L, Aricescu AR, Jones EY, Szedlacsek SE (2008) Protein tyrosine phosphatases: structure-function relationships. Febs J 275: 867-882
Takai Y, Nakanishi H (2003) Nectin and afadin: novel organizers of intercellular junctions. J Cell Sci 116: 17-27

Takeda A, Wu JJ, Maizel AL (1992) Evidence for monomeric and dimeric forms of CD45 associated with a 30-kDa phosphorylated protein. J Biol Chem 267: 16651-16659
Takeichi M (2007) The cadherin superfamily in neuronal connections and interactions. Nat Rev Neurosci 8: 11-20
Takeichi M, Hatta K, Nose A, Nagafuchi A (1988) Identification of a gene family of cadherin cell adhesion molecules. Cell Differ Dev 25 Suppl: 91-94
Tamir I, Dal Porto JM, Cambier JC (2000) Cytoplasmic protein tyrosine phosphatases SHP-1 and SHP-2: regulators of B cell signal transduction. Current Opinion in Immunology 12: 307-315
Tamura H, Fukada M, Fujikawa A, Noda M (2006) Protein tyrosine phosphatase receptor type Z is involved in hippocampus-dependent memory formation through dephosphorylation at Y1105 on p190 RhoGAP. Neurosci Lett 399: 33-38
Tanaka M, Maeda N, Noda M, Marunouchi T (2003) A chondroitin sulfate proteoglycan PTPzeta /RPTPbeta regulates the morphogenesis of Purkinje cell dendrites in the developing cerebellum. J Neurosci 23: 2804-2814
Tanoue T, Nishida E (2003) Molecular recognitions in the MAP kinase cascades. Cell Signal 15: 455-462
Tappe A, Kuner R (2006) Regulation of motor performance and striatal function by synaptic scaffolding proteins of the Homer1 family. Proc Natl Acad Sci U S A 103: 774-779
ten Dam GB, van de Westerlo EM, Purushothaman A, Stan RV, Bulten J, Sweep FC, Massuger LF, Sugahara K, van Kuppevelt TH (2007) Antibody GD3G7 selected against embryonic glycosaminoglycans defines chondroitin sulfate-E domains highly up-regulated in ovarian cancer and involved in vascular endothelial growth factor binding. Am J Pathol 171: 1324-1333
Tertoolen LG, Blanchetot C, Jiang G, Overvoorde J, Gadella TW, Jr., Hunter T, den Hertog J (2001) Dimerization of receptor protein-tyrosine phosphatase alpha in living cells. BMC Cell Biol 2: 8
Tessier-Lavigne M, Goodman CS (1996) The molecular biology of axon guidance. Science 274: 1123-1133
Thies E, Mandelkow EM (2007) Missorting of tau in neurons causes degeneration of synapses that can be rescued by the kinase MARK2/Par-1. J Neurosci 27: 2896-2907
Thomas GM, Huganir RL (2004) MAPK cascade signalling and synaptic plasticity. Nat Rev Neurosci 5: 173-183
Tidcombe H, Jackson-Fisher A, Mathers K, Stern DF, Gassmann M, Golding JP (2003) Neural and mammary gland defects in ErbB4 knockout mice genetically rescued from embryonic lethality. Proc Natl Acad Sci U S A 100: 8281-8286
Tiganis T, Bennett AM (2007) Protein tyrosine phosphatase function: the substrate perspective. Biochem J 402: 1-15
Toescu EC, Vreugdenhil M (2009) Calcium and normal brain ageing. Cell Calcium 47: 158-164
Togashi H, Abe K, Mizoguchi A, Takaoka K, Chisaka O, Takeichi M (2002) Cadherin Regulates Dendritic Spine Morphogenesis. Neuron 35: 77-89
Togashi H, Sakisaka T, Takai Y (2009) Cell adhesion molecules in the central nervous system. Cell Adh Migr 3: 29-35
Toker A, Newton AC (2000) Akt/Protein Kinase B Is Regulated by Autophosphorylation at the Hypothetical PDK-2 Site. Journal of Biological Chemistry 275: 8271-8274
Toledano-Katchalski H, Tiran Z, Sines T, Shani G, Granot-Attas S, den Hertog J, Elson A (2003) Dimerization in vivo and inhibition of the nonreceptor form of protein tyrosine phosphatase epsilon. Mol Cell Biol 23: 5460-5471

Tonks NK (2006) Protein tyrosine phosphatases: from genes, to function, to disease. Nat Rev Mol Cell Biol 7: 833-846
Torii S, Kusakabe M, Yamamoto T, Maekawa M, Nishida E (2004) Sef is a spatial regulator for Ras/MAP kinase signaling. Dev Cell 7: 33-44
Trudeau MM, Dalton JC, Day JW, Ranum LP, Meisler MH (2006) Heterozygosity for a protein truncation mutation of sodium channel SCN8A in a patient with cerebellar atrophy, ataxia, and mental retardation. J Med Genet 43: 527-530
Turkmen S, Guo G, Garshasbi M, Hoffmann K, Alshalah AJ, Mischung C, Kuss A, Humphrey N, Mundlos S, Robinson PN (2009) CA8 mutations cause a novel syndrome characterized by ataxia and mild mental retardation with predisposition to quadrupedal gait. PLoS Genet 5: e1000487
Uchida N, Honjo Y, Johnson KR, Wheelock MJ, Takeichi M (1996) The catenin/cadherin adhesion system is localized in synaptic junctions bordering transmitter release zones. J Cell Biol 135: 767-779
Valenzuela D, Han X, Mende U, Fankhauser C, Mashimo H, Huang P, Pfeffer J, Neer EJ, Fishman MC (1997) G alpha(o) is necessary for muscarinic regulation of Ca2+ channels in mouse heart. Proc Natl Acad Sci U S A 94: 1727-1732
Valko M, Leibfritz D, Moncol J, Cronin MT, Mazur M, Telser J (2007) Free radicals and antioxidants in normal physiological functions and human disease. Int J Biochem Cell Biol 39: 44-84
van den Maagdenberg AM, Bachner D, Schepens JT, Peters W, Fransen JA, Wieringa B, Hendriks WJ (1999) The mouse Ptprr gene encodes two protein tyrosine phosphatases, PTP-SL and PTPBR7, that display distinct patterns of expression during neural development. Eur J Neurosci 11: 3832-3844
van der Merwe PA, Barclay AN (1996) Analysis of cell-adhesion molecule interactions using surface plasmon resonance. Curr Opin Immunol 8: 257-261
van der Wijk T, Blanchetot C, Overvoorde J, den Hertog J (2003) Redox-regulated Rotational Coupling of Receptor Protein-tyrosine Phosphatase α Dimers. In, vol 278, pp 13968-13974
van Kuppevelt TH, Dennissen MA, van Venrooij WJ, Hoet RM, Veerkamp JH (1998) Generation and application of type-specific anti-heparan sulfate antibodies using phage display technology. Further evidence for heparan sulfate heterogeneity in the kidney. J Biol Chem 273: 12960-12966
Van Vactor D (1998) Protein tyrosine phosphatases in the developing nervous system. Curr Opin Cell Biol 10: 174-181
Vaskovsky A, Lupowitz Z, Erlich S, Pinkas-Kramarski R (2000) ErbB-4 Activation Promotes Neurite Outgrowth in PC12 Cells. Journal of Neurochemistry 74: 979-987
Verbeek DS, Knight MA, Harmison GG, Fischbeck KH, Howell BW (2005) Protein kinase C gamma mutations in spinocerebellar ataxia 14 increase kinase activity and alter membrane targeting. Brain 128: 436-442
Waites CL, Craig AM, Garner CC (2005) Mechanisms of vertebrate synaptogenesis. Annu Rev Neurosci 28: 251-274
Walchli S, Espanel X, Hooft van Huijsduijnen R (2005) Sap-1/PTPRH activity is regulated by reversible dimerization. Biochem Biophys Res Commun 331: 497-502
Walsh FS, Doherty P (1997) Neural cell adhesion molecules of the immunoglobulin superfamily: role in axon growth and guidance. Annu Rev Cell Dev Biol 13: 425-456
Wang Q, Lu L, Yuan C, Pei K, Liu Z, Guo M, Zhu M (2010) Potent inhibition of protein tyrosine phosphatase 1B by copper complexes: implications for copper toxicity in biological systems. Chemical Communications, Chem. Commun. 46: 3547-3549
Wang X, Michaelis EK (2010) Selective neuronal vulnerability to oxidative stress in the brain. Front Aging Neurosci 2: 12

Wang X, Pal R, Chen X-W, Kumar K, Kim O-J, Michaelis E (2007) Genome-wide transcriptome profiling of region-specific vulnerability to oxidative stress in the hippocampus. Genomics 90: 201 - 212
Wang X, Pal R, Chen X, Limpeanchob N, Kumar K, Michaelis E (2005) High intrinsic oxidative stress may underlie selective vulnerability of the hippocampal CA1 region. Brain Res Mol Brain Res 140: 120 - 126
Wang X, Zaidi A, Pal R, Garrett A, Braceras R, Chen X-w, Michaelis M, Michaelis E (2009) Genomic and biochemical approaches in the discovery of mechanisms for selective neuronal vulnerability to oxidative stress. BMC Neuroscience 10: 12
Waskiewicz AJ, Cooper JA (1995) Mitogen and stress response pathways: MAP kinase cascades and phosphatase regulation in mammals and yeast. Current Opinion in Cell Biology 7: 798-805
Wheelock MJ, Johnson KR (2003) Cadherins as modulators of cellular phenotype. Annu Rev Cell Dev Biol 19: 207-235
Wilde A, Beattie EC, Lem L, Riethof DA, Liu S-H, Mobley WC, Soriano P, Brodsky FM (1999) EGF Receptor Signaling Stimulates SRC Kinase Phosphorylation of Clathrin, Influencing Clathrin Redistribution and EGF Uptake. Cell 96: 677-687
Williams AF, Barclay AN (1988) The immunoglobulin superfamily--domains for cell surface recognition. Annu Rev Immunol 6: 381-405
Wishcamper CA, Coffin JD, Lurie DI (2001) Lack of the protein tyrosine phosphatase SHP-1 results in decreased numbers of glia within the motheaten (me/me) mouse brain. J Comp Neurol 441: 118-133
Wolosker H, Blackshaw S, Snyder SH (1999) Serine racemase: a glial enzyme synthesizing D-serine to regulate glutamate-N-methyl-D-aspartate neurotransmission. Proc Natl Acad Sci U S A 96: 13409-13414
Worley PF, Baraban JM, Van Dop C, Neer EJ, Snyder SH (1986) Go, a guanine nucleotide-binding protein: immunohistochemical localization in rat brain resembles distribution of second messenger systems. In, vol 83, pp 4561-4565
Worley PF, Zeng W, Huang G, Kim JY, Shin DM, Kim MS, Yuan JP, Kiselyov K, Muallem S (2007) Homer proteins in Ca2+ signaling by excitable and non-excitable cells. Cell Calcium, Calcium Channels and Transporters 42: 363-371
Wright GJ (2009) Signal initiation in biological systems: the properties and detection of transient extracellular protein interactions. Molecular BioSystems 5: 1405-1412
Xie L, Zhang Y-L, Zhang Z-Y (2002) Design and Characterization of an Improved Protein Tyrosine Phosphatase Substrate-Trapping Mutantâ€ Biochemistry 41: 4032-4039
Xie R, Li L, Goshima Y, Strittmatter SM (1995) An activated mutant of the alpha subunit of G(o) increases neurite outgrowth via protein kinase C. Brain Res Dev Brain Res 87: 77-86
Xu Z, Weiss A (2002) Negative regulation of CD45 by differential homodimerization of the alternatively spliced isoforms. Nat Immunol 3: 764-771
Yabe I, Sasaki H, Chen DH, Raskind WH, Bird TD, Yamashita I, Tsuji S, Kikuchi S, Tashiro K (2003) Spinocerebellar ataxia type 14 caused by a mutation in protein kinase C gamma. Arch Neurol 60: 1749-1751
Yagi T, Takeichi M (2000) Cadherin superfamily genes: functions, genomic organization, and neurologic diversity. Genes Dev 14: 1169-1180
Yamada M, Hashimoto T, Hayashi N, Higuchi M, Murakami A, Nakashima T, Maekawa S, Miyata S (2007) Synaptic adhesion molecule OBCAM; synaptogenesis and dynamic internalization. Brain Res 1165: 5-14
Yamagata M, Herman JP, Sanes JR (1995) Lamina-specific expression of adhesion molecules in developing chick optic tectum. J Neurosci 15: 4556-4571

Yamaguchi Y (2000) Lecticans: organizers of the brain extracellular matrix. Cell Mol Life Sci 57: 276-289
Yamauchi T (2005) Neuronal Ca2+/Calmodulin-Dependent Protein Kinase II—Discovery, Progress in a Quarter of a Century, and Perspective: Implication for Learning and Memory. Biological & Pharmaceutical Bulletin 28: 1342-1354
Yeatman TJ (2004) A renaissance for SRC. Nat Rev Cancer 4: 470-480
Yick LW, Cheung PT, So KF, Wu W (2003) Axonal regeneration of Clarke's neurons beyond the spinal cord injury scar after treatment with chondroitinase ABC. Exp Neurol 182: 160-168
York RD, Yao H, Dillon T, Ellig CL, Eckert SP, McCleskey EW, Stork PJ (1998) Rap1 mediates sustained MAP kinase activation induced by nerve growth factor. Nature 392: 622-626
Yoshimura Y, Sogawa Y, Yamauchi T (1999) Protein phosphatase 1 is involved in the dissociation of Ca2+/calmodulin-dependent protein kinase II from postsynaptic densities. FEBS Lett 446: 239-242
Zhang L, Oh SY, Wu X, Oh MH, Wu F, Schroeder JT, Takemoto CM, Zheng T, Zhu Z (2010) SHP-1 Deficient Mast Cells Are Hyperresponsive to Stimulation and Critical in Initiating Allergic Inflammation in the Lung. In, vol 184, pp 1180-1190
Zhang ZY (2002) Protein tyrosine phosphatases: structure and function, substrate specificity, and inhibitor development. Annu Rev Pharmacol Toxicol 42: 209-234
Zheng JQ, Poo M-m (2007) Calcium Signaling in Neuronal Motility. In, vol 23, pp 375-404
Zhukareva V, Chernevskaya N, Pimenta A, Nowycky M, Levitt P (1997) Limbic system-associated membrane protein (LAMP) induces neurite outgrowth and intracellular Ca2+ increase in primary fetal neurons. Mol Cell Neurosci 10: 43-55
Zimmermann D, Dours-Zimmermann M (2008) Extracellular matrix of the central nervous system: from neglect to challenge. Histochemistry and Cell Biology 130: 635-653

6.2 Abbreviations

AP, alkaline phosphatase

BSA, bovine serum albumine

CAM, cell adhesion molecule

CamkII, calcium/calmodulin-dependent kinase II

CNS, central nervous system

CNPase, 2'-3'-cyclic-nucleotide 3'-phosphodiesterase

Cx, connexin

CS, chondroitin-sulphate

DTT, Dithiothreitol

DMSO, Dimethyl sulfoxide

EA2, episodic ataxia 2

ECM, extracellular matrix

EGFR, epidermal growth factor receptor

ERK1/2, extracellular signal-regulated kinases 1/2

FCS, foetal calf serum

FGFR, fibroblast growth factor receptor

GAG, glycosaminoglycan

GPI, glycosylphosphatidylinositol

GSH, glutathione S-transferase

GJ, Gap junction

Gαo, guanine nucleotide-binding protein G(o) subunit alpha

HBSS, Hanks' balanced salt solution

HR, hydrophobic region

HRP, horseradish peroxidase

HS, heparan sulphate

IgSF, Immunoglobulin superfamly

IP3, inositol-(1,4,5)-triphosphate

JAK/STAT, Janus kinase/Signal transducer and activator of translation

KIM, kinase interaction motif

LTD, long-term depression

LTP, long-term potentiation

MAPK, mitogen-activated protein kinase

MAPKKK, Mitogen-activated protein kinase kinase kinase

MAM, mephrin/A5/RPTPμ

MKP, Mitogen-activated protein kinase phosphatase

NCAM, Neural cell adhesion molecule

NrCAM, neuron-glia-related cell adhesion molecule

NRG, neuregulin

Ntm, neurotrimin

OS, oxidative stress

PC, Purkinje cells

PG, proteoglycan

PKC, protein kinase C

PNN, perineuronal net

PSD, post synaptic density

PI3K, phosphatidilinositol-3-phosphate kinase

PLAP, placental alkaline phosphatase

PIP_2, phosphatidylinositol (4,5) bisphosphate

PIP_3, phosphatidylinositol-(3,4,5)-triphosphate

PLC, phospholipase C

pNPP, 4-nitrophenyldisodium orthophosphate

PTB, phosphotyrosine-binding

PTP, protein Tyrosine phosphatase

pTyr, phosphoTyrosine

PTK, protein Tyrosine kinase

RAP, receptor alkaline phosphatase

ROS, reactive oxygen species

RNS, reactive nitrogen species

RPTP, receptor-like protein Tyrosine phosphatase

RTK, receptor Tyrosine kinase

SCA, Spinocerebellar ataxia

SDS-PAGE, Sodium Dodecyl Sulphate - PolyAcrylamide Gel Electrophoresis

SH2, Src homology-2

Y2H, yeast two-hybrid

6.3 Plasmid Maps and Vector Constructs

Map of the pBG-flexilinker plasmid after modification with the linker EcoRI and KpnI

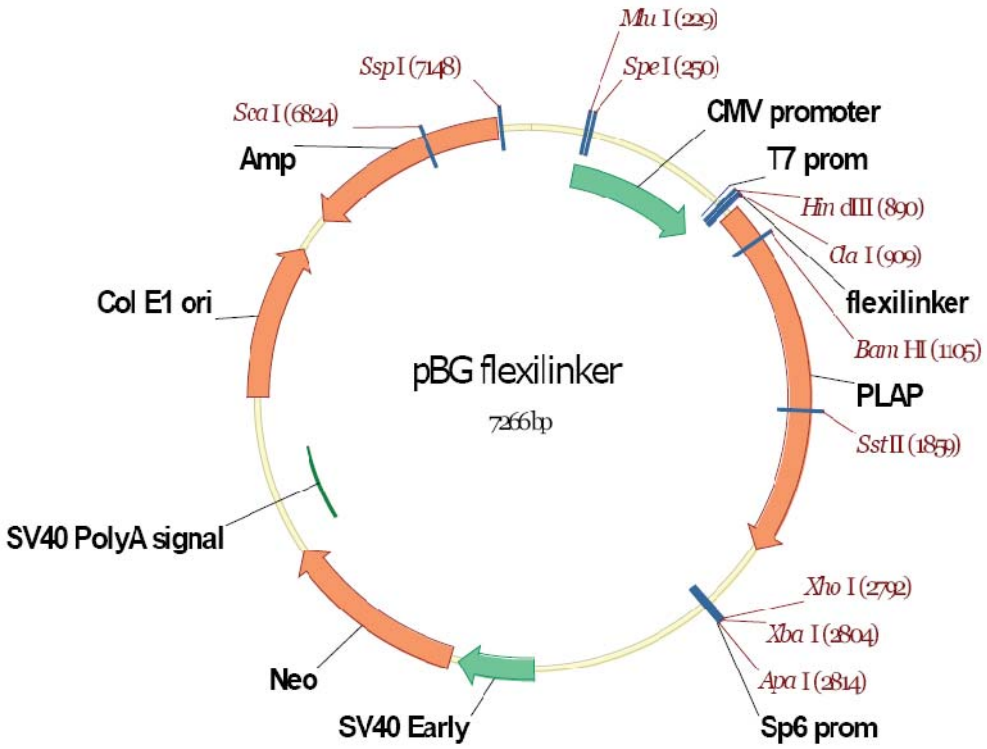

flexilinker

```
          S  L  P   R  S  G   S  I  G  G   G  G  S   G  G  G   G  S  P  I
889   AAGCTTGCCC AGATCTGGAT CGATCGGCGG AGGAGGTTCC GGAGGTGGCG GTTCACCGAT
      HindIII               ClaI
          I  P  V   E  E  E   N  P  D  F   W  N  R   E  A  A   E  A  L  G
949   CATCCCAGTT GAGGAGGAGA ACCCGGACTT CTGGAACCGC GAGGCAGCCG AGGCCCTGGG

          A  A  K   K  L  Q   P  A  Q  T   A  A  K   N  L  I   I  F  L  G
1009  TGCCGCCAAG AAGCTGCAGC CTGCACAGAC AGCCGCCAAG AACCTCATCA TCTTCCTGGG

          D  G  M   G  V  S   T  V  T  A   A  R  I
1069  CGATCGCATG GCGCTCTCTA CGCTGACACC TGCCACCATC C
                                          BamHI
```

Map of pHL sec plasmid

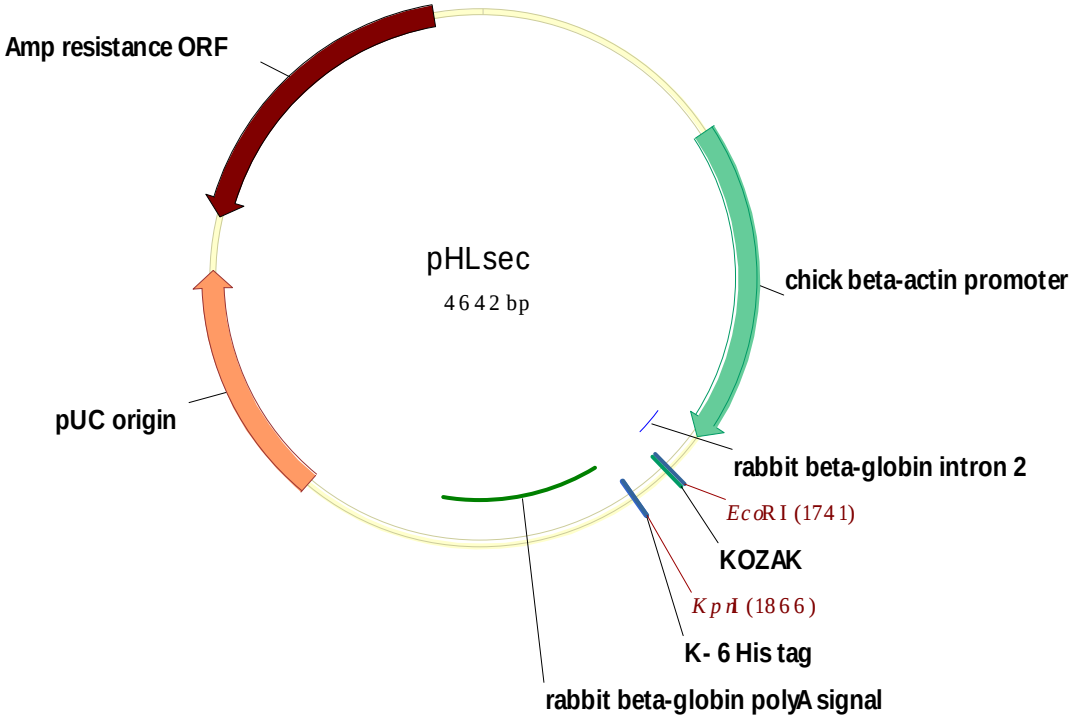

Map of pGEX-1N-Xho plasmid containing the PTP-SL phosphatase domain with C/S-D/A mutations

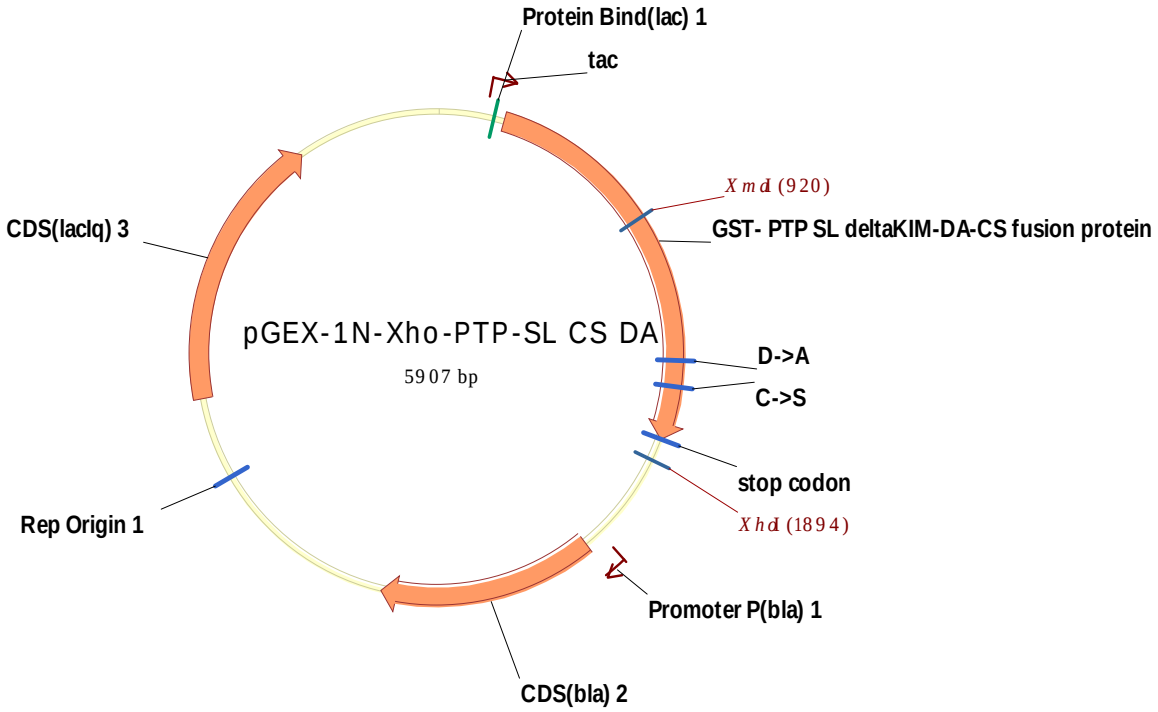

6.4 Supplementary tables

Table S1. Proteins affinity-purified by GST-PTP-SL and GST-PTP-BL (PTPN13) from brain lysates and identified by LC/MS-MS.
Mascot scores for proteins identified by LC-ESI-FT-MS/MS that were affinity-purified from brain lysates using GST-PTP-SL and GST-PTP-BL as baits. The scores for proteins identified in control isolates, using GST-PTP-BL as bait or the GST protein alone, are listed for each sample. Upper and lower refer to the two gel pieces in which each lane was divided before peptide extraction was applied.

Mascot results compiled from experiment:		GST-PT PSL wt upper	GST-PTP SL C/S D/A upper	GST lower	GST-PT PSL wt lower	GST-PTP SL C/S D/A lower	GST-PT PN13 wt upper	GST-PTN13 C/S upper	GST-PTPN13 wt lower	GST-PTPN13 C/S lower
Sample name										
PTPRR_MOUSE	Receptor-type tyrosine-protein phosphatase R OS=Mus musculus GN=Ptprr PE=1 SV=1	397	4250	123	467	2087	930	102	100	0
PTN13_MOUSE	Tyrosine-protein phosphatase non-receptor type 13 OS=Mus musculus GN=Ptpn13 PE=1 SV=2	0	47	0	0	43	3961	5310	2242	2303
KCC2A_MOUSE	Calcium/calmodulin-dependent protein kinase type II subunit alpha OS=Mus musculus GN=Camk2a PE=1 SV=2	145	449	0	0	0	1226	387	0	0
GNAO_MOUSE	Guanine nucleotide-binding protein G(o) subunit alpha OS=Mus musculus GN=Gnao1 PE=1 SV=3	0	0	69	0	0	0	0	126	227
NTRI_MOUSE	Neurotrimin OS=Mus musculus GN=Ntm PE=2 SV=2	0	0	0	0	0	33	0	0	0
AINX_MOUSE	Alpha-internexin OS=Mus musculus GN=Ina PE=1 SV=2	0	0	0	0	0	194	0	0	0
AP2M1_MOUSE	AP-2 complex subunit mu OS=Mus musculus GN=Ap2m1 PE=1 SV=1	0	0	0	0	0	33	0	0	0
KCC2D_MOUSE	Calcium/calmodulin-dependent protein kinase type II subunit delta OS=Mus musculus GN=Camk2d PE=1 SV=1	0	0	0	0	0	903	0	0	0

DSG1A_MOUSE	Desmoglein-1-alpha OS=Mus musculus GN=Dsg1a PE=2 SV=2	0	0	0	0	0	93	0	0	0
EF1G_MOUSE	Elongation factor 1-gamma OS=Mus musculus GN=Eef1g PE=1 SV=3	0	0	0	0	0	152	0	0	0
VATB2_MOUSE	V-type proton ATPase subunit B, brain isoform OS=Mus musculus GN=Atp6v1b2 PE=1 SV=1	0	0	0	0	0	182	0	0	0
RLA0_MOUSE	60S acidic ribosomal protein P0 OS=Mus musculus GN=Rplp0 PE=1 SV=3	0	0	99	47	0	0	0	53	0
ATS12_MOUSE	A disintegrin and metalloproteinase with thrombospondin motifs 12 OS=Mus musculus GN=Adamts12 PE=1 SV=1	0	0	0	0	0	31	0	0	0
ACTC_MOUSE	Actin, alpha cardiac muscle 1 OS=Mus musculus GN=Actc1 PE=1 SV=1	0	1254	0	0	0	508	0	369	0
ACTA_MOUSE	Actin, aortic smooth muscle OS=Mus musculus GN=Acta2 PE=1 SV=1	395	0	0	0	0	0	387	0	313
ACTB_MOUSE	Actin, cytoplasmic 1 OS=Mus musculus GN=Actb PE=1 SV=1	703	2069	252	273	235	824	622	685	386
ARP2_MOUSE	Actin-related protein 2 OS=Mus musculus GN=Actr2 PE=1 SV=1	0	0	0	0	31	51	46	48	33
ACTZ_MOUSE	Alpha-centractin OS=Mus musculus GN=Actr1a PE=2 SV=1	0	0	0	0	31	51	46	45	33
ANKR6_MOUSE	Ankyrin repeat domain-containing protein 6 OS=Mus musculus GN=Ankrd6 PE=1 SV=2	0	0	0	0	0	0	36	42	0
ASAP2_MOUSE	Arf-GAP with SH3 domain, ANK repeat and PH domain-containing protein 2 OS=Mus musculus GN=Asap2 PE=1 SV=3	0	31	0	0	0	0	0	35	0
ATPA_MOUSE	ATP synthase subunit alpha, mitochondrial OS=Mus musculus GN=Atp5a1 PE=1 SV=1	0	0	0	0	0	1040	306	0	0
ATPB_MOUSE	ATP synthase subunit beta, mitochondrial OS=Mus musculus GN=Atp5b PE=1 SV=2	0	0	0	0	0	390	0	0	0
ACTBL_MOUSE	Beta-actin-like protein 2 OS=Mus musculus GN=Actbl2 PE=2 SV=1	0	1148	0	0	0	0	0	0	0
BASP1_MOUSE	Brain acid soluble protein 1 OS=Mus musculus GN=Basp1 PE=1 SV=3	0	0	0	0	0	55	132	0	0
BCAS1_MOUSE	Breast carcinoma-amplified sequence 1 homologBreast carcinoma-amplified	0	0	47	0	93	0	0	0	0

	sequence 1 homolog OS=Mus musculus GN=Bcas1 PE=1 SV=2									
KCC2B_MOUSE	Calcium/calmodulin-dependent protein kinase type II subunit beta OS=Mus musculus GN=Camk2b PE=1 SV=2	0	0	0	0	0	1421	0	0	0
COR1A_MOUSE	Coronin-1A OS=Mus musculus GN=Coro1a PE=1 SV=5	0	0	0	0	0	0	49	0	0
COR1C_MOUSE	Coronin-1C OS=Mus musculus GN=Coro1c PE=1 SV=2	0	0	0	0	0	300	152	0	0
CT2NL_MOUSE	CTTNBP2 N-terminal-like protein OS=Mus musculus GN=Cttnbp2nl PE=1 SV=1	0	0	0	0	0	32	0	38	85
DEMA_MOUSE	Dematin OS=Mus musculus GN=Epb49 PE=1 SV=1	237	0	0	0	0	79	0	0	0
MSH6_MOUSE	DNA mismatch repair protein Msh6 OS=Mus musculus GN=Msh6 PE=1 SV=2	0	0	0	0	0	0	0	0	34
ENPP6_MOUSE	Ectonucleotide pyrophosphatase/phosphodiesterase family member 6 OS=Mus musculus GN=Enpp6 PE=2 SV=1	44	56	0	0	0	0	0	0	0
EF1A1_MOUSE	Elongation factor 1-alpha 1 OS=Mus musculus GN=Eef1a1 PE=1 SV=3	122	56	0	0	0	91	0	0	0
EF1A2_MOUSE	Elongation factor 1-alpha 2 OS=Mus musculus GN=Eef1a2 PE=1 SV=1	0	0	0	0	0	0	114	0	0
ERMIN_MOUSE	Ermin OS=Mus musculus GN=Ermn PE=1 SV=1	61	0	0	0	0	0	36	0	0
CAZA2_MOUSE	F-actin-capping protein subunit alpha-2 OS=Mus musculus GN=Capza2 PE=1 SV=3	0	0	35	0	88	0	0	92	0
FLOT1_MOUSE	Flotillin-1 OS=Mus musculus GN=Flot1 PE=1 SV=1	0	0	0	0	0	0	38	0	0
ALDOA_MOUSE	Fructose-bisphosphate aldolase A OS=Mus musculus GN=Aldoa PE=1 SV=2	0	0	0	0	0	0	0	113	0
CXA1_MOUSE	Gap junction alpha-1 protein OS=Mus musculus GN=Gja1 PE=1 SV=2	0	0	0	0	0	0	0	85	122
G3P_MOUSE	Glyceraldehyde-3-phosphate dehydrogenase OS=Mus musculus GN=Gapdh PE=1 SV=2	0	0	56	0	0	0	0	175	32
DIRA2_MOUSE	GTP-binding protein Di-Ras2 OS=Mus musculus GN=Diras2 PE=2 SV=1	0	47	0	0	0	0	0	0	0
GNAZ_MOUSE	Guanine nucleotide-binding protein G(z)	0	0	61	0	0	0	0	0	57

	subunit alpha OS=Mus musculus GN=Gnaz PE=2 SV=4									
GNA12_MOUSE	Guanine nucleotide-binding protein subunit alpha-12 OS=Mus musculus GN=Gna12 PE=1 SV=3	0	0	52	0	51	0	0	58	69
HBA_MOUSE	Hemoglobin subunit alpha OS=Mus musculus GN=Hba PE=1 SV=2	0	0	0	0	0	102	153	0	0
HBE_MOUSE	Hemoglobin subunit epsilon-Y2 OS=Mus musculus GN=Hbb-y PE=1 SV=2	0	0	0	0	0	71	43	41	0
HNRPF_MOUSE	Heterogeneous nuclear ribonucleoprotein F OS=Mus musculus GN=Hnrnpf PE=1 SV=3	0	82	0	0	0	0	0	0	0
HNRH1_MOUSE	Heterogeneous nuclear ribonucleoprotein H OS=Mus musculus GN=Hnrnph1 PE=1 SV=3	87	0	0	0	0	0	0	0	0
H4_MOUSE	Histone H4 OS=Mus musculus GN=Hist1h4a PE=1 SV=2	0	0	0	0	0	0	34	0	0
HOME1_MOUSE	Homer protein homolog 1 OS=Mus musculus GN=Homer1 PE=1 SV=2	221	176	0	0	0	178	43	0	0
PLAK_MOUSE	Junction plakoglobin OS=Mus musculus GN=Jup PE=1 SV=3	0	0	0	0	0	408	36	0	0
LANC1_MOUSE	LanC-like protein 1 OS=Mus musculus GN=Lancl1 PE=1 SV=1	0	0	103	0	63	0	0	161	64
LANC2_MOUSE	LanC-like protein 2 OS=Mus musculus GN=Lancl2 PE=1 SV=1	0	0	0	0	0	0	45	0	0
LSAMP_MOUSE	Limbic system-associated membrane protein OS=Mus musculus GN=Lsamp PE=1 SV=1	0	0	0	0	0	113	78	0	0
L12R1_MOUSE	Loss of heterozygosity 12 chromosomal region 1 protein homolog OS=Mus musculus GN=Loh12cr1 PE=2 SV=1	0	0	0	0	0	0	0	32	83
LA_MOUSE	Lupus La protein homolog OS=Mus musculus GN=Ssb PE=2 SV=1	0	58	0	0	0	0	0	0	0
MDHM_MOUSE	Malate dehydrogenase, mitochondrial OS=Mus musculus GN=Mdh2 PE=1 SV=3	0	0	94	0	0	0	0	0	0
TAU_MOUSE	Microtubule-associated protein tau OS=Mus musculus GN=Mapt PE=1 SV=3	84	32	0	0	0	43	44	0	0
MTA70_MOUSE	N6-adenosine-methyltransferase 70 kDa subunit OS=Mus musculus GN=Mettl3	0	0	0	0	0	43	52	0	0

	PE=2 SV=2									
NEGR1_MOUSE	Neuronal growth regulator 1 OS=Mus musculus GN=Negr1 PE=1 SV=1	129	94	0	0	0	121	111	0	0
SEPT3_MOUSE	Neuronal-specific septin-3 OS=Mus musculus GN=Sept3 PE=1 SV=2	0	0	32	35	37	0	0	53	57
NPM_MOUSE	Nucleophosmin OS=Mus musculus GN=Npm1 PE=1 SV=1	0	0	31	44	36	0	0	38	0
PK3CA_MOUSE	Phosphatidylinositol-4,5-bisphosphate 3-kinase catalytic subunit alpha isoform OS=Mus musculus GN=Pik3ca PE=1 SV=1	0	0	0	0	0	0	38	33	0
F164A_MOUSE	Protein FAM164A OS=Mus musculus GN=Fam164a PE=2 SV=1	0	0	58	0	85	0	0	41	0
FA98B_MOUSE	Protein FAM98B OS=Mus musculus GN=Fam98b PE=2 SV=1	65	120	0	0	0	0	0	0	0
ZER1_MOUSE	Protein zer-1 homolog OS=Mus musculus GN=Zer1 PE=1 SV=1	0	0	0	0	0	0	0	0	33
SMBT1_MOUSE	Scm-like with four MBT domains protein 1 OS=Mus musculus GN=Sfmbt1 PE=2 SV=1	0	0	0	0	0	0	39	0	0
SEP11_MOUSE	Septin-11 OS=Mus musculus GN=Sept11 PE=1 SV=4	0	0	0	0	0	219	80	0	0
SEPT4_MOUSE	Septin-4 OS=Mus musculus GN=Sept4 PE=1 SV=1	0	0	31	41	0	0	0	0	33
SEPT5_MOUSE	Septin-5 OS=Mus musculus GN=Sept5 PE=1 SV=2	0	0	78	54	63	0	0	413	202
SEPT7_MOUSE	Septin-7 OS=Mus musculus GN=Sept7 PE=1 SV=1	0	64	0	0	0	294	307	0	0
SEPT8_MOUSE	Septin-8 OS=Mus musculus GN=Sept8 PE=1 SV=4	0	0	0	0	0	140	0	0	0
2ABA_MOUSE	Serine/threonine-protein phosphatase 2A 55 kDa regulatory subunit B alpha isoform OS=Mus musculus GN=Ppp2r2a PE=1 SV=1	0	0	0	0	0	64	0	0	0
AT1B1_MOUSE	Sodium/potassium-transporting ATPase subunit beta-1 OS=Mus musculus GN=Atp1b1 PE=1 SV=1	78	43	0	0	0	0	0	0	0
SYN2_MOUSE	Synapsin-2 OS=Mus musculus GN=Syn2 PE=1 SV=2	0	0	0	0	0	295	0	0	0

TEFF1_MOUSE	Tomoregulin-1 OS=Mus musculus GN=Tmeff1 PE=2 SV=1	0	40	0	0	0	0	32	103	147
PURA_MOUSE	Transcriptional activator protein Pur-alpha OS=Mus musculus GN=Pura PE=1 SV=1	0	0	437	335	200	0	0	286	149
PURB_MOUSE	Transcriptional activator protein Pur-beta OS=Mus musculus GN=Purb PE=1 SV=3	0	0	161	97	152	0	0	146	135
TMOD1_MOUSE	Tropomodulin-1 OS=Mus musculus GN=Tmod1 PE=2 SV=1	0	0	0	91	39	0	0	75	0
TMOD2_MOUSE	Tropomodulin-2 OS=Mus musculus GN=Tmod2 PE=1 SV=2	0	0	102	177	107	0	0	253	56
TBA1A_MOUSE	Tubulin alpha-1A chain OS=Mus musculus GN=Tuba1a PE=1 SV=1	188	163	71	0	118	2020	1600	0	0
TBA1B_MOUSE	Tubulin alpha-1B chain OS=Mus musculus GN=Tuba1b PE=1 SV=2	0	0	0	0	0	1911	1185	0	0
TBA4A_MOUSE	Tubulin alpha-4A chain OS=Mus musculus GN=Tuba4a PE=1 SV=1	0	0	0	0	0	1445	900	0	0
TBB2A_MOUSE	Tubulin beta-2A chain OS=Mus musculus GN=Tubb2a PE=1 SV=1	416	87	0	62	89	3347	2280	71	0
TBB2C_MOUSE	Tubulin beta-2C chain OS=Mus musculus GN=Tubb2c PE=1 SV=1	426	0	0	0	0	3295	2491	0	0
TBB3_MOUSE	Tubulin beta-3 chain OS=Mus musculus GN=Tubb3 PE=1 SV=1	370	153	0	0	0	2939	2121	0	0
TBB4_MOUSE	Tubulin beta-4 chain OS=Mus musculus GN=Tubb4 PE=1 SV=3	0	0	0	0	0	3052	1851	0	0
TBB5_MOUSE	Tubulin beta-5 chain OS=Mus musculus GN=Tubb5 PE=1 SV=1	370	0	0	0	0	2873	2357	0	0
TBB6_MOUSE	Tubulin beta-6 chain OS=Mus musculus GN=Tubb6 PE=1 SV=1	169	0	0	0	0	2002	1381	0	0
UH1BL_MOUSE	UHRF1-binding protein 1-like OS=Mus musculus GN=Uhrf1bp1l PE=2 SV=1	33	0	0	0	0	0	0	0	0
VA0D1_MOUSE	V-type proton ATPase subunit d 1 OS=Mus musculus GN=Atp6v0d1 PE=1 SV=2	0	0	85	0	38	0	0	103	0
CN37_MOUSE	2~,3~-cyclic-nucleotide 3~-phosphodiesterase OS=Mus musculus GN=Cnp PE=1 SV=3	0	0	0	0	0	32	0	0	0
F262_MOUSE	6-phosphofructo-2-kinase/fructose-2,6-biphosphatase 2 OS=Mus musculus GN=Pfkfb2 PE=1 SV=2	0	0	0	0	0	34	0	0	0
GRP78_MOUSE	78 kDa glucose-regulated protein OS=Mus	0	0	0	0	0	0	0	0	30

	musculus GN=Hspa5 PE=1 SV=3									
ARP3_MOUSE	Actin-related protein 3 OS=Mus musculus GN=Actr3 PE=1 SV=3	55	0	0	0	0	0	0	0	0
APC1_MOUSE	Anaphase-promoting complex subunit 1 OS=Mus musculus GN=Anapc1 PE=1 SV=1	34	32	0	0	0	0	33	0	30
KCRU_MOUSE	Creatine kinase U-type, mitochondrial OS=Mus musculus GN=Ckmt1 PE=1 SV=1	42	0	0	0	0	0	0	0	0
CUL5_MOUSE	Cullin-5 OS=Mus musculus GN=Cul5 PE=1 SV=3	0	0	0	0	0	33	0	0	0
DEP1A_MOUSE	DEP domain-containing protein 1A OS=Mus musculus GN=Depdc1a PE=1 SV=1	0	0	0	0	0	31	0	0	0
DCR1A_MOUSE	DNA cross-link repair 1A protein OS=Mus musculus GN=Dclre1a PE=1 SV=2	0	0	0	0	0	0	32	0	0
ELAV2_MOUSE	ELAV-like protein 2 OS=Mus musculus GN=Elavl2 PE=2 SV=1	0	0	0	0	0	0	0	32	0
ELMO1_MOUSE	Engulfment and cell motility protein 1 OS=Mus musculus GN=Elmo1 PE=1 SV=2	0	0	0	31	0	0	0	0	0
CAZA1_MOUSE	F-actin-capping protein subunit alpha-1 OS=Mus musculus GN=Capza1 PE=1 SV=4	0	0	0	0	0	0	0	0	63
FABP5_MOUSE	Fatty acid-binding protein, epidermal OS=Mus musculus GN=Fabp5 PE=1 SV=3	0	0	0	0	0	42	0	0	43
FCSD2_MOUSE	FCH and double SH3 domains protein 2 OS=Mus musculus GN=Fchsd2 PE=1 SV=2	0	0	0	32	0	0	32	0	0
G3PT_MOUSE	Glyceraldehyde-3-phosphate dehydrogenase, testis-specific OS=Mus musculus GN=Gapdhs PE=1 SV=1	0	0	0	0	45	0	0	38	0
GNAL_MOUSE	Guanine nucleotide-binding protein G(olf) subunit alpha OS=Mus musculus GN=Gnal PE=1 SV=1	0	0	0	0	51	0	0	0	0
ROA3_MOUSE	Heterogeneous nuclear ribonucleoprotein A3 OS=Mus musculus GN=Hnrnpa3 PE=1 SV=1	0	0	0	0	0	0	0	69	0
HNRPD_MOUSE	Heterogeneous nuclear ribonucleoprotein D0 OS=Mus musculus GN=Hnrnpd PE=1 SV=2	0	0	0	0	54	0	0	0	0

IP3KA_MOUSE	Inositol-trisphosphate 3-kinase A OS=Mus musculus GN=Itpka PE=2 SV=1	0	0	0	0	0	31	0	0	0
LAMA1_MOUSE	Laminin subunit alpha-1 OS=Mus musculus GN=Lama1 PE=1 SV=1	0	0	0	41	0	0	0	0	0
KDM4A_MOUSE	Lysine-specific demethylase 4A OS=Mus musculus GN=Kdm4a PE=1 SV=2	0	0	0	0	0	0	30	0	0
NEUM_MOUSE	Neuromodulin OS=Mus musculus GN=Gap43 PE=1 SV=1	0	56	0	0	0	0	50	0	0
NR6A1_MOUSE	Nuclear receptor subfamily 6 group A member 1 OS=Mus musculus GN=Nr6a1 PE=1 SV=1	31	0	0	0	0	0	0	0	0
FA65C_MOUSE	Protein FAM65C OS=Mus musculus GN=Fam65c PE=2 SV=1	0	0	0	0	0	0	0	0	31
TDRD9_MOUSE	Putative ATP-dependent RNA helicase TDRD9 OS=Mus musculus GN=Tdrd9 PE=1 SV=3	0	0	0	0	0	0	0	0	31
FTSJ2_MOUSE	S-adenosyl-L-methionine-dependent methyltransferase FTSJD2 OS=Mus musculus GN=Ftsjd2 PE=1 SV=1	0	0	0	0	0	33	0	0	0
LACTB_MOUSE	Serine beta-lactamase-like protein LACTB, mitochondrial OS=Mus musculus GN=Lactb PE=1 SV=1	0	0	0	0	0	33	0	0	0
PP2BA_MOUSE	Serine/threonine-protein phosphatase 2B catalytic subunit alpha isoform OS=Mus musculus GN=Ppp3ca PE=1 SV=1	0	0	0	0	0	36	0	0	0
SYPH_MOUSE	Synaptophysin OS=Mus musculus GN=Syp PE=1 SV=2	0	0	35	0	0	0	0	0	0
SYTL2_MOUSE	Synaptotagmin-like protein 2 OS=Mus musculus GN=Sytl2 PE=1 SV=2	0	0	36	0	0	32	0	34	0
TBKB1_MOUSE	TANK-binding kinase 1-binding protein 1 OS=Mus musculus GN=Tbkbp1 PE=1 SV=1	0	0	0	0	0	0	34	0	0
TXD11_MOUSE	Thioredoxin domain-containing protein 11 OS=Mus musculus GN=Txndc11 PE=2 SV=1	0	0	31	0	0	0	0	0	0
UBIQ_MOUSE	Ubiquitin OS=Mus musculus GN=Rps27a PE=1 SV=1	0	0	0	0	0	0	0	0	44
CB063_MOUSE	Uncharacterized protein C2orf63 homolog OS=Mus musculus PE=2 SV=1	0	0	0	0	0	38	0	0	0

VIAAT_MOUSE	Vesicular inhibitory amino acid transporter OS=Mus musculus GN=Slc32a1 PE=1 SV=3	0	0	0	0	0	0	0	33	0
KCAB1_MOUSE	Voltage-gated potassium channel subunit beta-1 OS=Mus musculus GN=Kcnab1 PE=2 SV=1	0	0	0	0	0	32	0	34	0

Table S2 (next page). Proteins affinity-purified by BR7ecto226-His from brain lysates and identified by LC/MS-MS.

Mascot scores for proteins identified by LC-ESI-FT-MS/MS that were affinity-purified from brain lysates using BR7ecto226-His (BR7ecto) as bait. The scores for proteins identified in control isolates, using the His-tagged RPTPμ ectodomain (RPTPmu) as bait or nickel beads alone (Empty beads), are listed for two independent experiments (A, B). Underlined protein names are discussed in the text.

Mascot results compiled from experiment: Sample name	A Empty beads	A BR7ecto	A RPTPmu	B Empty beads	B BR7 ecto	B RPTPmu
Actin, cytoplasmic 1 OS=Mus musculus GN=Actb PE=1 SV=1	1193	992	1237	1740	2212	800
Tubulin alpha-1A chain OS=Mus musculus GN=Tuba1a PE=1 SV=1	3919	605	190	875	687	627
Tubulin beta-4 chain OS=Mus musculus GN=Tubb4 PE=1 SV=3	7362	598	0	1117	727	0
Tubulin beta-3 chain OS=Mus musculus GN=Tubb3 PE=1 SV=1	6474	568	0	1124	744	698
Tubulin beta-2C chain OS=Mus musculus GN=Tubb2c PE=1 SV=1	8624	549	0	1232	732	663
Tubulin beta-5 chain OS=Mus musculus GN=Tubb5 PE=1 SV=1	7411	528	0	1129	765	599
Tubulin beta-2A chain OS=Mus musculus GN=Tubb2a PE=1 SV=1	9102	435	84	1216	569	404
Myelin basic protein OS=Mus musculus GN=Mbp PE=1 SV=2	3025	280	137	1162	840	956
Beta-actin-like protein 2 OS=Mus musculus GN=Actbl2 PE=2 SV=1	659	229	0	0	689	249
Thy-1 membrane glycoprotein OS=Mus musculus GN=Thy1 PE=1 SV=1	0	157	51	80	116	43
Calcium/calmodulin-dependent protein kinase type II subunit alpha OS=Mus musculus GN=Camk2a PE=1 SV=2	0	153	69	38	200	45
Neuronal growth regulator 1 OS=Mus musculus GN=Negr1 PE=1 SV=1	0	147	62	97	62	0
Creatine kinase B-type OS=Mus musculus GN=Ckb PE=1 SV=1	2073	133	0	84	0	0
Receptor-type tyrosine-protein phosphatase R OS=Mus musculus GN=Ptprr PE=1 SV=1	0	117	0	0	952	0
Limbic system-associated membrane protein OS=Mus musculus GN=Lsamp PE=1 SV=1	0	104	0	43	74	40
Guanine nucleotide-binding protein G(o) subunit alpha OS=Mus musculus GN=Gnao1 PE=1 SV=3	0	85	0	0	139	0
Neurotrimin OS=Mus musculus GN=Ntm PE=2 SV=2	0	77	0	0	31	0
Guanine nucleotide-binding protein G(z) subunit alpha OS=Mus musculus GN=Gnaz PE=2 SV=4	0	73	0	0	0	0
Dihydropyrimidinase-related protein 2 OS=Mus musculus GN=Dpysl2 PE=1 SV=2	3598	72	0	71	107	0
ATP synthase subunit alpha, mitochondrial OS=Mus musculus GN=Atp5a1 PE=1 SV=1	235	59	0	170	0	97
Hemoglobin subunit epsilon-Y2 OS=Mus musculus GN=Hbb-y PE=1 SV=2	50	58	0	31	50	40

Elongation factor 1-alpha 1 OS=Mus musculus GN=Eef1a1 PE=1 SV=3	0	53	0	94	143	0
Ubiquitin OS=Mus musculus GN=Rps27a PE=1 SV=1	91	52	0	85	107	151
Histone H2A type 1-F OS=Mus musculus GN=Hist1h2af PE=1 SV=3	63	52	0	128	376	92
Myosin regulatory light chain 12B OS=Mus musculus GN=Myl12b PE=1 SV=2	0	48	0	129	67	0
N6-adenosine-methyltransferase 70 kDa subunit OS=Mus musculus GN=Mettl3 PE=2 SV=2	0	38	51	51	58	65
Desmoglein-1-alpha OS=Mus musculus GN=Dsg1a PE=2 SV=2	0	35	37	38	0	64
Heat shock cognate 71 kDa protein OS=Mus musculus GN=Hspa8 PE=1 SV=1	1144	34	0	169	196	0
Sodium/potassium-transporting ATPase subunit beta-1 OS=Mus musculus GN=Atp1b1 PE=1 SV=1	484	33	0	51	42	53
Tomoregulin-1 OS=Mus musculus GN=Tmeff1 PE=2 SV=1	0	33	54	0	0	0
Usher syndrome type-1C protein-binding protein 1 OS=Mus musculus GN=Ushbp1 PE=1 SV=1	0	32	0	31	0	0
Arf-GAP with SH3 domain, ANK repeat and PH domain-containing protein 2 OS=Mus musculus GN=Asap2 PE=1 SV=3	0	31	41	0	37	0
Histone H2B type 1-A OS=Mus musculus GN=Hist1h2ba PE=2 SV=3	0	31	0	32	0	35
V-type proton ATPase 116 kDa subunit a isoform 1 OS=Mus musculus GN=Atp6v0a1 PE=1 SV=2	0	0	0	90	319	65
Contactin-1 OS=Mus musculus GN=Cntn1 PE=1 SV=1	0	0	102	142	233	0
V-type proton ATPase subunit d 1 OS=Mus musculus GN=Atp6v0d1 PE=1 SV=2	0	0	0	127	222	0
Myosin-10 OS=Mus musculus GN=Myh10 PE=1 SV=2	0	0	132	906	193	0
Sodium/potassium-transporting ATPase subunit alpha-2 OS=Mus musculus GN=Atp1a2 PE=1 SV=1	0	0	74	511	192	0
Serum albumin OS=Mus musculus GN=Alb PE=1 SV=3	0	0	0	0	158	61
Glyceraldehyde-3-phosphate dehydrogenase OS=Mus musculus GN=Gapdh PE=1 SV=2	558	0	69	366	158	108
Transcriptional activator protein Pur-alpha OS=Mus musculus GN=Pura PE=1 SV=1	0	0	0	76	122	0
Microtubule-associated protein 1A OS=Mus musculus GN=Map1a PE=1 SV=2	94	0	0	0	114	0
Heterogeneous nuclear ribonucleoproteins A2/B1 OS=Mus musculus GN=Hnrnpa2b1 PE=1	0	0	0	0	97	0

6.5 Acknowledgements

"One never reaches home,
but wherever friendly paths intersect
the whole world looks like home for a time"
Herman Hesse

Writing acknowledgements at the end of this book one year after the experimental part of this work has been completed gives to the writer a strange feeling in the gut, a certain hesitancy on how to do, what to recall, where to begin from… Many things have changed in one year, a new house, a new job, old and young friendships have come knocking at the door, new challenges, new doubts and persistent perplexities on past and recent events. More than three years in The Netherlands added to six months spent in Germany, are no small thing, they are four years in total. Who could have guessed that Irene, the homebody, good student and churchgoer that her friends used to know would have undertaken such a journey in foreign lands, remote to the young minds of her friends, in the cold Nordic lands, wherefrom we only knew Germans were coming, those who were invading the Lake Garda shores every summer? I don't count on the fingers of one hand who among my acquaintances has had such an experience. Of course, there, during my travels, I met many. Four years, four years, are not few. And yet, when thought now, in this very moment, they seem as though they have flown away! A blow, a bracket, confined in the memory, that abandons remote days and rather quenches his thirst, lives and eventually satiates itself only with the recent past and present cares…

But now, now, I must go back to those four years, to whom, what, where,…Figures, yes, the figures of this book will help me! Behind each one of them there are faces, hands and words of the ones who set out with me to peer, to analyze, to try out this little piece of *Being* that had been consigned to me…PTPs, Protein Tyrosine Phosphatases, not all, one, PTPRR, in mouse brains.

And what should I do? Cloning! First of all cloning, yes. Cloning pieces of PTPRR in order to construct a sort of probes, baits, to be used in the future experiments. What future experiments? Ah, don't worry, now just clone, clone, that's that. And if Jan, "gouden handen", had not been there to teach me bases and tricks of good cloning practice, how would have I made it out? But I don't have the proper restriction sites to cut on!? So do a PCR and insert the restriction sites you need! Thank you Rick, master of the PCR, thanks a lot for the Herculase, that saved me from many empty PCR! And then? And now you need to prepare the mouse brains! Brains??????? Yes, you must cut them, prepare sections and see if your probes attach onto them. And don't forget controls! Thank you Ineke, for having sacrificed with me those poor mice and having taught me how to extract brains. And thank you Huib for the sections! Of 10 µm, watch out, otherwise experiments won't be comparable and reviewers won't accept the article! Really? Oh my gosh! And then what will I do?
But from now on you will see I will make it out! I go to London by Andrew Stoker to learn the RAP in situ. I go for 20 days. And if I have time I go also to Oxford to meet Radu Aricescu and test the other constructs too…maybe we get to obtain PTPRR crystals! Hurrah, I

set off again! Thanks Andrew, Radu, Viki and Thomas for the days spent in England! And thanks to the London mayor for the evening opening hours of museums, a manna for my curiosity!
Oops, and Switzerland? I will never forget the week spent at Merck-Serono in Geneva. Thank you Rob for your availability and Monique for your care! But now I must go back to Nijmegen… you will have to do many slides to see if the experiments you performed in London are reproducible and then do not forget to start testing also the candidate proteins obtained from your experiments in Switzerland! Yes, yes, not so fast! Sure, I will do everything!
But to obtain proteins I need to culture cells?! Lieke, Rinske, do you have COS-1 cells to gently give me? And is there anybody who has HEK293T cells? No? To the 7th floor I need to go, to the department of physiology? Ok, let's go!
And now I must start with all western blots. I need antibodies! Jaaaaaan! Olga, Samuel, Eric, do you have perhaps antibodies to HER4, HER3, HER2, N-cadherin…?
And Magda, I need to dispatch some samples, how can I do that? To the -1 floor, for the mail service and dry ice? Ok, I rush!
Frank, Jan, cells in culture are contaminated. I have taken all precautions you had suggested to me…I must also express viral constructs now. Well, you can ask Ad, he is a master in culturing viruses. Ok, let's try it!
Look here, do you see? Experiments have been repeated many times and they are not reproducible. I do not understand, sometimes I see protein bands, some other times I don't. Phosphorylation disappears and I can't get to the end of the experiment….What do you use to induce phosphorylation? Vanadium. Everybody uses it to induce and maintain tyrosine phosphorylation on proteins. Ok, let's try again!
Wiljan, I do not trust these compounds based on vanadium. To my opinion, they somehow inhibit also my PTPRR so that experiments in the end do not work, or maybe is something else….mmmhhh. I must find an alternative. And if I do purifications directly from mouse brains and I test interactions with mass spectrometry? In this way I go back to a relatively more familiar field. Thanks Nick for all your teachings on silver staining and mass spectrometry!
And thanks Huib again for helping me with the fluorescence microscope!

And then, what to say, the list would be very long! Wiljan, the accelerator, the gear, the brake, of the project-machine; sorry for I have often been just a squared wheel. All colleagues of Bé's, Pieter's, and Gerard's groups! All PhD students and post-docs with whom I had interesting and comforting talks during lunch breaks and evening hours around lab benches. A special thank to Lieke, Gerda, Susan, Mirthe, Rinske (my teacher of Dutch language, traditions and sometimes mother ☺), Marieke, Mietske, Olga, Bettina, Samuel and Antoine. Peter and Alie, thank you for hosting me in your house and for the wonderful day in Mantua!
All PTPNET members, with whom I spent unforgettable days among meetings, conferences and tables set with delicacies from all your countries. Barbara, Victoria, Monique, Deepika, Caroline, Vasu, Thomas, Vincent, Jeroen, Sujay, Leo and Deepankar! Heartily thank you Stefan, for treating me often as a daughter. And also to Frank, for your unconditional convidence in me and this project.

Behind these pages, I can't forget the other friends, those outside the lab, because there was some time left to the life outside! Igor and all my housemates; father Joop, Patsy and the members of the Nijmegen "church-group", without whom I would have lost my Christian reference points; Maria, Luminita, Peer, Gleb, Adriana, Olha and all members of the "Lost-in-Nijmgen" group with whom I have walked hundreds kilometres in the low lands!

And finally, a special thank to the students of the 1st and 2nd class of the "liceo scientifico" and 4th "ginnasio" of the Don Mazza high school in Verona, for their admirable commitment in having borne with me, novice teacher, during the 2011-2012 school year. Because maybe you will never know, but you, and what I owe you, have been the main lever that has made me accomplish this work with coherence and commitment.
Thank you because you have given new meaning to my life.

Here ends this journey. But no, I am wrong, this is just the beginning.

Other favourite quotes:

♫ Change does not roll in on the wheels of inevitability, but comes through continuous struggle. And so we must straighten our backs and work for our freedom. A man can't ride you unless your back is bent. Martin Luther King, Jr.

♫ A competent leader can get efficient service from poor troops, while on the contrary an incapable leader can demoralize the best of troops. John J. Pershing, general

♫ How important it is in life not necessarily to be strong but to feel strong, to measure yourself at least once, to find yourself at least once..." Primo Levi

♫ "Montag, take my word for it, I've had to read a few in my time, to know what I was about, and the books say nothing! Nothing you can believe or teach. They're about non-existent people, figments of imagination, if they're fiction. And if they're non-fiction, it's worse, one professor calling another an idiot, one philosopher screaming down another's gullet. All of them running about, putting out the stars and extinguishing the sun. You come away lost." Fahrenheit 451.

♫ Without words, without writing and without books there would be no history, there could be no concept of humanity. Herman Hesse

♫ Science can purify religion from error and superstition. Religion can purify science from idolatry and false absolutes. Joan Paul II

♫ All major religious traditions carry basically the same message, that is love, compassion and forgiveness. The important thing is they should be part of our daily lives. Dalai Lama

6.6 Lebenslauf - Curriculum vitae

Name: Chesini

Vorname: Irene Matilde

Geburtsdatum: 31.05.1981

Geburtsort: Verona, Italy

Staatsbürgerschaft: Italien

Familienstand: Ledig

Anschrift: Via Santa Caterina da Siena 22 – San Pietro in Cariano – Verona - Italien

1995-2000 Besuch des Gymnasiums "Liceo Scientifico G. Fracastoro", Verona, Italien

2000-2006 Ausbildung zum Master of Science im Fach " Agro-industrial Biotechnology"an der UniversitätVerona, Anfertigung und Verteidigung der Master-Arbeit unter Betreuung von Prof. G. Vallini

April - June 2006 Arbeit als Chemischer Analytiker in den "Chimica Servizi S.r.l." Laboratorien in Verona

September 2006 – March 2007 Praktikum im Bayer "Cropscience Centre", Monheim am Rhein, Deutschland, organisiert durch die **"**Italian Unipharma graduates organization"

May 2007 – September 2010 Arbeit als Doktorandin am Nijmegen Centre for Life Sciences (Nijmegen, The Netherlands) unter Betreuung von Prof. Dr. WJAJ Hendriks.

Spetember 2010 – June 2011 Arbeit als Biologie-Lehrerin am"Don Mazza" Gymnasium in Verona, Italien

E-mail: matilde.ch@libero.it

Telefonnummer: +39 3385212633

6.7 Selbstständigkeitserklärung

Hiermit erkläre ich, dass ich die vorliegende Arbeit selbstständig und nur unter Verwendung der angegebenen Hilfsmittel, Literatur und persönlichen Mitteilungen angefertigt habe.

Verona, den 11. September 2011
Irene Matilde Chesini

6.8 Erklärung zur Bewerbung

Hiermit erkläre ich, dass ich mich mit der vorliegenden Arbeit an keiner anderen Hochschule um den akademischen Grad Doctor rerum naturalium beworben habe und dass ich weder früher noch gegenwärtig die Eröffnung eines Verfahrens zum Erwerb des oben genannten akademischen Grades an einer anderen Hochschule beantragt habe. Die Promotions-Ordnung der Biologisch-Pharmazeutischen-Fakultät der FSU Jena ist mir bekannt.

Verona, den 11. September 2011
Irene Matilde Chesini

6.9 List of Posters and Publications

Some part of this work has already been presented at the following places.

Posters presented

Irene Matilde Chesini
Title: "PTPRR isoforms in neuronal cell signalling"
Presented at the PhD students meeting in Papendal, The Netherlands (April, 2008)

Irene M. Chesini, Andrew W. Stoker & Wiljan J.A.J. Hendriks
Title: "Hunting for extracellular PTPTRR signaling regulators"
Presented at the PhD students meeting in Papendal, The Netherlands (May, 2009)
and at the Europhosphatase Meeting in Alkmaar, The Netherlands (July, 2009)

Publications

Antonioli P, Lampis S, **Chesini I**, Vallini G, Rinalducci S, Zolla L, Righetti PG (2007) Stenotrophomonas maltophilia SeITE02, a new bacterial strain suitable for bioremediation of selenite-contaminated environmental matrices. Appl Environ Microbiol. Nov;73(21): 6854-63.

Chesini IM, Debyser G., Croes H, ten Dam GB, Devreese B, Stoker AW, Hendriks WJAJ (2011) PTPBR7 Binding Proteins in Myelinating Neurons of the Mouse Brain. Int J Biol Sci; 7(7): 978-991.